



HAL
open science

Development and evolution of the vertebrate mineralized skeleton : histomorphogenetic modeling applied to pteraspidomorph fossils

Guillaume Houée

► **To cite this version:**

Guillaume Houée. Development and evolution of the vertebrate mineralized skeleton : histomorphogenetic modeling applied to pteraspidomorph fossils. Paleontology. Sorbonne Université, 2023. English. NNT : 2023SORUS571 . tel-04861141

HAL Id: tel-04861141

<https://theses.hal.science/tel-04861141v1>

Submitted on 2 Jan 2025

HAL is a multi-disciplinary open access archive for the deposit and dissemination of scientific research documents, whether they are published or not. The documents may come from teaching and research institutions in France or abroad, or from public or private research centers.

L'archive ouverte pluridisciplinaire **HAL**, est destinée au dépôt et à la diffusion de documents scientifiques de niveau recherche, publiés ou non, émanant des établissements d'enseignement et de recherche français ou étrangers, des laboratoires publics ou privés.

Sorbonne Université

Ecole Doctorale « Sciences de la nature et de l'Homme : évolution et écologie »

– ED 227 –

Développement et évolution du squelette minéralisé des vertébrés : modélisation histomorphogénétique appliquée aux fossiles de ptéraspidomorphes

Par Guillaume HOUÉE

Thèse de doctorat de Paléontologie

Dirigée par :

Damien GERMAIN, Maître de conférences, CR2P, MNHN

Nicolas GOUDEMAND, Professeur des universités, IGFL, ENS de Lyon

Jérémie BARDIN, Ingénieur d'études, CR2P, SU

Présentée et soutenue publiquement le 18 décembre 2023

Devant un jury composé de :

Jukka JERNVALL	Professor, University of Helsinki, Finlande	Rapporteur
Sophie PANTALACCI	Directrice de recherche, Centre national de la recherche scientifique, France	Rapporteuse
Mélanie DEBIAIS-THIBAUD	Maîtresse de conférences, Université de Montpellier, France	Examinatrice
Joseph N. KEATING	Senior Research Associate, University of Bristol, Royaume-Uni	Examinateur
Alexandra HOUSSAYE	Directrice de recherche, Centre national de la recherche scientifique, France	Présidente
Damien GERMAIN	Maître de conférences, Muséum national d'Histoire naturelle, France	Directeur de thèse
Nicolas GOUDEMAND	Professeur des universités, École normale supérieure de Lyon, France	Codirecteur de thèse
Jérémie BARDIN	Ingénieur d'études, Sorbonne Université, France	Coencadrant de thèse

Je n'étais pas un bon élève lorsque j'étais enfant, et je n'avais aucune idée de ce que je voulais faire plus tard.

Mais, un jour, durant mes années de lycée, une flamme s'est allumée en moi :

Je veux devenir Paléontologue.

Aujourd'hui, dix ans plus tard, je suis en train de rédiger ma thèse de doctorat.

Quel étrange mélange d'émotions...

24.08.2023

REMERCIEMENTS

Je tiens tout d'abord à remercier mes encadrants de thèse, Damien Germain, Nicolas Goudemand et Jérémie Bardin, d'avoir construit ce sujet de thèse passionnant et de m'avoir encadré pendant sa réalisation. Ils forment un encadrement très complémentaire, que ce soit d'un point de vue des connaissances et des compétences, que d'un point de vue humain. Travailler avec eux a été à la fois particulièrement stimulant intellectuellement, favorisant notamment la créativité, et très agréable en raison de l'ambiance joyeuse qui était toujours présente lors de nos réunions. J'ai aussi beaucoup aimé confronter mon travail à leur regard critique. Leurs propositions étaient souvent challengeantes, mais c'est ce que je recherchais en me lançant dans l'aventure du doctorat. Je les remercie grandement de m'avoir soutenu et fait confiance durant ces trois années. Cela m'a notamment permis de prendre le temps nécessaire pour réfléchir et développer mes projets en autonomie. C'est aussi grâce à leur confiance que j'ai pu me lancer dans différents projets annexes qui me tenaient à cœur, comme l'enseignement, les terrains, ou encore un déplacement au Japon. Ce fut un réel plaisir de travailler avec vous. Je suis vraiment très heureux que tout se soit si bien passé, et j'espère que nous continuerons à travailler ensemble !

Une des rencontres marquantes que j'ai eues au cours de cette thèse a été celle avec Philippe Janvier. Dès mon arrivée dans l'équipe FOSFO du CR2P, il a eu la gentillesse de s'intéresser à mon sujet de thèse et à mes projets de recherche. Cela m'a encouragé à entrer en contact avec lui, et ce fut une rencontre formidable. Philippe Janvier a été particulièrement bienveillant envers moi et m'a aidé à plusieurs reprises à m'insérer dans le monde de la recherche. Il est finalement devenu comme un quatrième encadrant lors de cette thèse. C'est pourquoi je tiens à adresser un grand merci à Philippe Janvier pour le soutien et l'aide qu'il apporte encore aux jeunes chercheurs.

J'aimerais également remercier mes anciens encadrants de stage, Alexandra Houssaye, Jorge Cubo et Isabelle Rouget, pour m'avoir accompagné avant, mais aussi pendant le doctorat. C'est toujours un grand plaisir de vous revoir, d'échanger avec vous et de recevoir vos conseils. J'ai également une pensée pour Loïc Villier, qui m'a soutenu lors de ma candidature au Master SEP et en doctorat. C'est aussi le premier paléontologue que j'ai eu l'occasion de rencontrer lors de mon arrivée en licence.

Un grand merci à Alexandra Quilhac pour son soutien et son aide précieuse dans la gestion de ma mission d'enseignement. Alexandra Quilhac était l'une de mes professeures de biologie animale en licence, et ce fut une grande chance pour moi de pouvoir apprendre le métier avec quelqu'un d'aussi passionné par l'enseignement supérieur.

Je remercie également Sidney Delgado de m'avoir fait confiance en m'intégrant à l'étude "Expression of 20 SSCP genes during tooth and bone mineralization in Senegal bichir", avec l'aide de Jorge Cubo. Je suis particulièrement heureux d'avoir pu participer à ce projet sur les polyptères.

Un grand merci aux membres de mon Comité de Suivi Individuel : Stéphanie Bréhard, Mélanie Debiais-Thibaud, Alexandra Quilhac, Alan Pradel et Roland Zimm. Ils ont été particulièrement à l'écoute et bienveillants, que ce soit pendant ou entre les réunions annuelles. Ce fut un réel plaisir d'échanger avec eux au cours de mon doctorat.

Je remercie chaleureusement les membres de mon jury : Mélanie Debiais-Thibaud, Alexandra Houssaye, Jukka Jernvall, Joseph N. Keating et Sophie Pantalacci. Je suis particulièrement heureux de pouvoir partager avec eux le fruit de mon travail afin de solliciter leur retour critique et leurs conseils.

Je remercie le personnel administratif et d'appui du CR2P, de SU et du MNHN d'avoir permis la réalisation de mes divers projets. Merci à Angelina Bastos, Nadia Guerguadj, Suzy Colas, Anabela Guilliere, Peggy Vincent, Damien Germain, Colas Bouillet, Séverin Morel, Patricia Wils, Marta Bellato, Sylvain Charbonnier et Sylvie Crasquin. Je remercie particulièrement Vincent Rommevaux qui a pris de son temps pour m'initier à la réalisation de coupes histologiques.

De la même manière, je souhaite remercier le personnel de l'ED227 qui a toujours été à l'écoute et disponible en cas de besoin. Merci à Camille Vignes, Tiphanie Chica-Lefort, Jérôme Sueur, Julien Gasparini et Nathalie Machon.

Merci aux membres de l'association Rhinopolis, et notamment à Jean-Marc Pouillon, de m'avoir permis de m'investir dans l'organisation et la réalisation de chantiers de fouilles. En plus de m'apporter personnellement, ces expériences m'ont ouvert la voie à de nombreuses nouvelles rencontres et collaborations.

Je souhaite évidemment remercier mes amis, qui m'ont soutenu de près ou de loin pendant les périodes difficiles et m'ont permis de m'aérer l'esprit au quotidien. Un grand et chaleureux merci à Antoine Logghe, Lazare Elbaz, Erwan Courville, Rodolphe Paso, Nozomu Oyama, Alfred Lemierre, Valentin Buffa, Jordan Gonet, Elvis Guillam, Elie Mario Saliba, Paloma Maria Taraba, Lou de Montmiraille, Teddy Gaidon, Maël E Dor, François Clarac, Mathieu Faure-Brac et bien d'autres !

Ces amis font partie du monde de la recherche, mais je souhaite aussi grandement remercier mes autres amis qui me soutiennent depuis bien avant le doctorat. Un grand merci à Ludivine Tempelaere, Gabriel Colasante, David Sakana, Lou Moizo, Charles Bastide, Thomas Bergier et Sinan Cetiner.

C'est en grande majorité grâce à toutes ces personnes que j'ai pu réaliser cette thèse dans les meilleures conditions possibles. Ce fut réellement un grand plaisir de partager tous ces moments avec vous !

Finale­ment, rien de tout cela ne serait possible sans le soutien de longue date de ma famille et de mes proches. Je n'ai pas choisi le parcours le plus rassurant, mais je suis particulière­ment reconnaissant d'avoir pu être accom­pagné dans ce choix. Malgré les périodes de grosses difficultés, j'ai toujours pu garder la tête hors de l'eau grâce à votre soutien infaillible ! Un énorme merci à ma mère Armelle, mon père Michel, ma grande sœur Ophélie, ma petite sœur Mathilde, ma grand-mère Madeleine, la famille Mehta, Sylvie Fabulet, Xavier Pinel et la famille Chapelle !

Je souhaite dédier mes dernières lignes de remer­ciements à Ana Alves. Après avoir libéré une bourse à l'ED227, elle m'a permis de passer de premier sur liste d'attente à lauréat. Cette décision a changé ma vie d'une manière ou d'une autre. Depuis, nous avons eu l'occasion de devenir amis, et elle a été là à de nombreuses reprises pour me soutenir dans les moments difficiles. Un grand merci Ana !



Merci à Lazare Elbaz
pour cette magnifique
reconstruction d'*Astraspis* !

List of Contents

Résumé étendu	1
Extended abstract	5
General introduction.....	9
CHAPTER I: NEW ENAMELOID AND ENAMEL CONCEPTS.....	23
Objectives Chapter I.....	24
I.1. Introduction	25
I.2. Issues about enameloid definitions and identifications	26
State of the art	26
Issues with current enameloid concepts	29
Proposed solutions for the future	34
I.3. Overview of enamel and enameloid distribution and homologies.....	42
Distribution and primary homologies of enameloids and enamels	42
Ancestral states and secondary homologies of enameloids and enamels	46
I.4. Evo-devo: the dentin-enameloid-enamel continuum.....	48
Synthesis and creation of a general model of enameloid development.....	48
Enameloid-enamel transitions.....	52
I.5. Conclusion	56
Conclusion on the objectives of Chapter I	58
CHAPTER II: FROM ENAMELOID TO ENAMEL.....	59
Objectives Chapter II	60
II.1. Introduction.....	61
II.2. Materials and Methods	62
Modeling.....	62
Role of parameters	69
II.3. Results	74

II.4. Discussion	79
Impact of parameters and underlying mechanisms.....	79
Application of these results for <i>in vivo</i> studies	84
II.5. Conclusion	86
II.6. Appendix	87
Conclusion on the objectives of Chapter II.....	96
CHAPTER III: HISTOMORPHOGENESIS OF TEETH	97
Objectives Chapter III	98
III.1. Introduction	99
III.2. Materials and Methods.....	100
III.3. Results.....	101
Morphohistogenetic description of teeth.....	101
Morphohistogenetic description of simulations	103
III.4. Discussion.....	107
Impact of the initial epithelial curvature and the delayed activation of cells ...	107
Impact of a few primary transitions during a tooth-like growth.....	110
III.5. Conclusion.....	112
III.6. Appendix	113
Conclusion on the objectives of Chapter III	115
CHAPTER IV: PALEODEVELOPMENT OF ODONTODES.....	117
Objectives Chapter IV	118
IV.1. Introduction	119
IV.2. Materials and Methods.....	120
IV.3. Results.....	122
IV.4. Discussion	127
Capping tissue	128
Pulpar tissue.....	128
Developmental scenarios	132
Dual growth periodicity	138

IV.5. Conclusion.....	140
IV.6. Appendix.....	141
Conclusion on the objectives of Chapter IV	144
CHAPTER V: PALEODEVELOPMENT OF DERMAL PLATES	145
Objectives Chapter V	146
V.1. Introduction.....	147
V.2. Materials and Methods	148
V.3. Results	149
Basal layer of <i>Anglaspis</i>	149
Middle layer of <i>Anglaspis</i>	153
Odontodes of <i>Anglaspis</i>	157
Interaction between aspidin and odontodes in <i>Anglaspis</i>	159
Histology of another pteraspidomorph heterostracan	160
V.4. Discussion.....	162
Characterization of <i>Anglaspis</i> and other pteraspidomorphs' mineralized skeleton	162
Canal networks: looking for the vascular network	164
Developmental hypotheses of <i>Anglaspis</i> and other pteraspidomorphs' dermal skeleton	166
V.5. Conclusion.....	170
Conclusion on the objectives of Chapter V.....	171
General conclusions and perspectives	173
Experience feedback.....	181
References.....	189
General appendix	211

RESUME ETENDU

RESUME ETENDU

Le squelette minéralisé est une structure clé des vertébrés. À l'instar de nombreux autres groupes de métazoaires, celui-ci assure des fonctions essentielles (soutien, protection, alimentation et divers rôles physiologiques). Depuis son origine, ce squelette minéralisé s'est diversifié à plusieurs échelles. Aujourd'hui, il comporte une variété d'éléments, constitués de divers tissus, dont la composition et la structure peuvent varier. Pour mieux appréhender la répartition actuelle des propriétés histomorphologiques du squelette minéralisé des vertébrés, nous pouvons nous interroger sur les origines et l'histoire évolutive de cette diversité.

L'étude de la distribution des tissus minéralisés chez les vertébrés actuels et passés a permis de mieux comprendre leurs origines phylogénétiques et temporelles. Certains des tissus minéralisés parmi les plus anciennement connus ont été découverts chez les ptéraspidomorphes (stem-gnathostomes ; Ordovicien-Dévonien). Leur squelette dermique minéralisé prenant la forme de deux plaques céphalothoraciques, accompagnées de nombreuses écailles recouvrant le reste de leur corps. Ces structures se composaient de deux couches osseuses, une compacte et une spongieuse, surmontées d'odontodes (structures semblables à des dents) faites de dentine, parfois associées à de l'émailloïde (tissu semblable à l'émail). Bien que ces éléments fournissent des indications sur les origines et l'évolution des tissus chez les vertébrés, les mécanismes précis de leur diversification restent assez énigmatiques.

L'objectif de cette thèse est ainsi d'explorer, de manière intégrée, les mécanismes développementaux ayant pu favoriser l'émergence des tissus durant l'évolution du squelette minéralisé des vertébrés.

Une première partie a été consacrée à la révision des concepts liés aux tissus dentaires, à leur méthode d'identification, ainsi qu'à leur distribution actuelle et passée. Cela a contribué à clarifier la nomenclature et la validité des identifications antérieures des tissus dentaires, tout en proposant un cadre phylogénétique pour discuter de leurs étapes évolutives clés.

RESUME ETENDU

Une deuxième partie s'est portée sur la construction d'un modèle histogénétique actualiste de la dentine, l'émailloïde et l'émail. Celui-ci a permis d'étudier les mécanismes de transition entre les tissus en explorant *in silico* l'impact de paramètres développementaux sur la formation de tissus dentaires. Diverses modifications développementales menant à la transition entre émailloïde et émail ont ainsi pu être mis en évidence, suggérant que la mise en place de nouveaux tissus ne nécessite pas nécessairement l'acquisition de nouveaux gènes.

Une troisième partie, ajoutant une dimension morphogénétique au précédent modèle histogénétique, s'est intéressée à la formation des structures dentaires composées de dentine, d'émailloïde et d'émail. L'exploration *in silico* de l'impact de la courbure initiale de l'épithélium et du timing spatio-temporel d'activation des cellules a permis de montrer que la modification de ce type de paramètres intercellulaires influençait la présence et la répartition des tissus au sein d'une structure.

Une quatrième partie révisant la paléohistologie d'*Astraspis* avait pour but de reconstruire l'ontogénie de l'une des premières structures « dentaires ». En plus de renforcer l'identification du tissu recouvrant en tant qu'émailloïde, cela a permis de comparer les mécanismes de développement de ces premières structures avec ceux des actuelles. Une différence majeure étant que les odontodes des stem-gnathostomes semblaient se former suite à une activation synchrone, et non décalée, des cellules mésenchymateuses.

Une cinquième partie se penchait sur l'histomorphogénèse des structures en « empreinte digitale » et « nid-d'abeilles » présentes chez *Anglaspis*. Cela a permis de discuter des mécanismes de structuration, tels que les mécanismes de réaction-diffusion, qui ont pu influencer la formation du squelette des premiers vertébrés.

Mots-clés : paléontologie, vertébrés, ptéraspidormorphes, squelette minéralisé, tissus dentaires et osseux, développement, histogénèse, morphogénèse, histologie, microanatomie, modélisation.

EXTENDED ABSTRACT

EXTENDED ABSTRACT

The mineralized skeleton is a key structure in vertebrates. Like many other metazoan groups, it serves essential functions, including support, protection, feeding, and various physiological roles. Since its origin, this mineralized skeleton has diversified at multiple scales. Today, it comprises a variety of elements made up of different tissues, with varying composition and structure. To better understand the current distribution of histomorphological properties in the mineralized skeleton of vertebrates, we can examine the origins and evolutionary history of this diversity.

The study of the distribution of mineralized tissues in present and past vertebrates has enhanced our understanding of their phylogenetic and temporal origins. One of the oldest known mineralized tissues have been notably found in pteraspidomorphs (stem-gnathostomes; Ordovician-Devonian). Their mineralized dermal skeleton takes the form of two cephalothoracic plates, accompanied by numerous scales covering the rest of their bodies. These structures generally consisted of two bone layers, a compact one and a spongy one, topped with odontodes (tooth-like structures) made of dentine, sometimes associated with enameloid (a tissue similar to enamel). Although these elements provide insights into the origins and evolution of tissues in vertebrates, the precise mechanisms of their diversification remain quite enigmatic.

The objective of this thesis is to explore, in an integrated manner, the developmental mechanisms that may have favored the emergence of tissues during the evolution of the mineralized skeleton in vertebrates.

The first part was dedicated to the revision of concepts related to dental tissues, their method of identification, as well as their current and past distribution. This contributed to clarifying the nomenclature and validity of previous identifications of dental tissues, while also proposing a phylogenetic framework to discuss their key evolutionary stages.

The second part focused on constructing a current histogenetic model of dentin, enameloid, and enamel. This allowed for the study of transition mechanisms between

EXTENDED ABSTRACT

tissues by exploring the *in silico* impact of developmental parameters on the formation of dental tissues. Various developmental modifications leading to the transition between enameloid and enamel were thus identified, suggesting that the establishment of new tissues does not necessarily require the acquisition of new genes.

The third part, adding a morphogenetic dimension to the previous histogenetic model, focused on the formation of dental structures composed of dentin, enameloid, and enamel. The *in silico* exploration of the impact of the epithelium's initial curvature and the spatiotemporal activation timing of cells revealed that modifying such intercellular parameters influenced the presence and distribution of tissues within a structure.

The fourth part, revising the paleohistology of *Astraspis*, aimed to reconstruct the ontogeny of one of the earliest 'dental' structures. In addition to strengthening the identification of the covering tissue as enameloid, it allowed for a comparison of the developmental mechanisms of these early structures with those of contemporary ones. A major difference was that the odontodes of stem-gnathostomes appeared to form through synchronous, rather than delayed, activation of mesenchymal cells.

The fifth part delved into the histomorphogenesis of the 'fingerprint' and 'honeycomb' structures found in *Anglaspis*. This facilitated a discussion of structuring mechanisms, such as reaction-diffusion processes, that could have influenced the formation of the skeletons in early vertebrates.

Keywords: *paleontology, vertebrates, pteraspidormorphs, mineralized skeleton, dental and bone tissues, development, histogenesis, morphogenesis, histology, microanatomy, modeling.*

GENERAL INTRODUCTION

GENERAL INTRODUCTION

The mineralized skeleton is a key structure that is present in several groups of contemporary metazoans. It plays a crucial role in supporting and protecting soft tissues, as well as in animal physiology and feeding abilities. The mineralized skeleton evolved independently several times during metazoan evolution, leading to the acquisition of different compositions and structures (Fig. 1) (Murdock & Donoghue, 2011). They are based on silica, calcium carbonates, or calcium phosphates like the vertebrate mineralized skeleton mainly composed of apatite (Murdock & Donoghue, 2011; Hall, 2015; Berkovitz & Shellis, 2016).

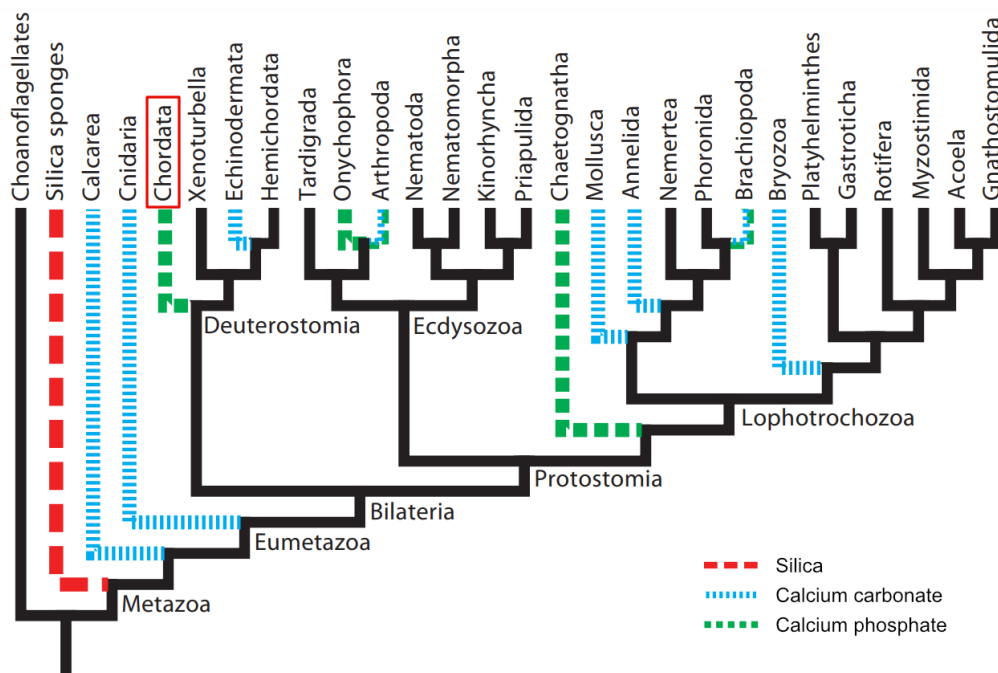


FIGURE 1. Distribution of biomimneralization across a phylum level animal tree. Terminal branches are coded to reflect known fossil or extant representatives with known mineralized tissues. The red box indicates the position of the vertebrates. Modified from Murdock & Donoghue (2011).

This mineralized skeleton is widespread in extant vertebrates and presents a diversity of elements, composed of a diversity of tissues, themselves presenting a diversity of histological and structural properties (Fig. 2 Context, Fig. 3) (Hall, 2015;

Berkovitz & Shellis, 2016). For example, the main tissues of the vertebrate mineralized skeleton are bone, dentin, enamel and intermediate tissues like enameloid, but these tissues may vary depending on the orientation of fibers, vascularity, cellularity, compactness, mineralization rate, etc (Hall, 2015; Berkovitz & Shellis, 2016; de Buffrénil *et al.*, 2021). These different properties impact the sensory and mechanical capacities of tissues (Sire & Kawasaki, 2012; Hall, 2015; de Buffrénil *et al.*, 2021) and thus have probably influenced vertebrate evolution.

From an evolutionary biology perspective, the observation of the existing diversity raises a general question (see Fig. 2: Problematics):

What are the origins and the evolutionary history of histological and structural diversity of the extant vertebrate mineralized skeleton?

This broad research question can be divided into three subproblematics:

- 1) **Where:** In which taxa did tissues emerge?
- 2) **When:** During which geological periods did tissues emerge?
- 3) **How:** Through which genetic acquisitions and developmental mechanisms did tissues emerge?

In order to improve our understanding of these evolutionary aspects, we are led to consider the paleontological record of the vertebrate mineralized skeleton in addition to the current one. The unique combinations of characters that can be found in certain fossils at key phylogenetic positions can enable us to better characterize the ancestral state of tissues ('Where?') and the associated dating ('When?'), thus reinforcing evolutionary hypotheses based on extant animals (see Fig. 2 Objectives). In this way, the early remains of vertebrate mineralized tissues have been well studied since the 19th century, as exemplified by Walcott's (1892) description of the oldest

vertebrate mineralized tissues of that time. Today, even though some aspects remain enigmatic, such as the origin(s) of cellular bone or endochondral ossification, the increasing number of studies has enabled us to build a detailed theoretical framework based on extant and extinct taxa (Fig. 4) (Smith & Hall, 1990; Donoghue & Sansom, 2002; Donoghue, Sansom & Downs, 2006; Sire, Donoghue & Vickaryous, 2009; Vickaryous & Sire, 2009; Sire & Kawasaki, 2012; Mondéjar-Fernández & Janvier, 2021). Regarding the question of 'How?' vertebrate mineralized tissues emerged, although the genetic context of extant and extinct vertebrates has been well documented (Sire & Kawasaki, 2012; Berkovitz & Shellis, 2016; Braasch *et al.*, 2016; Kawasaki *et al.*, 2021), the developmental mechanisms leading to the diversification of tissues are still poorly understood (Fig. 2 Objectives).

This issue involving the current and past distribution of structures, their relationships of ancestry, as well as their diversification mechanisms, leads us to adopt an approach of evolutionary and developmental paleobiology, or 'paleo-evo-devo'. The integration of these three disciplines, namely paleontology, evolutionary biology, and developmental biology (or, in earlier times, embryology), has been a gradual process since the late 18th century (see the following reviews for more details: Hall, 2002; Thewissen, Cooper & Behringer, 2012; Enault, 2015). The evolutionary interpretation of the fossil record, which initially lacked an evolutionary framework (e.g. Cuvier, 1769-1832), ruly gained ground with the works of Lamarck (1744-1829) and the publication of '*On the Origin of Species*' by Darwin (1859). One seeks, through the study of past life, to understand the evolution of organisms and their structures on a geological timescale. Similarly, after being established in the late 19th century, developmental biology was later integrated with evolutionary biology, forming 'evo-devo,' in order to understand the mechanisms of organism and structure formation and diversification. Given the shared objectives of these different disciplines in understanding the origins of diversity and the mechanisms of change over time, it was natural for the 'paleo-evo-devo' approach to emerge. It combines the formulation of

GENERAL INTRODUCTION

diversification hypotheses based on developmental and evolutionary biology with the assessment of these hypotheses in light of the fossil record, which provides anchoring points, such as novel character associations.

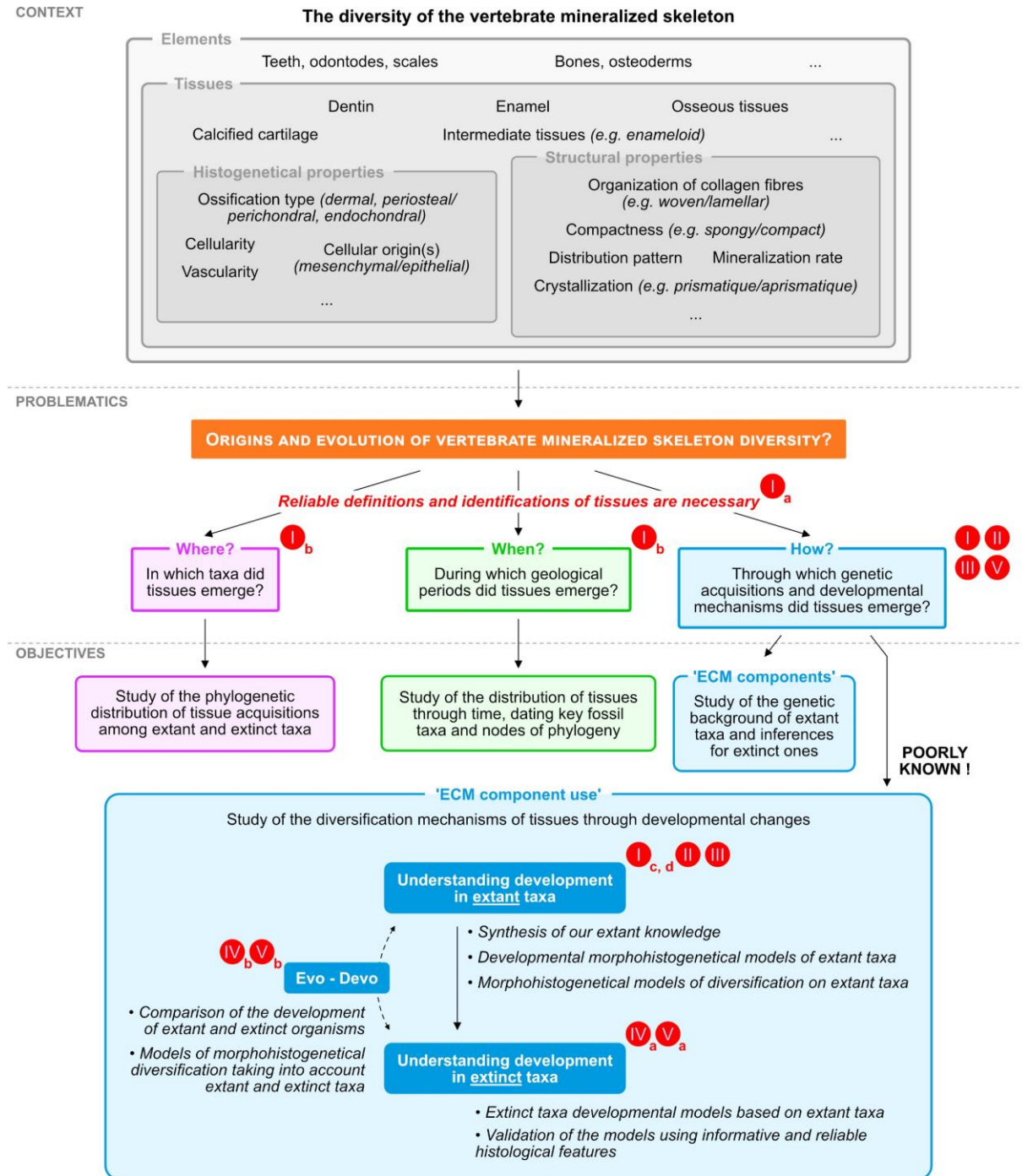


FIGURE 2. Flowchart summarizing the context, issues, and objectives of the thesis. Red circles refer to the contribution of the different chapters of the thesis.

GENERAL INTRODUCTION

The study of extant vertebrates is crucial to characterize tissues, to better understand their histomorphological developmental mechanisms, and finally to determine their diversification processes. However, to treat these questions (Fig. 2 Problematics), we also have to consider extinct vertebrates, especially stem-gnathostomes. The study of the composition and structure of the stem-gnathostome skeletons highlighted an old origin and a 'complex' early evolution of mineralized tissues (Fig. 4). Thus, the study of these early skeletons may enable us to better understand the current distribution of mineralized tissues. Among these early vertebrates, pteraspidomorphs stand out with an ancient fossil record, a skeleton composed of a diversity of mineralized tissues, and an early divergence from the other groups of vertebrates (Fig. 4).

Pteraspidomorphs are jawless stem-gnathostomes which have lived from the early-middle Ordovician to late Devonian (Fig. 4). Even if their phylogenetic relationships are not always well resolved (e.g. Keating, Marquart & Donoghue, 2015; Randle, Keating & Sansom, 2022), the distinction of three clades Arandaspida, Astraspida, and Heterostraci is generally accepted. They are the oldest known vertebrates to exhibit a fully developed mineralized skeleton throughout their entire body. It was composed of two cephalothoracic plates, tesserae, and numerous smaller scales, hence the name 'ostracoderms' (Fig. 5). These elements corresponded to a dermal skeleton, meaning that it directly formed inside the skin without differentiation of transitory cartilage, and their internal skeleton was presumably cartilaginous (Sire & Kawasaki, 2012). The mineralized skeleton of pteraspidomorphs is also recognized for harboring some of the most ancient remnants of bony and 'dental' tissues. Since at least the middle Ordovician, pteraspidomorphs exhibited a dermal skeleton constituted of two layers of anosteocytic osseous tissue, a compact basis and a spongy middle layer (known as aspidin), covered with a layer of odontodes (tooth-like structures) (Fig. 5D) (Sansom *et al.*, 1997; Sire *et al.*, 2009; Keating *et al.*, 2015, 2018; Lemierre & Germain, 2019). The odontodes of pteraspidomorphs are composed

GENERAL INTRODUCTION

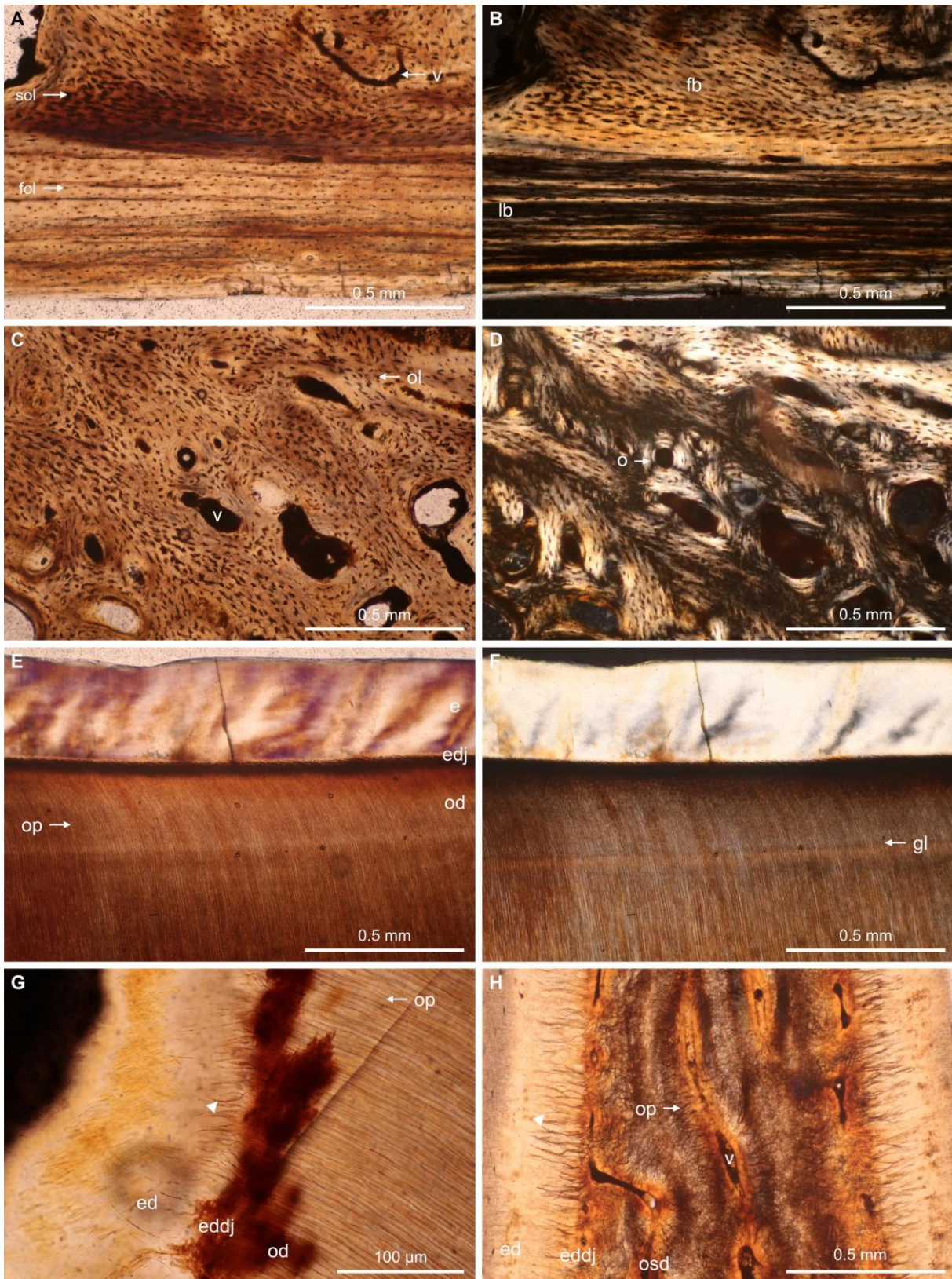


FIGURE 3. Examples of vertebrate mineralized tissue diversity. A, lamellar and fibrolamellar osseous tissue of a turtle osteoderm in natural light, and B, cross-polarized light. C, spongy osseous tissue of a turtle osteoderm in natural light, and D, cross-polarized light. E,

GENERAL INTRODUCTION

orthodentine and enamel of a mammalian tooth in natural light, and F, cross-polarized light. G, enameloid and orthodentine of a teleost tooth in natural light. H, enameloid and osteodentine of a selachian tooth in natural light. Note that well-visible odontoblastic projections are present in enameloid contrary to enamel (arrowhead). I collected these specimens in the Miocene of 'Faluns de Touraine', close to Angers in France. I learned to realize histological slices with these same specimens, thanks to the help of Vincent Rommeveaux (lithopreparator, CR2P). e, enamel. ed, enameloid. eddj, enameloid-dentin junction. edj, enamel-dentin junction. fb, fibrolamellar bone. fol, flat osteocyte lacunae. gl, growth line. lb, lamellar bone. o, osteon. od, orthodentine. ol, osteocyte lacunae. op, odontoblastic projection. osd, osteodentine. sol, starry osteocyte lacunae. v, vascularity.

by a pulpar tissue currently interpreted as dentin and some taxa also present a vitreous capping tissue identified as enameloid (Donoghue & Sansom, 2002; Sansom, Donoghue & Albanesi, 2005; Sire *et al.*, 2009; Lemierre & Germain, 2019; Mondéjar-Fernández & Janvier, 2021), although this identification remains questionable. In addition to being the oldest known vertebrates with a skeleton composed of bone, dentin, and enameloid, a diversity of compositions and structures have been observed in the mineralized skeleton of pteraspidomorphs (Fig. 6).

We can note that phosphatic fragments of an enigmatic taxon, resembling that of pteraspidomorph dermal skeleton, were found in the late Cambrian. This taxon was named *Anatolepis* and identified as a heterostracan (pteraspidomorph, vertebrate) due to its histological properties, then becoming the oldest pteraspidomorph (Repetski, 1978; Smith, Sansom & Cochrane, 2001). However, its attribution to pteraspidomorphs, and even to vertebrates, has been strongly questioned. In addition to the lack of data about *Anatolepis*, its remains also resemble that of arthropods (Smith *et al.*, 2001; Janvier, 2015). As some authors concluded that the attribution of *Anatolepis* is uncertain and requires more data, such as articulated specimens, we will not consider it in this manuscript. Similarly, since conodonts are considered as vertebrates, the phosphatic

GENERAL INTRODUCTION

mineralized tissues found in their oral elements correspond to the oldest remains of vertebrate mineralized tissues (Donoghue & Sansom, 2002). However, their enamel-like tissue is now assumed to be non-homologous to enamel, and the homology between their basal tissue and dentin is not confirmed (Murdock *et al.*, 2013; Donoghue & Keating, 2014). It is probable that vertebrates share common cellular mechanisms of mineralization, but that conodont tissues evolved independently of bone, dentin, enameloid and enamel.

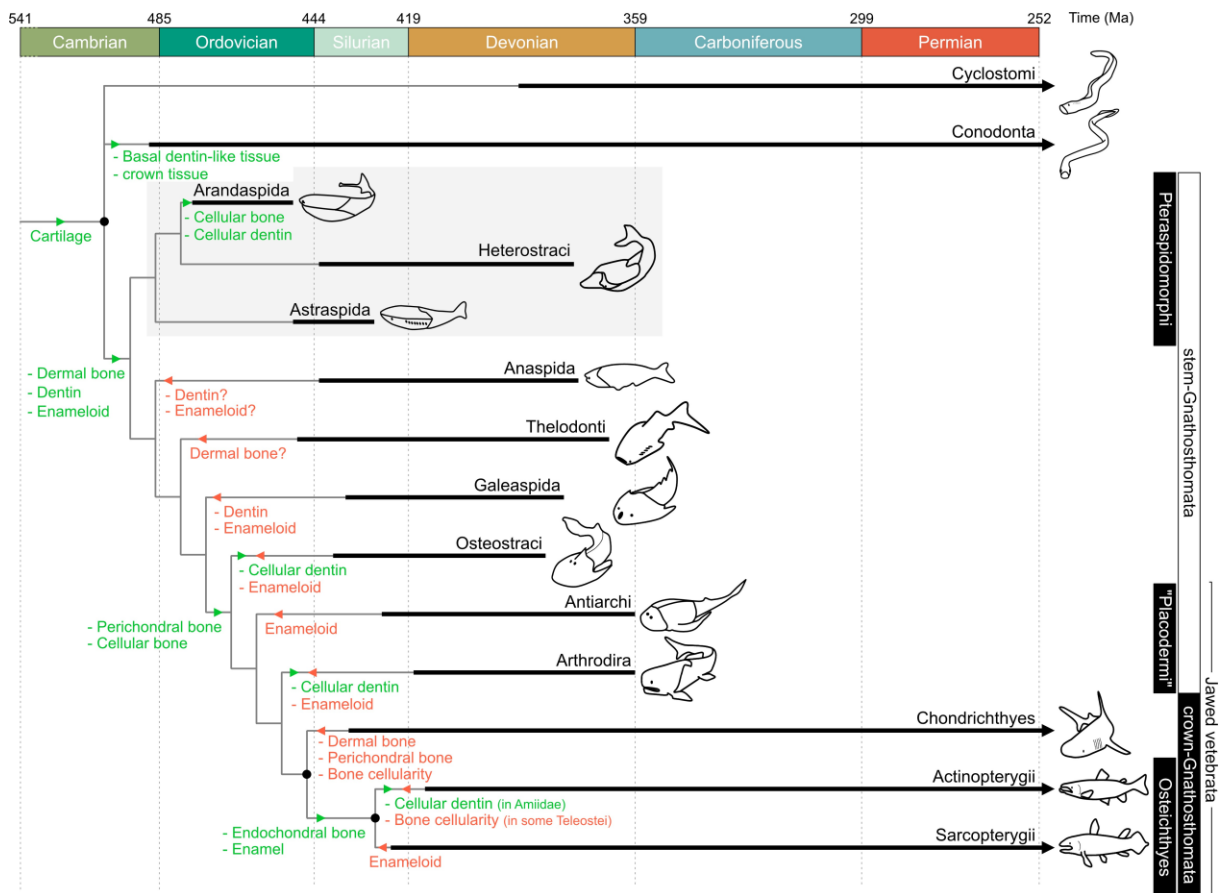


FIGURE 4. Vertebrate phylogeny, their fossil record distribution through time and the early evolution of the vertebrate mineralized skeleton. Note that the acquisition of mineralized cartilage is not mentioned, but is also a mineralized tissue that is present in most vertebrates. Pteraspidomorphi appeared as a key taxon to inform about the early evolution of bone, dentin and enameloid. Thick branches correspond to the fossil record, thin branches to the phylogeny (the length of branches does not reflect ages), dotted lines correspond to breaks in the timescale, and points to estimated divergence times. Green triangles correspond to the

GENERAL INTRODUCTION

acquisition of characters, and red triangles to the loss of characters. Phylogeny, fossil record distribution and characters are from Moss (1964), Sire, Donoghue & Vickaryous (2009), Murdock *et al.* (2013), Donoghue & Keating (2014), Hirasawa, Oisi & Kuratani (2016), Keating *et al.* (2018), Davesne *et al.* (2019), Fossilworks (<http://fossilworks.org/>), and estimated divergence times from Yu *et al.* (2023).

In this context, this PhD thesis aims at studying the origins and evolution of the vertebrate mineralized skeleton, with a focus on understanding how the diversity of vertebrate mineralized tissues emerged and using the development of extant and extinct taxa to probe the mechanisms of diversification. Since we lack direct access to the development of extinct animals, we will use extant mechanisms to infer extinct ones, building histomorphological models. Paleohistology is the science that studies the structure and composition of fossilized tissues, and combined with microanatomical descriptions, it enables us to have indirect access to tissue development (Francillon-Vieillot *et al.*, 1990; de Buffrénil *et al.*, 2021). Therefore, the accuracy of the inferred developmental mechanisms will be tested using the histomorphological properties observed in fossils.

After this **general introduction**, this doctoral thesis is structured into five chapters designed to contribute to our understanding of the origin and evolution of the vertebrate mineralized skeleton, particularly its developmental mechanisms of diversification. The subject of each chapter was chosen with the idea of exploring various topics, notably around histomorphogenesis, at different scales, from the tissue to the dermal plate, and considering both extant and extinct species. The contribution of each chapter is placed in the flowchart summarizing the context, issues, and objectives of the thesis (Fig. 2).

The **Chapter I** reviews some issues linked to bad practices in defining and identifying tissues in histology and paleohistology, taking the example of the dental tissues and more particularly the enigmatic enameloid. Based on new dental tissue

concepts, I review the phylogenetic distribution of these tissues among vertebrates, as well as the general developmental mechanisms of enameloid and enamel.

The **Chapter II** explores the developmental changes that could lead to an enameloid to enamel transition, and therefore, to the emergence of a new tissue. The exploration will be based on a computer modeling approach, whose advantages and disadvantages will be discussed.

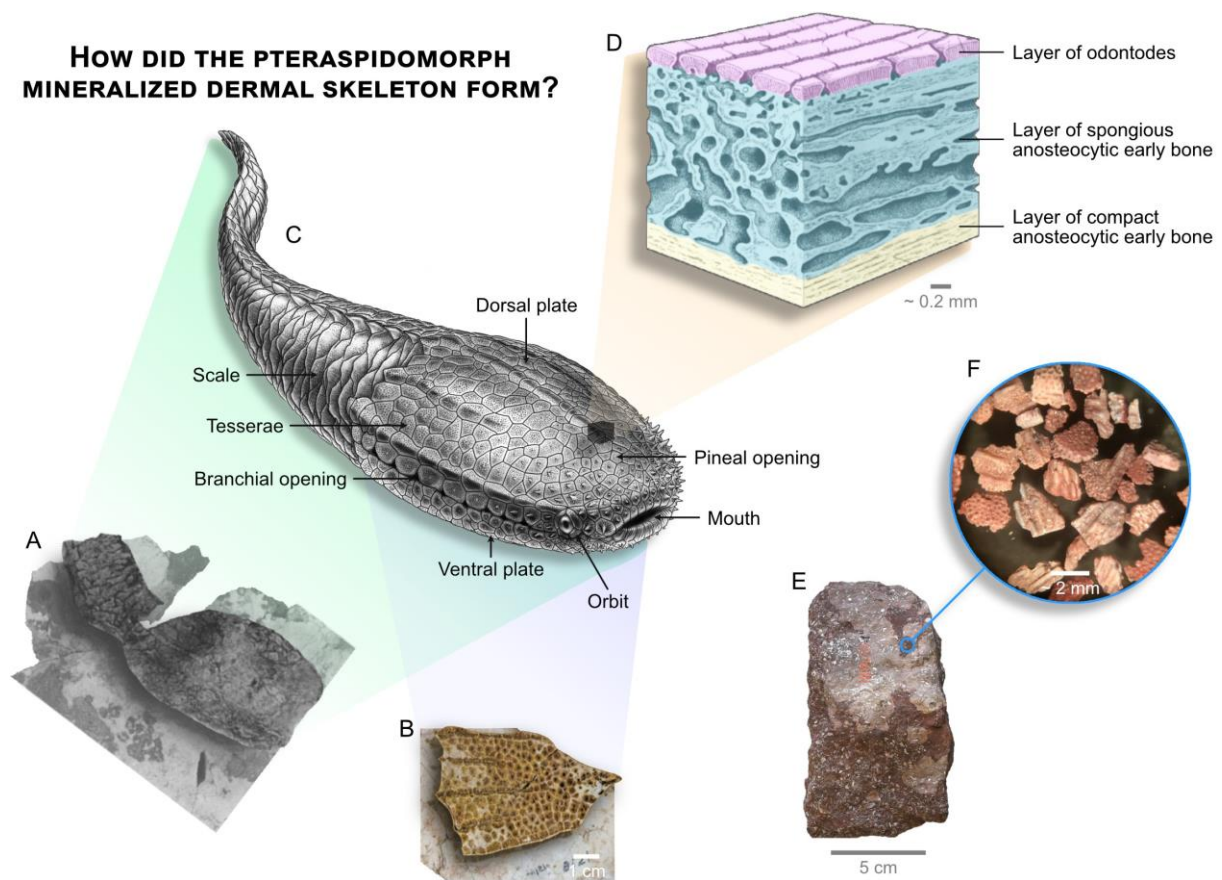


FIGURE 5. Anatomy of pteraspidomorphs. A-B, fossils of the pteraspidomorph *Astraspis* (A, Sansom *et al.*, 1997 ; B, USNM V 8121). C, reconstruction of *Astraspis* carried out for this thesis (© Lazare ELBAZ). D, general composition and structure of pteraspidomorph dermal skeleton (modified from Moy-Thomas, 1971). E-F, most of the pteraspidomorph remains correspond to fragments (an example of the Ordovician Harding sandstone, Colorado) (F, © ThePhysicist). Scales are unavailable for A and F.

The **Chapter III** briefly illustrates the possibility of extrapolating the histogenetic model from Chapter II to a histomorphogenetic model enabling the reconstruction of the formation of an extant tooth. At the same time, it tests the impact of new variables, this time intercellular, on the formation and distribution of dental tissues. As a case study, this Chapter focuses on the intriguing *Lepisosteus* tooth (Actinopterygian), composed of dentin, enameloid, and enamel.

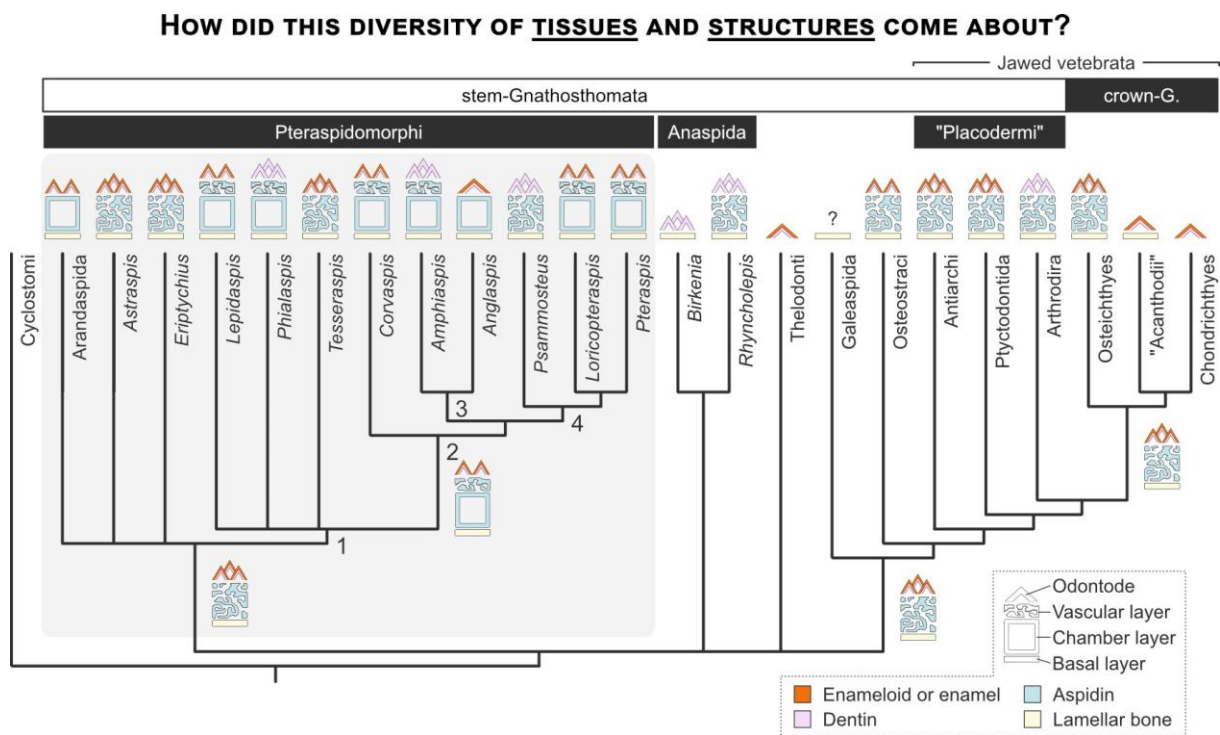


FIGURE 6. Diversity of compositions and structures of the dermal mineralized skeleton among vertebrates, and especially among pteraspido-morphs (conodonts are not represented). Note that we can distinguish two kinds of layers in the aspidin: a more compact one probably containing a network of vascular canals and a second one composed of large chambers. The 3D structure of the layer of chambers is still not well known, but will be studied in Chapter V. This figure also highlights that the phylogeny of pteraspido-morphs and other early vertebrates is debated. 1, heterostracans; 2, 'higher heterostracans'; 3, pteraspido-forms; 4, cyathaspido-forms. Modified after Keating, Marquart & Donoghue (2015), Mondéjar Fernández & Janvier (2021).

GENERAL INTRODUCTION

The **Chapter IV** extends this histomorphogenetic approach to the fossil record, proposing a new method to identify tissues using a modeling-based approach and to reconstruct their development in a paleontological context. The key and iconic fossil taxon, *Astraspis*, will be used as a case study.

After having focused on dental tissues in the previous chapters, **Chapter V** delves into the formation of the entire dermal plate, exploring the developmental sequence leading to the formation of various tissues and the patterning laws (e.g. Turing patterns) that could constrain vertebrate skeleton morphogenesis.

Finally, I **conclude** on the contributions of this thesis to our understanding of the origins and evolution of the vertebrate mineralized skeleton diversity and I share my **experience feedback** about conducting this exploratory research project.

CHAPTER I

***PALEO-EVO-DEVO IMPLICATIONS OF A REVISED
CONCEPTUALIZATION OF ENAMELOIDS AND ENAMELS***

Objectives Chapter I

Reliable definitions and identification methods of tissues are necessary to study the origins and evolution of the vertebrate mineralized skeleton (Fig. 2-Ia). However, these aspects can be still unclear for numerous tissues, especially in a paleontological context. Using the most abundant dental hypermineralized tissues (enameloid and enamel) as an example, the first chapter aims at highlighting the definition and identification issues that we can face in histology and paleohistology. Based on the newly proposed definitions and identification criteria, this chapter will also synthesize and interpret the current state of knowledge concerning the phylogenetic distribution of enameloid(s) and enamel(s) (Fig. 2-Ib), the enigmatic development of enameloid (Fig. 2-Ic) and the potential mechanisms of transition between dentin, enameloid and enamel (Fig. 2-Id).

This project I is close to the submission in *Biological Reviews*.

I.1. Introduction

The study of the origin and modification of the vertebrate mineralized skeleton is crucial to understand vertebrate evolution. Due to its involvement in protection, support, feeding capacities and physiology, the mineralized skeleton has undoubtedly greatly influenced the vertebrate diversification (Sire & Kawasaki, 2012; Hall, 2015; de Buffrénil *et al.*, 2021). In addition to the presence of mineralized tissue like bone and dentin, hypermineralized capping tissues emerged several times during vertebrate evolution. We notably recognize the crown tissue of conodonts (Donoghue, 1998; Murdock *et al.*, 2013; Zhuravlev, 2017), pleromin of chimaeroid (Ørvig, 1976; Didier, Stahl & Zangerl, 1994; Iijima & Ishiyama, 2020), petrodentine of dipnoans (Ishiyama & Teraki, 1990; Kemp, 2003), and more widely distributed, the enamel and enameloid (Berkovitz & Shellis, 2016). Besides to their extensive distribution, the homology of various enamels and enameloids has been the subject of extensive debate, making the reconstruction of their evolution challenging. The multiplication of developmental, genetic and paleontological studies has enabled the emergence of several phylogenetic trees and evolutionary scenarios proposing various hypotheses of homology between enamels and enameloids (e.g. Sire *et al.*, 2009; Qu *et al.*, 2015; Berkovitz & Shellis, 2016; Kawasaki *et al.*, 2021, 2022; Delgado *et al.*, 2023). However, over time and contribution accumulation, the terminology and definitions of these hypermineralized tissues have varied, especially concerning enameloids. As a result, there is a lack of uniformity in the definitions referring to enameloid or enamel, as well as in their usage. This questions the validity of the identification and phylogenetic distribution of these tissues, especially in extinct taxa, as well as the proposed evolutionary scenarios that result from them. Moreover, the development of enameloids is still enigmatic compared to that of enamel, hitherto hampering the formulation of developmental hypotheses for the inferred transitions between these tissues.

Therefore, after synthesizing current definitions and identification criteria for enameloid and enamel, this review aims at discussing the issues introduced above and

redefining the classification and terminology of hypermineralized tooth tissues. The focus is on enameloids, but discussions will be extended to enamels. These new enameloids and enamel concepts lead us to propose a more reliable synthesis of their phylogenetic distribution and ancestral states. Moreover, in addition to enabling a discussion on tissue homology, the revised phylogenetic distribution sheds light on our current knowledge gaps and the diversity of enameloid-enamel transitions that may have occurred during vertebrate evolution. Finally, a synthesis work on enameloid formation allows us to discuss more specifically the transition mechanisms between enameloid and enamel. This new approach of redefinition, synthesis on evolution and development, thus opens the door to robust evo-devo discussions and should be considered in the light of previous review works (Vickaryous & Sire, 2009; Sire & Kawasaki, 2012; Berkovitz & Shellis, 2016; Cuny, Guinot & Enault, 2018).

I.2. Issues about enameloid definitions and identifications: an outlook for the future

State of the art

Definitions

Dentin and its derivatives (e.g. 'orthodentine', 'mesodentine', 'semidentine') are defined as mineralized tissues of exclusively mesenchymal origin, whose matrix (predentine) is produced by odontoblasts and mostly composed of collagen (Sire *et al.*, 2009; Berkovitz & Shellis, 2016). Dentin can be cellular or acellular, and can present dentinal tubules or not (Sire *et al.*, 2009). Enamel and its derivatives (e.g., 'true enamel,' 'ganoin,' 'collar enamel,' 'ancestral enamel') are currently defined as hypermineralized tissues of exclusively epithelial origin, whose matrix is produced by ameloblasts or other types of inner dental epithelial cells, and composed of enamel matrix proteins (EMPs; e.g. AMEL, SCPP5, ENAM, AMBN) (Berkovitz & Shellis, 2016; Kawasaki *et al.*,

2021, 2021). Enamel hypermineralization is due to a maturation phase during which epithelial proteases (e.g. KLK4) degenerate and remove the matrix organic matter, allowing crystals to grow larger (Sire *et al.*, 2009; Berkovitz & Shellis, 2016).

Before the end of the nineteenth century, anatomists had already recognized mineralized dental tissues that intriguingly share features with both dentin and enamel (Williamson, 1849; Jaekel, 1891; Röse, 1898). Among these properties, the following have been recognized: a position above the dentin layer, the apparent implication of the odontoblasts in the matrix production, the potential presence of cytoplasmic processes and the initial presence of collagenous fibers that get lost during calcification (Kvam, 1960; Kerr, 1960). Depending on the context and authors, these intermediate tissues had been coined alternatively 'ganoïn layer' (Williamson, 1849), 'placoin layer' (Jaekel, 1891), 'vitrodentine' (Röse, 1898), 'mesodermal enamel' (Kvam, 1946) or 'durodentine' (Schmidt, 1957) reflecting alternative views on what features make them most similar or distinct from either enamel or dentin and hence implying competing evolutionary and developmental scenarios for their origin (see Baume (1980) for complementary information). In 1967, Poole (1967) and Ørvig (1967) coined the term 'enameloid' as a unifying name for these intermediate tissues. Poole (1967) defined enameloid as 'highly mineralized tissues, with affinities to dentin, which cover the teeth and scales of lower vertebrates'. Ørvig (1967) described it as a group of hard tissues (in hydroxyapatite or in fluorapatite) formed by hypermineralization after a mesodermal collagenous matrix reduction, situated between dermis and epithelium (on dentin) and frequently containing odontoblast processes. The involvement of epithelial cells in enameloid formation, and hence the dual origin (both mesenchymal and epithelial) of enameloid, was not clear at that time. A few years later, Shellis & Miles (1974) showed that epithelial cells were involved in the production of enameloid matrix proteins, which led Baume (1980) to redefine enameloid as referring to 'anyone of the varieties of highly mineralized enamel-like tissues of mesenchymal origin diffused by epithelial proteins which covers the top of teeth and scales of lower

vertebrates'. Later, these epithelial proteins have been identified as EMPs (Herold, Graver & Christner, 1980; Herold, Rosenbloom & Granovsky, 1989; Ishiyama, 1994; Kogaya, 1999; Satchell *et al.*, 2002; Sasagawa *et al.*, 2019; Kawasaki *et al.*, 2021). Collagen has been reported as well, for instance in a teleost (Huysseune *et al.*, 2008), or in a caudate larva (Assaraf-Weill *et al.*, 2014). The contribution of epithelial cells in the maturation of the tissue by degenerating and removing the organic matter has also been highlighted (Shellis & Berkovitz, 1976; Sasagawa, 1984, 1988, 2002; Davit-Beal, Allizard & Sire, 2007; Sasagawa *et al.*, 2019). This led to a revised definition of enameloid by Sire *et al.* (2009): 'enameloid is of mixed epithelial-mesenchymal origin, the collagenous matrix is mostly deposited by odontoblasts, but receives a matrix contribution (EMPs, such as amelogenin, and/or collagen) from the fully differentiated adjacent ameloblasts. Ameloblasts are also certainly involved in the degradation of the enameloid matrix by means of the synthesis of MMP20 (a collagenase)', which allows hypermineralization.

Before this overarching definition of enameloid was coined, implicitly assuming homology between the various enameloids, different names had been given to the enameloid-like tissues found in various clades: 'acrodin' has been proposed by Ørvig (1973) to refer to the hypermineralized tissue of fossil actinopterygians (see Ørvig (1978a)), later identified as enameloid with a specific matrix composition and mineralization mechanisms (see part I.4.), Shellis & Miles (1974) coined 'collar enameloid' to describe hypermineralized tissue found on the tooth shaft of teleosts resembling the enameloid of the teleost tooth tip, 'adameloid' by Sasagawa (2002) for enameloid of sharks (replacing the previous name 'coronoïn' (Bendix-Almgreen, 1983) based on fossil sharks) and the subcategory 'enameloid' included in enameloid by Kawasaki *et al.* (2021) to refer to what is not acrodin or collar enameloid.

Identifications

Practice of enameloid identification differs whether specimens are fossil or extant. When one has direct access to the development of a tissue, such as in most of the extant species, identifications are based on developmental data whereby the dual origin, the initial presence of matrix collagen and the epithelial hypermineralization may be evidenced directly (e.g. Sasagawa, 2002; Davit-Beal *et al.*, 2007; Sasagawa *et al.*, 2019; Kawasaki *et al.*, 2021). In addition, other features, such as matrix composition or microstructural details, can be used to identify some specific enameloid.

When direct, developmental evidence is not available, such as for fossils, one may use phylogeny, microstructure and other indirect evidence to infer the nature of hypermineralized tissues. In particular, the presence of tubules in a capping hypermineralized tissue, starting from the basal junction, has been used as the main indirect evidence of a dual mesenchymal and epithelial origin (e.g. Smith, Sansom & Smith, 1995; Friedman & Brazeau, 2010; Keating *et al.*, 2015; Lemierre & Germain, 2019).

Issues with current enameloid concepts

As the short state-of-art synthesis shows (see Fig. I-1A) the current set of definitions and identification criteria is problematic, for various reasons that we will now discuss.

Definition issues

In the preceding review, all authors used Aristotelian definitions: a given tissue *T* is part of a class *C* if it satisfies a given property *p*. Most of the time, the property defining a class is said to be ‘complex’ meaning that this property is the conjunction of

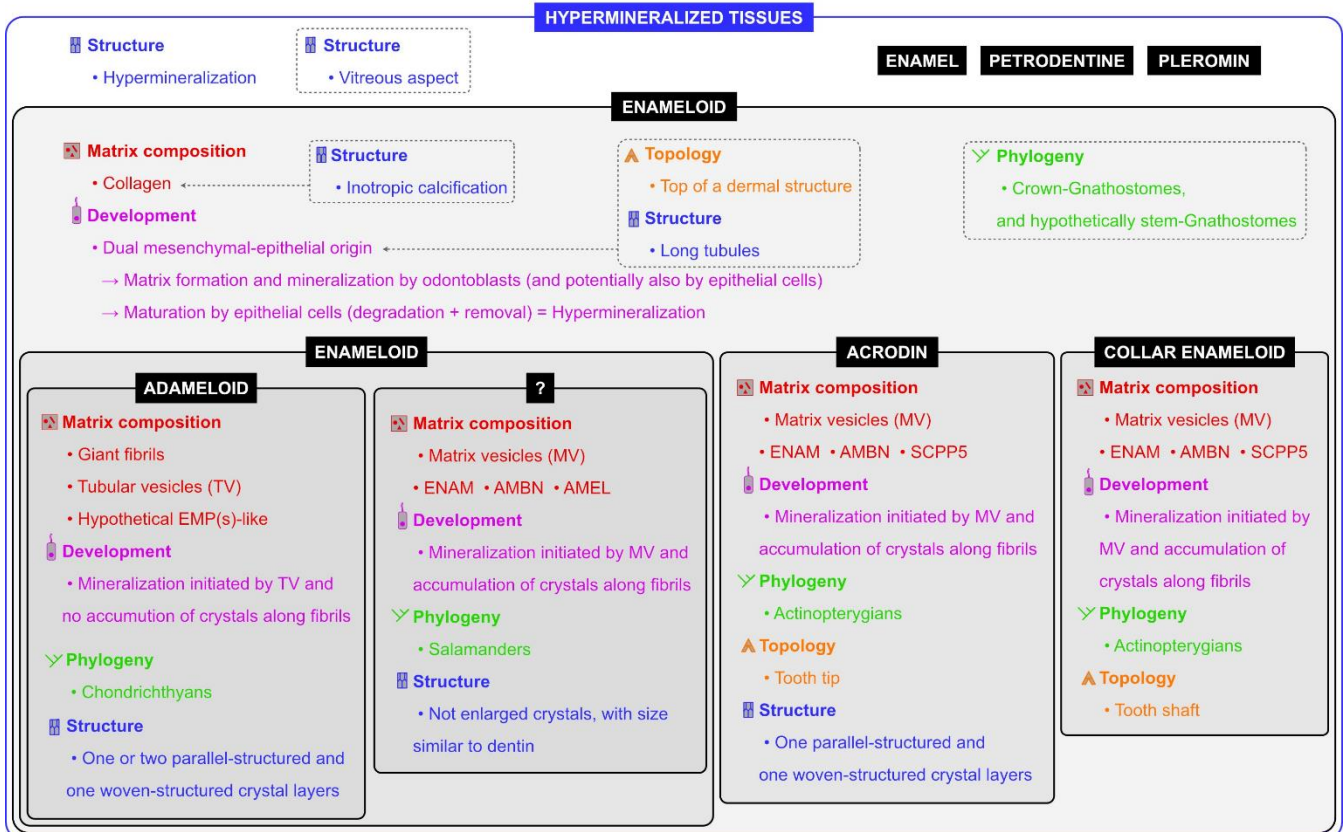
several elementary properties. For example, a tissue is said to belong to the class 'enameloid' if it is a hypermineralized tissue (*p1*), of mixed epithelial-mesenchymal origin (*p2*), and it incorporates a collagenous extracellular matrix (*p3*) (Fig. I-1A). This point is important for ensuring concepts consistency. However, depending on the authors, different sets of properties are used to define enameloid. For example, Sire *et al.* (2009) use the previously mentioned definition, composed of *p1-p3*, while other studies, e.g. Kawasaki & Amemiya (2014), Keating & Donoghue (2016), and O'Shea, Keating & Donoghue (2019), use only *p1* and *p2*. This lack of uniformity in definitions raises concerns about the equivalence of the resulting identifications. Similarly, when subcategories are defined, specific combinations of defining properties should be provided, which is for instance not the case for the 'enameloid' subcategory of Kawasaki *et al.* (2021).

Hierarchization issues

Classes describing units of life are hierarchies. Some properties of the class under scrutiny are inherited from its parent class, and ideally this should be made clear when defining subcategories and their hierarchy. In the case of enameloids, the hierarchy of subcategories has not been clearly defined, resulting in multiple subcategories with shared properties. For example, the subcategories 'enamel,' 'acrodin,' and 'collar enameloid' have some matrix components in common (Fig. I-1A). This also leads to a non-uniform usage of enameloid concepts. For example, Qu *et al.* (2015) discuss the acquisition of enameloid in actinopterygians and chondrichthyans using a subcategory name ('acrodin') in one case and the name of the overarching category ('enameloid,' rather than 'adameloid') in the other, not fully capturing the differences between these two enameloids. Finally, this also leads to the creation of 'catch-all' subcategories where tissues with distinct properties are grouped together, as in the already mentioned case of 'enameloid' in Kawasaki *et al.* (2021) (Fig. I-1A).

CHAPTER I – NEW ENAMELOID AND ENAMEL CONCEPTS

A - Interpretive synthesis of current concepts of enamelooids



B - Proposed concepts of enamelooids

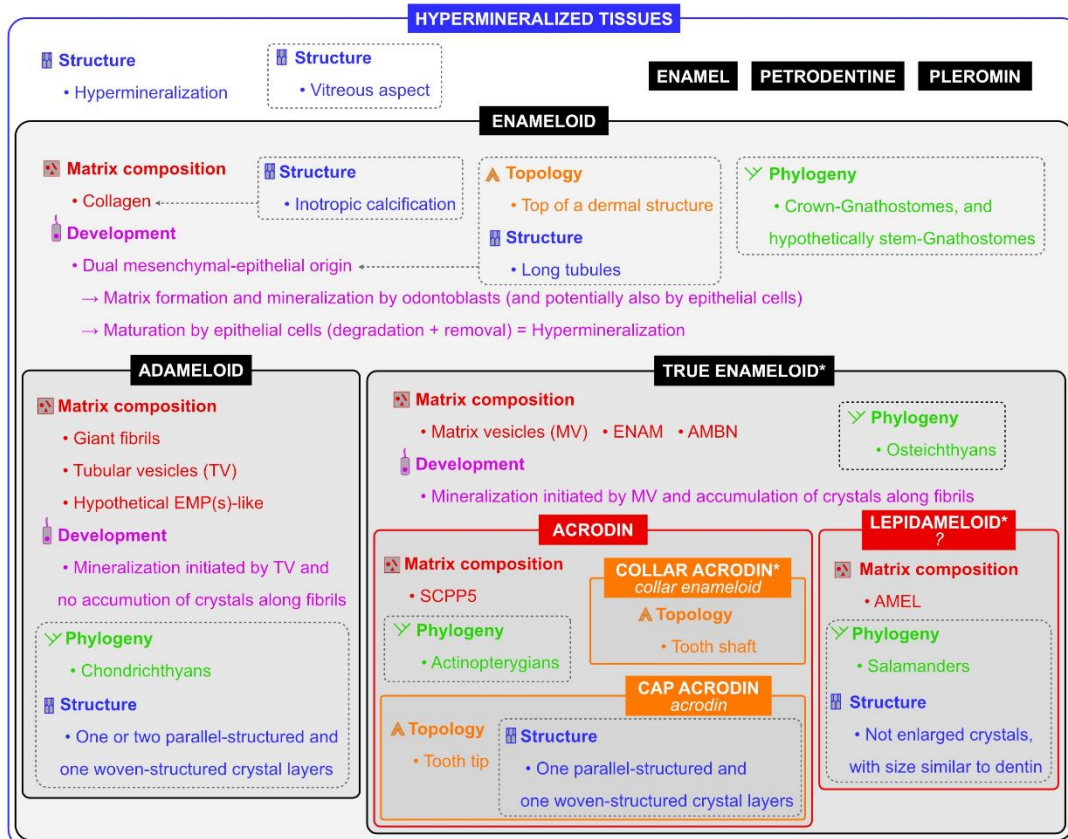


FIGURE I-1. Revision of enameloid concepts with a nested classification scheme, where each box corresponds to a concept. Defining and additional properties are listed within the boxes. The additional properties are separated from the defining properties by dashed boxes. Nested boxes inherit all the properties of their encompassing parent box. Additional properties are useful for inferring defining properties when the latter cannot be directly observed. Colors indicate different types of properties. The boxes are colored differently depending on the type of their respective defining properties, with black color indicating defining properties of mixed types. New terms introduced in this article have an asterisk (*). The terms in lowercase and italics below them are the traditional equivalents whose usage is discouraged here. For a comprehensive understanding of enameloid microstructures, refer to Berkovitz & Shellis (2016). We should also note that in the definition of 'adameloid' the presence, or absence, of EMP-like proteins in the matrix is not critical, as this aspect remains enigmatic (Berkovitz & Shellis, 2016). However, since epithelial cells have been observed to contribute to adameloid formation, it is likely that EMP-like proteins are involved in its maturation. The other vertebrate hypermineralized tissues (enamel, petrodentine and pleromin) are not detailed. The references used to construct this figure are detailed in parts I.3-4.

Nomenclatural issues

These hierarchical issues can also result in subcategories that lack clear and distinct names, as illustrated once more by the case of the 'enameloid' subcategory of 'enameloid' in Kawasaki *et al.* (2021) (Fig. I-1A).

Some names may also be misleading: let us consider for instance the term 'collar enameloid'. By including the term 'enameloid,' it implies that the subcategory would inherit only its attributes, with the distinctive 'collar' position being its sole unique feature, thus obscuring the additional developmental and phylogenetic properties of this subcategory (Fig. I-1A). This point raises an important and recurring question: should the name express the properties of the concept?

Identification issues: the use of additional properties

The defining properties of a given class are the properties that make identification of and assignment to this class absolutely sure. However, other properties may be used to hypothesize assignment to the class. In this case, a hypothesis is formulated regarding the relationship between defining and additional properties. If the latter are satisfied, it suggests that the former may as well be, allowing for a tentative assignment to the class. This practice is very common, especially in paleontology, where much (developmental) information may be missing. For example, *p2* (i.e. the mixed epithelial-mesenchymal origin) is hardly observable on any non-living specimen. Therefore, additional properties, such as the ‘presence of tubules in the hypermineralized tissue’ (*p5*), are frequently used to infer *p2* in order to identify an hypermineralized tissue as enameloid.

The ideal scenario for making such a deduction is when the extension of the additional property (*p5*) is encompassed within that of the defining property (*p2*). This means that, when the additional property (*p5*) is satisfied, the defining property (*p2*) is always satisfied. However, if this ideal scenario is not verified, the more cases where the additional property (*p5*) is present without the defining property (*p2*), the less suitable the use of this additional property becomes for assignment.

Concerning this example, it is known that before enamel formation, odontoblasts processes can penetrate the basal lamina and interpose themselves between the cells of the inner enamel epithelium forming ‘enamel spindles’ (Nanci, 2017), also called ‘enamel tubules’ (Poole, 1967). In some cases, e.g. in some mammals and reptiles, these tubules may pervade fully throughout the enamel (Williams, 1923; Ishiyama, 1984; Sasagawa & Ferguson, 1991; Stern, Song & Landis, 1992). Hence, the presence of long tubules in a hypermineralized tissue (*p5*) does not necessarily imply mesenchymal participation in the matrix production (partial *p2*), and is not restricted to enameloid. Therefore, *p5* is not a suitable additional property to assign a hypermineralized tissue to the class ‘enameloid’.

Finally, the diversity of enameloid concepts, the lack of a clear hierarchization between them, and the variety of properties used to characterize them (such as development, phylogenetic position, topology and microstructure), has blurred the true significance of some published identifications. As an example, the presence of collagen in the matrix is often disregarded when discussing fossil species (e.g. Kawasaki & Amemiya, 2014; Keating & Donoghue, 2016; O'Shea *et al.*, 2019), contrary to extant ones (e.g. Shellis & Miles, 1974; Davit-Beal *et al.*, 2007; Sasagawa *et al.*, 2019). It raises questions regarding the equivalency of the resulting identifications. This can be particularly problematic when inadvertent inferences about properties are made in taxa at key phylogenetic positions, especially when the identification of a given tissue as a subcategory of enameloid implies the presence of specific matrix proteins. For example, Schultze (2016) identified 'acrodin' in a potential stem-osteichthyan, *Ligulalepis toombsi*, without discussing the implications of his identification for the acquisition of SCPP5 in stem-osteichthyans.

Proposed solutions for the future

The issues mentioned above undermine the consistency of the terms used, and hence of the hypotheses of homology upon which any evolutionary scenario is based. This section aims at proposing solutions to standardize these various aspects.

Different types of properties

First of all, it is important to note that the properties used to define and identify morphological structures are highly diverse (see the review of Neumann & Neumann (2021)). We can notably distinguish (1) static properties that pertain to the phenotype of the studied object, without requiring observation at multiple stages of its development, (2) dynamic properties that involve the developmental time and

multiple observations along the ontogeny of the studied object (Webster & Zelditch, 2005), and (3) phylogenetic properties that are considered as shared by the members of a given taxon. Generally, static properties (as *p5*) have the advantage of being more easily observable, especially in a paleontological context. Conversely, dynamic properties, such as growth types and functional molecular aspects of development, may be trickier to assess (see *p2*). However, when both types of properties are available, dynamic ones are generally considered superior to static ones: they have demonstrated significant abilities to structure the observed diversity (Haeckel, 1866) and possess a causal meaning grounded in biological processes (Prondvai *et al.*, 2014; Bardin, Rouget & Cecca, 2017). Finally, phylogenetic properties have the advantage of reflecting the evolutionary history of taxa. However, their use may disconnect identifications from observable features when evolution modifies these properties, thus affecting the way we identify a structure. Indeed, apomorphies may not be good diagnostic traits. For example, gill arches are easily defined by associating developmental and phylogenetic properties but their huge morphological disparity in the tree of adult gnathostomes make static properties hardly usable.

In this review, we organize the enameloid properties into matrix composition, structural, topological, developmental and phylogenetical properties (Fig. I-1). The matrix composition, structure, and topology pertain to static properties, whereas development pertains to dynamic properties. We note that the 'enameloid' concept and, to a lesser extent, its subconcepts are strongly driven by the compositional and developmental properties (Fig. I-1).

Revised enameloid concepts

To overcome the definition, hierarchization and nomenclatural issues, we propose a revised, nested set of enameloid concepts that allows for a clear distinction of the defining and additional properties of enameloid and for an unambiguous

grouping of subconcepts into intermediate subcategories (Fig. I-1B). The subcategories 'acrodin' and 'collar enameloid' (Fig. I-1A) have been combined to account for their common properties (Fig. I-1B). Similarly, the new subcategory resulting from the merger of 'acrodin' and 'collar enameloid' has been grouped with the formerly unnamed sub-concept '?'. New terms are therefore introduced to represent these intermediate concepts: 'true enameloid', because it represents a well-documented subconcept of enameloid, and 'lepidameloid', referring to its presence in larval individuals (Fig. I-1B). Although the term 'acrodin' has been introduced historically to refer to the tooth tip (Ørvig, 1973), it has become clear that similar tissues (currently ambiguously coined 'collar enameloid') are found at the tooth collar. This has led some authors (e.g. Sasagawa *et al.*, 2009; Leuzinger *et al.*, 2020) to use the term 'cap acrocin' when referring specifically at the tissues found at the tooth tip. We propose to follow them and we further suggest using the term 'collar acrocin' to refer to 'collar enameloid', in order to better represent its properties. We can note that Ørvig (1978a) also proposed the terms 'verruciform acrocin' and 'tegmental acrocin', respectively corresponding to 'cap acrocin' and 'collar acrocin', but they are not currently in use. As enameloid concepts are primarily composed of matrix composition and developmental properties, we propose to base the definitions on these properties whenever possible. Therefore, the other properties, such as structure, phylogeny, and topology, are considered as additional properties and may be useful for identification purposes.

According to this hierarchy, the definitions of enameloids that we recommend are:

- Enameloid: a hypermineralized tissue with a dual mesenchymal and epithelial origin (matrix formation and mineralization by mesenchymal cells and potentially also by epithelial cells, and tissue maturation of epithelial origin), and with a collagenous matrix (Fig. I-1B). This definition is very similar to that of Sire *et al.*

(2009), but it is relaxed in terms of the nature of proteins (e.g. EMPs and MMP20) and epithelial cells (e.g. ameloblasts) involved, except in the case of collagen.

- Adameloid: in addition to enameloid properties, its matrix is composed of giant fibrils, tubular vesicles (TV), hypothetical EMP(s)-like (not yet identified), and its mineralization is initiated by the TV, with no accumulation of crystals along the fibrils (Fig. I-1B).
- True enameloid: in addition to enameloid properties, its matrix is composed of matrix vesicles (MV), ENAM and AMBN, and its mineralization is initiated by the MV, with accumulation of crystals along the fibrils (Fig. I-1B).
- Lepidameloid: in addition to true enameloid properties, its matrix also includes AMEL (Fig. I-1B).
- Acroclin: in addition to true enameloid properties, its matrix also includes SCPP5 (Fig. I-1B).
- Cap acroclin: in addition to acroclin properties, the tissue is situated on the tip of teeth (Fig. I-1B).
- Collar acroclin (previously 'collar enameloid'): in addition to acroclin properties, the tissue is situated on the shaft of teeth (Fig. I-1B).

Their definitions herein focus on matrix composition and developmental properties. When describing a new tissue, if one wishes to emphasize an additional property, we recommend using a terminology that highlights this additional property. For example, if one wants to refer to enameloid found in chondrichthyans, we suggest not only saying 'adameloid' but rather 'chondrichthyan adameloid'. We propose definitions that, in our view, should not constrain the concepts in terms of additional phylogenetic, structural, or topological properties. Therefore, for instance, it is not excluded that 'adameloid' could be identified in non-chondrichthyan taxa if all the defining properties are verified. Using lengthy yet explicit terminology should promote the precision of discussions, adapted to the message we want to convey.

Please note that, *sensu* this new terminology, ‘collar enameloid’ now simply refers to ‘enameloid’ positioned on the tooth shaft, not to a specific actinopterygian enameloid with a given matrix composition. Also note that the homologies of tissues are not explicit in the definitions, they will be discussed in the part I.3.

Identification

In the case of extant species, one may have direct access to the development of the tissue and assess all criteria of the enameloid definitions (Fig. I-1B) by studying various developmental stages (matrix formation, mineralization, maturation stages) and using complementary techniques (e.g. light and polarizing microscopy, transmission electron microscopy, immunohistochemistry) (e.g. Sasagawa, 1999; Davit-Beal *et al.*, 2007; Assaraf-Weill *et al.*, 2014; Sasagawa *et al.*, 2019).

At the matrix formation stage, one may attest to the secretion of collagen fibers between mesenchymal and epithelial cells, and the origin(s) of matrix components (mesenchymal and/or epithelial). Furthermore, one may look for the presence of giant fibrils, and EMPs or EMPs-like in the matrix, knowing that they can only be present during a short period at the beginning of the mineralization (Sasagawa *et al.*, 2019).

At the mineralization stage, one may attest to the origin(s) of components that initiate the mineralization (mesenchymal and/or epithelial). Furthermore, one may identify these components (e.g. matrix vesicles, tubular vesicles, and potentially EMPs as in enamel) and the mechanisms of mineralization.

At the maturation stage, one may attest to the degeneration and the removal of organic matter by epithelial cells, allowing the tissue to hyper-mineralize. One may then confirm the high degree of calcification and the putatively low amount of remaining organic matter.

To sum up, the dual mesenchymal and epithelial origin must be verified by the participation of mesenchymal cells in the matrix formation and mineralization, and the participation of epithelial cells in, at least, the maturation of the tissue.

In the case of extinct species, or non-model organisms for which developmental studies may be complicated, one has to use the additional properties to propose identification hypotheses (Fig. I-1B dotted boxes). However, we emphasize that the extension of these additional properties does not necessarily coincide with that of the defining properties, as exemplified with the property ‘presence of long tubules’. When using such additional properties, we advise discussing the reliability of the proposed identifications, recalling the defining properties to which additional properties refers and arguing on their link. Moreover, whenever one proposes an identification, but defining properties cannot be verified, we should mention them to contextualize the reliability of our attribution to an enameloid concept.

For example, a tissue may be identified as ‘enameloid’ if: (1) the hypermineralization is suggested by its more vitreous aspect compared to the underlying tissues, (2) the dual mesenchymal and epithelial origin is suggested by its position on the external surface of the structure (potential contact zone between mesenchymal and epithelial cells) and the presence of long cellular projections emanating from the base of the tissue, and (3) the initial presence of collagen is suggested by a microstructure with a fibrous appearance, considering that enameloid is assumed to be inotropic, meaning that crystallites organize along collagen fibers (Ørvig, 1967; Sasagawa, 1997). We can also consider comparing the studied tissue with other hypermineralized tissues of purely mesenchymal origin, such as pleromin and petrodentine, to rule out any connection with this tissue and further support its epithelial origin (Berkovitz & Shellis, 2016). In any case, the reliability of the identification inferred from additional properties should be discussed.

In order to discuss the reliability of a particular interpretation, it may be useful to use an approach such as the one introduced in Chapter IV: the theoretical outcomes of several hypotheses of developmental processes (e.g. epithelium initial shape, spatiotemporal activation of cells, matrix origin(s) of the capping tissue) are simulated (using computer models if necessary) and the scenario whose phenotypic outcome is closest to the observed histomorphology is retained as the one with the strongest support. This method enables to infer the developmental properties of extinct tissues. In regard to properties formalization, this approach corresponds to deducing additional properties from defining ones via an integrative developmental model.

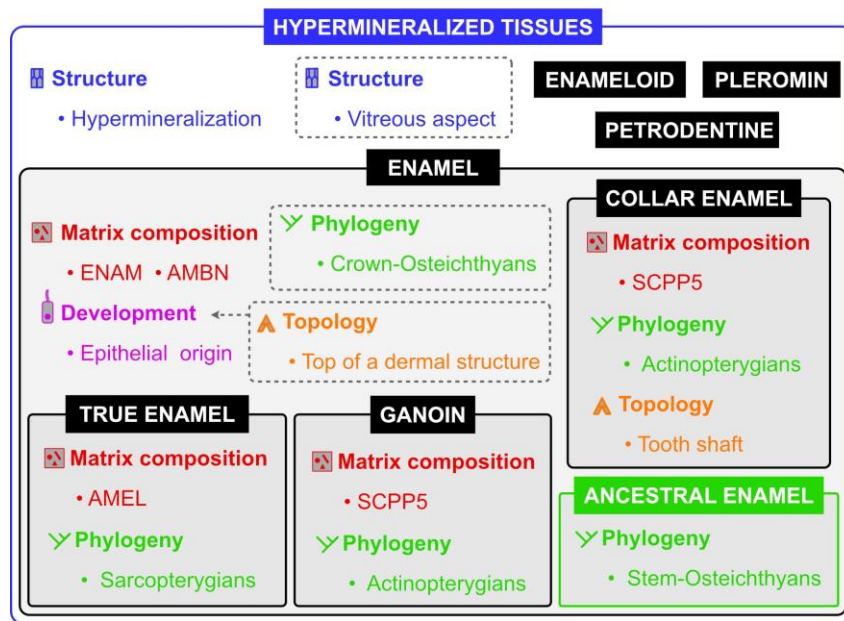
Once a tissue is identified as enameloid (or enameloid is the most likely hypothesis), one may use information, for instance on the phylogenetic position of the taxa, to refine the classification at the subcategory level. The same methodology can be applied using additional properties related to microstructure. However, it is important to note that some microstructures may be convergent (e.g. the one parallel-structured and one woven-structured crystal layers of 'adameloid' and 'cap acrodin', see Figure 1B), and one should therefore exercise caution with such properties. Of course, if a new microstructure is described, it can be clarified as an adjective (e.g. the 'monocrystalline enameloid' of *Astraspis* described in Donoghue *et al.* (2006)) for specifying a new subcategory.

A similar framework for enamel

Since the usage of enamel subcategories may be inconsistent (for instance, the unexpected differentiation between 'enamel' and 'ganoin' in their Figure 5 of Kawasaki *et al.* (2021), despite initially defining 'ganoin' as a subcategory of 'enamel' in their Figure 1), we propose to extend this revision to enamel and its subcategories (Fig. I-2). We proceed similarly with a nested classification scheme emphasizing developmental and compositional properties and we apply the same identification methodology as for enameloid.

CHAPTER I – NEW ENAMELOID AND ENAMEL CONCEPTS

A - Interpretive synthesis of current concepts of enamelooids



B - Proposed concepts of enamels

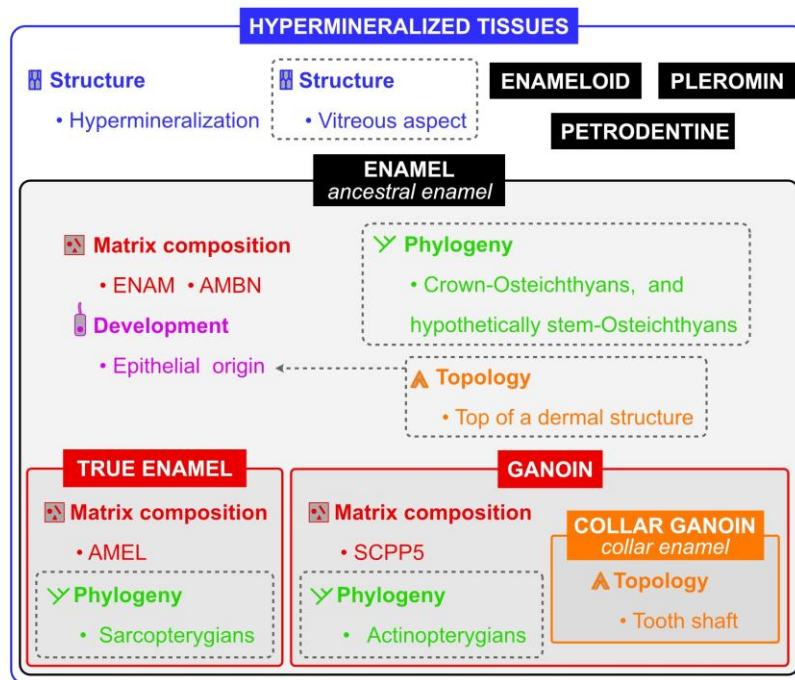


FIGURE I-2. Revision of enamel concepts with a nested classification scheme, where each box corresponds to a concept. Defining and additional properties are listed within the boxes. The additional properties are separated from the defining properties by dashed boxes. Nested boxes inherit all the properties of their encompassing parent box. Additional properties are useful for inferring defining properties when the latter cannot be directly observed. Colors indicate different types of properties. The boxes are colored differently depending on the type

of their respective defining properties, with black color indicating defining properties of mixed types. The box names are the new, preferred terms. The terms in lowercase and italics below them are the traditional equivalents whose usage is discouraged here. Please note that AMEL and SCPP5 do not seem necessary to form a thin enamel layer (Kawasaki *et al.*, 2021). The other vertebrate hypermineralized tissues are not detailed (enameloid, petrodentine and pleromin). The references used to construct this figure are detailed in parts I.3-4.

I.3. Overview of enamel and enameloid distribution and homologies

Dentin emerged in the first stem-gnathostomes, at least during the upper Ordovician, and the homology of its derivatives is admitted (Cuny *et al.*, 2018; Keating *et al.*, 2018; Lemierre & Germain, 2019). Since its acquisition, enameloid and enamel can be found on top of it. However, their evolution is less clear than that of dentin.

Distribution and primary homologies of enameloids and enamels

Extant taxa

Actinopterygians

Enameloid is found on the apex of teeth and as a layer on the surface of the tooth shaft (Berkovitz & Shellis, 2016). These structures are respectively named acrodin and collar enameloid, but could be rather called cap acrodin and collar acrodin due to the presence of matrix vesicles and EMPs (ENAM, AMBN, SCPP5) in the matrix (Fig. I-1 and see Fig. 1 in Kawasaki *et al.*, 2021). These two tissues are considered homologous because of their similar development (Shellis & Miles, 1974; Sasagawa & Ishiyama, 1988; Kawasaki *et al.*, 2021). We differentiate them into cap and collar acrodin owing to their different degrees of mineralization and their different positions within teeth, a junction being usually present between them (Sasagawa & Ishiyama,

1988). Cap acroдин is present in various extant and extinct actinopterygians (Shellis & Miles, 1974; Sasagawa *et al.*, 2013; Schultze, 2016; Kawasaki *et al.*, 2021), whereas collar acroдин would have secondarily evolved in teleosts (Fig. I-3) (Kawasaki *et al.*, 2021), replacing the collar ganoin (collar enamel) found in non-teleost actinopterygians. Collar ganoin is considered homologous to the true enamel found in sarcopterygians (Fig. I-3) (Sire *et al.*, 1987; Sasagawa *et al.*, 2013; Qu *et al.*, 2015b; Berkovitz & Shellis, 2016; Kawasaki *et al.*, 2021, 2022). Ganoin is also found in the odontodes of non-teleost actinopterygians (Sire *et al.*, 2009; Qu *et al.*, 2015b). The absence of enamel in teleost could be due to the lack of two modules (P/Q and DE) in their SCPP5 genes, whereas non-teleost actinopterygian SCPP5 genes have a similar modular structure with that of sarcopterygian AMEL (Kawasaki *et al.*, 2021). A few matrix proteins have been secondarily lost in certain teleosts (AMBN and/or ENAM) (Lv *et al.*, 2017), suggesting a modification or a loss of their enameloid, but more studies on teleost tissues are necessary (Kawasaki *et al.*, 2021).

Sarcopterygians

The teeth of most sarcopterygians and the odontodes of non-tetrapod sarcopterygians are capped with true enamel, a tissue considered homologous to the ganoin of actinopterygians (Sire *et al.*, 1987; Sasagawa *et al.*, 2013; Qu *et al.*, 2015b; Berkovitz & Shellis, 2016; Kawasaki *et al.*, 2021, 2022). In urodeles, and only in urodeles so far, enameloid, more precisely lepidameloid (as indicated by the presence of matrix vesicles and probably of ENAM, AMBN, AMEL proteins in the matrix (Fig. I-1B) (Davit-Beal *et al.*, 2007; Assaraf-Weill *et al.*, 2014)), is found as a cap in larval teeth (Fig. I-3). Lepidameloid is gradually replaced by true enamel during ontogeny, with the teeth of juveniles and adults ultimately consisting of only dentin and true enamel (Kogaya, 1999; Davit-Beal *et al.*, 2007; Assaraf-Weill *et al.*, 2014). This unique presence of enameloid among sarcopterygians suggests an independent origin of enameloid in urodeles (Kawasaki *et al.*, 2021).

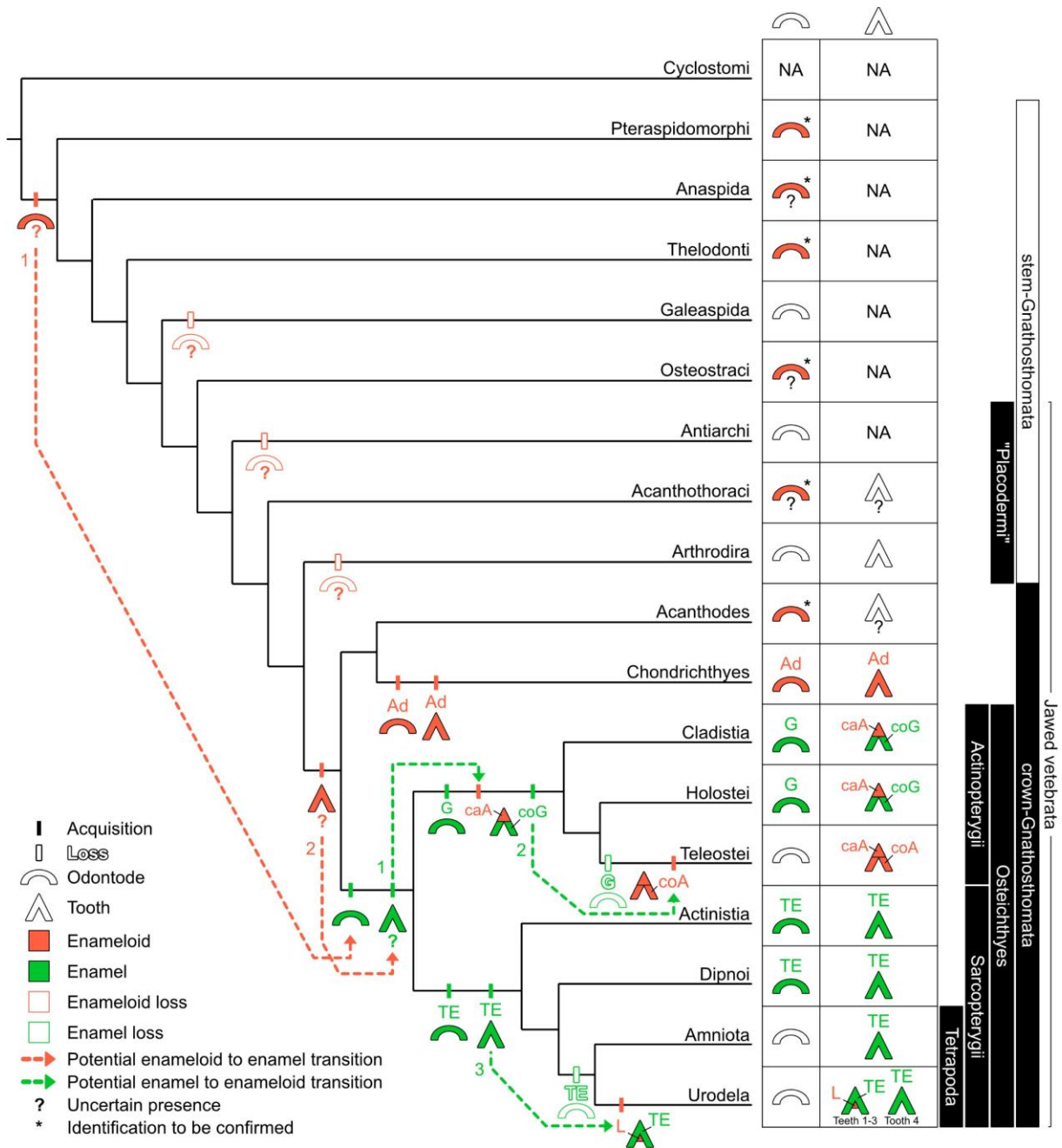


FIGURE I-3. Phylogenetic distribution of enameloids and enamels among vertebrates, along with its uncertainties, and its evo-devo implications. The hypothesis illustrated here is the most parsimonious and corresponds to a common origin of enameloid among stem-gnathostomes followed by potential losses. Alternatively, several independent acquisitions of enameloid in early vertebrates could also be possible. This tree is after Keating *et al.* (2018), Rücklin & Donoghue (2019), and Kawasaki *et al.* (2021). Distribution of characters is mostly based on Sire *et al.* (2009) and Mondéjar Fernández & Janvier (2021), and see also part I.3 and

references therein. A, acrodin. Ad, adameloid. ca, cap. co, collar. G, ganoin. L, lepidameloid. TE, true enamel. See figure 1C for definitions.

Chondrichthyans

In chondrichthyans, the hypermineralized part of the teeth and odontodes is made of a type of enameloid, namely adameloid (Enault *et al.*, 2015; Berkovitz & Shellis, 2016) (Fig. I-3). The structure of adameloid varies between sharks and rays (Enault *et al.*, 2015; Berkovitz & Shellis, 2016). Chondrichthyan adameloid seems to have evolved independently of that of actinopterygians and sarcopterygians as suggested by its matrix composition and its specific mineralization processes (see part I.4.) (Sasagawa, 2002; Kawasaki *et al.*, 2021). However, their developmental differences could also be due to the independent evolution of enameloid in chondrichthyans and osteichthyans from a common ancestral enameloid.

Extinct taxa

Several groups of jawless stem-Gnathostomata possessed odontodes covered by a layer of a hypermineralized tissue identified as enameloid (Sire *et al.*, 2009; Mondéjar-Fernández & Janvier, 2021). It was the case of Pteraspidomorphi (Keating *et al.*, 2015; Lemierre & Germain, 2019), Thelodonti (Sire *et al.*, 2009), and potentially Anaspida (Keating & Donoghue, 2016), as well as Osteostraci (Qu *et al.*, 2015a). *Romundina* (Acanthothoracid, 'Placoderm'), a taxa of jawed stem-Gnathostomata, also seems to have an enameloid layer on its odontodes (Giles, Rücklin & Donoghue, 2013; Rücklin & Donoghue, 2015, 2016; Meredith Smith *et al.*, 2017), as few Acanthodes type scales ('Acanthodii') (Fig. I-3) (Burrow, Trinajstić & Long, 2012; Mondéjar-Fernández & Janvier, 2021).

However, most of these identifications as enameloid are solely based on the presence of tubules in a capping hypermineralized tissue. As discussed in part I.2., this feature is not diagnostic of enameloid only, hence further observations (e.g. histology, microstructure) are needed to exclude potential alternatives.

Ancestral states and secondary homologies of enameloids and enamels

Some ancestral states can be inferred based on the enameloid and enamel distribution detailed in the previous section (Fig. I-3). They either correspond to acquisition or loss of one of these tissues (or their subcategories) in odontodes and/or teeth:

- Acquisition of adameloid in the odontodes and teeth of chondrichthyans.
- Acquisition of enamel in the odontodes of osteichthyans. This acquisition may be linked to the emergence of AMBN and ENAM in stem-osteichthyans (Kawasaki *et al.*, 2021). These EMPs are known to be essential for enamel formation in extant mammals (Gibson *et al.*, 2001; Smith *et al.*, 2016; Liang *et al.*, 2019; Kawasaki *et al.*, 2020).
- Acquisition of ganoin in the odontodes and tooth shaft, and acrodin in the tooth tip of actinopterygians, as partially proposed by Kawasaki *et al.* (2021). They are both linked to the emergence of SCPP5.
- Loss of ganoin in the odontodes of teleosts and replacement by acrodin in the tooth shaft of teleost.
- Acquisition of true enamel in the odontodes and teeth of sarcopterygians, linked to the emergence of AMEL (Kawasaki *et al.*, 2021).
- Loss of true enamel in odontodes of tetrapods, and acquisition of lepidameloid in the first teeth of urodeles.

Some key ancestral states remain uncertain:

Was AMEL (forming true enamel) or SCPP5 (forming ganoin) already present in early osteichthyans, as proposed by Kawasaki *et al.* (2021)? Then, one might have evolved from the other, and that other would be considered the plesiomorphic condition in osteichthyans (Kawasaki *et al.*, 2021).

Was tooth enamel first acquired in the first osteichthyans, as proposed by Qu *et al.* (2015)? This point is key to determining if tooth enamel was acquired independently in actinopterygians and sarcopterygians, as proposed by Kawasaki *et al.* (2021). Moreover, the cap acrodin of first actinopterygians could have derived from this putative enamel of first osteichthyans (Fig. I-3 green arrow 1). The discovery of a stem-osteichthyan with tooth enamel would clarify this contention point.

Was tooth enameloid first acquired in the first crown-gnathostomes? This point is key to understanding whether the enamel found in osteichthyans teeth derived from enameloid (see part I.4. and Fig. I-3 red arrow 2), and whether the hypermineralized tissues of chondrichthyans and osteichthyans emerged independently. The discovery of a stem-gnathostome with tooth enameloid would resolve this question.

The evolutionary history of enameloid in the odontodes of stem-gnathostomes remains blurry. The most parsimonious hypothesis is represented in Figure I-3: all odontodes composed of enameloid share a common origin and a few reversions are present (Galeaspida, Antiarchi and Arthrodira). More reliable identifications of mineralized tissues and phylogenies of stem-gnathostomes would play a critical role in clarifying this history. This would also clarify whether extant enamel is derived from enameloid, such as the one found in the Ordovician pteraspidomorph *Astraspis* (Sire *et al.*, 2009).

I.4. Evo-devo: the dentin-enameloid-enamel continuum

Synthesis and creation of a general model of enameloid development

On the one hand, despite the numerous available studies about enameloid development, it is still enigmatic in terms of matrix composition, cellular origin of matrix components, their timing of secretion and their distribution (Berkovitz & Shellis, 2016). On the other hand, even if enameloid(s) might not be homologous, they seem to share some similar developmental pathways. Here, we propose to synthesize the shared developmental pathways of enameloid development among vertebrates and to organize them in a general model of enameloid development. It will facilitate interpretations of the development of enameloid in stem-gnathostome fossil taxa and help deciphering the mechanisms of enameloid-enamel transition.

Matrix formation stage

Enameloid matrix (named 'preenameloid' by Poole (1967) and Ørvig (1967)) is produced between mesenchymal and epithelial cells (Berkovitz & Shellis, 2016). Preenameloid has two main components (Fig. I-4). First, there is collagen produced by odontoblasts (mesenchymal origin) (Berkovitz & Shellis, 2016), and potentially by inner dental epithelial (IDE) cells (epithelial origin) as it has been demonstrated in a teleost (Huysseune *et al.*, 2008) and in a caudate larva (Assaraf-Weill *et al.*, 2014). 'Giant fibers' are also present in chondrichthyan preenameloid (Sasagawa & Akai, 1992; Sasagawa, 2002). Second, there are matrix vesicles (MVs) in the case of osteichthyans (Sasagawa, 1988; Davit-Beal *et al.*, 2007), and tubular vesicles (TVs) in the case of chondrichthyans (Sasagawa, 2002), both produced by odontoblasts. In osteichthyans, preenameloid is mainly composed of collagen fibers, while it is dominated by TVs, which occupy most of the space, in chondrichthyans (Sasagawa, 2002; Davit-Beal *et al.*, 2007). As in pre-dentin, the participation of odontoblasts in preenameloid formation

can induce the presence of odontoblast processes in the preenameloid (Sasagawa, 2002; Davit-Beal *et al.*, 2007; Sasagawa *et al.*, 2019). At the beginning of its secretion, preenameloid does not seem to include enamel matrix proteins (or EMPs-like), even if an expression of enamel proteins (e.g. AMBN, ENAM and SCPP5) have been found in inner dental epithelial (IDE) cells (Satchell *et al.*, 2002; Assaraf-Weill *et al.*, 2014; Sasagawa *et al.*, 2019; Kawasaki *et al.*, 2021). We can note that EMPs (AMBN, ENAM and SCPP5) are also expressed by odontoblasts in teleosts (Kawasaki, Suzuki & Weiss, 2005; Kawasaki *et al.*, 2021; Kawasaki, 2009), which may have led to a modification of their acroдин compared to the non-teleost (Kawasaki *et al.*, 2021). A basal lamina can be initially present between odontoblasts and IDE cells, but it is degraded at the latest before the maturation stage (Berkovitz & Shellis, 2016).

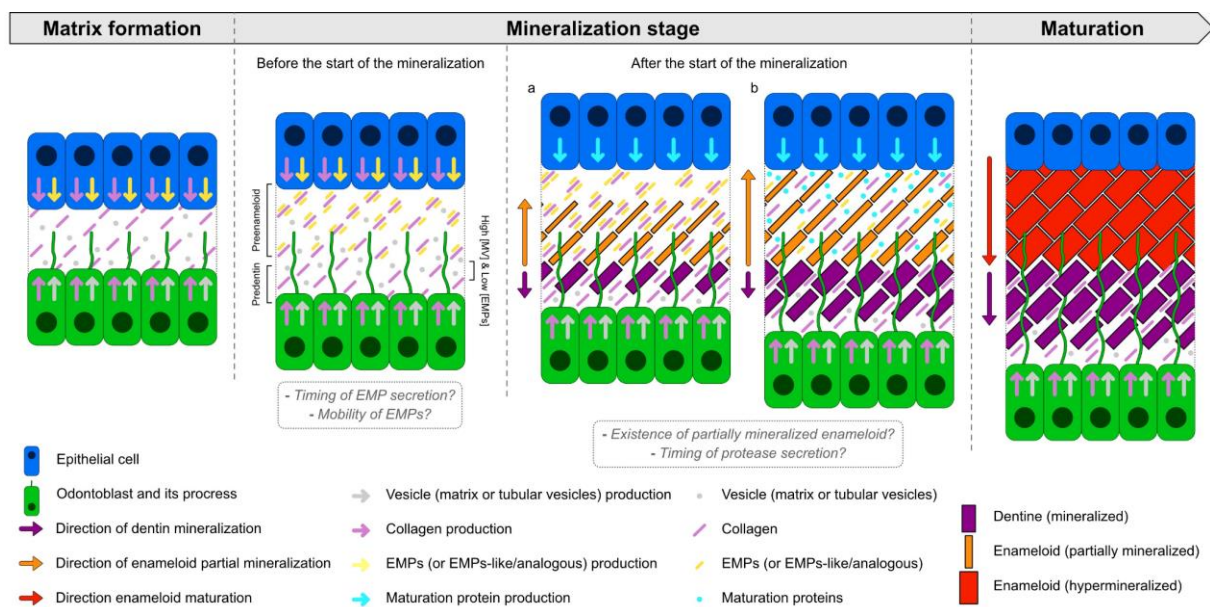


FIGURE I-4. Interpretation of dentin-enameleoid histogenesis in vertebrates. Even if enameloids present developmental differences among vertebrates, they share similar general developmental mechanisms. Mineralization is initiated by vesicles, then the mineralization spreads in dentin and enameloid. Mineralization of enameloid is probably initially partial, because of the presence of EMPs (or EMPs-like/analogous) in the matrix, but becomes high after the degradation of EMPs by maturation proteins. The basal lamina is not represented here.

Matrix mineralization stage

Before mineralization starts (Fig. I-4a), IDE cells continue to produce EMPs (e.g. SCPP5 in actinopterygians, AMEL in sarcopterygians, and probably AMBN in osteichthyans, perhaps ENAM) or EMPs-like. Those have been documented in the preenameloid of actinopterygians (Sasagawa *et al.*, 2019; Kawasaki *et al.*, 2021) and are likely present in the preenameloids of sarcopterygian and chondrichthyan (Shellis, 1978; Slavkin *et al.*, 1983; Graham, 1984, 1985; Assaraf-Weill *et al.*, 2014; Berkovitz & Shellis, 2016). In chondrichthyans, the expression of genes similar to SCPP genes has been detected in IDE cells (Leurs *et al.*, 2022), but these genes are not orthologous to AMEL, SCPP5, AMBN, ENAM (Kawasaki *et al.*, 2022). When they are detected in preenameloid, EMPs are associated with collagen fibrils and their concentrations are higher near the outer surface and decrease toward the dentin-enameloid junction, close to odontoblasts (Sasagawa *et al.*, 2019; Kawasaki *et al.*, 2021, 2022). However, we do not know exactly when these epithelial proteins start to be secreted nor whether they have the ability to invade the matrix, or are secreted from the beginning of the matrix formation without having been detected. Neither do we know the exact function(s) of these proteins, but we suspect that they have analogous functions to those of enamel (Sasagawa *et al.*, 2019; Kawasaki *et al.*, 2021, 2022). At this stage, preentin may be found near odontoblasts, notably where EMPs are not or poorly present (Sasagawa, 2002; Davit-Beal *et al.*, 2007; Sasagawa *et al.*, 2019). Electron-dense fibrous structures (EDFS) derived from MVs were also detected in actinopterygians, prior to the detection of EMPs (Sasagawa *et al.*, 2019). They are highly concentrated in the inner layer, where the mineralization will start (Sasagawa *et al.*, 2019).

When mineralization starts, all the preenameloid is formed and IDE cells stop their matrix production (Fig. I-4b).

Initialization of preenameloid mineralization by MVs takes place near the preentin-preenameloid junction and progresses toward the surface of the enameloid

in actinopterygians (Sasagawa *et al.*, 2019). It is still unknown why the mineralization starts near odontoblasts, rather than in the first formed layers of preenameloid where the mineralization appears to be inhibited. It might be due to a high concentration of vesicles and/or a low concentration of EMPs at the position of the future junction (Sasagawa, 1988). Then, crystal deposition occurs on the collagen fibrils, and potentially EDFs when they are present (Shellis & Berkovitz, 1976; Sasagawa, 1988, 1997; Sasagawa *et al.*, 2019; Kawasaki *et al.*, 2022). In chondrichthyans, the initialization of the mineralization by TVs is more scattered in the preenameloid, and there is no specific portion where the initial crystals gather (Sasagawa, 2002). Furthermore, crystals are not really concentrated along fibrils (collagen and giant fibers), probably because of the low concentration of fibrils in the matrix (Sasagawa, 1998, 2002). This could also be due to the acquisition of new mineralization mechanisms that are based on ODAM and novel P/Q-SCPP genes coding for enamel matrix proteins, rather than mechanisms based on SCPP genes (Berkovitz & Shellis, 2016; Kawasaki *et al.*, 2021). At the end of this stage, at least in actinopterygians, collagen and EMPs are barely found in the preenameloid, suggesting that degeneration or modification has started (Sasagawa *et al.*, 2019; Kawasaki *et al.*, 2022). Dentin starts to mineralize at the same time as the enameloid (Davit-Beal *et al.*, 2007), or afterward (Sasagawa, 2002).

While no studies have yet focused on this point, it is likely that the preenameloid is only partially mineralized before the maturation stage. In enamel, mineralization remains limited to about 30 percent before maturation, which will allow for protein transport/removal during the maturation phase (Nanci, 2017). Once the limiting matrix proteins (probably AMEL (Margolis, Kwak & Yamazaki, 2014), SCPP5 and/or collagen fibers (Sasagawa *et al.*, 2019)) are removed due to protease activity, crystals can grow further and tighter. Without such a limiting mechanism, preenameloid may mineralize to about 60 percent, as does dentin (Nanci, 2017), thus preventing further protein transport/removal and further crystal growth.

Maturation stage

The hypermineralization of enameloid is achieved by the transport of mineral ions into the matrix, the degeneration and the removal of the organic matrix (e.g. collagen and giant fibers), enabling the crystallites to increase in size (Fig. I-4) (Sasagawa, 2002; Sasagawa, Ishiyama & Akai, 2006; Davit-Beal *et al.*, 2007; Berkovitz & Shellis, 2016). The degeneration of the matrix proteins is achieved by proteases, probably MMP20 as in enamel, or related genes such as the teleost gene MMPF20L (Kawasaki & Suzuki, 2011). Based on teleosts, ODAM, expressed by IDE cells, is also suspected to have functions in enameloid maturation, as it is the case for enamel (Kawasaki, 2009, 2013; Berkovitz & Shellis, 2016). The removal of matrix components is carried out by the IDE cells (Berkovitz & Shellis, 2016), which reduce their height, induce extended extracellular spaces and ruffled borders in the case of osteichthyans (Shellis, Miles & Harrison, 1997; Davit-Beal *et al.*, 2007). As discussed above, these steps of degeneration and removal of the organic matrix might be possible only if enameloid is partially mineralized, thus enabling the displacement of the organic components of the matrix. In the end, bundles of thick crystallites occupy the enameloid, and collagen as well as EMPs are no longer present. Predentin mineralization progresses towards the odontoblasts, which keep on producing predentin. Maturation probably spreads, as in enamel, from the outer layers to the inner layers near the dentin-enameloid junction (see Fig. 1A in Simmer & Hu (2002)). We note that the outer part of the enameloid may be more highly mineralized than its inner parts (e.g. the collar enameloid in Sasagawa & Ishiyama (1988)).

Enameloid-enamel transitions

Several evolutionary transitions may have occurred between enameloid and enamel during the evolution of vertebrate odontodes and teeth (Fig. I-3). These

transitions could be explained by simple independent loss of an initial tissue, followed by the acquisition of a new one. However, commonalities in the development of enamel and enameloid rather suggest that those transitions may be explained more parsimoniously by a few developmental shifts. In the following, we explore this hypothesis. A more in-depth simulation-based analysis is available in Chapter II.

Dentin, enamel and enameloid can develop in the same dental structure. As dentin is a tissue of mesenchymal origin, enamel of epithelial origin, and enameloid of both origins, one may consider they form a kind of continuum, whereby dentin and enamel may be viewed as the two poles and enameloid as an intermediate state sharing similarities between both dentin and enamel (Shellis & Miles, 1974; Kawasaki *et al.*, 2021). Based on this idea, developmental variations have been proposed to explain the transitions between dentin-enameloid and dentin-enamel formation (Poole, 1971; Smith & Tchernov, 1992; Smith, 1995). This means, for instance, that the emergence of enamel in stem-osteichthyans might have occurred through a few developmental changes, without implying drastic genetic changes (Fig. I-3 red arrows). Several developmental hypotheses have been proposed to explain such transition: (H1) a prolonged epithelial cell activity (Poole, 1971; and see Kawasaki *et al.* (2022) who propose a similar hypothesis where the SCPP5 production is reduced in enameloid compared to enamel), (H2) a delayed epithelial cell activity (Shellis & Miles, 1974), and (H3) a modification of the epithelial cells' production (from mostly collagen to mostly enamel proteins) (Assaraf-Weill *et al.*, 2014) (Fig. I-5). Please note that the opposite transition (from enamel to enameloid) may have occurred too, and could be explained by the dual version of these hypotheses. For example, Kawasaki *et al.* (2021) proposed that collar ganoin found in non-teleost actinopterygians was replaced by collar acrodin in teleost, supported by the expression of SCPP5, AMBN and ENAM in both tissues (Fig. I-3 green arrow 2).

CHAPTER I – NEW ENAMELOID AND ENAMEL CONCEPTS

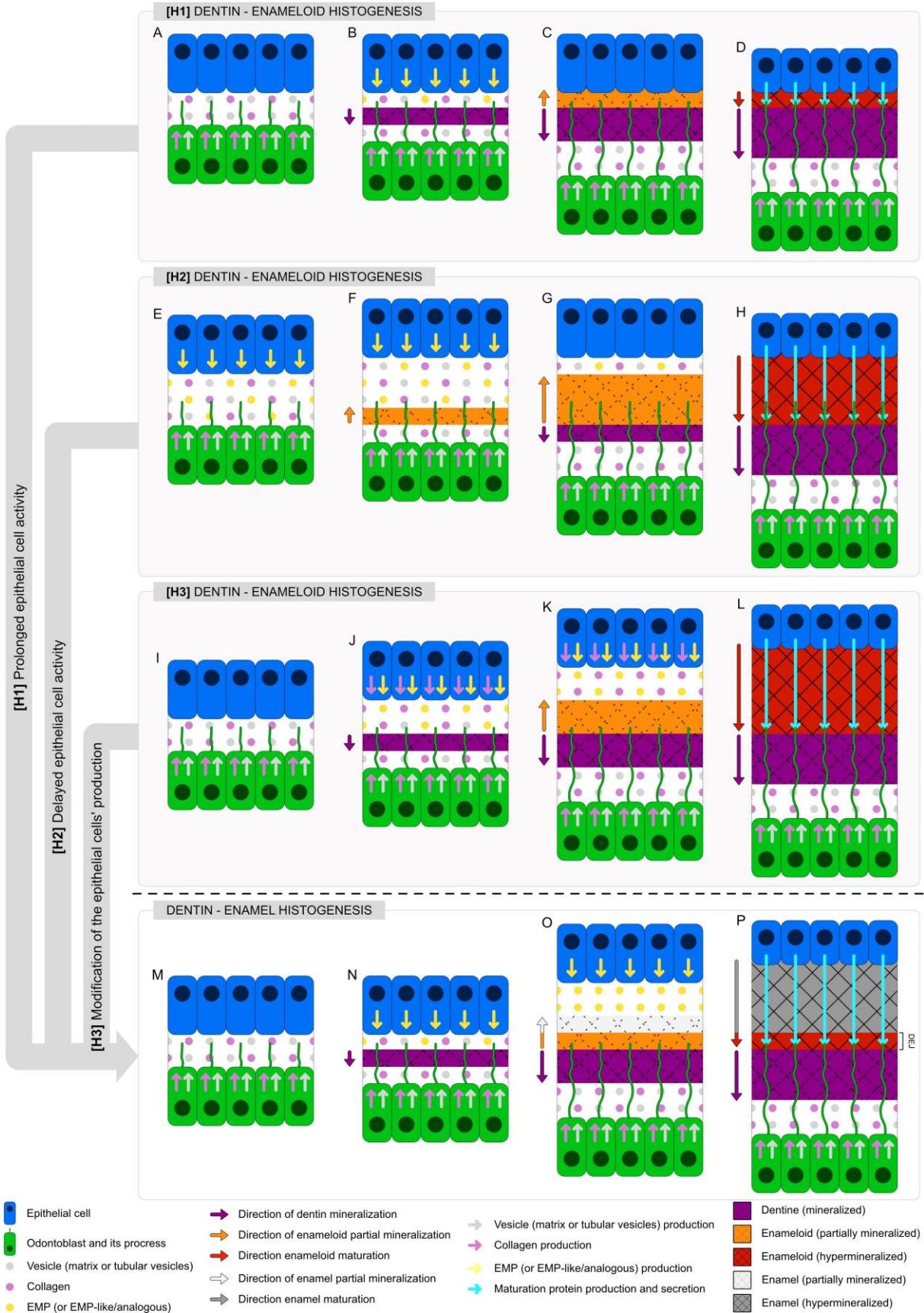


FIGURE I-5. Main hypotheses of enameloïd-enamel transition via developmental changes. M-P, note that, during the dentin-enamel formation, a thin layer of matrix is composed of both pre-dentin and pre-enamel at the dentin-enamel junction (DEJ) and can be interpreted as enameloïd. These hypotheses are based on the general model of enameloïd development presented in part I.4.

The idea that such transition (in one way or the other) may be 'evolutionary easy' is supported by some examples in extant organisms, where similar transitions have been documented: in some urodeles, larval teeth are made of dentin, lepidameloïd, and a thin layer of true enamel, whereas the teeth after metamorphosis, in the juveniles and adults, show a greater proportion of true enamel and an apparent loss of lepidameloïd (Kogaya, 1999; Davit-Beal *et al.*, 2007; Assaraf-Weill *et al.*, 2014); in some actinopterygian teeth, the junction between collar ganoin and cap acrodin may show some continuous gradation rather than a clear-cut distinction between two very different tissues (see Fig. 16B in Richter & Smith (1995)). In those cases, clear junctions between enameloïd and enamel are visible, but this may not always be the case. Combined with the fact that the matrix components that define those respective tissues 'diffuse' from the secreting cells and hence their concentrations likely present a gradient up to the junction, those examples suggest that *sensu stricto* if enamel is present then enameloïd must be present too, and vice versa: as suggested by Sasagawa *et al.* (2019), one may expect that a (arguably very thin) layer of enameloïd-like tissue is present near most dentin-enamel junctions, as some pre-dentin may get mixed with pre-enamel before the secretion of EMPs (Uchida, Tanabe & Fukae, 1989; and see Fig. 7-22B in Nanci (2017)); and similarly, the outermost layer of many enameloïds may appear shinier (in sharks and teleosts, see Herold (1974), Shellis *et al.* (1997), Berkovitz & Shellis (2016)) and could be considered as a kind of enamel lacking the participation of true EMPs (Berkovitz & Shellis, 2016). The presence of a thin layer of pre-enamel (preganoin) onto the cap acrodin of the actinopterygian *Polypterus* (Sasagawa *et al.*,

2012; Delgado *et al.*, 2023) supports this latter hypothesis. It would be critical to test for the presence of those putative concentration gradients of matrix components.

These considerations, as well as the very possibility of 'easy' transitions between enameloid and enamel hinge on the assumption that the protein(s) secreted by the IDE cells are qualitatively similar in enameloid versus enamel formation. It has been documented that IDE cells may secrete specific matrix components during the formation of some enamels (Berkovitz & Shellis, 2016) but it is not clear whether those differences in matrix components with enameloid may have been derived secondarily along some phylogenetic branches or are indeed necessary for such tissue transitions. The evolution of vertebrate hypermineralized tissues was probably driven both by spatio-temporal developmental shifts AND modifications of the involved matrix proteins (Kawasaki *et al.*, 2021) and disentangling the respective roles of developmental vs compositional factors will likely require, beyond the classical histological studies, the use of *in silico* exploratory models such as the one discussed in the next chapter(s).

I.5. Conclusion

Enameloid definitions and nomenclature have been, and still are, widely debated. This has led to ambiguous usage of terms referring to enameloids, thereby questioning the consistency of former identifications. We propose a nested scheme of revised enameloid concepts that will hopefully set a standard for future studies. We introduce new terms such as 'true enameloid', 'collar acrodin', and 'lepidameloid', and encourage our colleagues to use our scheme to define and properly name new subcategories whenever necessary. A similar scheme is proposed also for enamel concepts. The other parts of this Chapter I were notably used as application examples and tests of these new definitions.

We also discuss the criteria that can be used to identify those tissues, in particular in taxa without extant relatives (e.g. stem-gnathostomes). This is further discussed in Chapter IV.

Armed with our revised definitions, we also reassess and synthesize the current knowledge about the phylogenetic distribution of enameloids and enamels and discuss their homologies as well as the likely occurrence, in vertebrate evolution, of several transitions between the two tissues.

We propose also general, hypothetical models for the formation of extant enameloids, or enamels respectively, whose comparison highlights potential developmental trajectories for putative transitions between the two tissues (see also Chapter II). Thereby we also suggest that, strictly speaking, the presence of one tissue may imply the presence of the other.

Acknowledgements. We warmly thank Ichiro SASAGAWA and Sidney DELGADO for the discussions we had about enamel and enameloid formation.

Contributions. **Conceptualization** Guillaume Houée (GH), Jérémie Bardin (JB), Nicolas Goudemand (NG), Damien Germain (DG); **Investigation** GH; **Formal Analysis** GH; **Methodology** GH; **Project Administration** GH; **Supervision** DG, NG, JB; **Validation** GH, JB, NG, DG; **Visualization** GH, JB; **Writing – Original Draft Preparation** GH, JB, NG, DG.

Conclusion on the objectives of Chapter I

In Chapter I we:

- Redefined the different concepts of enameloids and enamels (Fig. 2-1a).
- Clarified identification criteria of these tissues (Fig. 2-1a).
- Compiled their present and past phylogenetic distribution (Fig. 2-1b).
- Proposed a developmental model of enameloid (Fig. 2-1c).
- Described developmental hypotheses of evolutionary transitions between enameloid and enamel (Fig. 2-1d).

CHAPTER II

MODELING THE HISTOGENETIC SWITCH BETWEEN ENAMELOID AND ENAMEL

Objectives Chapter II

This second chapter aims at studying the mechanisms of tissue diversification through developmental modifications, taking as a case study the transitions between enameloid and enamel. As highlighted in Chapter I, the development of these tissues is closely linked, and several enameloid-enamel or enamel-enameloid transitions have been suggested to have occurred during vertebrate evolution. In addition to these macroevolutionary hypotheses, similar transitions can be observed during salamander ontogeny or during non-teleost actinopterygian tooth development, enabling potential direct studies on the transition mechanisms. As the developmental mechanisms involve many actors and parameters, it seems convenient to first explore the parameter space using computer modeling (Fig. 2-II). This has the advantage of working within a simplified theoretical framework, where actors are known and the parameters are purposely limited, which enables exhaustive exploration of the parameter space.

This project II is close to the submission in *Journal of dental research*.

II.1. Introduction

The vertebrate skeleton is composed of a diversity of calcium-phosphate mineralized tissues (Sire *et al.*, 2009; Vickaryous & Sire, 2009; de Buffrénil *et al.*, 2021). 'Dental tissues' such as dentin, enamel and enameloid are the main components of teeth and odontodes (tooth-like structures). Teeth and odontodes are classically structured with a basal dentinous tissue, capped by a hypermineralized tissue (i.e. with a low fraction of organic matter) such as enamel or enameloid (Sire *et al.*, 2009).

In a nutshell, these three tissues are classically distinguished by their matrix composition and their cellular origin. Dentin is a mineralized tissue of mesenchymal (ectomesenchymal) origin. Its matrix (predentin) is mostly composed of collagen produced by odontoblasts (Sire *et al.*, 2009; Berkovitz & Shellis, 2016). Enamel is a hypermineralized tissue of epithelial origin. Its matrix (preenamel) contains enamel matrix proteins (EMPs, such as amelogenin, enamelin, ameloblastin and SCPP5) produced by inner dental epithelial cells (IDEC) named ameloblasts. Enamel hypermineralization is due to a maturation phase during which IDEC degenerate and remove the organic fraction of the matrix, using proteases (such as metalloproteinase 20 and kallikrein-4). The maturation phase allows crystals to grow larger/tighter, especially in width (Sire *et al.*, 2009; Berkovitz & Shellis, 2016). Enameloid is also a hypermineralized tissue, but of dual epithelial and mesenchymal origin. Its matrix (preenameloid) is constituted of collagen (produced mostly by the odontoblasts and possibly by the IDEC) and EMPs (or EMP-like proteins in the case of chondrichthyans). Its hypermineralization is also obtained via a maturation phase, similar to that of enamel (Sire *et al.*, 2009; Berkovitz & Shellis, 2016; Sasagawa *et al.*, 2019).

Enamel and dentin development are relatively well understood, whereas that of enameloid remains enigmatic on several aspects: the composition of its extracellular matrix (ECM), the cellular origin(s), timing of secretion and distribution of its matrix components (Berkovitz & Shellis, 2016; Chapter I).

Given that enameloid has a dual mesenchymal and epithelial origin, whereas enamel has only epithelial origin, it has been suggested that one might have derived from the other, possibly as a result of some heterochronic shifts (Poole, 1971). The precedence of enameloid in the fossil record suggests an enameloid to enamel transition in stem-osteichthyans (Chapter I). However, it is also possible that this transition occurred several times, in one or the other direction, during vertebrate evolution. Several developmental hypotheses have been proposed to explain this transition (Fig. II-1): (H1) a delayed epithelial cell activity (Shellis & Miles, 1974), (H2) a prolonged epithelial cell activity (Poole, 1971), and (H3) a modification of the epithelial cells' production (from mostly collagen to mostly enamel proteins) (Assaraf-Weill *et al.*, 2014). These hypotheses consider that similar EMPs, or EMPs-like, are involved in enameloid and enamel formation, and thus that acquiring new genes is not necessary to transition (Berkovitz & Shellis, 2016).

In this study, we use a biomodeling approach to explore the impact of various developmental parameters on the relative proportions of dentin, enameloid and enamel formed. This allows us to test *in silico* the above-mentioned developmental hypotheses and to propose alternative ones.

II.2. Materials and Methods

Modeling

We used the open-access software EmbryoMaker to build our histogenetic model. EmbryoMaker allows us to model, in three dimensions and at the cellular scale, developmental mechanisms such as ECM secretion, while considering physical parameters like cellular and ECM cohesion (e.g. Marin-Riera *et al.*, 2016, 2018; Hagolani *et al.*, 2019, 2021).

CHAPTER II – FROM ENAMELOID TO ENAMEL

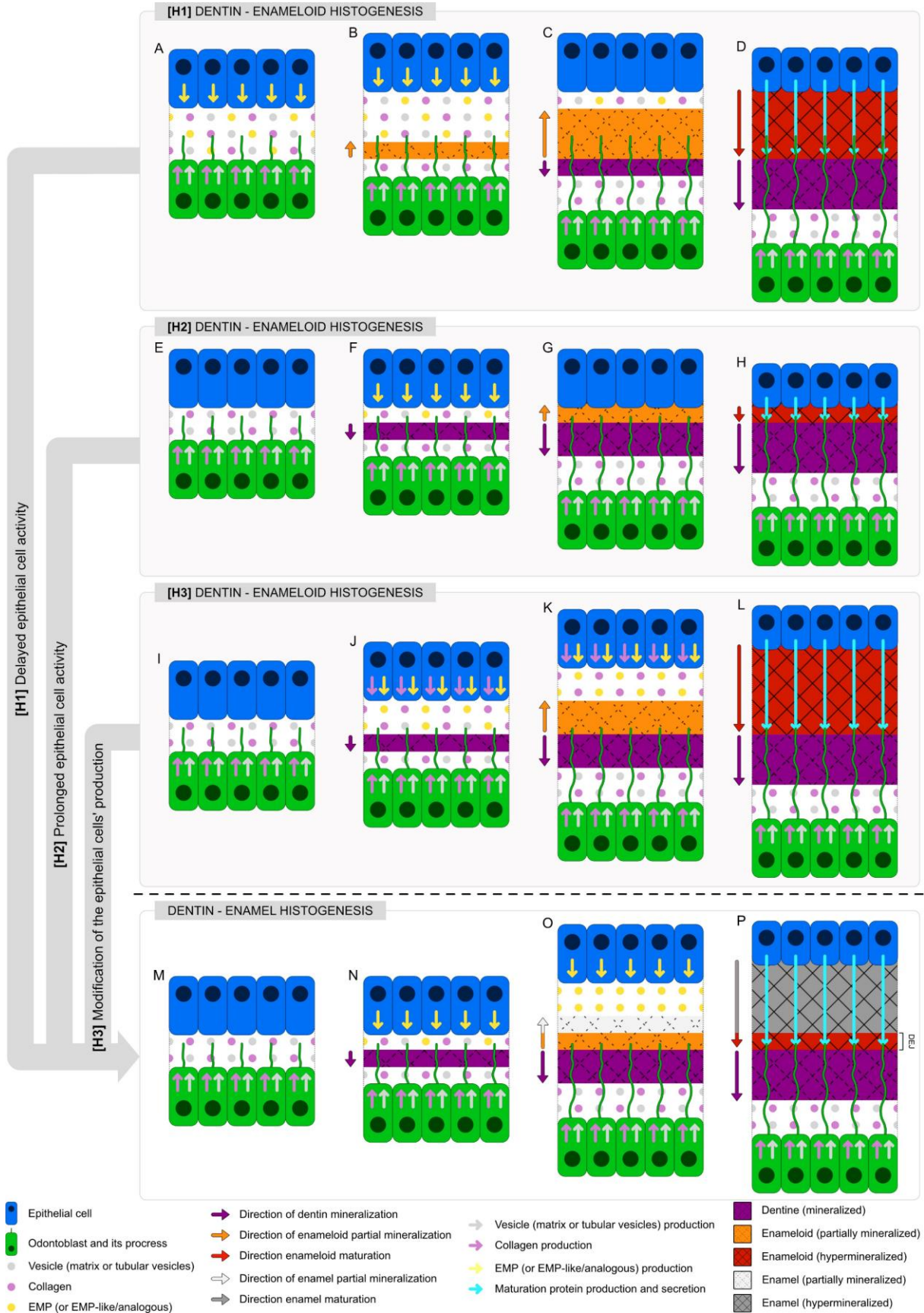


FIGURE II-1. Main hypotheses of enameloïd-enamel transition via developmental changes. M-P, note that, during the dentin-enamel formation, a thin layer of matrix is composed of both predentin and preenamel at the dentin-enamel junction (DEJ) and can be interpreted as enameloïd. Modified from the Figure I-5.

In our histogenetic model, polarized cells (IDeC and odontoblasts) are represented by double cylinders, which correspond respectively to the apical and basal poles (Fig. II-2, 3). These cylinders also define the physical boundaries of the simulations. The relative volumes occupied by mineralized tissues (MTv, including both dentin and hypermineralized tissues), partially mineralized tissues (pMTv, preenamel and preenameloïd) and ECM (ECMv, including collagen, vesicles or EMPs) are discretized and represented by spheres of different colors (Fig. II-2, 3). Using relatively small spheres compared to the cylinder-cells ensures they are sufficiently free to move around in the simulations, thereby simulating diffusion and mixing. Distinguishing between partially mineralized and mineralized tissues is critical because partially mineralized are porous to matrix components whereas mineralized tissues are not (that is, they block their diffusion) (Fanchon *et al.*, 2004).

In addition to the initial conditions, the model considers three developmental stages: matrix formation, matrix mineralization, and, in hypermineralized tissues, maturation (Berkovitz & Shellis, 2016).

At the initiation, and as we do not study differentiation mechanisms, epithelial and mesenchymal cells are already differentiated into IDeC and odontoblasts respectively (Fig. II-3). Cells are arranged in two lines facing each other: an epithelium of IDeC and a pseudo-epithelium of odontoblasts (Berkovitz & Shellis, 2016). For simplicity, all cells of a given type are assumed to behave in the same way and hence only three cells of each type are represented. Please note that a model using only one cell of each type would have been possible. The chosen option anticipates the potential

CHAPTER II – FROM ENAMELOID TO ENAMEL

evolution of the model to account for the non-uniformity of some parameters along the tissue (see Chapter III). The extremities of these polarized cells define the model physical boundaries for the x and y axes, but cells are able to move along the z axis.

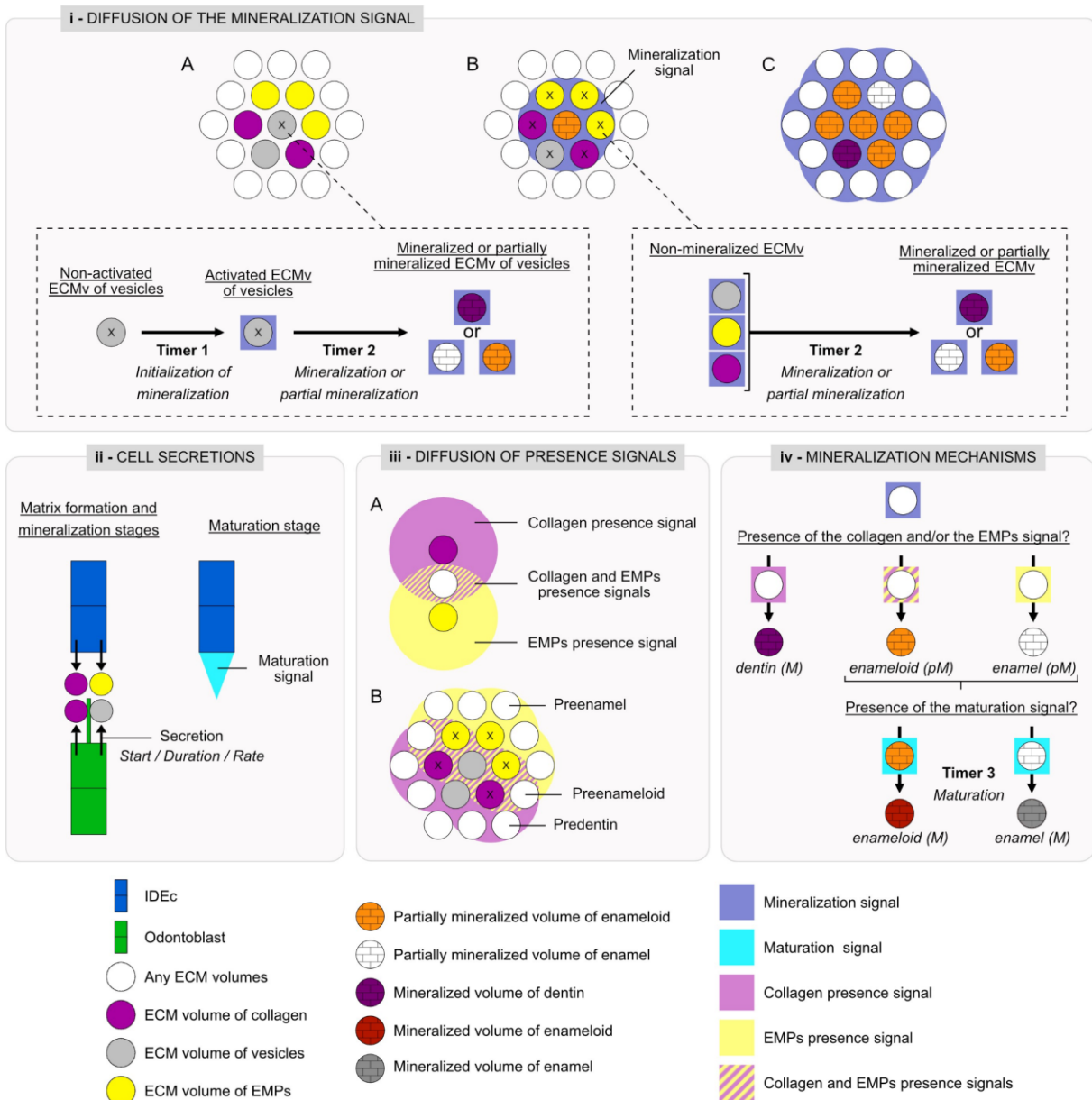


FIGURE II-2. Model mechanisms. M, mineralized. pM, partially mineralized. ECMv, the volume of extracellular matrix. EMPs, enamel matrix proteins. IDEc, cell of the inner dental epithelium.

During matrix formation, ECMv (collagen, vesicles and/or EMPs) are secreted by odontoblasts and/or IDEc just off their respective apical poles, that is, in between the two (sub)epithelial sheets (Fig. II-2ii, 3) (Berkovitz & Shellis, 2016). Spheres of ECMv are considered cohesive (set via a cohesion property in EmbryoMaker), which constrains their spacing. They have the possibility to move along the z axis, and also on the x-y plane (within the limit of the physical boundaries previously introduced) as they have a smaller diameter than cells. Because it has been suggested that EMPs can invade the ECM (Shellis & Miles, 1974; Fanchon *et al.*, 2004; Goldberg *et al.*, 2004; Sasagawa *et al.*, 2019; Kawasaki *et al.*, 2021), we set the corresponding EMP volumes as particularly motile (we attribute them a displacement property in EmbryoMaker). Furthermore, once secreted, vesicle volumes are associated with an activation timer (*timer 1*, arbitrarily defined as 1000 iterations) (Fig. II-2i) that delays the start of mineralization locally, whereas both EMP and collagen volumes ‘diffuse’ in their close vicinity (Fig. II-2iii) a non-physical ‘*presence signal*’ that conditions the matrix nature of neighboring ECMv: once a given ECMv is about to mineralize (that is, once *timer 1* goes off), its mineralization status depends on the presence of collagen and/or EMPs in its vicinity (that is, whether the *presence signals* of the corresponding proteins has reached this ECMv). If only collagen is ‘sensed’ in the vicinity, the corresponding ECMv becomes a volume of predentin. If only EMPs are sensed, it becomes a volume of preenamel and if both collagen and EMPs are sensed, then it becomes a volume of preenameloid (we consider that similar EMPs, or EMPs-like, are involved in enameloid and enamel formation). The secreting cells are set to be ‘repulsed’ by ECMv, which means they tend to move away from their secretions as those accumulate at the interface (Fig. II-3). The positions of odontoblasts are monitored through the simulation and their trajectories are used to display avatars of their processes, whose distribution may be used as a criteria (Sasagawa, 2002; Davit-Beal *et al.*, 2007; Sasagawa *et al.*, 2019; but see also Chapter I).

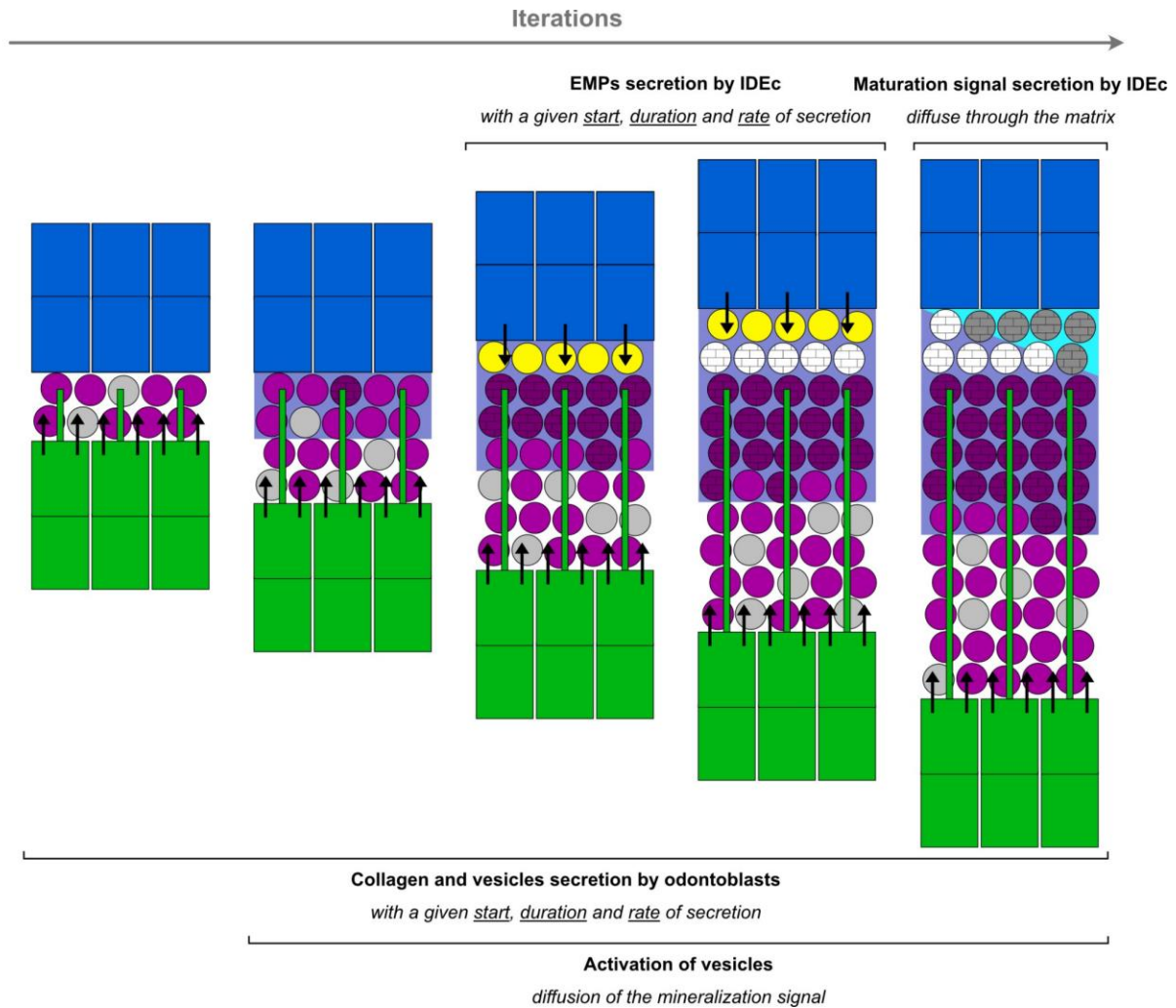


FIGURE II-3. Illustration of a simulation run, with an example of dentin-enamel formation. For the sake of simplicity, some mechanisms are not shown. See Figure II-2 for a legend.

Once the mineralization starts (that is when the vesicle activation timer *timer 1* goes off), a mineralization timer (*timer 2*, arbitrarily defined as 250 iterations) is set that models that (partial) mineralization actually takes time (Fig. II-2i). When *timer 2* goes off, vesicle volumes either mineralize in dentin (MTv) or partially mineralize in enameloïd or enamel (pMTv) depending on the nature of the matrix (predentin, preenameloïd, preenamel), itself depending on the presence signals of collagen and EMPs (Fig. II-2iv). Then these newly mineralized volumes diffuse in turn a non-physical signal of mineralization to the neighboring volumes of ECM (ECMv, Fig. II-2i), which sets the mineralization timer (*timer 2*) for those ECMv, thereby spreading a

wave of mineralization throughout the ECM volumes. Volumes of mineralized dentin (MTv) are set to be fixed in space and to block the diffusion of signals other than the mineralization signal and the displacement of EMP volumes. We have not considered the possibility that EMPs may play the role of nucleation spots for the mineralization: here only the vesicles play this role.

During tissue maturation, 1000 iterations after the end of collagen and EMPs secretion, IDEc change their secretory behaviors. They start to diffuse a non-physical signal of maturation throughout the ECMv and pMTv (Fig. II-2ii, 3). When received by a pMTv, this signal starts a timer of maturation in these volumes, which enables their mineralization (hypermineralization) (Fig. II-2iv). This timer corresponds to the time of degradation and removal of the organic matter (like collagen and EMPs) by maturation proteins, and also the time to crystals to grow larger (timer 3, arbitrarily defined as 250 iterations) (Sasagawa, 2002; Sasagawa *et al.*, 2009; Margolis *et al.*, 2014; Berkovitz & Shellis, 2016). These proteins are not represented by real volumes because, *in vivo*, they do not participate in the volume gain. Indeed, at the maturation stage, future hypermineralized tissues have reached their full thickness (Berkovitz & Shellis, 2016). As previously explained (see the previous paragraph about the mineralization stage), MTv keep a fixed position and block the diffusion.

After a given number of iterations (here 1000 iterations after the end of EMPs and collagen secretion), IDEc change their secretory behavior: instead of secreting EMPs and collagen, they start to secrete maturation proteins, here modeled as a diffusive, non-physical signal of maturation that spreads through the volumes of ECM (ECMv) and the volumes of partially mineralized tissues (pMTv, Fig. II-2ii, 3). Once a pMTv detects such signal of maturation, it sets a maturation timer (*timer 3*, arbitrarily defined as 250 iterations) (Fig. II-2iv), which models the time necessary for the degradation and removal of the organic matter (like collagen and EMPs) by proteases, and the time necessary for crystals to grow larger (Sasagawa, 2002; Sasagawa *et al.*, 2009; Margolis *et al.*, 2014; Berkovitz & Shellis, 2016). These maturation proteins are

not modeled using volumes (spheres) because, *in vivo*, they do not participate in the volume gain: it has been documented that hypermineralizing tissues already reach their full thickness before maturation (Berkovitz & Shellis, 2016).

Role of parameters

Exploration of the parameter space

In the final model there are 12 parameters of interest: when the two types of secreting cells start to secrete any of the three types of ECM, how long they do so and with what secretion rate. We have scanned those 12 parameters extensively, thereby exploring the 12-dimension parameter space, and we have quantified the proportions of enameloid and enamel in the resulting outputs (Tab. II-1). Varying the initialization time for IDEc relative to odontoblasts (1) allows us to test the hypothesis of delayed epithelial cell activity (H1) (Shellis & Miles, 1974). Similarly, varying the time period during which IDEc secrete EMPs (2) allows us to test the hypothesis of a prolonged epithelial cell activity (H2) (Poole, 1971), and varying the relative rates at which they secrete either collagen or enamel proteins (3) allows us to test for a modification of the epithelial cells' production activity (H3) (Assaraf-Weill *et al.*, 2014) (Tab. II-1). The other variables are used to explore alternative scenarios.

In order to explore both the independent and interaction impacts of the parameters, we have performed a multidimensional grid search, rather than a random search (Fig. II-4A). We have run 551 124 simulations with different initial conditions (see Table II-1 for details). The computations have been performed on an intensive computing platform (Plateforme de Calcul Intensif et Algorithmique PCIA, Muséum national d'histoire naturelle, Centre national de la recherche scientifique, UAR 2700 2AD, CP 26, 57 rue Cuvier, F-75231 Paris Cedex 05, France).

TABLE II-1. List of input parameters, their range of variation and associated hypotheses. For the ‘Start’ parameters, iteration 1 corresponds to a secretion at the beginning of the simulation, iteration 6001 to a secretion when the mineralization front is already formed (when vesicles are secreted at the first iteration), and iteration 3001 to a secretion at an intermediate stage during which the mineralization front is forming (when vesicles are secreted at the first iteration). For duration and rate values, we have explored one order of magnitude between extreme cases. A duration of 1000 iterations allows secretion to cease before the formation of the mineralization front, while 10000 iterations correspond to secretion that continues after the front formation. RCE may take the value of zero, because IDEc do not secrete collagen during enamel formation. We have performed an entire grid search, except for the multiple similar simulations presenting a RCE of 0 where it is not necessary to explore the impact of SCE and DCE. For H1 and H2 IDEc are assumed to secrete only EMPs (no epithelial collagen). 'volume', adimensional volume. +, increase. -, decrease.

Input parameters	Abbreviations	Hypotheses	Variation			
Start of collagen secretion by odontoblasts (<i>iteration</i>)	SCO	/	1	3001	6001	
Start of vesicles secretion by odontoblasts (<i>iteration</i>)	SVO	/	1	3001	6001	
Start of collagen secretion by IDEc (<i>iteration</i>)	SCE	/	1	3001	6001	
Start of EMPs secretion by IDEc (<i>iteration</i>)	SEE	H1 (SEE+)	1	3001	6001	
Duration of collagen secretion by odontoblasts (<i>iterations</i>)	DCO	/	1000	5500	10000	
Duration of vesicles secretion by odontoblasts (<i>iterations</i>)	DVO	/	1000	5500	10000	
Duration of collagen secretion by IDEc (<i>iterations</i>)	DCE	/	1000	5500	10000	
Duration of EMPs secretion by IDEc (<i>iterations</i>)	DEE	H2 (DEE+)	1000	5500	10000	
Rate of collagen secretion by odontoblasts (<i>volume/iteration</i>)	RCO	/	0.1	0.55	1	
Rate of vesicles secretion by odontoblasts (<i>volume/iteration</i>)	RVO	/	0.1	0.55	1	
Rate of collagen secretion by IDEc (<i>volume/iteration</i>)	RCE	H3 _{1/2} (RCE-)	0	0.1	0.55	1
Rate of EMPs secretion by IDEc (<i>volume/iteration</i>)	REE	H3 _{2/2} (REE+)	0.1	0.55	1	

Simulations are set to end when the mineralization and the maturation are stabilized. At the end of each simulation, we compute the following outputs: (1) the amount of each ECM_v, pMT_v and MT_v, (2) the stacking order of tissues, (3) the order in which tissues mineralized (partially or fully), (4) the respective polarities of partial mineralization, mineralization and maturation, (5) the presence ratio of odontoblast processes in tissues, and (6) the cellular origin of tissues (proportion of production by odontoblasts and IDEc).

Data analysis

As a preprocessing step, we have screened the outputs and retained only the simulations that satisfy a set of eligibility criteria based on biological observations:

- 1) Either enameloid or enamel must be present.
- 2) The stacking order of tissues must be (dentin)-enamel, (dentin)-enameloid, or (dentin)-enameloid-enamel from the bottom to the top (Fig. II-4A). Volumes of partial or full mineralization (pMT_v, MT_v respectively) are not distinguished here.
- 3) In simulations of dentin+enamel, dentin must mineralize first.
- 4) The polarity of mineralization must primarily be toward the odontoblasts for dentin and toward the IDEc for partially mineralized enameloid and enamel.
- 5) For enamel, the polarity of maturation must primarily be toward the junction. No such constraint is imposed for enameloid because of a lack of experimental data.
- 6) The dentin and enamel volumes (either partially or fully mineralized) must be, respectively, mostly (>95%) of mesenchymal and epithelial origin, while enameloid must be of dual origin ($5\% \leq \text{mesenchymal origin} \leq 95\%$).
- 7) The presence ratio of odontoblast processes must be high in dentin ($\geq 90\%$), significant in enameloid ($\geq 5\%$) and negligible in enamel (<5%). pMT_v and MT_v are not distinguished here. Note that odontoblast processes may be found in enamel (notably known as enamel spindles). Their formation process is not explicitly considered in the current model.

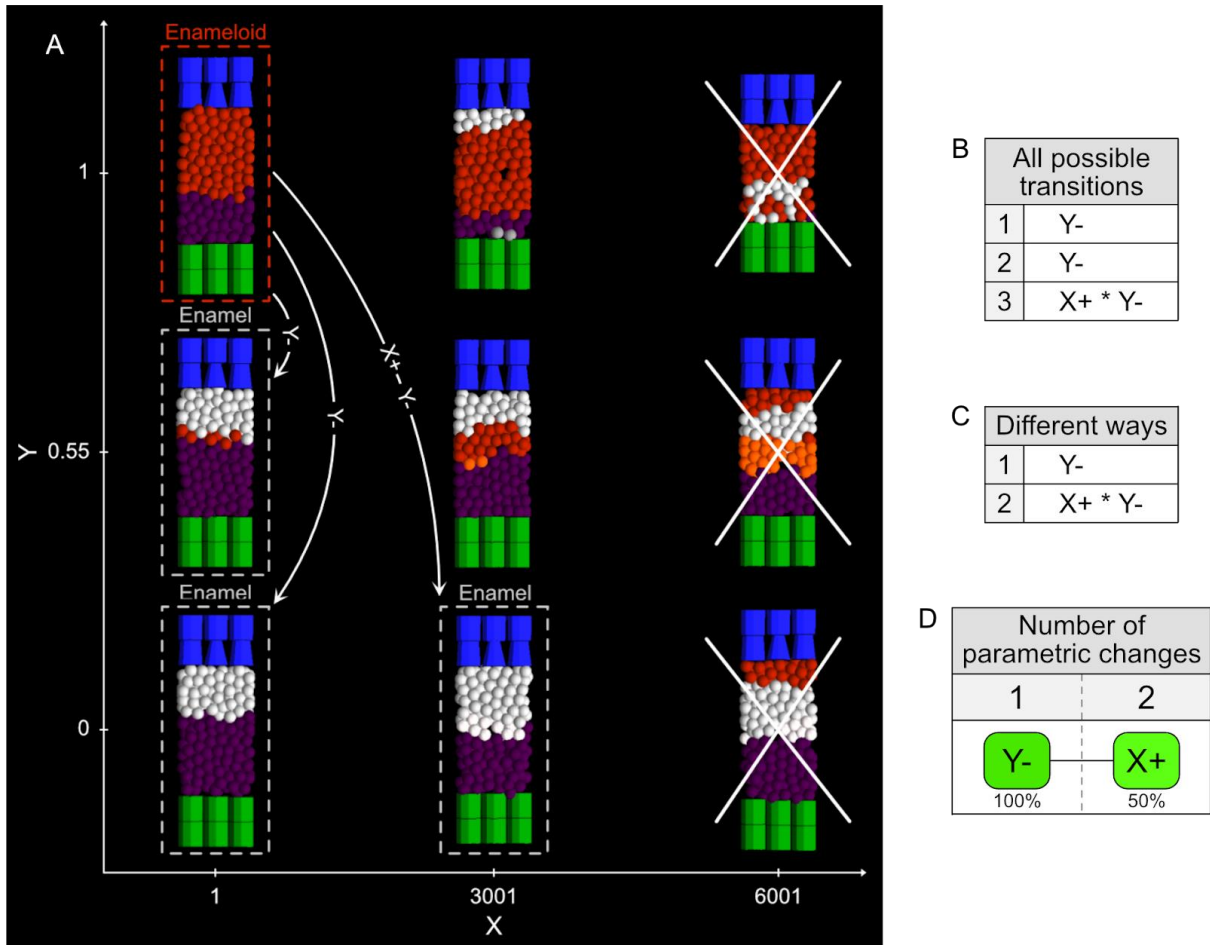


FIGURE II-4. A, a fictional example of a 2D (X, Y) parameter space to illustrate the selection process and the identification of the diversity of possible transitions. In this study, the same methodology is used on a 12D parameter space (see Tab. II-1). Enamel and enameloid cases respectively correspond to the simulations with a $P_{enamel} > 95\%$ and with a $P_{enamel} < 5\%$ (dotted boxes). White crosses indicate simulations that are filtered out using the criteria about tissue stacking order (six other criteria are also used in the study). White arrows show the several enameloid to enamel transitions and their associated parameter changes. B, the three possible transitions. C, the two different ways to do the transition. D, the *primary transition* 'Y-' (composed by one *primary shift*) sufficient to carry out the transition, and the *additional shift* 'X+', with their respective implication rate. The legend of the model components is available in Fig. II-2. +, increase. -, decrease.

In order to determine which developmental shifts may induce a complete (dentin)-enameloid to (dentin)-enamel transition, we have focused our analysis on simulations having a significant ratio of enamel versus enameloid ($Penamel > 95\%$), or vice versa ($Penamel < 5\%$), with:

$$Penamel = \frac{(Q_{enamel} + Q_{partialenamel}) \times 100}{Q_{enamel} + Q_{partialenamel} + Q_{enameloid} + Q_{partialenameloid}}$$

Where $Penamel$ is the percentage of enamel formed compared to the total amount of enamel and enameloid, and Q is the amount of given pMTv or MTv at the end of a simulation. Note that we considered pMTv and MTv to calculate this proportion to avoid the exclusion of not fully matured enamel or enameloid. We end up with two categories of simulations: (1) simulations that lead to the formation of (dentin)-enameloid ($Penamel < 5\%$, enameloid case), and (2) those that lead to the formation of (dentin)-enamel ($Penamel > 95\%$, enamel case) (Fig. II-4).

In order to visualize the influence of input parameters on the distribution of enamel and enameloid cases we have performed a PCA on the resulting reduced dataset using the package FactoMineR (Lê, Josse & Husson, 2008) on Rstudio (Team, 2020). In order to determine which input parameters maximize the separation between enamel and enameloid cases we have performed a LDA using the package MASS (Ripley *et al.*, 2013) (code available in Appendix II.6).

All possible transitions between the enameloid and enamel cases have been analysed by comparing in each pair of simulations the input parameters one by one (Fig. II-4A). For each comparison, the differences in input parameters have been recorded as developmental shifts, associated with a polarity of variation ('+' for increase, '-' for decrease) (Fig. II-4B). We have then compiled all the sets of possible developmental shifts (Fig. II-4C) and extracted the parameter shifts or associations of parameter shifts that may be considered as sufficient for an enameloid-enamel transition (those are referred to as '*primary shifts*', forming '*primary transitions*', as

opposed to '*additional shifts*', which may be combined with '*primary shifts*') (Fig. II-4D). In addition, the implication rate, that is the frequency at which a particular *primary shift* or *additional shift* is involved in all possible sets of developmental shifts that may lead to an enameloid-enamel transition, is used to rank the different scenarios (Fig. II-4D).

II.3. Results

Among the 551 124 simulations computed with different initial conditions, 42 571 have been retained using the 7 criteria presented in part II.2. They correspond to the simulations that fit most with the biological observations made on extant forms of dentin, enameloid and enamel. Among those, 33 435 simulations correspond to 'enameloid cases' ($P_{\text{enamel}} < 5\%$) and 1 913 to 'enamel cases' ($P_{\text{enamel}} > 95\%$).

To have a first global idea of the link between the parameters and the production of enamel or enameloid, we performed a PCA on all the input parameters as well as a binary output variable (enamel or enameloid). The first two axes of the PCA, which represent 25.2% of the variance (12.9% and 12.3% respectively; supplementary Tab. II-4), do not allow us to clearly distinguish between enameloid and enamel cases due to an important overlapping (Fig. II-5). The axes are essentially driven by DEE, DCE and, to a lesser extent, SVO in the case of the first axis, and SVO, SCO and, to a lesser extent, DEE in the case of the second one. This analysis seems to suggest that there are many ways to produce enamel or enameloid with our model.

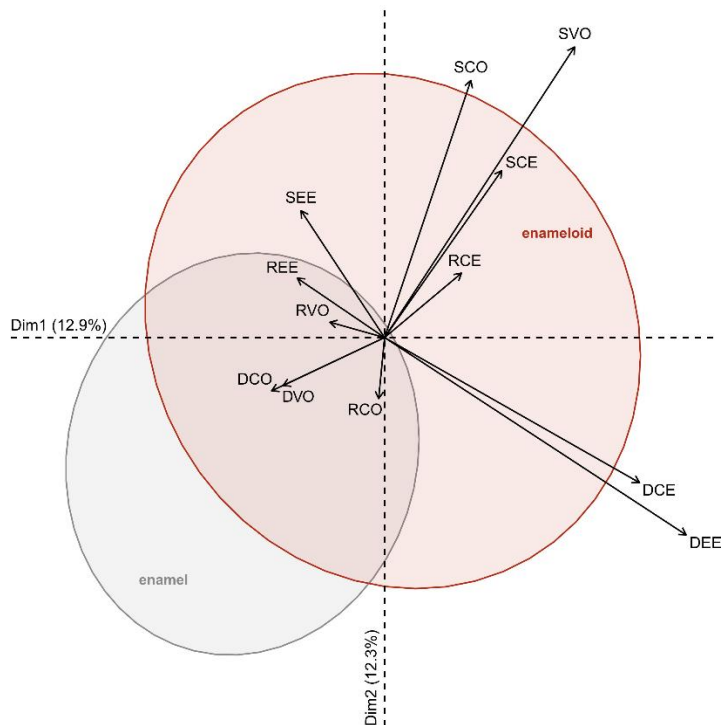


FIGURE II-5. PCA of the enamel and enameloid cases. Ellipses encompass 95% of enamel and enameloid data (points not displayed for readability). Results of the PCA are given in the Table 1 of the supplementary data.

In order to determine which input parameters maximize the separation between enamel and enameloid cases we have performed a LDA. The LDA shows that enamel cases tend to be characterized by smaller values of SVO, DCE, and, to a lesser extent, SCO, as suggested also by the PCA. It reveals also that enamel cases tend to be associated with a larger SEE or DEE and a smaller RCE. The LDA corroborates the idea that there are several possible shifts to induce a transition.

In order to better identify the parameter shifts that can lead to a transition, in particular those that may be necessary or sufficient, we have run 63 961 155 comparisons of the initial conditions for all pairs of enameloid and enamel cases (that is, a comparison corresponds to a transition between enameloid and enamel) (Fig. II-4B). After consolidation, we have identified 186 355 unique combinations of 1 to 12 parameter changes, that is, different ways to induce an enameloid to enamel transition (Fig. II-4C). Among those, 38 parameter changes or associations of parameter changes are considered as sufficient on their own and constitute a set of independent *primary transitions* (Fig. II-6, supplementary Tab. II-3).

These *primary transitions* hence correspond to 38 independant ways to induce the transition, and each of them combine 1 to 6 *primary shift(s)*. All 186 355 different transitions necessarily include one or more of these 38 *primary transitions*, plus various *additional shifts*. They are more or less present among the 186 355 transitions, as highlighted by their implication rate (Fig. II-6, supplementary Tab. II-3).

Of the three main hypotheses encountered in the literature, only H1 corresponds to a *primary transition*, that is, H1 may explain an enameloid-enamel transition on its own. Moreover, its implication rate is high (53.0%; Fig. II-6 number 2, supplementary Tab. II-3 *primary transition 2*).

TABLE II-2. Correlation values of input parameters with the axe of the LDA, ordered in absolute. Positive values of correlation mean that the input parameter is higher in enameloid than in enamel cases. Cross validation has a success rate of 99.5%.

Input parameters	Abbreviations	Correlation values
Start of vesicles secretion by odontoblasts	SVO	0.68
Start of EMPs secretion by IDEc	SEE	- 0.45
Rate of collagen secretion by IDEc	RCE	0.29
Duration of collagen secretion by IDEc	DCE	0.28
Duration of vesicles secretion by odontoblasts	SCE	0.20
Start of collagen secretion by IDEc	DVO	-0.19
Rate of vesicles secretion by odontoblasts	RVO	- 0.17
Duration of EMPs secretion by IDEc	DEE	- 0.14
Start of collagen secretion by odontoblasts	SCO	0.14
Duration of collagen secretion by odontoblasts	DCO	- 0.11
Rate of collagen secretion by odontoblasts	RCO	- 0.09
Rate of EMPs secretion by IDEc	REE	0.04

H2 must be combined with at least one other parameter shift. The highest implication rate of H2 is as an *additional shift* in combination with the *primary transition* SVO- (21,8%), or in combination with DVO+ (14.6%) as a pair forming a *primary transition* (Fig. II-6 number 7, supplementary Tab. II-3 *primary transition* 7).

The two parameter changes corresponding to H3 also need to be combined with at least one other parameter, but the two are never found in combination within the same *primary transition*. Their highest implication rates within a *primary transition* are found when H3_{1/2} is in interaction with SCE+ (10,8%), and H3_{2/2} with SCO- (10.7%) (Fig. II-6 number 11, 12; supplementary Tab. II-3 *primary transitions* 11, 12). As *additional shifts*, their highest implication rates are found when they are combined with the *primary transition* SVO- (22.3% for H3_{1/2}, 19.7% for H3_{2/2}), as for H2 (Fig. II-6 number 1).

Many *primary transitions* correspond to or combine parameter changes that have never been proposed as such in the literature (SCO-, SCO+, SCE-, SCE+, DCO-, DCO+, DVO-, DVO+, DCE-, DCE+, RCO-, RCO+, RVO+, RCE+ and REE-; supplementary Tab. II-3). Among them, several can induce a transition by themselves (SVO-, RVO+, SCE-, SCO+ and RCO-). SVO- stands out for its very high implication rate (58.6%; Fig. II-6 number 1; supplementary Tab. II-3 *elementary changes* 1). Finally, only four (SVO+, SEE-, DEE- and RVO-) of the 24 possible parameter changes are never involved in any of the 38 *primary transitions*.

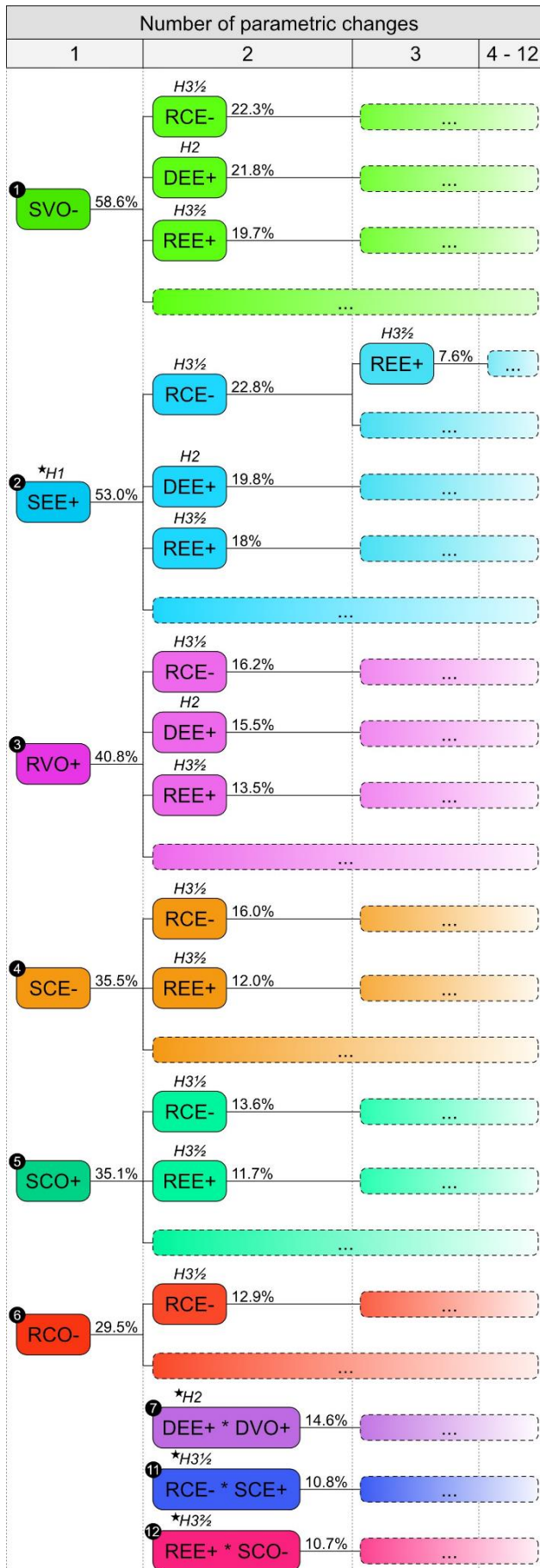


FIGURE II-6. Partial illustration of the compiled *primary changes*, forming *primary transitions*, and their optional *additional shifts* that may induce an enameloid-enamel transition (see supplementary Tab. II-3 for a full list of *primary transitions*). Each independent transition pathway is associated with a different color, the leftmost box corresponding to the *primary transition* itself and the other boxes corresponding to *additional shifts*. When several parameter changes are indicated within a single box, they need to be combined (symbol *) to induce the transition. The *primary transitions* are ranked by decreasing implication rates (to the right of each box). The main hypotheses of the literature are indicated as H1, H2, H3½ and H3¼, with stars corresponding to their highest implication rate in a *primary transition*. See Table II-1 for the abbreviations. Dotted boxes represent *additional shifts* that are not detailed. +, increase in parameter value. -, decrease in parameter value.

II.4. Discussion

Impact of parameters and underlying mechanisms

The results of the PCA (Fig. II-5, supplementary Tab. II-4) and LDA (Tab. II-2) suggest parameter changes that may favor enameloid-to-enamel transitions (such as SVO-, SEE+ (H1), or DCE-), but they do not confirm the ability of these parameter changes to induce a complete transition through their modification alone. It is also difficult to have access to the potential parameter interactions that are necessary for transitions. Therefore, it is not possible to test the relevance of the three hypotheses and to clearly identify different independent manners to induce the transition with the PCA and LDA. The data analysis developed for this study, based on one by one comparison of the initial conditions of each enameloid and enamel cases (Fig. II-4A), solves these problems.

The comparative analysis revealed 38 independent ways to achieve transitions between enameloid and enamel (Fig. II-6, supplementary Tab. II-3). These *primary transitions* imply between one to six developmental shift(s) in combination. In the following we analyse the main modalities of transition in order to extract the main mechanisms and how they can be combined to induce an histogenetic transition (Fig. II-7, 8).

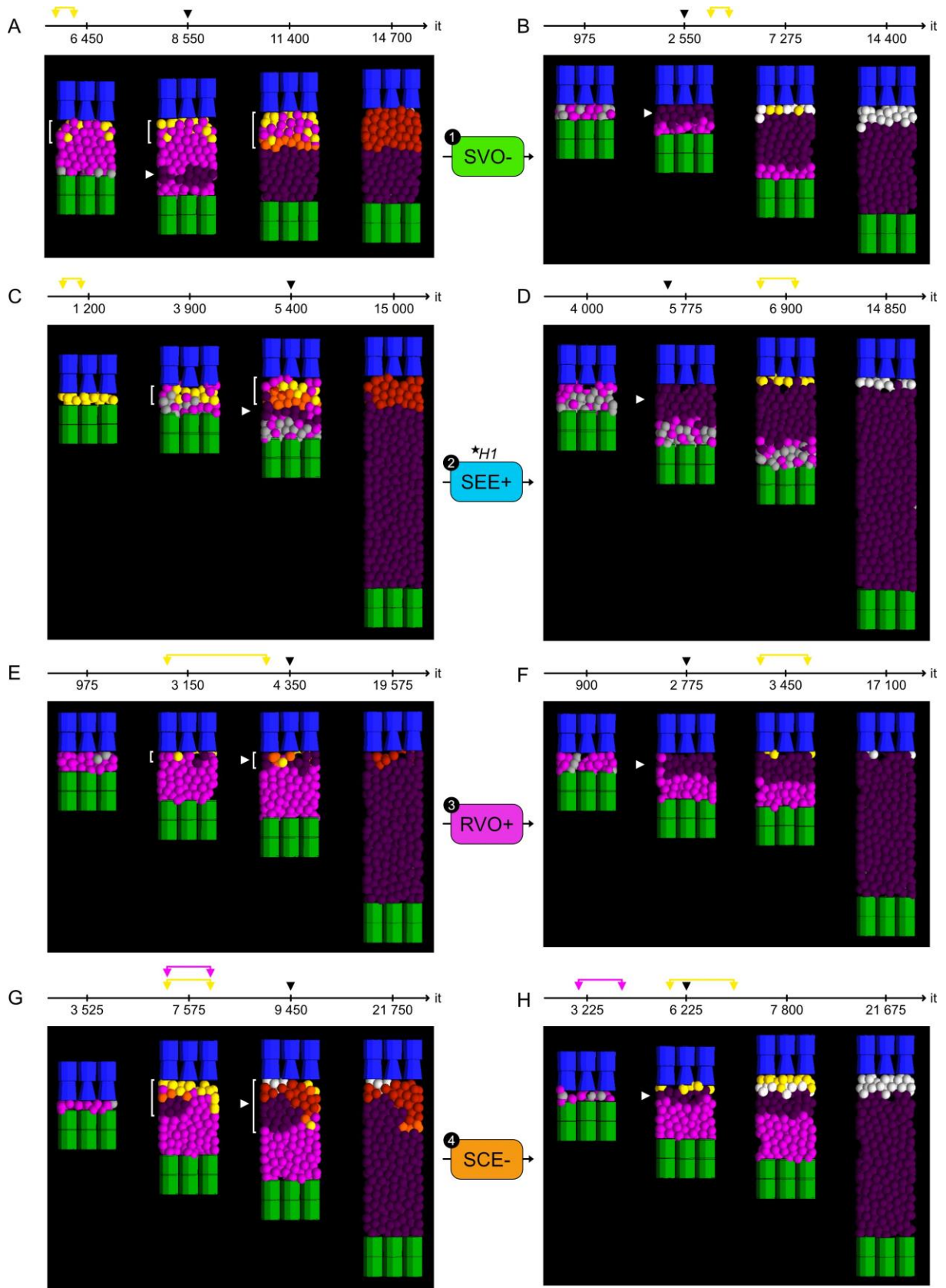
Among the three introduced hypotheses of developmental shift(s), H2 and H3 are partially rejected in the exploration of this model. Indeed, H2 (DEE+), a prolonged epithelial cell activity (Poole, 1971), has to be in interaction with at least one more parameter change, such as DVO+, to induce a transition (Fig. II-6 number 7). However, H2 interacts with other parameter changes in a number of *primary transitions* (supplementary Tab. II-3 *primary transitions* 7, 8, 19-21, 23, 25-28, 30, 31 and 33-36), suggesting that DEE+ strongly promotes enamel formation. In addition to another parameter change(s), such as DVO+ favoring a faster mineralization of the front close

to IDEc, DEE+ promotes the formation of a great amount of EMPs above a small amount of collagen already present in the matrix, leading to the formation of a small quantity of enameloid at the junction under a greater quantity of enamel (Fig. II-7 number 7, II-8).

Concerning H3, a modification of the epithelial cells' production (from mostly collagen to mostly enamel proteins) (Assaraf-Weill *et al.*, 2014), the two parameter changes associated are not been found in interaction in a same *primary transition*. However, they can independently explain transitions when they are in interaction with other developmental changes, such as SCE+ for H3_{1/2} (RCE-) and SCO- for H3_{2/2} (REE+) (Fig. II-6 numbers 11 and 12). H3_{1/2} facilitates enamel formation by reducing the quantity of epithelial collagen produced compared to that of EMPs, but the transition is mainly possible due to the production delay, preventing simultaneous secretion (Fig. II-7 number 11, II-8). H3_{2/2} promotes enamel formation by increasing the number of EMPs produced compared to that of collagen present under the IDEc, but it requires a faster mineralization front formation primarily (Fig. II-7 number 12, II-8). The *primary transition* number 15 emphasizes more on the underlying mechanisms related to H3. The reduction of RCE and DCE unbalances the formation of epithelial collagen and EMPs, limiting the formation of a thick layer of blend (Fig. II-7 number 15, II-8). However, a faster formation of the mineralization front close to IDEc remains necessary.

Only H1 (SEE+), a delayed epithelial cell activity (Shellis & Miles, 1974), can explain a transition on its own, and this shift is frequently involved (Fig. II-6 number 2), thereby corroborating the results of the LDA (Tab. II-2). The delayed secretion of EMPs enables the formation of the mineralization front close to IDEc before the presence of EMPs in the matrix, which will prevent its mix with previously secreted collagen (Fig. II-7 number 2, II-8). This late secretion of EMPs, relative to the timing of matrix mineralization near IDEc, is commonly observed *in vivo* during enamel formation, contrary to enameloid formation (Berkovitz & Shellis, 2016).

CHAPTER II – FROM ENAMELOID TO ENAMEL



CHAPTER II – FROM ENAMELOID TO ENAMEL

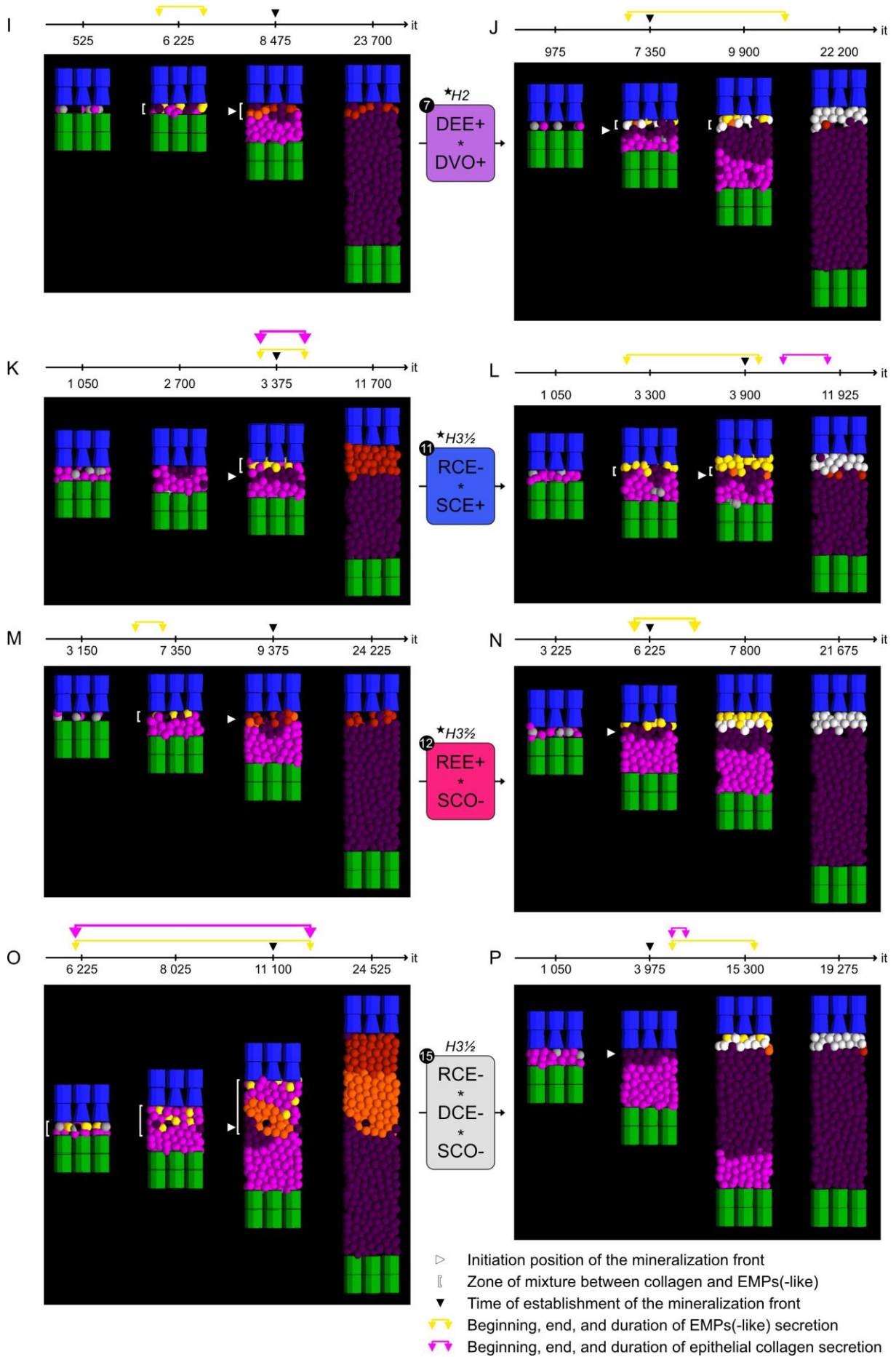


FIGURE II-7. Illustration of the differences between enameloid (A, C, E, G, I, K, M and O) and enamel (B, D, F, H, J, L, N and P) formation for various *primary transitions*. A-F, secretion of EMPs before the mineralization front formation near IDEc (enameloid), versus after due to a faster and closer mineralization (A, B), a delayed secretion of EMPs (C, D), or a faster mineralization (E, F) (enamel). G, H, balanced secretion of epithelial collagen and EMPs (enameloid), versus unbalanced secretions and faster mineralization near IDEc (enamel). I, J, end of EMPs production before the front formation (enameloid), versus production continuing after the front formation due to a longer secretion duration and a faster mineralization (enamel). K, L, simultaneous secretion of epithelial collagen and EMPs (enameloid), versus delayed due to a later secretion of the collagen, also promoted by a reduction of its rate of secretion (enamel). M, N, termination of EMPs production before the formation of the front (enameloid), versus production continuing after the formation of the front due to a faster mineralization and a higher rate of EMPs secretion (enamel). O, P, balanced secretion of epithelial collagen and EMPs (enameloid), versus unbalanced secretions, also promoted by faster mineralization close to IDEc (enamel). The legend for the components is available in Figure II-2. Complete dynamic simulations are given in the Appendix II.6. it, iterations.

Five other, hitherto unsuspected, parameter changes can also explain transitions on their own, and with great implication rates (Fig. II-6 numbers 1 and 3-6). Variation in the start of matrix vesicles secretion by odontoblasts (SVO-) stands out with the higher implication rate (Fig. II-6 number 1), corroborating the results of the PCA and LDA (Fig. II-5 and Tab. II-2). If matrix vesicles are secreted late relative to collagen production, it shifts away, both in time and space, the formation of the early mineralization front (Fig. II-7 number 1, II-8). This dual impact of SOV- on the timing and position of the early mineralization front constrains the timing of the matrix mineralization in front of IDEc. Finally, depending on the presence of a mineralized isolating layer in front of IDEc, EMPs secreted by IDEc will be more or less able to mix with previously secreted collagen, and thus to form enameloid. The establishment of an early mineralization front closer to odontoblasts than to IDEc, as obtained in the model with a late secretion of matrix vesicles, is a feature observed *in vivo* during

enameloid formation (see Chapter I). Even though a late secretion of matrix vesicles has not been noticed *in vivo*, Sasagawa (1988) highlighted a delayed activation of the matrix vesicles during enameloid formation in teleosts, with similar consequences (a late initiation of mineralization and closer to odontoblasts than IDEc). Similarly, the other *primary transitions* involving a single parameter shift also affect the timing (Fig. II-7 numbers 3, 4), or both the timing and position, of the mineralization front initialization (Fig. II-8 numbers 3-6), suggesting those are key to such transitions, they may be themselves induced by several independent developmental changes.

Concerning the *primary transition 4*, a case with no enamel formation on the enameloid layer was achieved only once, despite several attempts. This suggests that this parameter change may ultimately not allow a complete transition between enameloid and enamel. The reduction of SCE- is supposed to prevent the simultaneous secretion of epithelial collagen and EMPs and promote a faster formation of the mineralization front.

Application of these results for in vivo studies

The diversity of independent ways (*a minima* the 38 *primary transitions*) suggests that, if several independent transitions occurred during vertebrate evolution (Fig. I-3), their transitional modalities may have been quite different. It would be relevant to identify and compare the transition mechanisms for the different cases, in light of the *in silico* results presented here (Fig. II-6, 8, supplementary Tab. II-3).

Attention should be given to the role of the identified differences between enameloid or enamel formation in a transition. The possible addition of non-essential modifications to primary ones observed in our results suggests that they may also be present *in vivo*. They could correspond to derived developmental changes, evolving after a transition, and have to be distinguished from essential ones. For example, both a reduction in the rate of secretion of epithelial collagen (H3_{1/2}) and an increase in the

rate of secretion of EMPs (H3_{2/2}) have been documented *in vivo* during the ontogeny of urodeles (Assaraf-Weill *et al.*, 2014). However, as these changes are not found to define a *primary transition* (supplementary Table II-3), one of these changes at least may have evolved after the transition.

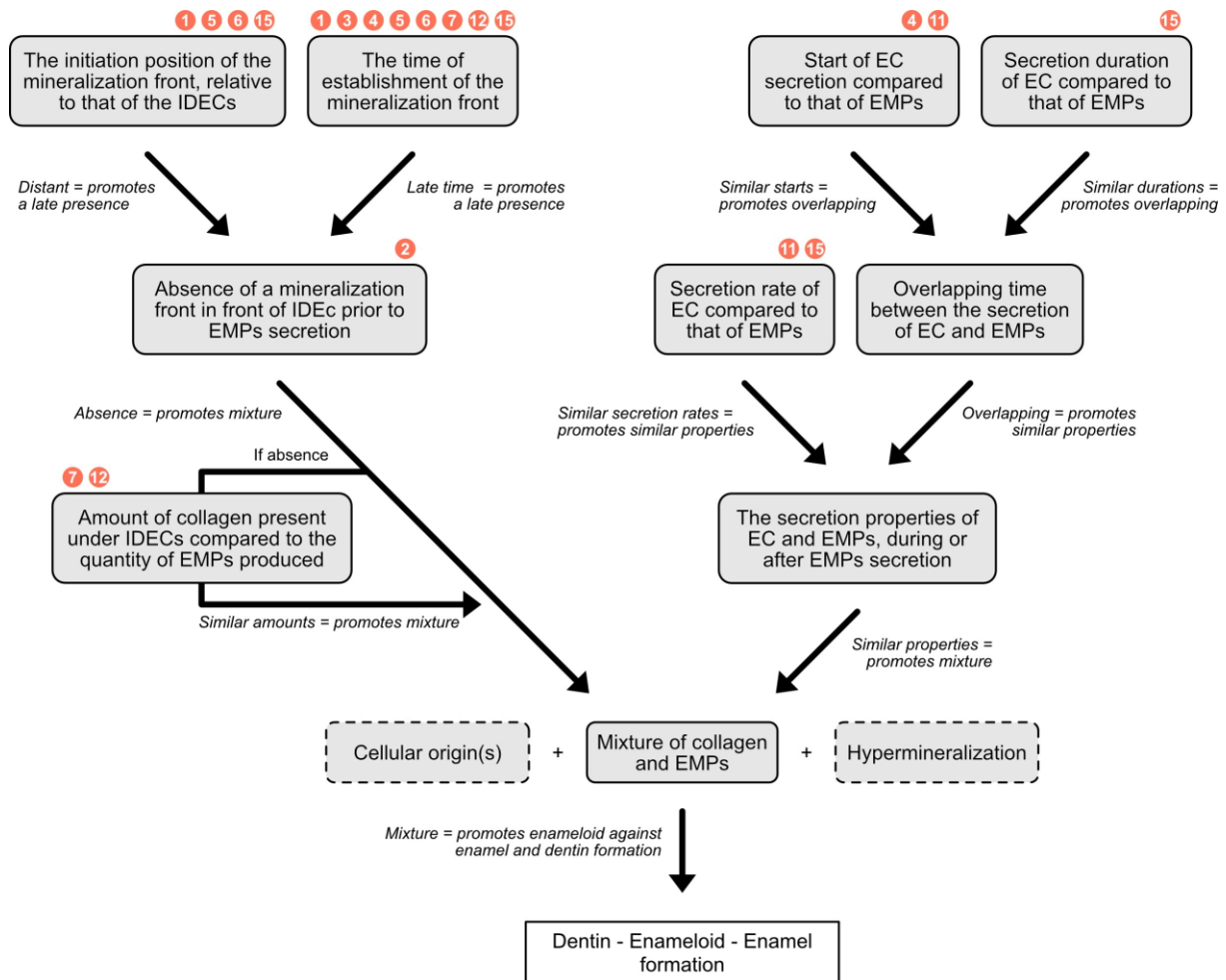


FIGURE II-8. Identified mechanisms controlling the amount of dentin, enameloid and enamel formed, and therefore, the transition between dentin-enameloid and dentin-enamel. Examples of developmental changes impacting these various mechanisms are provided (see *primary transition* numbers indicated in the orange circles). Note that certain *primary transitions* impact different mechanisms simultaneously (e.g. 1, 5, 6, 7 and 12). EC, epithelial collagen. EMPs, enamel matrix proteins (as well as EMPs-like with similar functions).

It is also important to remind that in the framework of this model and exploration, we considered that similar EMPs, or EMPs-like, are involved in enameloid and enamel formation, without considering the acquisition of new genes between these two cases. However, if different proteins, with different functions, are required to form enameloid and enamel, the transition will not depend on only few histogenetic developmental shifts (Berkovitz & Shellis, 2016).

II.5. Conclusion

Thanks to the development of a new histogenesis model and a novel multivariate analysis methodology, this study demonstrates the possibility of *in silico* transitions between enameloid and enamel through a few developmental shifts. There appear to be several independent pathways to achieve this transition, such as the modification of the timing of initiation of vesicle secretion, or of EMPs secretion (H1). On the other hand, the prolonged epithelial cell activity (H2) and the shift in epithelial cells' production from predominantly collagen to mostly enamel proteins (H3) do not enable transitions on their own within the frame of our model. In general terms, the timing of matrix mineralization in front of IDEc emerges as a major factor controlling the transition.

Acknowledgements. We warmly thank Roland ZIMM and Fayçal ALLOUTI for the assistance they provided in using EmbryoMaker and the intensive computing platform (PCIA).

Contributions. **Conceptualization** Guillaume Houée (GH), Nicolas Goudemand (NG), Jérémie Bardin (JB), Damien Germain (DG); **Data Curation** GH; **Formal Analysis** GH; **Investigation** GH; **Methodology** GH; **Project Administration** GH; **Resources** GH;

Supervision DG, NG, JB; Validation GH, NG, JB, DG; Visualization GH; Writing – Original Draft Preparation GH, NG, JB, DG.

II.6. Appendix

TABLE II-3. Complete list of the *primary transitions* allowing an enameloid to enamel transition and their implication rate. Inversely, the direction (increase or decrease) of parameter changes can be reversed to explain enamel to enameloid transitions. '+', increase in parameter value. '-', decrease in parameter value. '*', interaction between parameter changes.

<i>Primary transition number</i>	<i>Number of parameter changes</i>	<i>Primary shifts and hypotheses</i>	<i>Implication rate</i>
1	1	SVO-	58.6%
2	1	SEE+ (H1)	53.0%
3	1	RVO+	40.8%
4	1	SCE-	35.5%
5	1	SCO+	35.1%
6	1	RCO-	29.5%
7	2	DVO+ * DEE+ (H2)	14.6%
8	2	SCO- * DEE+ (H2)	12.2%
9	2	SCO- * DVO+	11.9%
10	2	SCO- * DCO+	10.8%
11	2	RCE- (H3 _{1/2}) * SCE+	10.8%
12	2	SCO- * REE+ (H3 _{2/2})	10.7%
13	2	RCO+ * SCO-	10.6%
14	2	SCO- * REE-	9.4%
15	3	SCO- * RCE- (H3 _{1/2}) * DCE-	5.8%
16	3	DCO+ * DVO+ * DCE-	5.6%
17	3	DVO+ * DCE- * REE+ (H3 _{2/2})	5.2%
18	3	DVO+ * DCE- * REE-	5.1%

CHAPTER II – FROM ENAMELOID TO ENAMEL

19	3	DCE- * REE- * DEE+ (H2)	5.0%
20	3	DCO+ * DCE- * DEE+ (H2)	4.9%
21	3	RCO+ * DCO+ * DEE+ (H2)	4.6%
22	3	DVO+ * SCE+ * DCE-	4.5%
23	3	DCO- * DCE- * DEE+ (H2)	4.3%
24	3	RCO+ * DVO+ * REE+ (H3 _{2/2})	4.2%
25	3	RCO+ * REE+ (H3 _{2/2}) * DEE+ (H2)	4.1%
26	3	DCO+ * REE+ (H3 _{2/2}) * DEE+ (H2)	4.0%
27	3	RCO+ * DCO- * DEE+ (H2)	3.9%
28	3	SCE+ * REE+ (H3 _{2/2}) * DEE+ (H2)	3.5%
29	3	RCO+ * DCO- * DVO+	3.5%
30	3	DCO- * REE+ (H3 _{2/2}) * DEE+ (H2)	3.3%
31	3	DCO- * DVO- * DEE+ (H2)	3.2%
32	4	DCO- * DVO+ * RCE- (H3 _{1/2}) * DCE-	1.9%
33	4	DCO- * RCE- (H3 _{1/2}) * REE- * DEE+ (H2)	1.7%
34	4	DVO- * DCE- * REE+ (H3 _{2/2}) * DEE+ (H2)	1.3%
35	5	RCE+ * SCE+ * DCE+ * REE- * DEE+ (H2)	0.60%
36	5	RCO+ * RCE+ * SCE+ * DCE+ * DEE+ (H2)	0.60%
37	6	RCO+ * DCO+ * RCE+ * SCE+ * DCE+ * REE+ (H3 _{2/2})	0.17%
38	6	RCO+ * DCO+ * DVO+ * RCE+ * SCE+ * DCE+	0.17%

CHAPTER II – FROM ENAMELOID TO ENAMEL

TABLE II-4. Results of the PCA.

	comp 1	comp 2	comp 3	comp 4	comp 5	comp 6	comp 7	comp 8	comp 9	comp 10	comp 11	comp 12
Eigenvalue	1,54226883	1,4819233	1,35714315	1,26934086	1,20778349	1,07501443	1,01420668	0,96338615	0,73445732	0,57808885	0,43894512	0,33744181
Percentage of variance	12,8522402	12,3493608	11,3095262	10,5778405	10,0648624	8,95845362	8,45172232	8,02821793	6,1204777	4,81740709	3,65787603	2,81201511
Cumulative percentage of variance	12,8522402	25,201601	36,5111273	47,0889678	57,1538302	66,1122838	74,5640061	82,5922241	88,7127018	93,5301089	97,1879849	100
RCO	-0,01440302	-0,14265062	0,17241625	0,15421526	0,37591293	0,27239503	0,77623773	-0,03294003	-0,23793621	0,22280281	0,02127812	0,00930103
SCO	0,21024079	0,60104986	0,31521741	-0,03200021	-0,43193014	0,12721096	0,31478697	-0,05439944	0,22399652	-0,06742639	-0,36624432	-0,02235567
DCO	-0,2752784	-0,1244502	0,68098153	-0,08948353	0,00904183	0,11658705	-0,41086735	0,20108547	-0,24665148	0,33307323	-0,20500396	0,01636484
RVO	-0,13309494	0,03592049	-0,017068	0,06377037	0,05107955	0,8787732	-0,13584786	0,32027867	0,1402028	-0,22308296	0,10385212	-0,02334206
SVO	0,46293074	0,67915562	0,07832925	0,1211096	-0,19490552	0,08558307	-0,12839962	-0,01216776	-0,26182962	0,19939452	0,33811171	0,13805861
DVO	-0,24731658	-0,11226468	0,7652414	-0,15517629	-0,18177408	-0,22054873	0,19583757	0,02053444	0,08550325	-0,30060796	0,31368148	0,00524223
RCE	0,18736472	0,15056828	-0,07322631	-0,68808372	0,19523524	-0,11524119	0,11816829	0,47264016	0,29298664	0,25151333	0,09811018	-0,12620151
SCE	0,28510138	0,38998704	0,17003403	-0,07224226	0,6775347	-0,13656769	-0,12003762	0,07254189	-0,28322847	-0,35626768	-0,11797192	-0,11857083
DCE	0,62138522	-0,33930155	0,20458606	0,52709657	-0,12855132	-0,04672457	-0,06276509	0,13931009	0,09946375	0,07067246	0,04727823	-0,3462518
REE	-0,21248157	0,13863844	-0,09026402	0,54187565	0,00837217	-0,32210707	0,11497353	0,68872791	0,04098825	-0,04585046	-0,05552476	0,18868159
SEE	-0,20347986	0,29646171	0,22776987	0,35776173	0,5201905	-0,02811812	-0,1511575	-0,30534137	0,51652566	0,17619264	0,06185098	0,04116974
DEE	0,73473599	-0,46117558	0,19010765	-0,12482664	0,14773186	0,0646036	-0,0456689	0,01097523	0,16394676	-0,06890582	-0,07837871	0,36025447

CHAPTER II – FROM ENAMELOID TO ENAMEL

TABLE II-5. Selected simulations to illustrate the 38 *primary transitions*. *, highlights parameter changes between the enameloid and enamel simulations.

<i>Primary transition number</i>	Tissue	Simulation	RCO	SCO	DCO	RVO	SVO	DVO	RCE	SCE	DCE	REE	SEE	DEE
1	Enameloid	235878	0.55	1	10000	0.55	6001*	1000	0	0	0	0.1	3001	10000
	Enamel	231342	0.55	1	10000	0.55	1*	1000	0	0	0	0.1	3001	10000
2	Enameloid	303517	0.55	3001	10000	1	3001	10000	0.55	3001	1000	0.55	1*	1000
	Enamel	303523	0.55	3001	10000	1	3001	10000	0.55	3001	1000	0.55	6001*	1000
3	Enameloid	408271	1	1	10000	0.1*	1	1000	0.1	1	1000	0.1	3001	1000
	Enamel	415075	1	1	10000	0.55*	1	1000	0.1	1	1000	0.1	3001	1000
4	Enameloid	469690	1	3001	10000	0.1	1	1000	0.1	6001*	1000	1	6001	1000
	Enamel	469609	1	3001	10000	0.1	1	1000	0.1	3001*	1000	1	6001	1000
5	Enameloid	424168	1	1*	10000	1	3001	1000	0.1	1	1000	1	6001	1000
	Enamel	485404	1	3001*	10000	1	3001	10000	0.1	1	1000	1	6001	1000
6	Enameloid	418120	1*	1	10000	0.55	3001	5500	0.1	1	1000	1	6001	1000
	Enamel	50704	0.1*	1	10000	0.55	3001	5500	0.1	1	1000	1	6001	1000

CHAPTER II – FROM ENAMELOID TO ENAMEL

7	Enameloid	530746	1	6001	10000	0.1	1	1000*	0.1	1	1000	0.1	6001	1000*
	Enamel	532260	1	6001	10000	0.1	1	10000*	0.1	1	1000	0.1	6001	10000*
8	Enameloid	530746	1	6001*	10000	0.1	1	1000	0.1	1	1000	0.1	6001	1000*
	Enamel	408276	1	1*	10000	0.1	1	1000	0.1	1	1000	0.1	6001	10000*
9	Enameloid	510325	1	6001*	5500	0.1	1	1000*	0	0	0	1	6001	1000
	Enamel	388609	1	1*	5500	0.1	1	5500*	0	0	0	1	6001	1000
10	Enameloid	510325	1	6001*	5500*	0.1	1	1000	0	0	0	1	6001	1000
	Enamel	408265	1	1*	10000*	0.1	1	1000	0	0	0	1	6001	1000
11	Enameloid	225904	0.55	1	10000	0.1	1	5500	1*	3001*	1000	1	3001	1000
	Enamel	225499	0.55	1	10000	0.1	1	5500	0.1*	6001*	1000	1	3001	1000
12	Enameloid	530827	1	6001*	10000	0.1	1	1000	0.1	3001	1000	0.1*	6001	1000
	Enamel	469609	1	3001*	10000	0.1	1	1000	0.1	3001	1000	1*	6001	1000
13	Enameloid	347011	0.55*	6001*	10000	0.1	1	1000	0	0	0	0.1	6001	1000
	Enamel	408247	1*	1*	10000	0.1	1	1000	0	0	0	0.1	6001	1000

CHAPTER II – FROM ENAMELOID TO ENAMEL

14	Enameloid	510325	1	6001*	5500	0.1	1	1000	0	0	0	1*	6001	1000
	Enamel	387844	1	1*	5500	0.1	1	1000	0	0	0	0.55*	6001	1000
15	Enameloid	531207	1	6001*	10000	0.1	1	1000	0.55*	6001	10000*	0.1	6001	10000
	Enamel	408438	1	1*	10000	0.1	1	1000	0.1*	6001	1000*	0.1	6001	10000
16	Enameloid	267685	0.55	3001	5500*	0.1	3001	1000*	0.1	1	5500*	0.1	6001	1000
	Enamel	288826	0.55	3001	10000*	0.1	3001	5500*	0.1	1	1000*	0.1	6001	1000
17	Enameloid	267685	0.55	3001	5500	0.1	3001	1000*	0.1	1	5500*	0.1*	6001	1000
	Enamel	268432	0.55	3001	5500	0.1	3001	5500*	0.1	1	1000*	1*	6001	1000
18	Enameloid	204196	0.55	1	5500	0.1	1	1000*	0.1	1	5500*	1*	3001	1000
	Enamel	204916	0.55	1	5500	0.1	1	5500*	0.1	1	1000*	0.55*	3001	1000
19	Enameloid	204196	0.55	1	5500	0.1	1	1000	0.1	1	5500*	1*	3001	1000*
	Enamel	204152	0.55	1	5500	0.1	1	1000	0.1	1	1000*	0.1*	3001	5500*
20	Enameloid	267775	0.55	3001	5500*	0.1	3001	1000	0.1	3001	5500*	0.55	6001	1000*
	Enamel	288162	0.55	3001	10000*	0.1	3001	1000	0.1	3001	1000*	0.55	6001	10000*
21	Enameloid	81655	0.1*	3001	5500*	0.1	1	1000	0	0	0	0.1	6001	1000*

CHAPTER II – FROM ENAMELOID TO ENAMEL

	Enamel	469484	1*	3001	10000*	0.1	1	1000	0	0	0	0.1	6001	5500*
22	Enameloid	224608	0.55	1	10000	0.1	1	1000*	0.1	1*	5500*	1	3001	1000
	Enamel	225499	0.55	1	10000	0.1	1	5500*	0.1	6001*	1000*	1	3001	1000
23	Enameloid	408307	1	1	10000*	0.1	1	1000	0.1	1	5500*	0.55	3001	1000*
	Enamel	387870	1	1	5500*	0.1	1	1000	0.1	1	1000*	0.55	3001	10000*
24	Enameloid	81655	0.1*	3001	5500	0.1	1	1000*	0	0	0	0.1*	6001	1000
	Enamel	449836	1*	3001	5500	0.1	1	5500*	0	0	0	0.55*	6001	1000
25	Enameloid	81655	0.1*	3001	5500	0.1	1	1000	0	0	0	0.1*	6001	1000*
	Enamel	265382	0.55*	3001	5500	0.1	1	1000	0	0	0	1*	6001	5500*
26	Enameloid	267739	0.55	3001	5500*	0.1	3001	1000	0.1	3001	1000	0.1*	6001	1000*
	Enamel	288162	0.55	3001	10000*	0.1	3001	1000	0.1	3001	1000	0.55*	6001	10000*
27	Enameloid	40864	0.1*	1	10000*	0.1	1	1000	0.1	1	1000	0.55	3001	1000*
	Enamel	387870	1*	1	5500*	0.1	1	1000	0.1	1	1000	0.55	3001	10000*
28	Enameloid	387940	1	1	5500	0.1	1	1000	0.1	3001*	1000	0.1*	3001	1000*

CHAPTER II – FROM ENAMELOID TO ENAMEL

	Enamel	388032	1	1	5500	0.1	1	1000	0.1	6001*	1000	0.55*	3001	10000*
29	Enameloid	40864	0.1*	1	10000*	0.1	1	1000*	0.1	1	1000	0.55	3001	1000
	Enamel	204916	0.55*	1	5500*	0.1	1	5500*	0.1	1	1000	0.55	3001	1000
30	Enameloid	408271	1	1	10000*	0.1	1	1000	0.1	1	1000	0.1*	3001	1000*
	Enamel	387870	1	1	5500*	0.1	1	1000	0.1	1	1000	0.55*	3001	10000*
31	Enameloid	473380	1	3001	10000*	0.1	3001	10000*	0.1	3001	1000	0.55	6001	1000*
	Enamel	452214	1	3001	5500*	0.1	3001	5500*	0.1	3001	1000	0.55	6001	10000*
32	Enameloid	510804	1	6001	5500*	0.1	1	1000*	0.55*	6001	10000	0.55	6001	10000
	Enamel	490851	1	6001	1000*	0.1	1	5500*	0.1*	6001	1000	0.55	6001	10000
33	Enameloid	408532	1	1	10000*	0.1	1	1000	0.55*	1	1000	1*	3001	1000*
	Enamel	387870	1	1	5500*	0.1	1	1000	0.1*	1	1000	0.55*	3001	10000*
34	Enameloid	473344	1	3001	10000	0.1	3001	10000*	0.1	1	10000*	0.1*	6001	1000*
	Enamel	472545	1	3001	10000	0.1	3001	5500*	0.1	1	1000*	0.55*	6001	10000*
35	Enameloid	387850	1	1	5500	0.1	1	1000	0*	0*	0*	1*	3001	1000
	Enamel	387870	1	1	5500	0.1	1	1000	0.1*	1*	1000*	0.55*	3001	10000

CHAPTER II – FROM ENAMELOID TO ENAMEL

36	Enameloid	81655	0.1*	3001	5500	0.1	1	1000	0*	0*	0*	0.1	6001	1000*
	Enamel	449099	1*	3001	5500	0.1	1	1000	0.1*	1*	1000*	0.1	6001	5500*
37	Enameloid	81655	0.1*	3001	5500*	0.1	1	1000	0*	0*	0*	0.1*	6001	1000
	Enamel	469609	1*	3001	10000*	0.1	1	1000	0.1*	3001*	1000*	1*	6001	1000
38	Enameloid	81655	0.1*	3001	5500*	0.1	1	1000*	0*	0*	0*	0.1	6001	1000
	Enamel	287395	0.55*	3001	10000*	0.1	1	10000*	0.1*	3001*	1000*	0.1	6001	1000

Access to complete dynamic simulations, data and code:

<https://drive.google.com/drive/folders/1S6S8LmVngriwCKwIwucy6oHRxxXRX-xZ?usp=sharing>



Conclusion on the objectives of Chapter II

In Chapter II we:

- Proposed a new *in silico* approach for assessing evo-devo hypotheses.
- Tested hypotheses from the literature to explain transitions between enameloid and enamel (Fig. 2-II).
- Identified new developmental modifications allowing for transitions between enameloid and enamel (Fig. 2-II).

CHAPTER III

MODELING THE HISTOMORPHOGENESIS OF TEETH: PRELIMINARY NOTES

Objectives Chapter III

As seen in Chapter II, the transition between enameloid and enamel may be induced by histogenetic changes such as alterations in the relative dynamics of ECM production. In this chapter, we are interested in testing whether, in addition to histogenetic changes, morphogenetic alterations can also influence the nature and distribution of the formed tissues. In *Lepisosteus* teeth, both enameloid and enamel are present, and their spatial distribution (enameloid being present at the tip and enamel at the lateral edges) suggests that both histogenetic and morphogenetic changes could influence their formation. Using computer models, we propose to assess the relative roles of histo- and morphogenetic parameters (Fig. 2-III).

III.1. Introduction

In chapters I and II, we studied the developmental mechanisms that could lead to the transition between enameloid and enamel, thus explaining how new dental structures could be established without requiring the acquisition of new matrix components (Fig. I-3). Thanks to a computer-assisted exploration, we were also able to identify various independent ways to theoretically achieve these modifications (Fig. II-6).

In addition to this histogenetic dimension, tooth formation also includes a morphogenetic one. Indeed, contrary to the straight alignment of cells assumed in the initial conditions of previous models, the epithelium and pseudo-epithelium of odontoblasts display an initial curvature at the beginning of extracellular matrix secretion and mineralization (see Chapter 9 in Berkovitz & Shellis (2016) and Chapter 5 in Nanci (2017)). This curvature notably constrains the final shape of the tooth or odontode, and potentially the blending of matrix elements, and therefore the histomorphogenesis of dentin, enameloid, and enamel.

In extant vertebrates, the matrix-secreting cells do not differentiate (e.g. ameloblasts or odontoblasts) and activate simultaneously along the tooth profile (Thesleff, Keranen & Jernvall, 2001; Lisi *et al.*, 2003), contrary to what has been considered in previous models. However, this spatio-temporal parameter could also have an impact on the histomorphogenesis of dental structures.

Therefore, this chapter aims at assessing the impact of the initial curvature of the epithelial-mesenchymal cell interface, the spatio-temporal gradient of cell differentiation, and the histogenetic changes (called '*primary transitions*') highlighted in Chapter II on the histomorphogenesis of a dental structure. The outputs of the simulations under consideration are: (1) the nature of tissues formed, (2) the shape of their junctions with neighboring tissues, and (3) the shape of the dentin growth lines.

III.2. Materials and Methods

As a case study, we chose to investigate and model the formation of non-teleost actinopterygian teeth. Indeed, they have the advantage of being composed of pulp dentin, cap enameloid, and collar enamel (more specifically ‘cap acrodin’ and ‘collar ganoin’, see Chapter I). Moreover, several studies are available about *Lepisosteus* and *Polypterus* tooth development (e.g. Sasagawa *et al.*, 2012, 2019; Kawasaki *et al.*, 2021; Delgado *et al.*, 2023).

We will use the histological model of dentin, enameloid, enamel formation developed on EmbryoMaker in Chapter II. The epithelium and the pseudo-epithelium of odontoblasts will be both represented by 35 cells, providing sufficient length to achieve an actinopterygian tooth-like morphology. The model will still be in pseudo-3D, meaning that cells will be arranged in 2D, but, as matrix elements are smaller than cells, they will be able to move in a three-dimensional space beneath them. These pseudo-3D simulations have the advantage of being directly comparable to histological slices while limiting calculation time. We added the possibility for the formation of growth lines in dentin based on the mineralization timing of elements. This notably allows simulating the formation of initially spherical growth lines (forming calcospherites), then linear ones following the progressive fusion of the calcospherites, as observed during the formation of dental structures (Berkovitz & Shellis, 2016; Dean, 2017; Nanci, 2017). Even though all the cells involved in tooth formation will be present from the start of the simulations, we will be able to delay their activation, starting from the middle of the cellular layer and progressing towards the extremities, as observed during extant tooth development (see Fig. 3 of Kawasaki & Weiss, 2008; Fig. 7 and 5 of Sasagawa *et al.*, 2012, 2019; Fig. 2A of Kawasaki *et al.*, 2021; Fig. 1A of Delgado *et al.*, 2023)

To firstly independently test the impacts of the initial curvature of the epithelium and the delayed activation of cells, we will simulate four cases of dentin, enameloid, and enamel formation, where epithelium can be straight or curved and

cells can activate synchronously or with a delay. As initial conditions for these four cases, we have chosen those from the illustration of the *primary transitions* with the higher implication rate, SVO- (supplementary Tab. II-3, II-5 lines 1 and 2, III-3). We took an intermediate value of 3001 for SVO, between the maximum of 6001 for enameloid formation, and the minimum of 1 for enamel formation, to promote both enamel and enameloid formation for this test.

Then, we will test the theoretical impact of a few *primary transitions*, with the higher implication rates, highlighted in Chapter II (see supplementary Tab. II-3 numbers 1-6). For these six cases, the epithelial curvature and the delayed activation of cells will be activated. For each case, initial conditions correspond to those of the *primary transition* illustrative simulations (supplementary Tab. II-5 lines 1-12, III-3). The varying parameter will gradually change on each side of the structure, from the center (enameloid value) to the edges (enamel value), over nine cells. Finally, we will quantitatively describe the results of the simulations, comparing them to histomorphological properties observed in longitudinal tooth sections of *Lepisosteus aculeatus* (Neopterygii, Actinopterygii), and more generally non-teleost actinopterygian teeth.

III.3. Results

Morphohistogenetic description of teeth

The teeth of *Lepisosteus aculeatus* are composed of the following structures: 1) pulpar orthodentine with visible cellular projections throughout the tissue, 2) a cap of enameloid at the tooth tip with cellular projections visible in almost the entire tissue thickness, which are in continuity with those of dentin, and 3) a thin collar of enamel at the edges, partially covering the cap of enameloid (Fig. III-1A-D). The enameloid is thicker at the center of the tip and gradually tapers towards the edges, in contrast to



FIGURE III-1. Thin sections of actinopterygian teeth composed of dentin, cap enameloid and collar enamel (A, D and E-H, cross-polarized light; B, natural light). Note the shapes of enamel-dentin, enameloid-dentin, and enamel-enameloid junctions. A-D, extant *Lepisosteus aculeatus* (MNHN-F-Histos 3154). A, well developed tooth with a growth line partially visible (arrow).

B, zoom on a triple point of A. C, scheme of B. D, a probably not fully formed tooth, revealing the morphology of a potential growth line (arrow and dotted line), as well as a sigmoid shape of the inner dentin boundary. Paleontological examples of actinopterygian teeth from Richter & Smith (1995). E, F, *Saurichthys* sp. (Trias). G, pycnodontiform (Cretaceous). H, *Lepidotes sphaerodus* (Jurassic). ac, acrodin (cap enameloid). cg, collar ganoin (collar enamel). de, dentin.

enamel, which generally maintains a constant thickness. There is an exception at the sigmoid-shaped enamel-enameloid junction, where the thickness of enameloid gradually decreases from the tip to the base of the cap, giving way to a thicker layer of enamel (Fig. III-1B, C). Regarding dentin, the initial layers formed at the tip appear to be partially covered by the cap of enameloid (Fig. III-1D). The dentin growth lines are rarely observable. However, when they are partially observable, growth lines are not parallel to the inner boundary of dentin and seem to come into contact with the enamel at the edges (Fig. III-1A, D arrows), forming discordances (triple points). It is also noteworthy that sometimes the inner boundary of dentin takes on a sigmoid shape (Fig. III-1D).

This structure is very similar to that of various fossil non-teleost actinopterygians (Fig. III-1E-H), as well as *Polypterus* (Sasagawa *et al.*, 2012; Delgado *et al.*, 2023). The sigmoid shape of the enamel-enameloid junction is particularly visible in *Saurichthys* (Fig. III-1F).

Morphohistogenetic description of simulations

Results of the simulations testing the impact of the initial epithelial curvature and the delayed activation of cells are given in the Figure III-2 and described in the Table III-1.

Results of the simulations testing the impact of a few *primary transitions* on an initially curved epithelium with a delayed activation of cells are given in the Figure III-3 and described in the Table III-2.

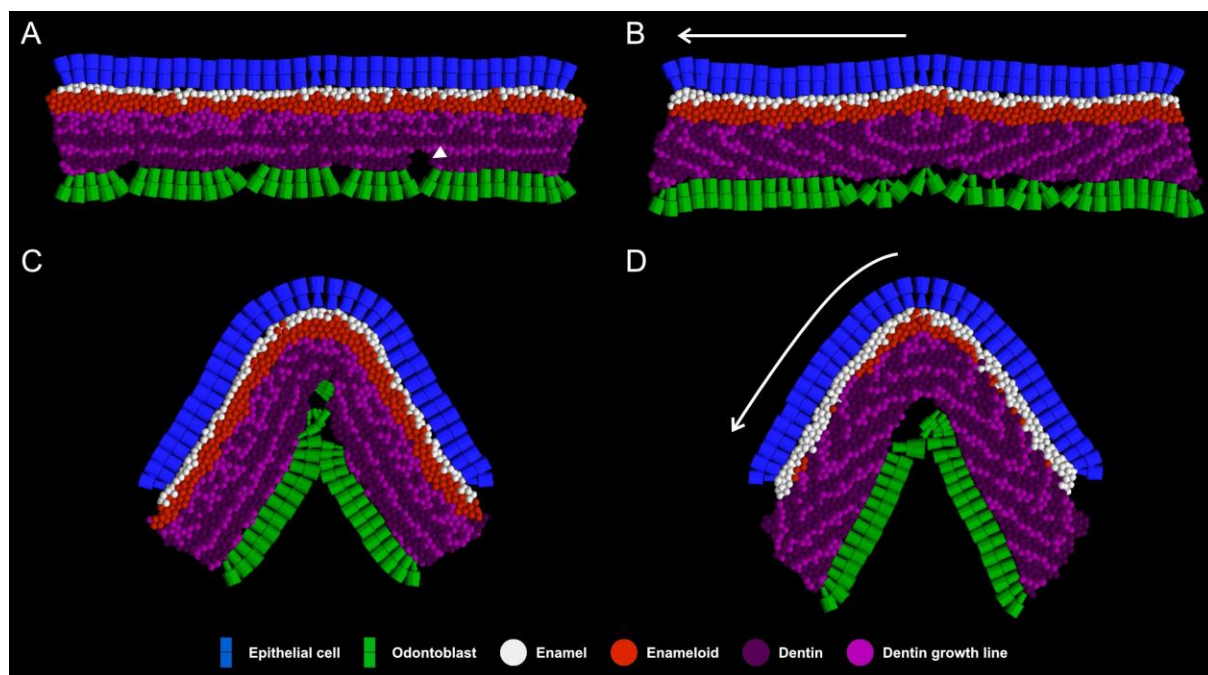


FIGURE III-2. Results of the simulations modeling dentin, enameloid and enamel formation, considering, or not, an initial epithelial curvature and a delayed activation of cells (from the middle to the edges; arrows). The arrows are shown on one side only to simplify the figure, but the delay occurs on both sides. Note that cells may have lost their cohesion during ECM secretion, sometimes inducing anomalies during the tooth formation (arrow head). The shape of the cells can also vary during formation, illustrating the physical constraints with neighboring cells, but this does not affect their secretion properties. Complete dynamic simulations are given in Appendix III.6, as well as the initial conditions in the supplementary Table III-3.

TABLE III-1. Description of the histomorphological properties of interest at the end of the simulations testing the impact of the initial epithelial curvature and the delayed activation of cells (see Fig. III-2).

		Histomorphological properties	
		Enameloid and Enamel distribution	Growth line morphology
Different initial conditions	<ul style="list-style-type: none"> • Straight epithelium (Fig. III-2A) 	<p>There is a globally similar distribution of enameloid and enamel thickness. Similar to B and C.</p>	<p>Calcospherite-like structures are found beneath hypermineralized tissues, followed by growth lines parallel to the dentin inner surface. Similar to C.</p>
	<ul style="list-style-type: none"> • Straight epithelium • Delayed activation (Fig. III-2B) 	<p>Similar to A and C. We can simply note a slight elevation at the starting zone.</p>	<p>Chevron-like growth lines that are in discordance with the enamel(oid)-dentin junction. Similar to D. We can note a slight elevation at the starting zone.</p>
	<ul style="list-style-type: none"> • Curved epithelium (Fig. III-2C) 	<p>Similar to A and B.</p>	<p>Similar to A.</p>
	<ul style="list-style-type: none"> • Curved epithelium • Delayed activation (Fig. III-2D) 	<p>The concentration of enameloid is high at the cap, with only a few traces of enameloid observable at the junction between enamel and dentin at the edges. A thin layer of enamel is present on the pseudo-cap.</p>	<p>Similar to B.</p>

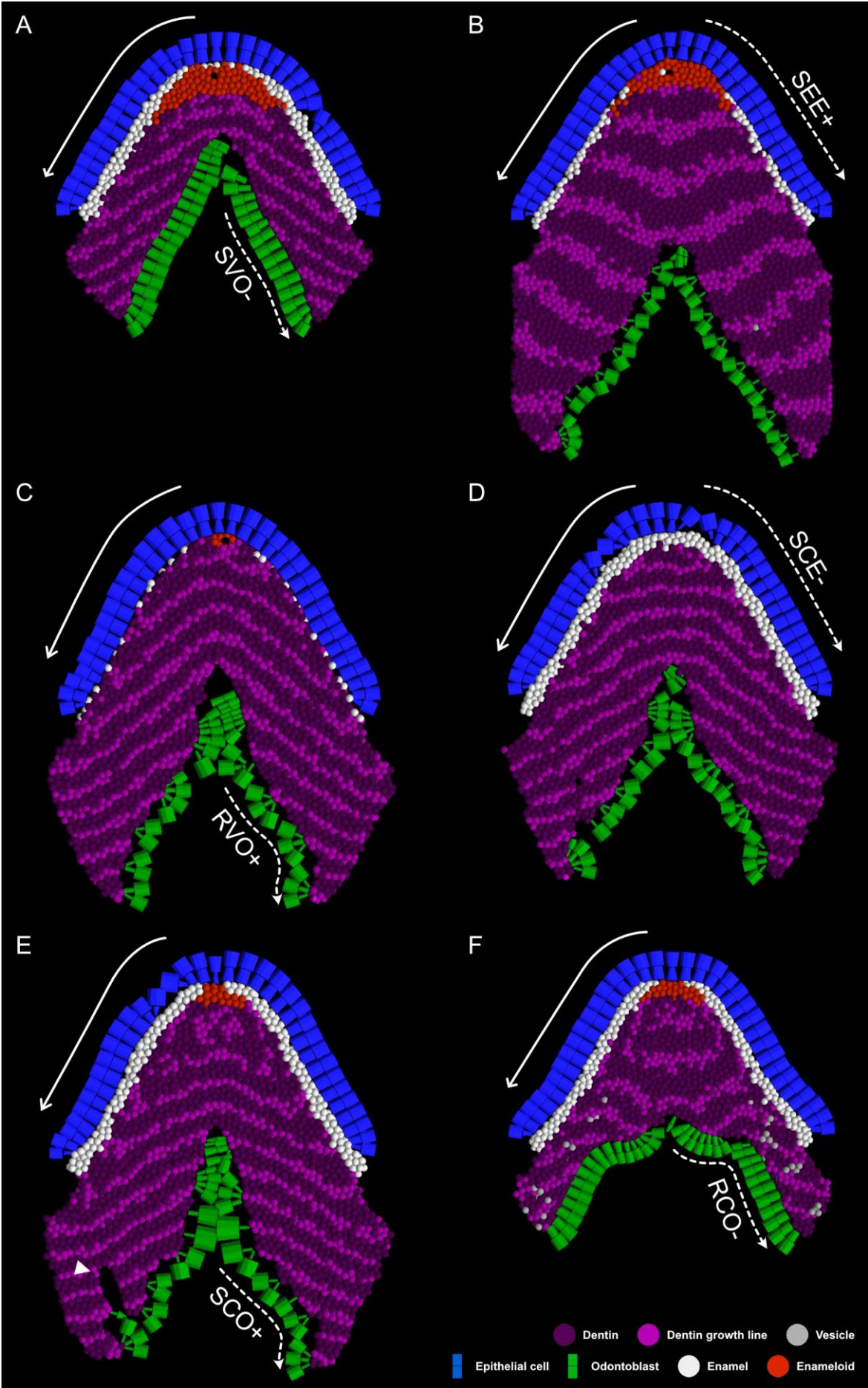


FIGURE III-3. Results of the simulations modeling dentin, enameloid and enamel formation, considering an initial epithelial curvature, a delayed activation of cells (from the middle to the edges; arrows) and developmental changes corresponding to *primary transitions* (also from the middle to the edges, on the first nine cells; dotted arrows). The arrows are shown on one side only to simplify the figure, but the modifications occur on both sides. Note that cells may have lost their cohesion during ECM secretion, sometimes inducing anomalies during the tooth formation (arrow head). The shape of the cells can also vary during formation, illustrating the physical constraints with neighboring cells, but this does not affect their secretion properties. Occasionally, vesicles do not well mineralize due to the lack of collagen or EMPs around. The dentin inner surface of most simulations is sigmoid-like in shape, especially F. Dynamic simulations are given in App. III.6, as well as the initial conditions in the supp. Table III-3.

III.4. Discussion

Impact of the initial epithelial curvature and the delayed activation of cells

In Chapter II, we identified a set of mechanisms controlling the formation of dentin, enameloid, and enamel (Fig. II-8), which could be influenced by a variety of intracellular changes, such as alterations in the relative dynamics of extracellular matrix (ECM) production (supplementary Tab. II-3). The results of this Chapter suggest that, in addition to the previously identified *primary shifts* (supplementary Tab. II-3), intercellular changes (such as the delayed cellular activation and the initial curvature) are also likely to influence these mechanisms of dentin, enameloid, and enamel formation (Fig. II-8).

When they vary in interaction, the curvature of the epithelial-mesenchymal interface and the cell activation delay can either enable or prevent the differential formation of tissues in a dental structure (Fig. III-2 and Tab. III-1). It can notably induce a concentration of enameloid under the tip and enamel on edges, forming a *Lepisosteus* tooth-like structure (Fig. III-2D). This is explained by the influence of these parameters

TABLE III-2. Description of the histomorphological properties of interest at the end of the simulations testing the impact of a few *primary transitions* on an initially curved epithelium with a delayed activation of cells (see Fig. III-3). Comparisons are made with tooth sections of *Lepisosteus aculeatus*, and more generally non-teleost actinopterygian teeth. Green boxes, presence of the property. Orange boxes, intermediate cases. Red boxes, absence of the property. White boxes, non-applicable.

		Histomorphological properties			
		Cap enameloid	Enamel on edges	Enameloid-Enamel junction morphology	Growth line morphology
Different initial conditions	PT1 SVO- (Fig. III-3A)	Presence, with a low amount of enamel above.	Presence.	Similar to real teeth. The enameloid appears 'to dig' into the thickness of the enamel, contrary to E and F.	Similar to real teeth.
	PT2 SEE+ (Fig. III-3B)	Presence.	Presence.	Similar to real teeth.	Not similar to real teeth, they exhibit a downward curvature. We can also note that growth lines are thicker than those of A, C, D and E.
	PT3 RVO+ (Fig. III-3C)	Presence, but in small quantity.	Presence, but in small quantity.	Not visible.	Similar to real teeth.
	PT4 SCE- (Fig. III-3D)	Absence.	Presence.	-	Similar to real teeth.
	PT5 SCO+ (Fig. III-3E)	Presence, but in limited quantity.	Presence.	Similar to real teeth. The enamel thickness appears to be constant, contrary to A.	Generally similar to real teeth, the only differences are found beneath the cap, where a form of concentric mineralization and interferences close to the enamel are visible.
	PT6 RCO- (Fig. III-3F)	Presence.	Presence.	Similar to real teeth. The enamel thickness appears to be constant, contrary to A.	Not similar to real teeth, they exhibit a concentric mineralization below the cap, with a downward curvature. We can also note that growth lines are thicker than those of A, C, D and E.

on the key mechanisms controlling the formation of dental tissues, such as the position and timing of mineralization front formation (Fig. II-8 and refer to supplementary animations III-2 in Appendix III.6). Thus, the formation of a cap enameloid and collar enamel appears to be favored by a relatively faster lateral propagation of the mineralization front at the level of epithelial cells along the edges, preventing the mixing of matrices on the sides, a property influenced by the interaction of curvature and cellular activation delay. It also seems likely that the curved area may modify the matrix blends, and therefore the amount of enameloid produced at the tip.

In addition to influencing tissue distribution, the cellular activation delay also seems to constrain the morphogenesis of growth lines that can be more or less parallel to the mesenchymal cellular arrangements (Fig. III-2 and Table III-1). In the case of synchronous cell activation, this can be explained by simultaneous mineralization initiation (by the vesicles), following the arrangement of secreting cells (odontoblasts) throughout the dental structure. The calcospherites thus formed subsequently merge, leading to the formation of a front parallel to the odontoblasts. For delayed cell activation, mineralization initiation will occur at the location of the first secreting cells, resulting in concentric mineralization propagation from the initiation site. It's worth noting that the chevron-like growth line morphology, which tends to form when mineralization propagates concentrically (e.g. Fig. III-2B, D), resembles the structure observed in some conodonts (see figure 4 of Murdock *et al.*, 2013).

Thus, as there is a wide variety of dental structure morphologies (Sire *et al.*, 2009; Berkovitz & Shellis, 2016; Ungar & Sues, 2019), and the activation timing of cells appears to be different in early vertebrates (see Chapter IV), the curvature and cell delayed activation parameters could have contributed to histomorphological changes during vertebrate evolution.

Impact of a few primary transitions during a tooth-like growth

The various elemental changes appear to influence the shape and even the thickness of the growth lines, the morphology of the enamel(oid)–dentin junction, and the distribution of hypermineralized tissues (Fig. III-3 and Tab. III-2). They also seem to impact the morphology of the enamel-enameloid junction, where more or less enamel can cover the enameloid cap. Therefore, it confirms that developmental shift(s) such as *primary shift* highlighted in Chapter II can also participate in the formation of a cap enameloid and collar enamel with specific enamel-enameloid-dentin junction shapes, in addition to the curvature and cell delayed activation parameters.

According to this model considering an initially curved epithelium as well as a delayed activation of cells, the *primary transition 1* (SVO-; reduction in the onset of vesicle secretion by odontoblasts) induces the histomorphogenesis that fit the most with biological observations (Fig. III-3A, Tab. III-2). The enameloid covers a portion of the dentin, the transition between enameloid and enamel forms a sigmoidal junction, and dentin growth lines are curved towards the tip of the tooth and exhibit discordances with the enamel on lateral edges (Fig. III-4). The presence of a thin layer of enamel on the enameloid cap is not surprising, as it is also partially observed in certain taxa such as *Lepisosteus* (Fig. III-1) or *Polypterus* (Sasagawa *et al.*, 2012; Delgado *et al.*, 2023). Considering the results from Chapter II, this suggests that modifying the onset of vesicle secretion by odontoblasts plays a central role in the formation of this type of dental structure.

On the contrary, the *primary transition 4* (SCE-; reduction in the onset of collagen secretion by epithelial cells) does not appear to allow for the formation of an enameloid cap (Fig. III-3D, Tab. III-2). Considering that its influence on the enamel-enameloid transition was previously debated in Chapter II, these histomorphogenetic findings suggest that altering the initiation of epithelial collagen secretion does not have a central role in the formation of this type of dental structure.

In actinopterygian the cell activation is delayed (e.g. Sasagawa *et al.*, 2012, 2019; Kawasaki *et al.*, 2021), but from a theoretical standpoint, simultaneous cell activation (as suspected in some fossil stem-gnathostomes; see Chapter IV) would primarily result in altering the shape of growth lines in taxa exhibiting this type of dental structure (Fig. III-4). The growth lines would be more parallel to the inner surface of dentin, forming preferentially discordances with the enameloid located at the tip, and more numerous calcospherites.

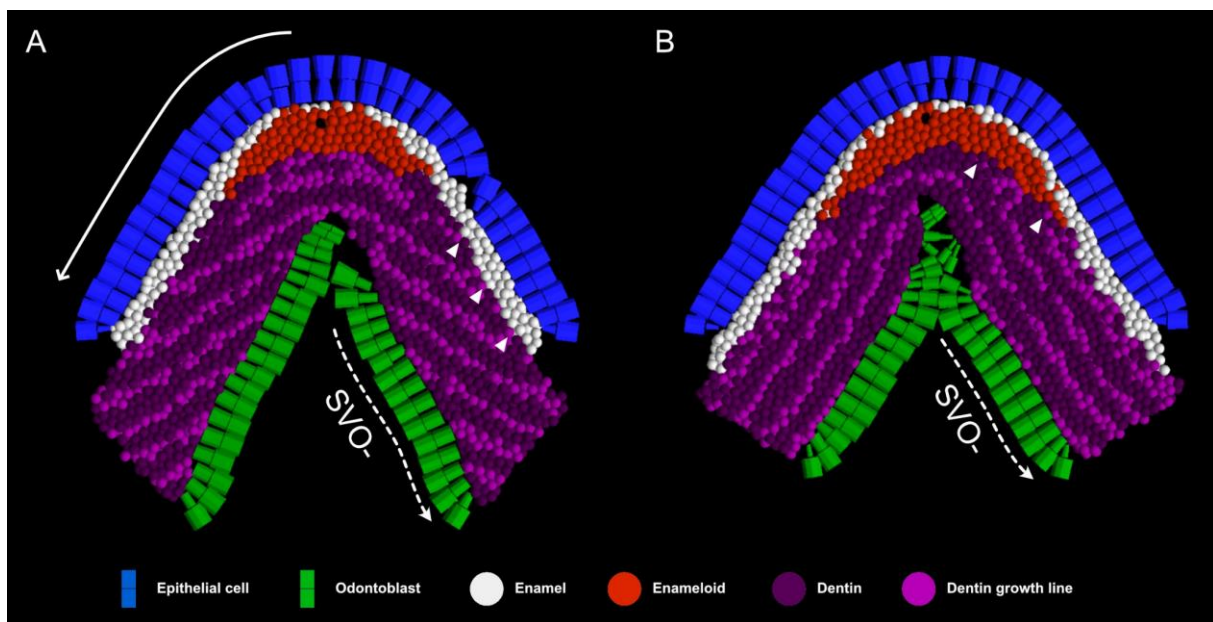


FIGURE III-4. Illustration of the theoretical impact of the delayed activation of cells (A, with, and B, without; arrow) on the histomorphology of dental structures composed of a cap enameloid, collar enamel, and basal dentin. This illustration is based on the *primary transition* 1 (on the first nine cells; dotted arrow), as it seems to produce the most consistent histomorphogenesis with that of real teeth (see Fig. III-3A and Tab. III-2). The growth lines preferentially form discordances with the enamel located on the lateral edges in A, and with the enameloid located at the tip in B (arrow heads). Note that cells may have lost their cohesion during ECM secretion. The shape of the cells can also vary during formation, illustrating the physical constraints with neighboring cells, but this does not affect their secretion properties. Complete dynamic simulations are given in App. III.6, as well as supplementary simulations with an initial straight epithelium. Initial conditions are given in the supp. Table III-3.

We can note that the inner boundary of dentin can sometimes take the form of a sigmoid in the simulations (Fig. III-3C-F), reminiscent of that observed in the figure III-1D. Further studies could therefore focus on how this morphology develops and the factors that constrain it. We can also note that, in the case of enameloid, the surface of the tissue generally corresponds to the initial position of the epithelium, whereas this initial position corresponds more to the junction in the case of enamel (see the complete dynamic simulations in Appendix III.6).

Please bear in mind that the histomorphological properties observed in the simulations are undoubtedly influenced by the chosen initial conditions. In the future, it would be relevant to perform similar tests with different initial conditions whenever possible in order to strengthen the results. Moreover, as this project is still in production, the next objective would be to test the impact of various curvature levels, as well as different values of cell activation delay. This would notably help to better characterize the critical relationship between these two parameters in the formation, or not, of an enameloid cap.

III.5. Conclusion

Based on computer-assisted modeling, this study showed that, along with the developmental shift(s) such as *primary shifts* of Chapter II, the initial curvature of the epithelium and the timing of activation of cells constrain the formation of tissues and growth lines in dental structures. Therefore, the alteration of these developmental parameters could be vectors of histomorphological diversification during vertebrate evolution. This study also supports the hypothesis that modifying the start of secretion or activation of vesicles is a good candidate for inducing transitions between enameloid and enamel. In general, it reinforces the idea that it is possible to simulate the development of bioconstructed structures to better understand the mechanisms

constraining their formation. This opens up the possibility of using this type of study on fossilized structures, which have no current representatives, in order to better understand their developmental mechanisms.

Acknowledgements. We warmly thank Roland ZIMM for the assistance he provided in using EmbryoMaker.

Contributions. **Conceptualization** Guillaume Houée (GH); **Data Curation** GH; **Formal Analysis** GH; **Investigation** GH; **Methodology** GH; **Project Administration** GH; **Resources** GH; **Supervision** Damien Germain (DG), Nicolas Goudemand (NG), Jérémie Bardin (JB); **Validation** GH, DG, NG, JB; **Visualization** GH; **Writing – Original Draft Preparation** GH, DG, NG, JB.

III.6. Appendix

Access to complete dynamic simulations and code:

https://drive.google.com/drive/folders/1h3OTdWgBDs9O_TObHpZtWee13zIxL7wC?usp=sharing



CHAPTER III – HISTOMORPHOGENESIS OF TEETH

TABLE III-3. Initial conditions of the simulations. Arrows indicate the parameters that gradually change on each side of the structure, from the center (enameloid value) to the edges (enamel value), over nine cells.

Figure	Simulation	Primary transition	RCO	SCO	DCO	RVO	SVO	DVO	RCE	SCE	DCE	REE	SEE	DEE	Curvature	Delayed activation
III-2	A	-	0.55	1	10000	0.55	3001	1000	0	0	0	0.1	3001	10000	deactivated	deactivated
III-2	B	-	0.55	1	10000	0.55	3001	1000	0	0	0	0.1	3001	10000	deactivated	activated
III-2	C	-	0.55	1	10000	0.55	3001	1000	0	0	0	0.1	3001	10000	activated	deactivated
III-2	D	-	0.55	1	10000	0.55	3001	1000	0	0	0	0.1	3001	10000	activated	activated
III-3	A	SVO-	0.55	1	10000	0.55	6001 → 1	1000	0	0	0	0.1	3001	10000	activated	activated
III-3	B	SEE+	0.55	3001	10000	1	3001	10000	0.55	3001	1000	0.55	1 → 6001	1000	activated	activated
III-3	C	RVO+	1	1	10000	0.1 → 0.55	1	1000	0.1	1	1000	0.1	3001	1000	activated	activated
III-3	D	SCE-	1	3001	10000	0.1	1	1000	0.1	6001 → 3001	1000	1	6001	1000	activated	activated
III-3	E	SCO+	1	1 → 3001	10000	1	3001	1000	0.1	1	1000	1	6001	1000	activated	activated
III-3	F	RCO-	1 → 0.1	1	10000	0.55	3001	5500	0.1	1	1000	1	6001	1000	activated	activated
III-4	A	SVO-	0.55	1	10000	0.55	6001 → 1	1000	0	0	0	0.1	3001	10000	activated	activated
III-4	B	SVO-	0.55	1	10000	0.55	6001 → 1	1000	0	0	0	0.1	3001	10000	activated	deactivated

Conclusion on the objectives of Chapter III

In Chapter III we:

- Demonstrated that the modification of the epithelial initial curvature and of the spatiotemporal activation timing of cells impact the presence and distribution of tissues within a dental structure (Fig. 2-III).

CHAPTER IV

*DEVELOPMENTAL MODELS SHED LIGHT ON THE EARLIEST
DENTAL TISSUES, USING ASTRASPIS AS AN EXAMPLE*

Objectives Chapter IV

After studying the extant development of the main dental tissues (Chapters I, II) and the histomorphogenesis of the extant teeth composed of these tissues (Chapters II, III), this chapter IV aims at inferring the development of extinct teeth and odontodes. Indeed, these kinds of inferences may help to better understand how the early tissues developed and emerged (Fig. 2-IVa), and also to discuss the potential developmental differences between early vertebrate dental tissue development and extant ones (Fig. 2-IVb). As an application example, we choose to work on the iconic *Astraspis* (pteraspidomorph) due to its key phylogenetic position (Fig. 4) and the exceptional preservation of its histological properties. *Astraspis* fossils also correspond to one of the oldest osseous and dental tissue remains.

This project IV was accepted in *Palaeontology* and is very close to the publication.

IV.1. Introduction

While vertebrate mineralized skeleton is composed of a large diversity of mineralized tissues (Sire *et al.*, 2009; Vickaryous & Sire, 2009), it is mainly constituted of osseous tissues, dentin, enamel and intermediate tissues like enameloid (Hall, 2015). Osseous tissues constitute bones, whereas ‘dental’ tissues, such as dentin, enamel and enameloid, mainly compose teeth and odontodes (‘tooth-like structures’). Teeth and odontodes are classically composed of a pulpar dentinous tissue, covered by a hypermineralized tissue, like enamel or enameloid. In this study, we will use simplified definitions of these tissues, that do not take into account the nature of proteins: dentin is a tissue of mesenchymal origin, enamel of epithelial origin, and enameloid of dual mesenchymal and epithelial origin (Berkovitz & Shellis, 2016; Nanci, 2017).

Pteraspidomorphs (jawless stem-gnathostomes, ‘ostracoderms’, middle Ordovician to late Devonian) present some of the oldest remains of these bony and ‘dental’ tissues. Indeed, since at least the late Ordovician, pteraspidomorphs such as *Astraspis* exhibited a dermal skeleton (two cephalothoracic plates, tesseræ, and numerous smaller scales) constituted of a layer of lamellar anosteocytic osseous tissue, and a layer of spongy anosteocytic osseous tissue (aspidin), covered with a layer of star-shaped odontodes (Sansom *et al.*, 1997; Sire *et al.*, 2009; Keating *et al.*, 2015, 2018; Lemierre & Germain, 2019). The odontodes of pteraspidomorphs are composed by a pulpar tissue which has been interpreted as orthodentine on the basis of the presence of radially oriented tubules throughout the entire thickness of the tissue and the absence of cell lacunae (Sire *et al.*, 2009; Lemierre & Germain, 2019). In few taxa, such as *Astraspis*, the pulpar tissue is also covered by a vitreous capping tissue identified as enameloid, rather than enamel, because the presence of tubules suggested the participation of mesenchymal cells in its formation (Donoghue & Sansom, 2002; Sansom *et al.*, 2005; Sire *et al.*, 2009; Lemierre & Germain, 2019). However, these criteria and hence these identifications are questionable. Indeed, the pulpar tissue had also

been interpreted as aspidin (Ørvig, 1967), or astraspidin (Halstead, 1987), the tubules being then considered as fibers. Moreover, short tubules (known as “enamel spindles”) or even well-developed tubules can also be found in enamel (at least in some marsupial and placental enamel) (Williams, 1923; Stern *et al.*, 1992; Nanci, 2017), which contradicts the common hypothesis that they would be present exclusively in enameloid. Thus, the presence of tubules in the hypermineralized capping tissue is not sufficient to conclude on its enameloid or enamel nature.

This study aims at bringing forth new, model-based histological features for the interpretation of fossil hypermineralized tissues. The integrative analysis of these features allows one to discriminate between the various possible developmental scenarios that may have led to the tissues under scrutiny. As a case study we show how we use this approach to reinterpret the odontode tissues of *Astraspis*, in particular, whether mesenchymal and/or epithelial cells contributed to the formation of its capping tissue.

IV.2. Materials and Methods

This study focuses on *Astraspis* dermal skeleton remains found in the Harding Sandstone Formation, and more precisely on their odontodes, which correspond to one of the oldest known remains of ‘dental’ tissues. The Harding Sandstone Formation, dated to the upper Ordovician, is composed of a diversity of early vertebrates remains: e.g. conodonts, pteraspidomorphs such as *Astraspis desiderata*, *Eriptychius americanus* and *Eriptychius orvigi*, potential thelodonts, potential stem-chondrichthyans, and the enigmatic *Skiichthys halsteadi* (Walcott, 1892; Vaillant, 1902; Bryant, 1936; Ørvig, 1958, 1989; Denison, 1967; Smith & Hall, 1990; Sansom, Smith & Smith, 1996; Sansom *et al.*, 1997; Smith & Sansom, 1997; Allulee & Holland, 2005). Although few articulated specimens of *Astraspis* and *Eriptychius* have been discovered (Bryant, 1936; Denison, 1967; Elliott, 1987; Sansom *et al.*, 1997), most of the remains are fragments of the

mineralized skeleton, prompting histological studies (Walcott, 1892; Bryant, 1936; Ørvig, 1958, 1989; Denison, 1967; Smith & Hall, 1990; de Ricqlès, 1995; Sansom *et al.*, 1996, 1997; Smith & Sansom, 1997; Lemierre & Germain, 2019).

Histological sections have been prepared from blocks of Harding red sandstone (collection number MNHN.F.1891-20) (de Ricqlès, 1995; Lemierre & Germain, 2019), collected in 1891 by Marcellin BOULE and Albert GAUDRY, Professors at the Museum national d'Histoire naturelle (Paris, France), during a field trip organized by Charles Doolittle WALCOTT in the framework of the Fifth International Geological Congress. We have studied the *Astraspis* odontodes found in these thin sections. They were polished to a thickness of about 80 to 100 µm. These odontodes are histologically recognizable from that of other taxa, and especially from those of the other pteraspidomorph genus, *Eriptychius*, whose larger dentin tubules are branching (Bryant, 1936; Smith & Hall, 1990). Moreover, most *Eriptychius*' odontodes do not exhibit a capping tissue (Smith & Hall 1990). The preservation of the Astraspid remains from the Harding Sandstone is exceptional, especially for Ordovician fossils, thus allowing observation of histological and morphological features that are key to developmental interpretations. In particular, we have sampled the best preserved *Astraspis* odontodes, that is, those where cellular projections, growth lines, tissue junction or patterns of mineralization are visible and where the external and inner surfaces are not or poorly eroded. Interestingly, these histological features are particularly visible in those parts of the sections that are covered with an orange-brown film (oxide precipitation?), contrary to those that are white and translucent. Since the sections are randomly oriented in a bioclastic sandstone, and in order to work with the most comparable sections, we have selected preferentially longitudinal sections passing through the pulp cavity. Pictures were taken with a digital camera (Canon EOS 6D) adapted on a microscope Olympus CX31P with the Micro Tech Lab DSLRCFTC_Pro and TUST42C models. Measurements have been done using the "Measure" tool of ImageJ 1.53k (Abràmoff, Magalhães & Ram, 2004).

None of the studied odontodes exhibits all of the features of interest. We have assumed this to reflect preservation biases rather than true variation. Hence, we have selected several sections with complementary information to reconstruct a virtual odontode that synthesizes all our observations. Note that the molecular and cellular mechanisms involved in the formation of teeth or that of tooth-like organs (odontodes) have been documented to be similar (Fraser *et al.*, 2010; Witten, Sire & Huysseune, 2014; Berio & Debiais-Thibaud, 2021), and although they have been documented only on a few extant gnathostomes, all we know so far suggests that the main developmental aspects of those tissues are shared by most vertebrates. As a consequence, and unless we are able to falsify this hypothesis during the course of our analyses, we will assume that the odontodes of *Astraspis* were formed using similar mechanisms. Still, several scenarios are possible. By confronting our reconstructed, virtual odontode based on observations to the phenotypes obtained theoretically under those various scenarios we can decipher which scenario is the most plausible.

IV.3. Results

Astraspis odontodes are arranged on top of the dermal skeleton, over a layer of spongy and vascularized aspidin (a tissue that resembles anosteocytic bone) and a layer of lamellar anosteocytic osseous tissue (Fig. IV-1) (Sire *et al.*, 2009). The junction between odontodes and the underlying aspidin may be conspicuous (Fig. IV-2A).

Astraspis odontodes are fold-shaped. They are composed of a pulp cavity, a pulpar tissue and a capping tissue, the latter being delimited by a well-marked pulpar-capping junction (PCJ) (Fig. IV-2B). The capping tissue is present on the apical portion of odontodes only, and it tapers towards the edges (Fig. IV-2-4). It is not always well visible because lateral portions are often eroded, which could be due to a secondary resorption of tissues. The capping tissue has a vitreous aspect (Fig. IV-2-4). Depending on the external morphology of odontodes and on the plans of slicing, the external

surface of the odontodes can appear either smooth or undulated with more or less marked ridges, as the growth lines of the pulpar tissue (Fig. IV-2B, C and Fig. IV-4A). The PCJ on the other hand are always smooth and never exhibit large waves or ridges (Fig. IV-2-4). They may however exhibit small-scaled wavy patterns (wavelength of 4-8 μm , whose tips are oriented towards the pulpar tissue) (Fig. IV-2F, G).

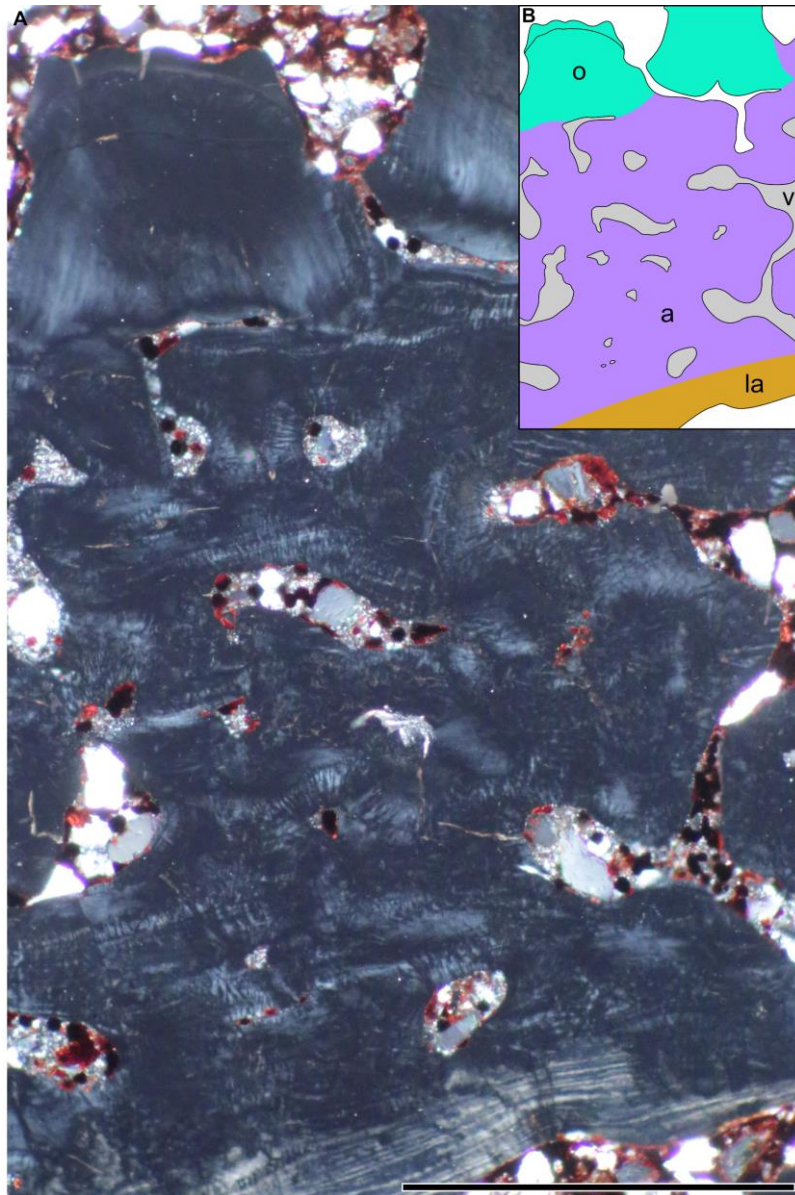


FIGURE IV-1. A, transversal section of an *Astraspis* dermal element, where the three layers are visible (cross-polarized light) (MNHN-Histos 3253). B, interpretive drawing of A. a, aspidin. la, lamellar anosteocytic osseous tissue. o, odontode. v, vascularities. Scale bar: 0.5 mm.

Within the pulpar tissue, numerous well-marked growth lines are visible, delimiting superimposed layers of tissue (Fig. IV-2). Among these growth lines, it is sometimes possible to distinguish long and short-period growth lines, where long-periods include 4-18 short-periods (Fig. IV-3 and supplementary Fig. IV-7). The thickness of short-period layers decreases from outer layers inwards, respectively from 5 to 0.5 μm , and that of long-period layers varies without clear tendency, around 4-70 μm . The thickness of layers appears to be constant along the outer edge of the odontode. However, the observed thicknesses correspond to a projection of the 'true' growth thicknesses onto the thin section plane and hence are influenced by the orientation of the section. The growth lines are parallel to the lateral edges of the pulpar tissue and the contour of the pulp cavity, but may be discordant with the PCJ (Fig. IV-2). This implies the presence of unconformities (triple points) at the PCJ (Fig. IV-2D, E). Also, the most external layers of the pulpar tissue are only present on the lateral edges of the odontodes. The shape of the growth lines changes gradually within the pulpar tissue, it is particularly visible when the lines transition from an initially angular morphology (outer layers) to a smooth one (inner layers) (Fig. IV-4A). We observe no growth lines within the capping tissue.

Calcospherites of various sizes are often visible within the pulpar tissue, especially within the external layers, although not within the most external layers (Fig. IV-4B). More internally, these calcospherites tend to fuse, thereby forming a mineralization front that becomes gradually smoother inwards.

Thin and seemingly continuous tubules pervade the whole thickness of the pulpar tissue. They are oriented subperpendicularly to growth lines and as such tend to be straight in regions where the growth lines are smooth and may be curved in regions where the growth lines are folded (Fig. IV-4C). We observe no tubule ramifications, suggesting that the number of tubules is constant throughout the thickness of the pulpar tissue. As a consequence, tubule density increases from the

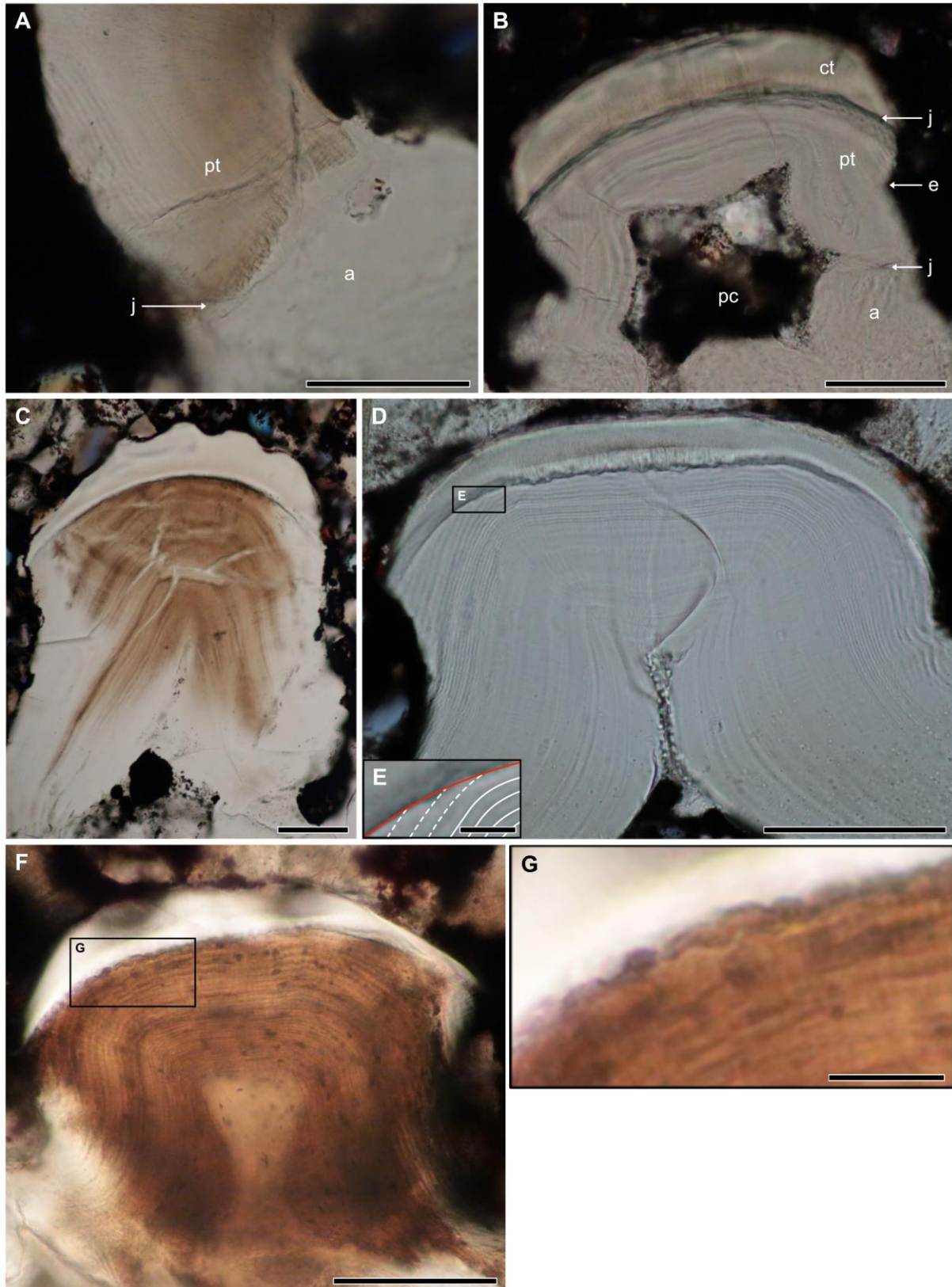


FIGURE IV-2. Longitudinal sections of *Astraspis* odontodes. A, clear junction between the pulpar tissue of an odontode and the underlying aspidin (MNHN-Histos 3255). B, an odontode with a smooth external surface (MNHN-Histos 3256). C, an odontode with a folded

external surface (MNHN-Histos 3245). D, an odontode whose well visible growth lines parallel the contour of the pulp cavity and the non-eroded right lateral edge (MNHN-Histos 3247). E, zoom on the overlapping over the growth lines of the pulpar tissue (dashed lines). F, an odontode with a scalloped junction (MNHN-Histos 3255). G, zoom on the small-scaled wavy patterns in F. a, aspidin. ct, capping tissue. e, erosion. j, junction. pc, pulp cavity. pt, pulpar tissue. Scale bars represent: 100 μm (A-D, F); 20 μm (G); 10 μm (E).

external layers inwards. This is particularly clear in regions where tubules are curved (Fig. IV-4C). Their diameter is about 0.8-1.2 μm . Based on transverse views of these tubules in the pulp cavity of some odontodes, their density is estimated to reach about 320 000-360 000 tubules/ mm^2 internally (18 ± 1 tubules/ $53 \mu\text{m}^2$, see Fig. IV-4D, E). In agreement with this estimation, a 21 μm portion of a longitudinal view of tubules near the pulp cavity shows about 10 probable mesenchymal cells impressions (Fig. IV-4D). As the perimeter of the cavity measures about 600 μm , we can estimate that around 250-300 cells were involved in the formation of the inner layers of this section. We observe no cell lacunae. Thin tubules are also present within the whole thickness of the capping tissue (Fig. IV-4F, G). Our sampling does not allow us to observe the connection between tubules of the basal and the capping tissues, but they are interpreted as being continuous (Sansom *et al.*, 1997).

Figure IV-5 synthesizes these morphological and histological observations gathered from the analysis of several odontodes and sections in a virtual *Astraspis* odontode. The construction and confrontation of the developmental scenarios will arise from the discussion of this virtual odontode.

IV.4. Discussion

Inferring the nature of *Astraspis*' tissues from these observations is not as straightforward as one may think. Most traits usually used for such interpretations are not actually specific of one single type of tissue. In order to conclude about the nature of these mineralized tissues, we argue that it is necessary to adopt an integrative approach that considers all observations (see below) and confront them with the theoretical phenotypes (virtual odontodes) that we would expect as outcomes of the various possible developmental scenarios. The most plausible developmental scenario is then the one whose virtual odontode is the most congruent with the empirical observations.

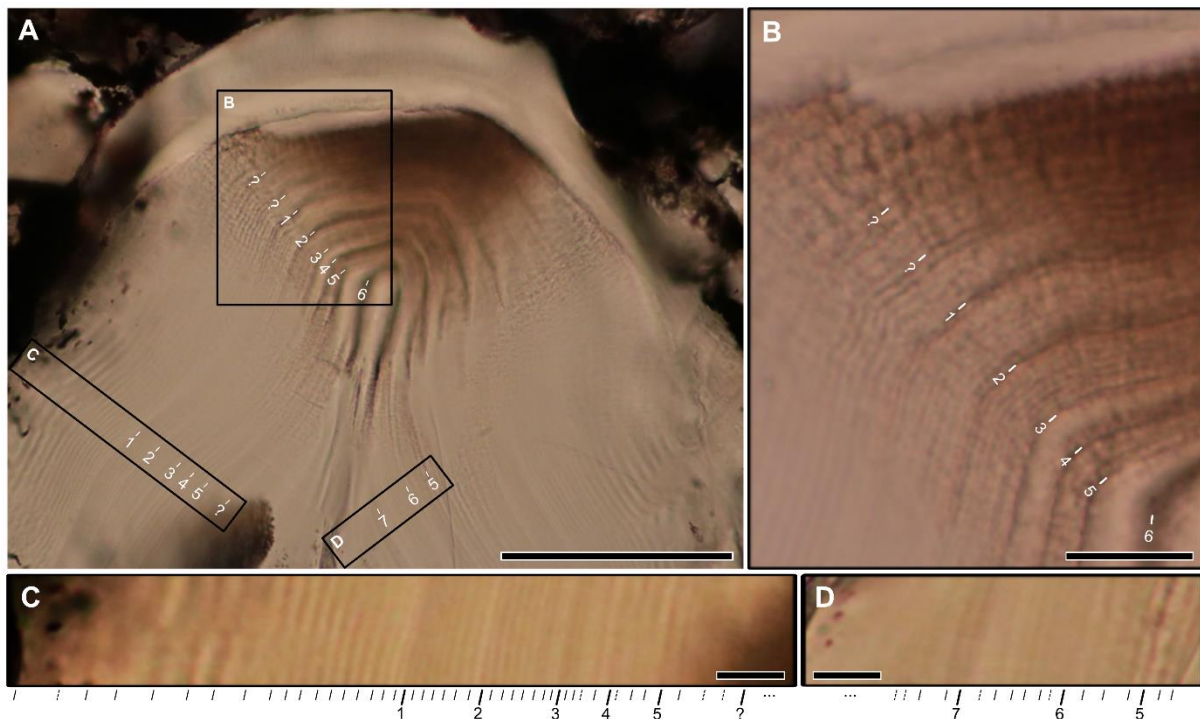


FIGURE IV-3. A, potential short and long-period growth lines in the pulpar tissue of an odontode of *Astraspis* (MNHN-Histos 3251). B, zoom on the growth lines where the dual periodicity is well-visible. C-D, enlargements of areas of the section used for counting the growth lines across the whole thickness of the structure. Scale bars represent: 100 μm (A); 20 μm (B); 10 μm (C, D).

Capping tissue

The vitreous aspect of the capping tissue, in addition to the well-marked PCJ, suggests that the capping tissue of *Astraspis* was hypermineralized (Fig. IV-2-4). Moreover, its distal location on the external surface of the dermal skeleton (Fig. IV-1) is compatible with a fully epithelial (enamel tissue) or partially epithelial (enameloid tissue) origin (Berkovitz & Shellis, 2016). The presence of tubules that are in connection with those of the pulpar tissue has been used to infer the contribution of mesenchymal, odontoblast-like cells and thus to identify it as an enameloid (Fig. IV-4G) (Donoghue & Sansom, 2002; Sansom *et al.*, 2005; Sire *et al.*, 2009; Lemierre & Germain, 2019). However, some marsupial and placental enamels are known to present long tubules (Williams, 1923; Stern *et al.*, 1992), thereby questioning this trait as being presumably specific to enameloid. As a consequence, we consider that these observations are not sufficient to conclude at this stage.

Pulpar tissue

The size (0.8-1.2 μm), density (ca. 320 000 tubules/ mm^2), and orientation of the tubules in the pulpar tissue of *Astraspis* are compatible with the current interpretation of this tissue as orthodontine: similarly sized tubules are known in reptiles (Brink *et al.*, 2016) and teleosts (Deang *et al.*, 2018; Deng *et al.*, 2022), similarly dense tubules have been documented in teleosts (230 000 tubules/ mm^2 (Deang *et al.*, 2018; Deng *et al.*, 2022)), and subparallel tubules crossing the growth lines perpendicularly throughout the acellular, avascular tissue are characteristic of gnathostome orthodontine (Fig. IV-4C) (Sire *et al.*, 2009). In other words, this pulpar tissue was likely produced by odontoblasts or odontoblast-like cells and these tubules are probably homologous to Tomes' fibers (also called odontoblast processes) (Berkovitz & Shellis, 2016; Nanci, 2017) which refutes the identification of tubules as fibers. Please note that the tubules

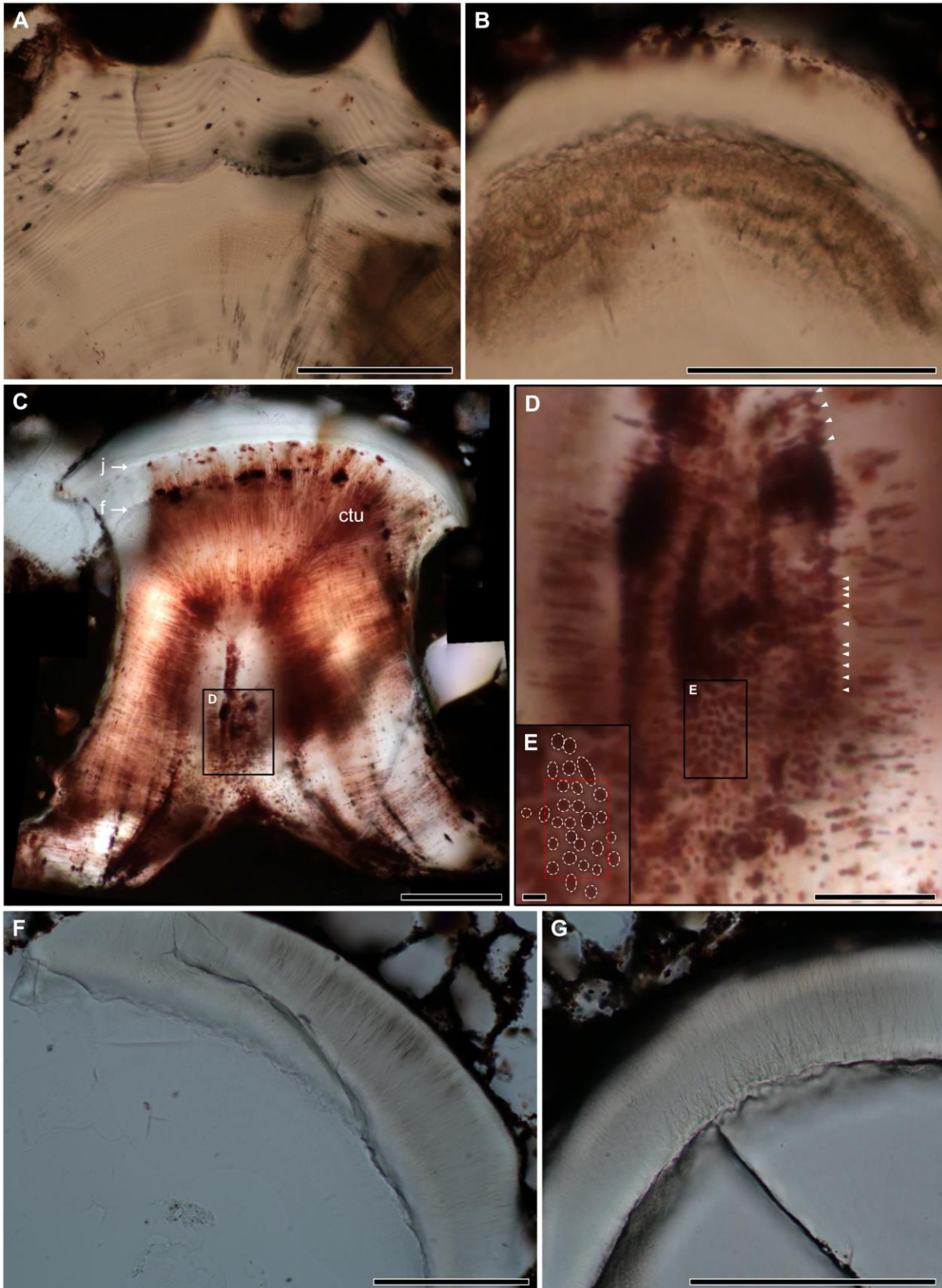


FIGURE IV-4. Sections of *Astraspis* odontodes. A, an odontode with a ridged external surface and ridged growth lines in the pulpar tissue, ridges (and valleys) progressively fade out

inwards (MNHN-Histos 3251). B, calcospherites within the first incremental (external) layers of the pulpar tissue (MNHN-Histos 3251). C, an odontode in which the thin tubules are well visible (MNHN-Histos 3251). D, zoom on the pulp cavity of C enabling us to observe the potential impression of some mesenchymal cells (arrowheads) and transversal sections of the thin tubules (see E). E, zoom on transversal sections of the thin tubules enabling quantification of the density (quantification made in the dashed red box). F, the thin tubules extend across the whole thickness of the capping tissue (MNHN-Histos 3248). G, the thin tubules originate at the junction between the capping and the basal tissue (MNHN-Histos 3248). ctu, curved tubules. f, fracture. j, junction. Scale bars represent: 100 μm (A-C, F, G); 20 μm (D); 2 μm (E).

in *Astraspis* tend to be smaller than what we know of other vertebrates, which is consistent with the fact that their density is also the highest ever documented. This may suggest the presence of smaller, more compacted, odontoblast-like cells. The presence of periodic patterns of incremental lines alternating in color and opacity (see further below) is reminiscent of similar patterns observed in the orthodontine of other vertebrates and corroborates the interpretation of the pulpar tissue as orthodontine.

The frequent presence of calcospherites within the pulpar tissue, as also observed in the odontodes of other stem-gnathostomes (e.g. Smith & Hall, 1990; Keating & Donoghue, 2016), suggests the corresponding external part of the pulpar tissue can be further characterized as globular orthodontine (Dean, 2017; Waugh *et al.*, 2018). Note that this kind of mineralization ('Liesegang rings') can also be found in other mineralized tissues, such as globular calcified cartilage (Kemp & Westrin, 1979; Smith & Hall, 1990), and can also form abiotically (Sadek, Sultan & Lagzi, 2010). The presence of well-marked calcospherites within dentin may imply the initial presence of nucleating matrix vesicles in the corresponding external layers (Nanci, 2017). Therefore, matrix vesicles-based mineralization was likely already present and widespread in stem-gnathostomes. The gradual fusion of the calcospherites towards the pulpar cavity, leading to the formation of a linear mineralization front, suggests a centripetal propagation of a gradually slowing mineralization front (Nanci, 2017) (also

suggested by the gradually thinner growth lines, see below). We can note that the size of globules could inform about the rate of orthodontine deposition, with higher rates where globules are largest (Nanci, 2017).

The well-marked junction sometimes observed between the pulpar tissue and the aspidin suggests structural and/or compositional differences between these tissues (Fig. IV-2A), contradicting the identification of the both tissues as similar aspidin (Ørvig, 1967).

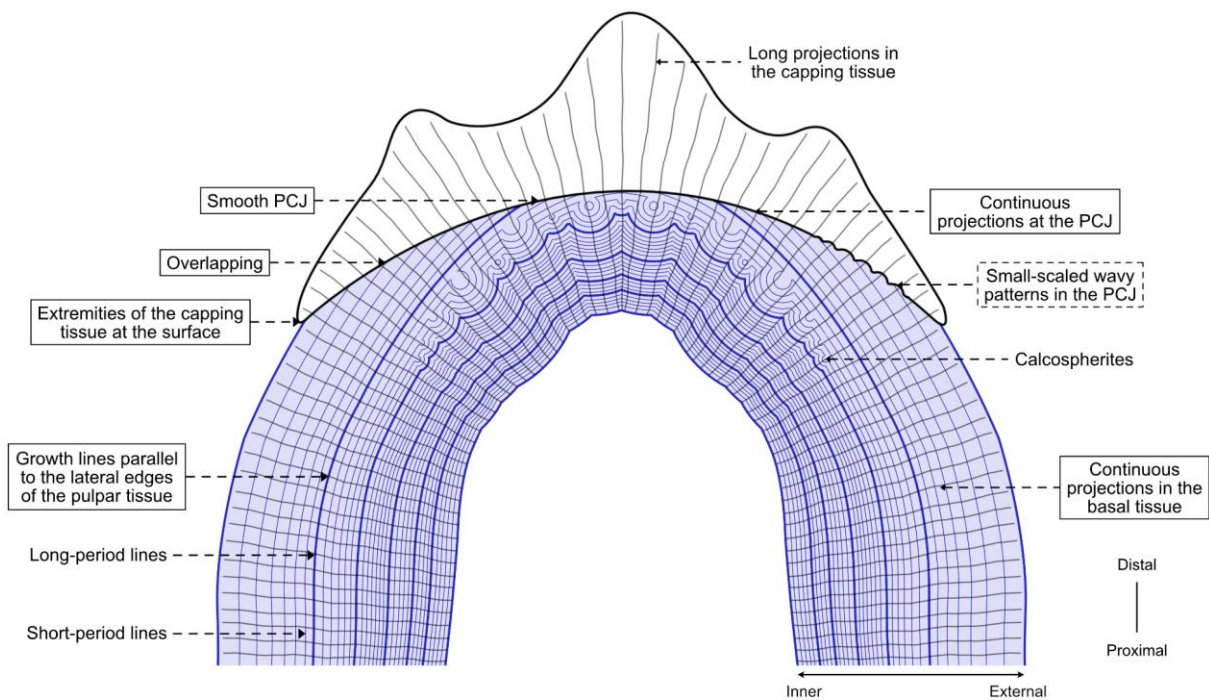


FIGURE IV-5. Virtual *Astraspis* odontode based on the compilation of the morphological and histological observations of several specimens. Some features are critical for the inference of the developmental scenario (boxes), while one is more ambiguous (dashed box). Note that the orientation of the tubules within a folded capping tissue is so far not well-constrained. Blue tissue, basal tissue (orthodontine). White tissue, capping tissue (enameloid or enamel). PCJ, pulpar-capping junction.

Developmental scenarios

The folded external surface of the *Astraspis* odontodes suggests either that the mineralization of the capping tissue was not uniform (giving rise to a wavy external surface from an initially smooth epithelium-mesenchyme interface) or that the epithelium-mesenchyme interface was similarly folded before the start of the matrix secretion. Depending on the nature of the capping tissue, the initial position of the epithelium-mesenchyme interface could correspond to either the PCJ, the external surface of the odontode, or an intermediate position between the PCJ and the external surface. In extant enamels, the initial position of the epithelium-mesenchyme interface corresponds to the position of the dentin-enamel junction because the upper layer of dentin mineralizes against the epithelium. In extant enameloid, it corresponds either to the external surface, or to an intermediate position between the dentin-enameloid junction and the external surface, depending on the relative contribution of the secreting epithelial cells in the matrix production and on the invading rate of the corresponding matrix components (Meinke & Thomson, 1983; Berkovitz & Shellis, 2016). Note that the initial shape and position of the epithelium-mesenchymal interface may be strongly related with the shape of the growth lines within the dentin, because it corresponds also to the initial position of the odontoblasts and may constrain their movements during secretion and mineralization. In extant (enameloid-bearing) gnathostomes, the shape of the dentin-enameloid junction seems to be constrained essentially by the epithelial protein distribution in the matrix (Sasagawa *et al.*, 2019). Interestingly, the inner boundary of the distribution range of the epithelial proteins, which delineates the future shape of the junction, does not necessarily parallel the shape of the epithelium. Instead, it depends on the pervading gradient of these proteins in the matrix (Shellis & Miles, 1974; Fanchon *et al.*, 2004; Goldberg *et al.*, 2004; Sasagawa *et al.*, 2019; Kawasaki *et al.*, 2021), and on the position of the odontoblasts if epithelial proteins reach their position. Moreover, during enameloid formation, some of the early secretion fronts of the odontoblasts that could have become 'growth lines'

within the dentin, may be ‘erased’ by the propagating epithelial proteins. This may explain the presence of the unconformities (triple points) observed between the pulpar growth lines and the junction in *Astraspis*, notably at the periphery of the capping tissue (Fig. IV-2D, E). Dentin growth lines at the periphery of a capping enameloid are not well documented in crown-gnathostomes. However, in our opinion, this kind of unconformities are visible at least in actinopterygians (see Richter & Smith (1995), their Fig. 17, and possibly their figs. 18–19, or Ørvig (1978a), his Fig. 47). These features are thus critical for deciphering the nature and developmental history of fossil mineralized tissues and consequently we consider the two extreme initial positions of the epithelium-mesenchyme interface in our ‘identification key’ (Fig. IV-6 step 2) and the possibility to form enamel or enameloid (Fig. IV-6 step 5). We also added a case of initial position corresponding to the first complete pulpar tissue growth line to illustrate the hypothesis of overlapping formation through secondary, external and centrifugal deposition of pulpar tissue (Fig. IV-6 steps 2 and 6) (Smith & Hall, 1990).

It is noteworthy that contrary to what we usually observe in the orthodentine of extant gnathostomes, the growth lines in *Astraspis* are parallel to the lateral edges of the pulpar tissue, when erosion is not present (D’Emic *et al.*, 2013; Meunier, Germain & Otero, 2018; Emken *et al.*, 2021). In extant gnathostomes, differentiation of the mineralizing cells (odontoblasts in the mesenchyme and ameloblasts in the epithelium) seems to occur first at the tips of the cusps, where putative signaling centers are present (see Debais-Thibaud *et al.*, 2015; Thiery *et al.*, 2022; Zimm *et al.*, 2023), and then spreads to the rest of the tooth or odontode (Thesleff *et al.*, 2001; Lisi *et al.*, 2003). This induces the development of growth lines that, in longitudinal sections, appear discordant (not parallel, presence of triple points) with the lateral edges of the orthodentine (D’Emic *et al.*, 2013; Meunier *et al.*, 2018; Emken *et al.*, 2021). The fact that in *Astraspis*, the growth lines are parallel to the lateral edges of the pulpar tissue suggests instead that odontoblasts differentiated and started secreting subsynchronously over the whole periphery of the odontode. Similar dentin growth

line shapes have been observed in other stem-gnathostomes, e.g. *Eriptychius* (Smith *et al.*, 1995), Heterostraci (Keating *et al.*, 2015), Thelodonti (Janvier, 1996), providing further evidence of synchronous formation of dentin during development. This is thus the kind of phenotypic features that may allow discrimination among otherwise similar developmental scenarios and we have included the two corresponding developmental hypotheses (spreading or synchronous differentiation) in our identification key (Fig. IV-6 step 3, see details below). Furthermore, we distinguish spreading from the top (as observed in extant gnathostomes) and from a hypothetical case of lateral spreading.

Alternatively, as cases of erosion can be observed in odontodes (Ørvig, 1976, 1978c), teeth (LeBlanc *et al.*, 2023), and conodont elements (Shirley *et al.*, 2018), the vertical unconformities could also be formed via erosion of the top orthodentine and secondary deposition of the capping tissue (illustrated as an irregular erosion front in Fig. IV-6 step 4).

The small-scaled wavy patterns (scallop patterns occasionally observed in the PCJ in *Astraspis*) are reminiscent of those sometimes observed at the dentin-enamel junction of mammals (e.g. primates (Whittaker, 1978), notoungulates (Braunn, Ferigolo & Ribeiro, 2021), litopternes (Oliveira, Bergqvist & Line, 2001)). Their size in *Astraspis* (4-8 μm) is comparable to that in *Homo* (2-5 μm (Marshall *et al.*, 2003)), although they are known to show variability between individuals, teeth or even within a given tooth (Whittaker, 1978; Brauer, Marshall & Marshall, 2010). In mammals, these scallops seem to be induced by the formation of dentin on a folded epithelium whose expansion is confined (Radlanski & Renz, 2007). This seems to suggest that these scallops are not compatible with enameloid formation, as the epithelium should be in contact with the odontoblasts during the formation of the first layer of dentin (Berkovitz & Shellis, 2016). Yet, Velasco-Hogan *et al.* (2021) mentioned the presence of a scalloped dentin-enameloid junction in a teleost, suggesting they are not specific of one or the other hypermineralized tissue (enamel vs. enameloid). Furthermore, in mammals the tips of

these U-shaped scallops are oriented outwards (towards the enamel) (e. g. Whittaker 1978; Marshall *et al.* 2003), whereas the tips of those found in *Astraspis* are oriented inwards, i.e. toward the dentin (Fig. IV-2G). Note that these small-scaled wavy patterns may also correspond to an erosion front (as in Ørvig 1976, 1978b; LeBlanc *et al.* 2023). It is thus unclear for now whether and how the presence and shape or orientation of these scallops can be used to favor one developmental hypothesis over another.

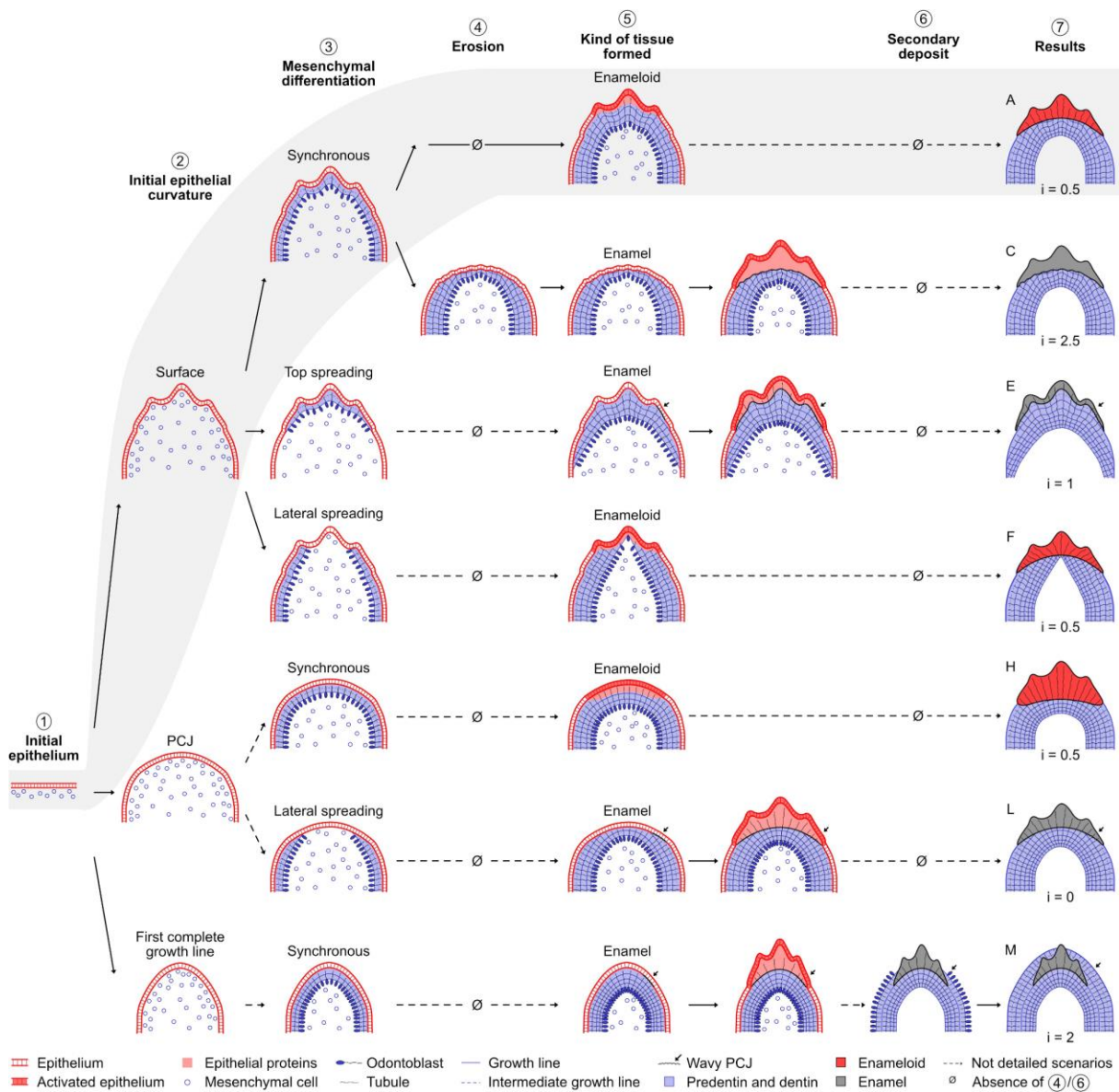


FIGURE IV-6. A selection of theoretical developmental scenarios for the formation of an *Astraspis* odontode (scenarios B, D, G and I–K are provided in Fig. IV-8, as well as a more

detailed selection procedure in high resolution). Developmental steps are listed from 1 to 7. The most congruent ontogenetic scenario (A) is highlighted in grey, based on a low index of incongruence (excluding C, E and M), the consideration of the lateral spreading as being unlikely (excluding F and L), and the reflection of the external surface shape in growth lines that can be verified in some odontodes (promoting A over H; see Fig. IV-4A). Please note that when not all scenarios are illustrated (dotted arrows), only the incongruences shared by all scenarios in this section of the 'tree' are used to calculate the index of incongruence. i , index of incongruence, where the lack of a critical feature adds 1, and 0.5 when it is an ambiguous one (see Fig. IV-5 boxes). PCJ, pulpar-capping junction.

Finally, among all the developmental hypotheses illustrated in our identification key, scenarios A, F, H and L (Fig. IV-6 and supplementary Fig. IV-8 for the most complete and detailed one) appear to be the most congruent with our observations (Fig. IV-2–5). In particular, scenario L ticks all the boxes, but it implies a hypothetical (and unlikely?) lateral spreading differentiation that has never been documented in any animal. On the other hand, scenario A is the only one that explains the presence of pulpar tissue growth lines that resemble the shape of the odontode external surface (as observed in Fig. IV-4A, and potentially in Fig. IV-2C) and it does fit with what we understand of the development of teeth and odontodes in extant vertebrates. These results strongly suggest that the odontodes of *Astraspis* are composed of (partially globular) orthodontine and a capping tissue of dual mesenchymal-epithelial origin. This corroborates previous interpretations of the capping tissue as enameloid (Fig. IV-6A) (Donoghue & Sansom, 2002; Sansom *et al.*, 2005; Sire *et al.*, 2009; Lemierre & Germain, 2019). Furthermore, it suggests that the initial epithelium-mesenchyme interface was similar in shape to the final external surface of the odontode, and that the differentiation of the odontoblast-like cells likely occurred synchronously throughout the epithelium-mesenchyme interface. The observation, in putative juveniles of other pteraspidomorphs, of partially mineralized odontodes that are similar in shape and size to the fully mineralized odontodes, but

lack centripetal dentin infilling the pulp cavity, supports these inferences (see Denison (1964), his Fig. 159, and Denison (1973), his Text-fig. 2). Under this scenario, the overlapping originates from the penetration of epithelial proteins through the matrix, and the pulpar growth lines partially preserve the initial shape of the epithelium-mesenchyme interface. When this initial shape of the epithelium-mesenchyme interface is folded, the incremental lines within the pulpar tissue are also folded, although it is also expected that the corresponding ridges and valleys will progressively fade out as growth increments of the pulpar tissue are added inwards (Fig. IV-4A). Hence, depending on the thickness of the enameloid, that is the relative size of the overlapping, the shape of the incremental lines within the pulpar tissue may reflect more or less the initial folded epithelium-mesenchyme interface (Fig. IV-2C, 4A). In the latter case, when the potentially folded part of the incremental lines within the pulpar tissue is secondarily masked by the overlapping, it may be tricky to distinguish the outcomes of scenarios A and H (smooth initial interface but folded surface of the capping tissue), except if we have access to tubules orientations in the capping tissue. Please note that we produced extreme cases in our developmental steps and that, depending on the odontode observed, traits can correspond to intermediate states.

The subsynchronous differentiation of the odontoblast-like cells assumed under scenario A may imply greater secretion of predentin at the lateral edges (supplementary Fig. IV-8A, D), and hence may promote overlapping, as compared to an 'actinopterygian' scenario where differentiation of those cells initiates at the top (see Richter & Smith (1995), their Fig. 17, and possibly their figs. 18–19, or Ørvig 1978*a*, his Fig. 47). At the scale of an individual odontode, it also implies that the whole epithelium is almost in place at the beginning of the secretion, and thus that no additional epithelial surface is added at the odontode extremities during its formation. Concerning the growth of the whole mineralized skeleton, either new odontodes are added at the periphery, or the odontodes already present at an earlier stage should

correspondingly grow in size. Our conclusions seem to reject the latter hypothesis for *Astraspis*, unless its odontodes were mineralized at the adult stage only.

Dual growth periodicity

Incidentally, our detailed analysis of odontodes of *Astraspis* also evidence for the first time a dual periodicity of the growth lines in the orthodontine (Fig. IV-3). Although incremental lines have already been reported in *Astraspis* (e.g. Sansom et al. 1997; Lemierre & Germain 2019) and compared with the von Ebner lines found in amniotes (Sansom *et al.*, 1997), there is no mention of a dual periodicity. In the dentin of amniotes, dual periodicity is common: short-period lines are called von Ebner lines, and long-period lines are called Andresen lines (Dean & Scandrett, 1996). It is also considered homologous among amniotes due to the morphological similarities (alternating opaque zones, line trajectories paralleling the contour of the pulp cavity, and widths ranging between 1 and 30 μm) observed between mammals, crocodylians, dinosaurs, mosasaurs, early synapsids, early reptiles and stem-amniotes (Erickson, 1996a, 1996b; Hillson, 2005, 2014; Gren & Lindgren, 2014; García & Zurriaguz, 2016; Maho *et al.*, 2022). In non-amniote vertebrates, incremental lines have been identified in non-amniote osteichthyans (e.g. Miller & Hobdell, 1968; Herold & Landino, 1970; Shellis & Berkovitz, 1976; Shellis & Poole, 1978; Kerebel & Le Cabellec, 1979), but no dual periodicity has ever been formally described. Yet, we suggest such dual periodicity is visible in at least one teleost (see Berkovitz & Shellis (2016), their Fig. 11.1). In chondrichthyans, an alleged triple periodicity has been described in the dentin of an extinct taxon (Soler-Gijón, 1999). In *Astraspis* the thickness of the short-period lines (0.5-5 μm) lies within the range of values measured for von Ebner lines of amniote orthodontine (1-34 μm) (Erickson, 1996a; Dean, 1998; Gren & Lindgren, 2014). The number of short-period growth lines per long-period (4-18) is close to that of primates (5-9) (Kawasaki, Tanaka & Ishikawa, 1979; Dean, 1987; Dean *et al.*, 1993). Note that in

other taxa, long-periods may comprise many more incremental lines (e.g. 11-128 in reptiles (Gren & Lindgren, 2014), and ca. 365 in *Delphinapterus leucas* (Waugh *et al.*, 2018)). Moreover, the short-period growth lines in *Astraspis* are found to interact with calcospherites (Fig. IV-3B), as in, for instance, mammal orthodontine (Dean, 2017; Waugh *et al.*, 2018). Therefore, we suggest that the dual periodicity observed in *Astraspis* orthodontine is, at least primarily, homologous to von Ebner and Andresen lines as defined in amniotes. To our knowledge, this is the most basal record of these periodic lines in the vertebrate phylogeny, and it may be shared within gnathostomes clade. In amniotes, von Ebner growth lines correspond to daily deposition and mineralization of dentin, under the influence of circadian rhythms (Yilmaz, Newman & Poole, 1977; Kawasaki *et al.*, 1979; Rosenberg & Simmons, 1980; Dean & Scandrett, 1996; Dean, 1998; Ohtsuka-Isoya, Hayashi & Shinoda, 2001; Iinuma *et al.*, 2002; D’Emic *et al.*, 2013; Waugh *et al.*, 2018; Papakyrikos *et al.*, 2020; Emken *et al.*, 2021). If short-period lines of *Astraspis* also correspond to a daily deposition and mineralization, we can estimate that the orthodontine, and probably the whole odontode (including the capping tissue), grew in about 60-70 days with a rate of 0.5-5 $\mu\text{m}/\text{day}$ (note that a day lasted about 21 hours during the Ordovician (Denis *et al.*, 2011)). The periodicity of Andresen lines is more enigmatic as it could reflect annual (Waugh *et al.*, 2018) or seasonal periods (Berkovitz & Shellis, 2016). Both types of lines are likely due to cyclic variations in the orientation of the fibrous matrix and/or in the matrix composition (Yilmaz *et al.*, 1977; Kawasaki *et al.*, 1979). A detailed analysis of this pattern is beyond the scope of this manuscript but it may be very informative about e.g. the ecology of *Astraspis*. Hopefully, this discovery will motivate developmental studies on extant non-amniote gnathostomes in order to test for the presence of daily growth lines (von Ebner lines).

IV.5. Conclusion

The fossils of *Astraspis* from the Harding sandstone feature odontodes that are considered as some of the oldest vertebrate ‘dental’ tissues. Although pivotal to our understanding of the gradual assembly of the vertebrate skeleton, homology of their mineralized tissues remained controversial to date. Here we show how a total evidence approach combined with even simple models of the development of vertebrate mineralized tissues is able to resolve such long-term debates about the nature of fossil mineralized tissues. Within the odontodes of *Astraspis* we identify the pulpar tissue as orthodentine and the capping tissue as enameloid. Moreover, integrative analyses of histogenetic features such as the one proposed here may allow to infer additional aspects about the development of these tissues: the most plausible developmental scenario for the odontodes of *Astraspis* suggests their external surface mirrors the shape of the initial epithelium-mesenchyme interface and the differentiation of the odontoblast-like cells occurred most likely subsynchronously across that interface. Our analysis also shows how superficially similar morphologies may be attained via very different developmental scenarios and how often overlooked details may be critical for histological identifications. In the future, this kind of developmental approach could be extended to the study of other pteraspidomorph’s odontodes, and more generally, other tissues of extinct taxa. As a conclusion, we are tempted to stress out that it is not mere the ‘phenotype’ that matters, it is the developmental journey.

Acknowledgements. We warmly thank Severin MOREL for preparing the thin sections, Alfred LEMIERRE for our rich discussions about *Astraspis* histology and Nozomu OYAMA for his great suggestions to improve the figures.

Contributions. **Conceptualization** Guillaume Houée (GH), Nicolas Goudemand (NG), Jérémie Bardin (JB), Damien Germain (DG), Philippe Janvier (PJ); **Data Curation** GH; **Formal Analysis** GH; **Investigation** GH; **Methodology** GH; **Project Administration** GH; **Resources** DG; **Supervision** DG, NG, JB; **Validation** GH, NG, JB, DG, PJ; **Visualization** GH, NG, JB, DG, PJ; **Writing – Original Draft Preparation** GH, NG, JB, DG, PJ; **Writing – Review & Editing** GH, NG, JB, DG, PJ.

IV.6. Appendix

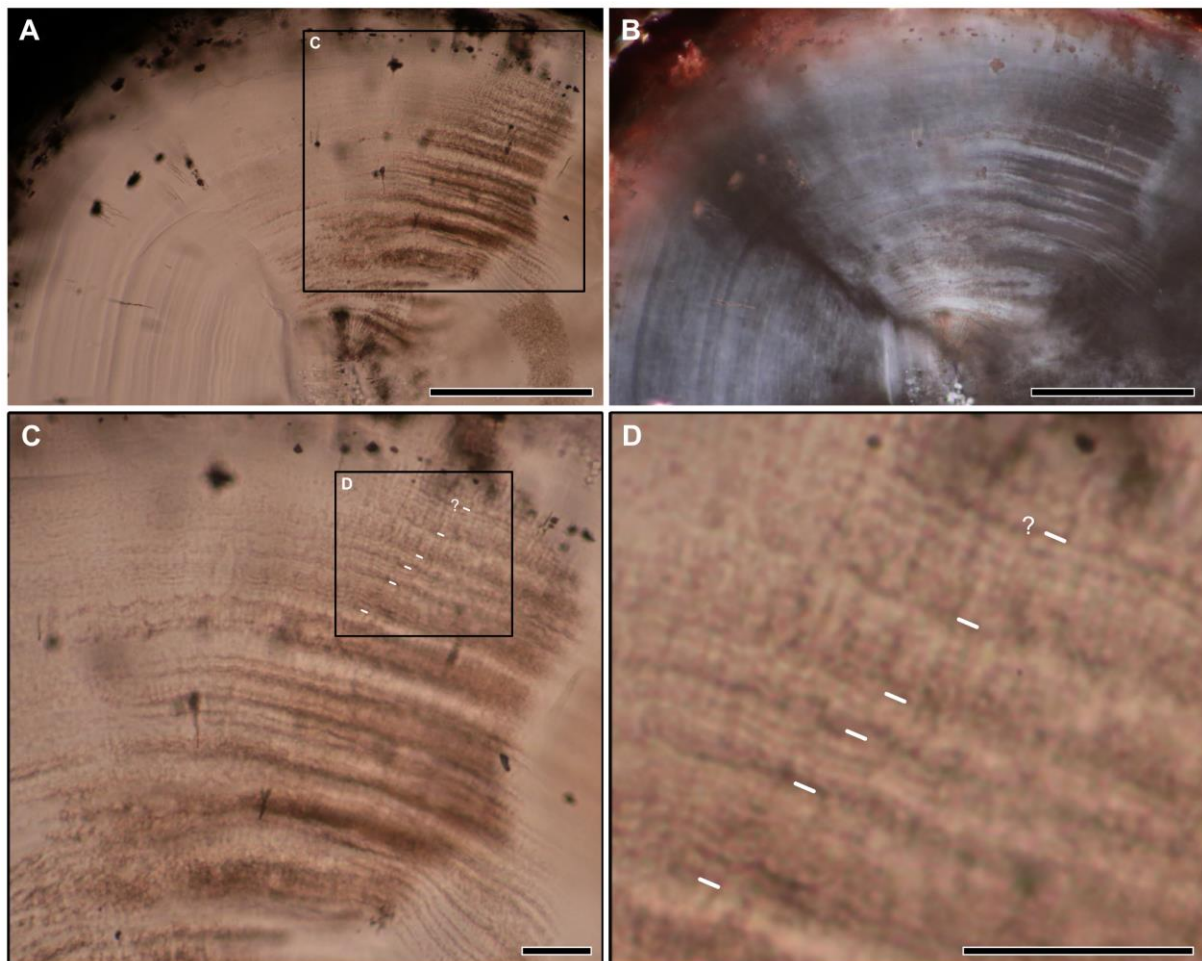


FIGURE IV-7. Supplementary example of dual growth periodicity in an odontode of *Astraspis* (MNHN-Histos 3251). A, natural light. B, same section in cross-polarized light. C, zoom in A. D, zoom in C to see the short-period growth lines between the long-period growth lines (white lines). Scale bars represent: 100 μm (A, B); 20 μm (C, D).

CHAPTER IV – PALEODEVELOPMENT OF ODONTODES

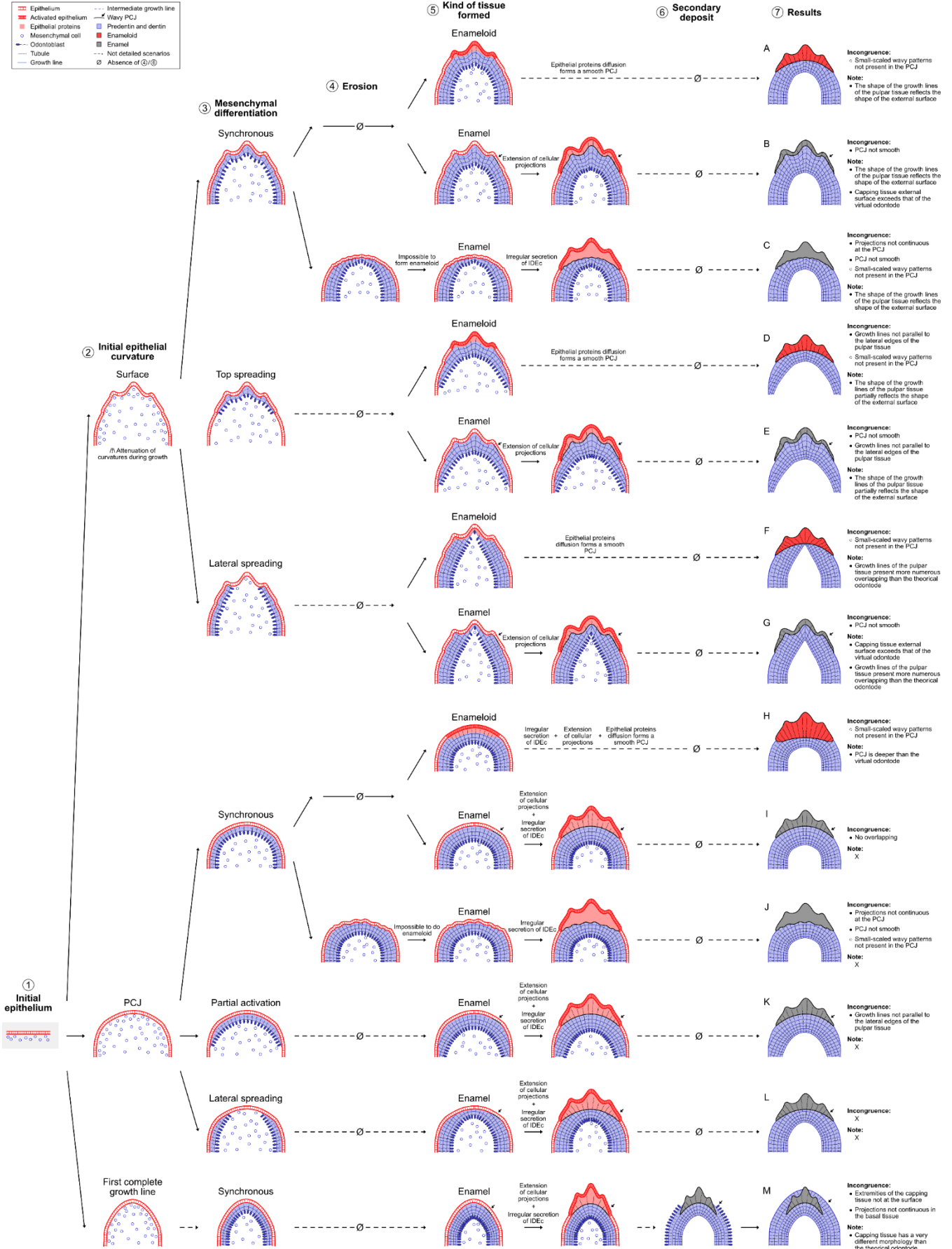
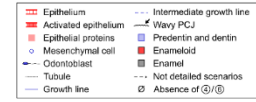


FIGURE IV-8. Theoretical developmental scenarios for the formation of an *Astraspis* odontode (the high-resolution figure is available on the provided google drive link below). Developmental steps are listed from 1 to 7. The most congruent ontogenetic scenario (A) is highlighted in grey, based on a low index of incongruence (excluding B, C, D, E, G, I, J, K and M), the consideration of the lateral spreading as being unlikely (excluding F and L), and the reflection of the external surface shape in growth lines that can be verified in some odontodes (promoting A over H; see Fig. IV-4A). Please note that when not all scenarios are illustrated (dotted arrows), only the incongruences shared by all scenarios in this section of the 'tree' are listed near the illustrated scenario. *i*, index of incongruence, where the lack of a critical feature adds 1, and 0.5 when it is an ambiguous one (see Fig. IV-5 boxes). PCJ, pulpar-capping junction.

Figures in high resolution and an additional simulation proposing a reconstruction of *Astraspis* odontode development:

https://drive.google.com/drive/folders/1dXuW_3O5hsByHnJ-zvG1BoW7Dt7_Sz0t?usp=sharing



Conclusion on the objectives of Chapter IV

In Chapter IV we:

- Revised the histomorphology of the key Ordovician early vertebrate *Astraspis*.
- Proposed a new approach to make developmental inferences and identify tissues by comparing multiple ontogenetic scenarios (Fig. 2-IVa).
- Showed that stem-gnathostome odontodes appeared to form through synchronous, rather than delayed, activation of mesenchymal cells (Fig. 2-IVb).
- Identified what seems to be the oldest occurrence of vertebrate daily growth lines ever reported.

CHAPTER V

***DEVELOPMENT OF THE PTERASPIDOMORPH DERMAL PLATE:
PRELIMINARY NOTES***

Objectives Chapter V

After focusing on the histomorphogenesis of dental tissues and structures in pteraspidomorphs (Chapter IV), Chapter V aims at exploring also the ossification of the mineralized plates on top of which odontodes grow, and how this process interacts with the patterning of the odontodes at the body scale (Fig. 2 Va). As for Chapter IV, such paleodevelopmental inferences about pteraspidomorphs may help us characterizing the events and mechanisms of vertebrate diversification by providing plesiomorphic states (Fig. 2 Vb). Special attention is given here to the description and interpretation of the formation of intriguing patterns in the skeleton of *Anglaspis*.

V.1. Introduction

Pteraspidomorphs were jawless stem-gnathostomes ('ostracoderms') that lived from the early-middle Ordovician to the late Devonian. They are considered as representing some of the oldest remains of vertebrate mineralized skeleton (Janvier, 1996; Sire *et al.*, 2009; de Buffrénil *et al.*, 2021). They exhibited a dermal skeleton that includes in particular two cephalothoracic plates constituted, from the internal surface to the external surface, of: (1) a layer of compact lamellar anosteocytic osseous tissue, and (2) a layer of cancellar anosteocytic osseous tissue (aspidin), covered with (3) a layer of odontodes (tooth-like structures) (Keating *et al.*, 2015). Structurally speaking, there is variation among the pteraspidomorph skeletons: the aspidin may be arranged more or less geometrically (forming canal networks or chambers, see Fig. 6), and the odontodes may be shaped as either 'spots' or 'strips' (Tarlo, 1967; Pernègre, 2003; Keating *et al.*, 2015). Because these patterns are reminiscent of those formed by chemical reaction-diffusion mechanisms (Turing, 1952; Garfinkel *et al.*, 2004; Kondo & Miura, 2010), they have been interpreted as being possibly produced via Turing-like processes (Tarlo, 1967). Owing to pteraspidomorphs' key phylogenetic position near the origin of vertebrates, these skeletal patterns are likely to shed light on the first mechanisms of skeletogenesis in vertebrates.

Among pteraspidomorphs, the cephalothoracic plates of a few heterostracans such as *Anglaspis* exhibit an intriguing combination of patterns: above the basal compact and lamellar anosteocytic osseous tissue, aspidin presents a honeycomb-like structure (Janvier, 1996), upon which odontodes are shaped and arranged in a 'fingerprint-like' manner (e.g. see Figure 150 in Denison (1964)). Unlike the already described patterns of odontodes, the characterization of the internal honeycomb-like bone structure has been limited to descriptions of fractured specimens or histological sections (e.g. Denison, 1964; Blicek, Goujet & Janvier, 1987). Today X-ray microtomography allows for full-body, non-destructive, virtual histology of these

plates. This has notably enabled the description of the 3D structure of spongy bone (not forming honeycomb-like structures) in a heterostracan (see Figure 2c in Keating *et al.* (2018)), as well as in other early vertebrates (e.g. Qu *et al.*, 2015a; O’Shea *et al.*, 2019). Using X-ray microtomography, we are keen to explore the distribution of the honeycomb-like bone throughout dermal plates, and more particularly the possible interactions between this cancellous bone structure and the ‘fingerprint-like’ pattern of odontodes situated above. As vascular and sensory networks of canals have been identified in heterostracans (Denison, 1964), as well as internal organ impressions (Denison, 1964), we also aim at clarifying the 3D distribution of canal networks and their interactions with the soft and mineralized structures. Finally, based on reconstructed histomorphological features of *Anglaspis*, we consider the developmental stages that led to the formation of pteraspidomorph dermal skeleton.

V.2. Materials and Methods

We conducted scans of a complete dorsal (MNHN.F.SVD606) and ventral (MNHN.F.SVD615) cephalothoracic plate of *Anglaspis insignis* Wills, 1936 (ex Kiaer, 1932) (Heterostraci) from the Devonian of Spitsbergen. These scans were conducted using high-resolution computed tomography at the AST-RX platform of the Muséum National d’Histoire Naturelle, Paris (UAR 2700 2AD; GE phoenix|X-ray v|tome|xs 240 L), with reconstructions performed using DATOX/RES software (phoenix datos|x). The voxel size was about 10 μm in all cases. Segmentations were performed on Amira and Avizo 2021.2 (<https://www.fei.com/software/amira-avizo/>).

Transversal and longitudinal thin sections have been prepared from a subcomplete dorsal cephalothoracic plate of *Anglaspis* from the Devonian of Spitsbergen (MNHN.F.SVD2219b). As most strip-like odontodes are subaligned with the anteroposterior axis, these sections are also transversal and longitudinal for at least

a few odontodes, allowing access to the histological properties of these organs in three dimensions. Transverse histological sections were also prepared from another heterostracan (MNHN.F.SVD2998) exhibiting an intermediate aspidin structure composed of both spongy and cancellous areas for comparison. All sections were polished to a thickness of about 70 to 100 μm . Pictures were taken with a digital camera (Canon EOS 6D) adapted on a microscope Olympus CX31P with the Micro Tech Lab DSLRCFTC_Pro and TUST42C models. We also discuss a synchrotron-based image illustrated in Keating *et al.* (2015).

V.3. Results

Postmortem fractures apart, each dorsal or ventral plate presents a cohesive structure without any discernible demarcation, fusion zone, or apparent growth lines (Fig. V-1A, 2A). As mentioned above, these plates are made of three layers: a basal layer, a middle layer and an odontode layer, whose respective structure and histology are described here in detail.

Basal layer of Anglaspis

Structure

The basal layer is continuous on each plate (Fig. V-1B purple layer, H). A number of small pores are visible, which could correspond either to canal positions or to alteration pit marks, with no particular distribution (Fig. V-1H). As already described by Denison (1964), the dorsal cephalothoracic plates of *Anglaspis* may preserve imprints of some internal organs (e.g. semi-circular canals, gill archs...) (Fig. V-1H).

CHAPTER V – PALEODEVELOPMENT OF DERMAL PLATES

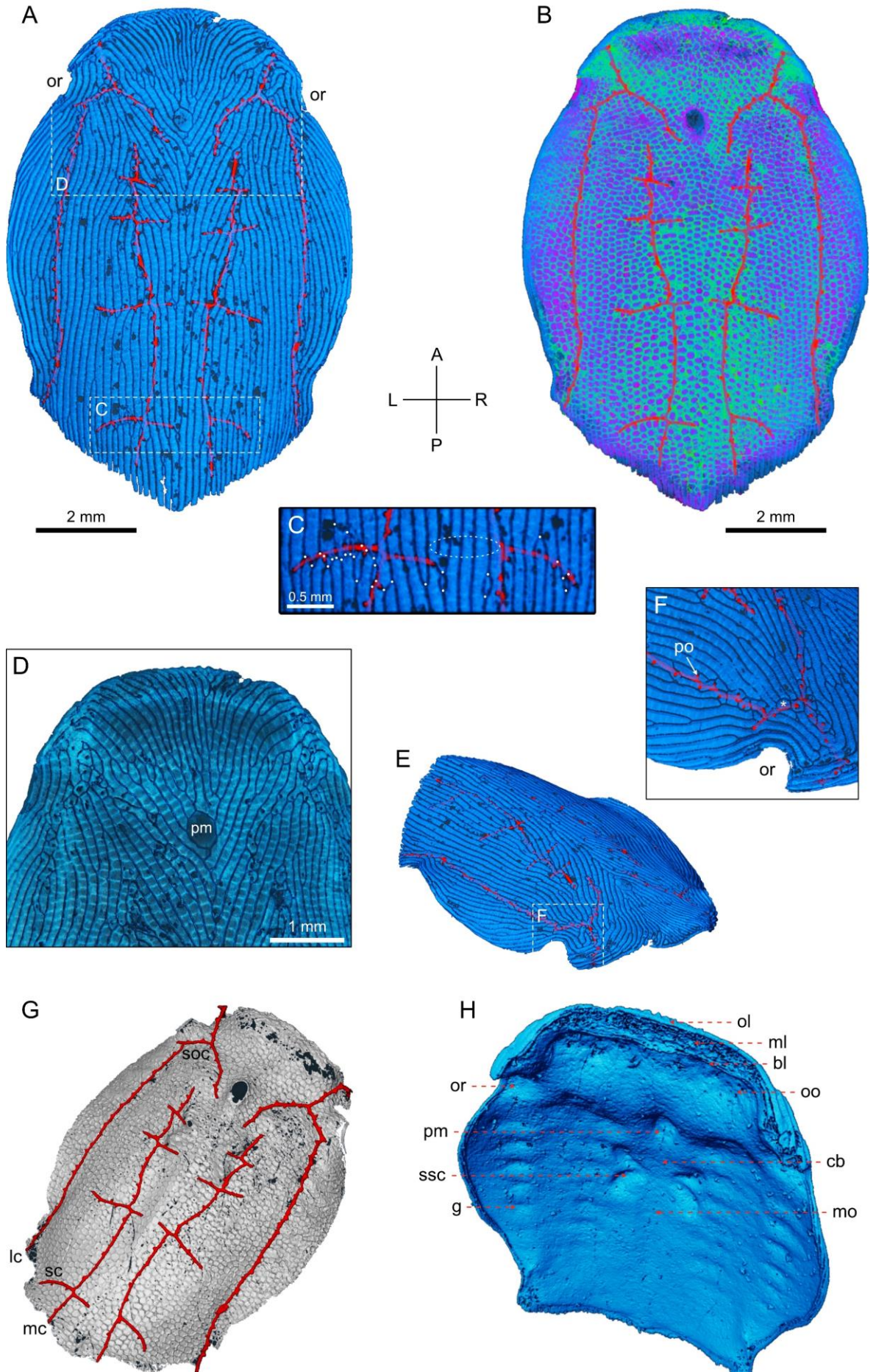


FIGURE V-1. 3D reconstructions of the dorsal dermal plate of *Anglaspis insignis*. A, dorsal view of the fingerprint-like pattern of odontodes. The openings and the low transparency allow for the visualization of the network of wide canals (red). B, same as A with the three layers set as semi-transparent (blue, layer of odontodes; green, middle layer; purple, basal layer), thereby highlighting the honeycomb-like pattern of the middle osseous layer. C, detail of A: the dotted ellipse indicating the location of a missing secondary branch of the canal network. The white dots indicate triple junctions between the odontodes. Note their absence in the region where the missing secondary branch would be expected if the canal network were bilaterally symmetrical. D, detail of A viewed in transparency, thereby highlighting the alignment of the fingerprint-like and honeycomb-like patterns. E, oblique antero-lateral view of the same specimen detailing the network of canals and pores in the orbital region (F). Note the presence of smaller, 'truncated', subcircular odontodes along the canal (*). G, oblique dorsal view of the basal layer together with the canal network, detailing the arrangement of secondary branches of this network around the central nervous system, known to be located beneath the plate. H, oblique ventral view showing the imprints left by internal organs on the dorsal plate (Janvier, 1996). bl, basal layer. g, gill. cb, cerebellum. lc, lateral canal. mc, medial canal. ml, middle layer. mo, medulla oblongata. ol, odontode layer. oo, olfactory organ. or, orbit. pm, pineal macula. po, pore. sc, secondary canal. scc, semicircular canal. soc, supraorbital canal. Orientation: Anterior, Posterior, Right, Left.

Histology

The basal layer is made of a compact anosteocytic osseous-like tissue (Fig. V-3-5). Under cross-polarized light it presents an alternation of light and dark thin sublayers that are generally straight and parallel to the inner surface of the layer, as in lamellar bone. Note that what appears as the topmost part of this basal layer may be formed by the centripetal deposition of aspidin around the chambers, and may correspond to the middle layer. Some discontinuities (Fig. V-3A arrow head) may be interpreted as canals crossing the basal and middle layers and opening inside the chambers. Locally we observe thin fibers perpendicular to the growth lines (Fig. V-4E).

CHAPTER V – PALEODEVELOPMENT OF DERMAL PLATES

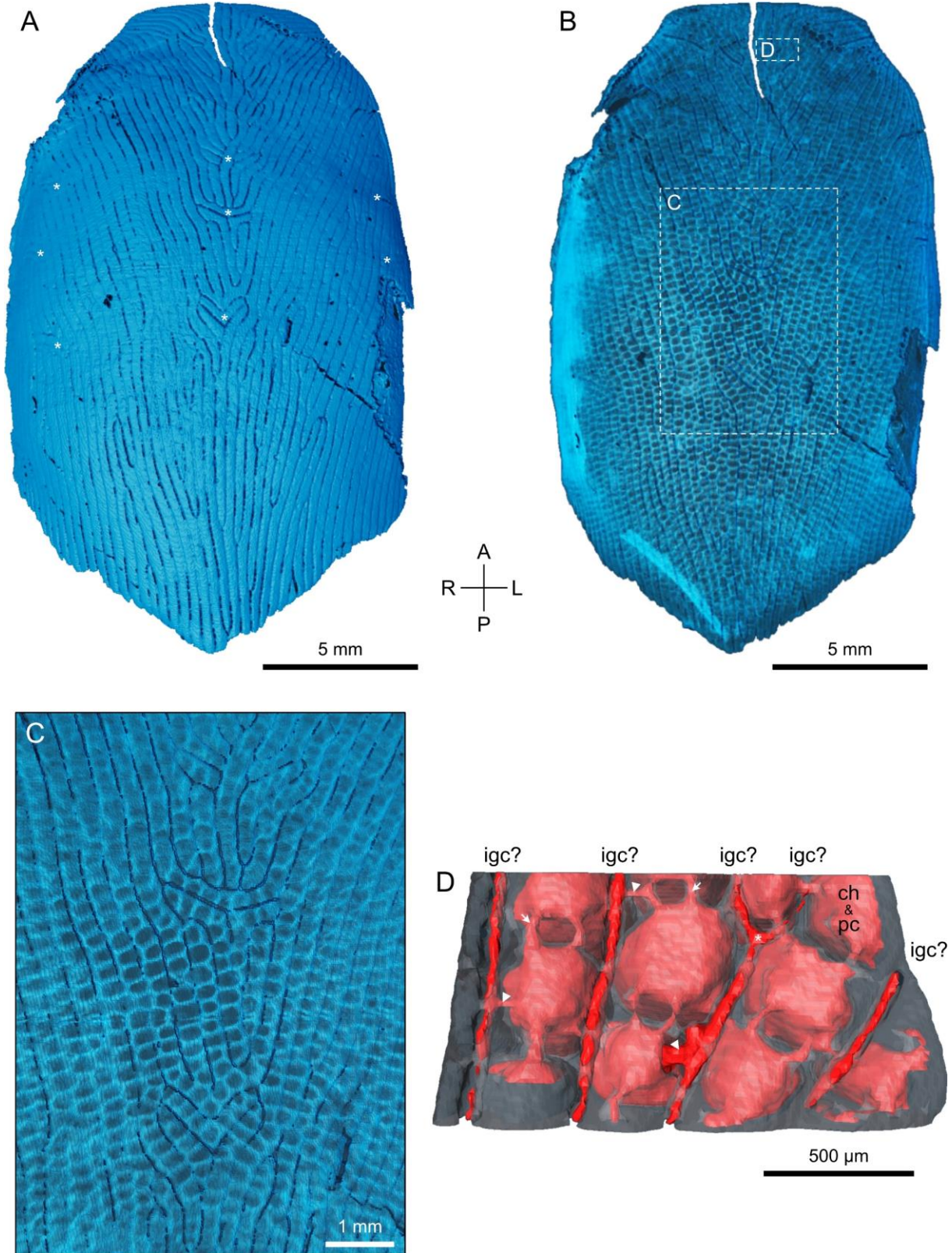


FIGURE V-2. 3D reconstructions of the ventral dermal plate of *Anglaspis insignis*. A, ventral view of the fingerprint-like pattern of odontodes. Most odontodes align with the antero-posterior axis, but in some regions (indicated by a white asterisk) they are either arranged subperpendicularly or they are U- or V-shaped and centered on the symmetry axis. B, same view as A with the layers set as semi-transparent, thereby highlighting the honeycomb structure of the aspidin. C, detail of B, highlighting the alignment of the fingerprint-like and honeycomb-like patterns. D, reconstruction of the network of chambers and canals in the region D of B. Note that the chambers, including the pulp cavities, are interconnected with each other (indicated by arrows), and with the network of intercostal grooves (indicated by arrowheads), which is also interconnected (*), via small canals. Additional canals were likely present at the base of the structure, not visible in this view. ch, chamber. igc, intercostal groove canal. pc, pulp cavity. Orientation: Anterior, Posterior, Right, Left.

Middle layer of Anglaspis

Structure

In dorsal view, this layer presents a honeycomb pattern: uniformly packed, polygonal, mostly hexagonal, chambers, separated by pillar walls, fill the volume of this layer over the entire plate (Fig. V-1B, D and 2B, C). These chambers correspond to the cavities of this middle layer, as well as to the pulp cavities of the odontodes with which they are fused (Fig. V-3B, 4C and 5). Many canals connect the chambers together (Fig. V-3A, 4A and 5 arrow head) in their upper part, or connect them to the ‘intercostal grooves’ (Denison, 1964) that separate odontodes (Fig. V-2D). In cross-section, the middle layer takes essentially the form of I- or Y-shaped parallel pillars, perpendicular to both the basal and upper layers (Fig. V-3-5). The bifurcation of the conspicuously Y-shaped pillars corresponds to a section in a neighboring chamber (Fig. V-4A-D) or to wide canals (Fig. V-3E, wc; see the following paragraph).

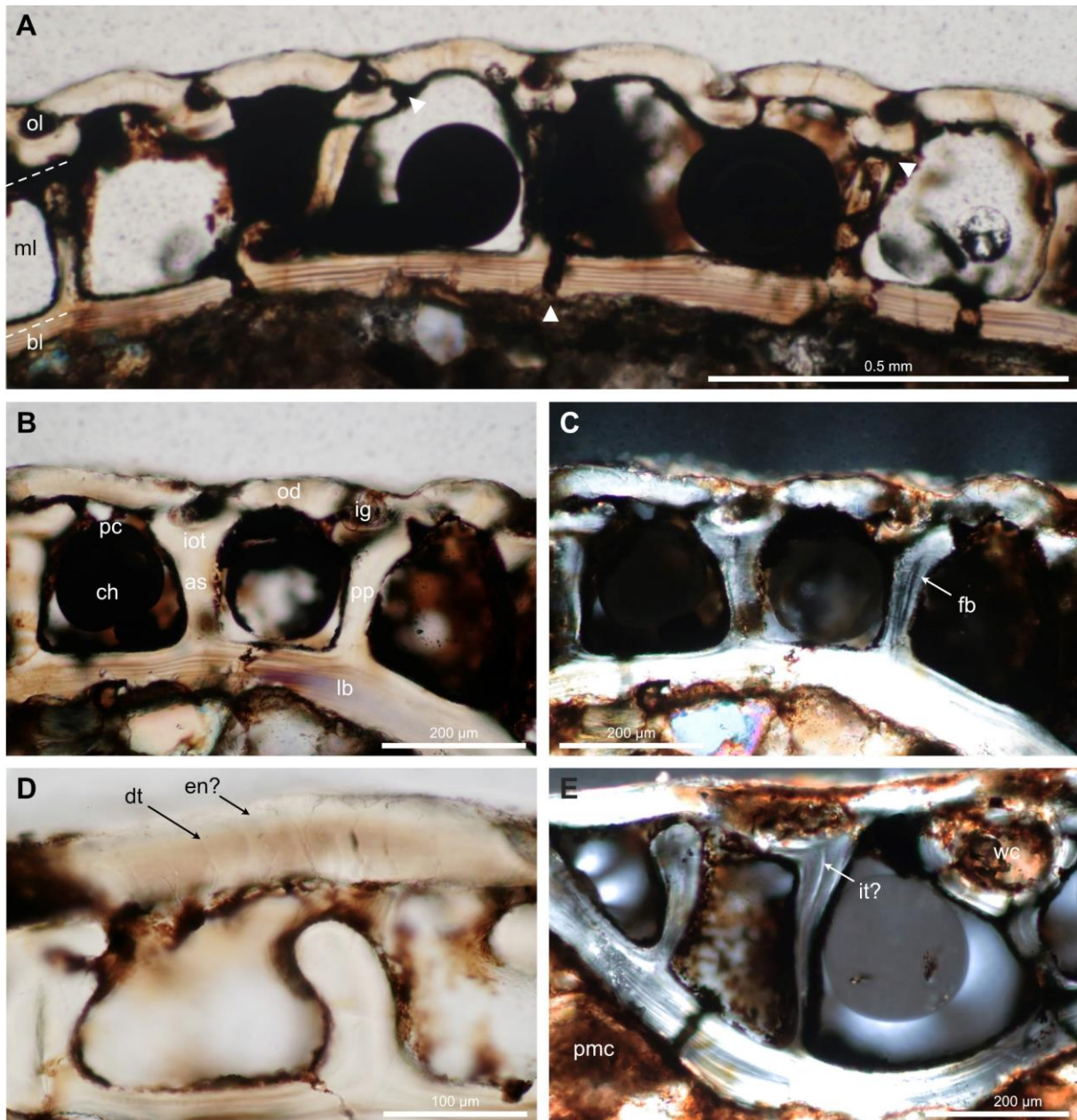


FIGURE V-3. Transversal thin sections of the dorsal dermal plate of *Anglaspis* in polarized (A, B, D) and cross-polarized light (C, E). Please note that the same pattern is repeated laterally: on top, bean-shaped odontodes are separated by intercostal grooves whose sides form a subtriangular void (canal?); in the middle layer, spacious, interconnected (arrowheads), inner chambers are separated by pillars of aspidin, each chamber being aligned below an odontode and housing its pulp cavity and each pillar supporting an intercostal groove; a compact lamellar tissue forms the base. A-C, F-Histos 3267. D, E, F-Histos 3268. as, aspidin. bl, basal layer. ch, chamber. dt, dentin tubule. en, enameloid. fb, fiber. ig, intercostal groove. it, initial trabeculae. iot, intermediate osseous tissue. lb, lamellar bone. ml, middle layer. od, odontode.

ol, odontode layer. pmc, pineal medulla cavity. pp, parallel pillars. pc, pulp cavity. wc, wide canal.

In the upper part of the dorsal plate middle layer, wide canals form a bilaterally subsymmetrical network along the anteroposterior axis (Fig. V-1A, B). Those canals are easily distinguishable in cross-section because of the concentric tissue deposition around them (Fig. V-3E, wc). This canal network is composed of four disconnected parts, or branches, two on each side of the symmetry axis. The two proximal branches present 7-8 smaller, secondary branches, usually organized in opposing pairs. The distance between two consecutive pairs increases linearly towards the posterior end. They are positioned very close to the neural area (marked by a X-shaped imprint on the ventral side of the dorsal plate), itself positioned under the dermal plate on the symmetry axis, with some of the secondary branches heading towards the semicircular canals (Fig. V-1G). We have not found any evidence of a connection between this canal network and the organs situated beneath the basal layer. Intriguingly, although the geometry of this canal network appears mostly symmetrical, the posteriormost secondary branch on the left side does not have a counterpart on the right side MNHN.F.SVD606 (Fig. V-1C). The two hook-shaped, mostly distal branches are located within the mid-lateral depressions, then they extend anteriorly around the orbits and bifurcations curve back to the top of the head, close to the pineal macula (Fig. V-1G). All of these wide canals are connected to the plate's exterior via a system of regularly-spaced pores that traverse the odontodes (Fig. V-1F). These pores are situated on either side of the canals, generally alternating between right and left (Fig. V-1F). No such pores or wide canals have been observed within the ventral plate.

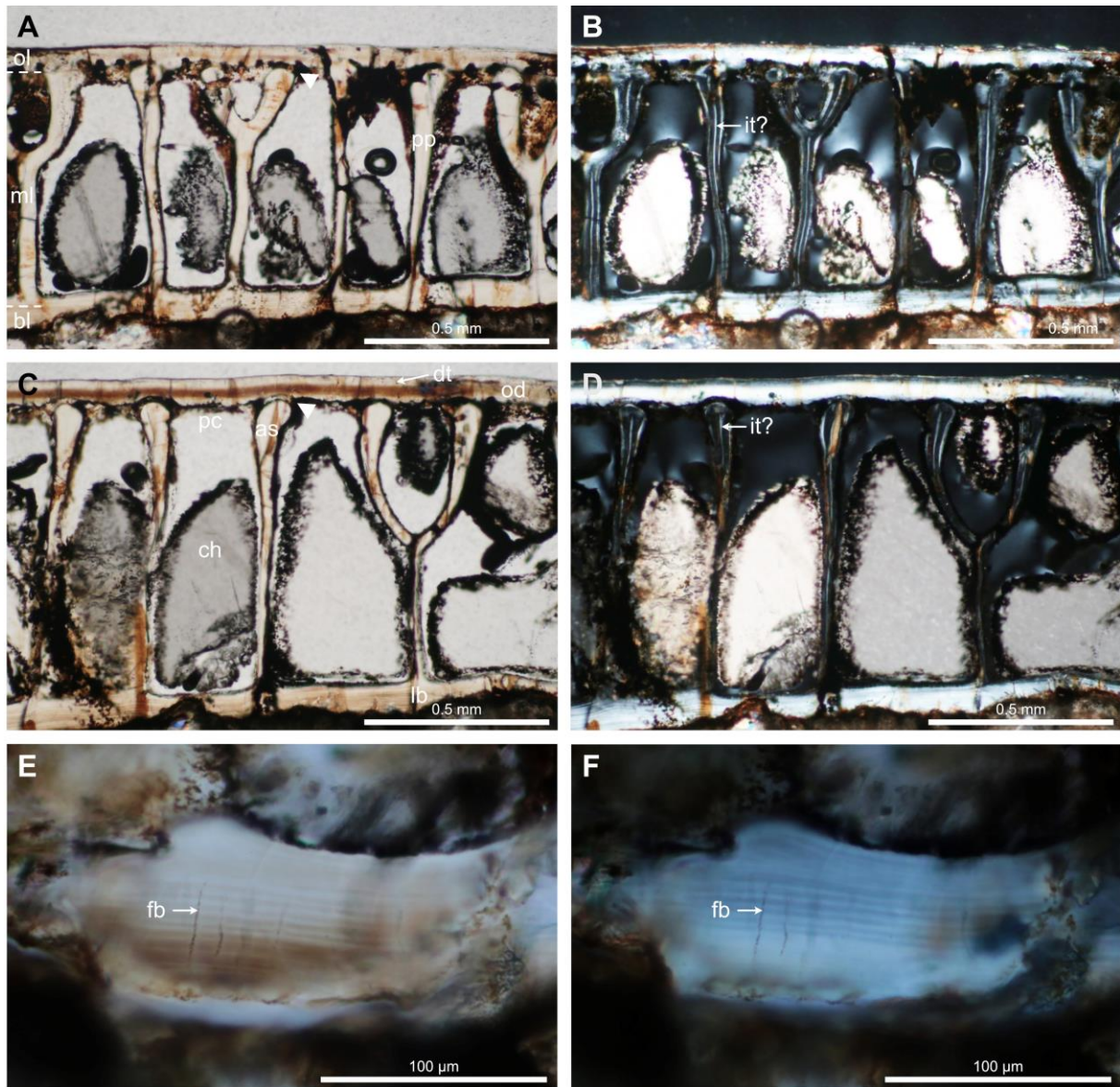


FIGURE V-4. Longitudinal thin sections of the dorsal dermal plate of *Anglaspis* (F-Histos 3269) in polarized (A, C, E) and cross-polarized light (B, D, F). A-D, please note the arrangement of parallel pillars corresponding to the walls of the chambers. They appear fused with the basal layer, but they are often separated from the odontode layer, possibly due to secondary erosion (canals?; arrowheads). E, F, large fibers in the basal compact lamellar layer. as, aspidin. as, aspidin. bl, basal layer. ch, chamber. dt, dentin tubule. fb, fiber. it, initial trabeculae. lb, lamellar bone. lma, lamella aspidin. ml, middle layer. od, odontode. ol, odontode layer. pp, parallel pillars. pc, pulp cavity. sr, secondary resorption.

Histology

The periphery of the inner chambers is made (as for the basal layer) of a lamellar anosteocytic osseous-like tissue (Fig. V-3C, E, 4B, D and 5), corresponding to aspidin (historically referring to the tissue of the middle layer of heterostracan dermal skeleton; Gross, 1930; Keating *et al.*, 2018). The growth lines are parallel to the periphery of the chambers, and under cross-polarized light the sublayers alternate between black and white. Within these sublayers, we observe thin tubules/fibers that are perpendicular to the growth lines (Fig. V-3C, 5, fb). Between these lamellar peripheral depositions, we tentatively distinguish thin anosteocytic osseous initial trabeculae (Fig. V-3E, 4B, D and 5, it). These putative trabeculae are anchored in the basal layer, contrary to the upper odontode layer, where trabeculae are most of the time separated by a canal (Fig. V-2D, 5). These canals sometimes overlap the growth lines and the aspidin pillar (Fig. V-5).

Odontodes of Anglaspis

Structure

The odontodes of *Anglaspis* present a fingerprint-like pattern (Fig. V-1A, F, 2A): most odontodes are strip-like shaped, their length being much larger than their width; some odontodes may be much shorter and then subcircular in shape; the width of all odontodes is very uniform across a plate. The pattern is bilaterally subsymmetrical, although details at the odontode level may vary between the left and the right sides. On the dorsal plate, odontodes are mostly aligned along the anteroposterior axis, except in the anterior region where odontodes seem to radiate from the pineal macula. The odontodes seem to be ‘truncated’ (that is, smaller than one would expect by comparison with its neighboring odontodes) when they ‘meet’ a wide canal (Fig. V-1C, F). In such cases they may also be crossed by a pore near their extremity. On the

ventral plate, most odontodes also align with the antero-posterior (AP) axis, the angle between the main axis of the odontodes and the AP axis decreasing progressively from the anterior to the posterior. In some regions (Fig. V-2A, *) the odontodes may be either arranged subperpendicularly to the AP axis or they are U- or V-shaped and centered on the symmetry axis. The latter U- or V-shaped odontodes appear at three distinct locations along the AP axis.

In transversal section, odontodes have a bean shape, with angular edges overlapping circular intercostal groves (Fig. V-3, 5, od and ig). These intercostal grooves are present between odontodes, have a tubular shape and are all connected in a branched pattern (Fig. V-2D, *). The U-shaped base of these intercostal grooves is made of an osseous-like tissue that connects neighboring odontodes (Fig. V-3B, 5, iot).

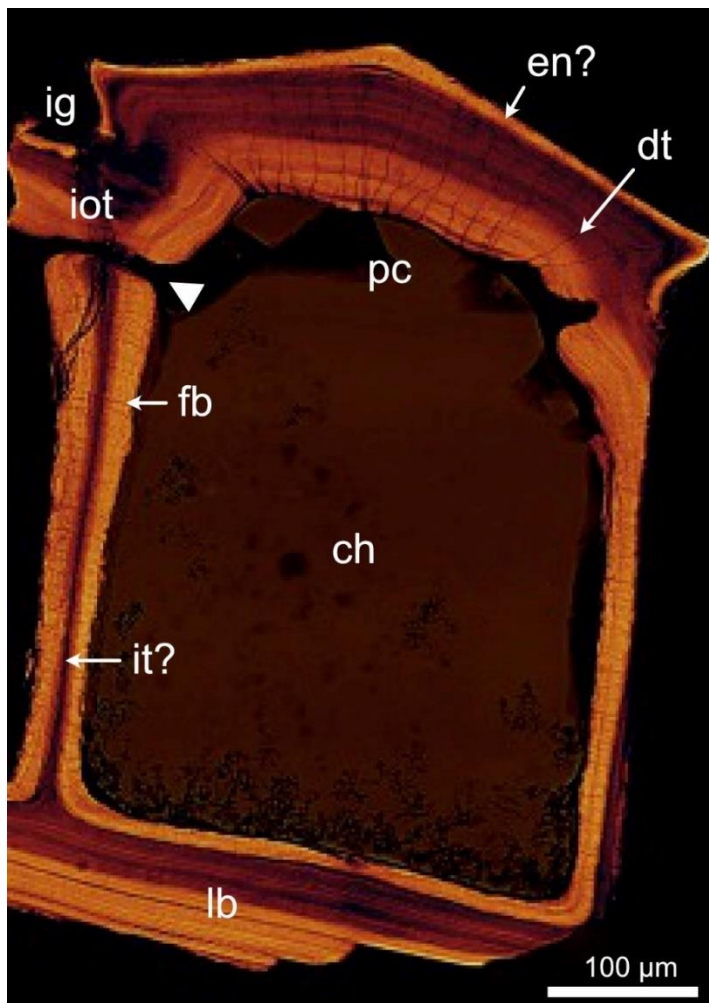


FIGURE V-5. Synchrotron radiation X-ray tomographic microscopy section of *Anglaspis macculoughi* (from Keating *et al.* (2015)). Please note the morphology of the growth lines within the orthodentine. ch, chamber. dt, dentin tubule. en, enameloid. fb, fiber. ig, intercostal groove. iot, intermediate osseous tissue. arrow head, vascular canal. it, initial trabeculae. lb, lamellar bone. pc, pulp cavity.

Histology

Odontodes are made of an anodontocytic tissue, traversed by long, ramified and relatively wide tubules that are generally perpendicular to the growth lines, resembling to orthodentine (Fig. V-3D, 5). As mentioned above, odontodes are connected via acellular tissue that lacks wide tubules and surrounds the base of the intercostal grooves, more compatible with an osseous-like tissue (Fig. V-3, 5, od and ig). Presence of aspidin-like fibers cannot be verified in this intermediate osseous tissue with these sections. In both tissues, discernible growth lines are globally parallel to the external and internal peripheries (Fig. V-5). The growth lines appear to connect between the orthodentine and the osseous tissue surrounding the intercostal grooves, with the exception of those found in the inner orthodentine layers (Fig. V-5), which may be linked to osseous deposition at the chamber periphery. The intermediate osseous tissue is often fused with the aspidin pillars of the middle layer (Fig. V-3). Some resorption areas are visible and discordant with the growth lines of the orthodentine within the pulp cavity. In longitudinal sections, such resorption areas are frequently present around the top of the aspidin pillars (Fig. V-4C, D). As already mentioned, small canals connect the pulpar cavity with the intercostal grooves, crossing the osseous tissue, and the pores of the wide canal network cross the odontodes (Fig. V-1F, 2D). On the polished sections, no capping tissue is easily identifiable on the orthodentine (MNHN.F.SVD2219b), only a more vitreous surface is sometimes observed (Fig. V-3D, en; MNHN.F.SVD2219b), contrasting with what we observe on tomographic microscopy sections (Fig. V-5, en; NHM P.73620).

Interaction between aspidin and odontodes in Anglaspis

The honeycomb-shaped chambers in the middle, aspidin, layer are aligned with fingerprint shaped odontode strips and spots (Fig V-1D, 2B, C). Indeed, the edges of

chambers are generally positioned beneath those of odontodes, or perpendicular to them. It is also visible at the end of strips, where we can observe chambers with a reduced size. This alignment between chambers and odontodes notably enable a fusion of chambers with pulp cavities (Fig. V-3B, 4C and 5).

Histology of another pteraspidomorph heterostracan

The histology of the dermal skeleton of this other (probably a cyathaspid) heterostracan is generally similar to that of *Anglaspis*. It is also composed of a basal compact layer of anosteocytic lamellar bone, a layer of cancellar aspidin, and a layer of odontodes at the external surface (Fig. V-6). However, some differences can be observed compared to *Anglaspis*. The middle layer is not only composed of areas of large chambers with parallel pillars (Fig. V-6E, F), but also of areas with more irregular chambers (Fig. V-6C, D). In these same areas, a well-defined vascular network can be identified above the putative chambers (Fig. V-6A, B). Always in these areas, an intermediate tissue, non-lamellar and rich in fibers, can be easily distinguished from the lamellar tissue deposited around the cavities (Fig. V-6B-D, lma and *). Potential traces of this intermediate aspidin tissue can be identified between the large chambers (Fig. V-6F-H, *) (see also Fig. 15.9F in Mondéjar Fernández & Janvier (2021)). The large chambers are not topped by a single odontode, but rather by two to three odontodes (Fig. V-6E, F). These odontodes are capped by a hypermineralized-like tissue, possibly enameloid as suggested by the presence of cellular projections inside (Fig. V-6B, en). However, its identification needs to be confirmed (see Chapters I and IV).

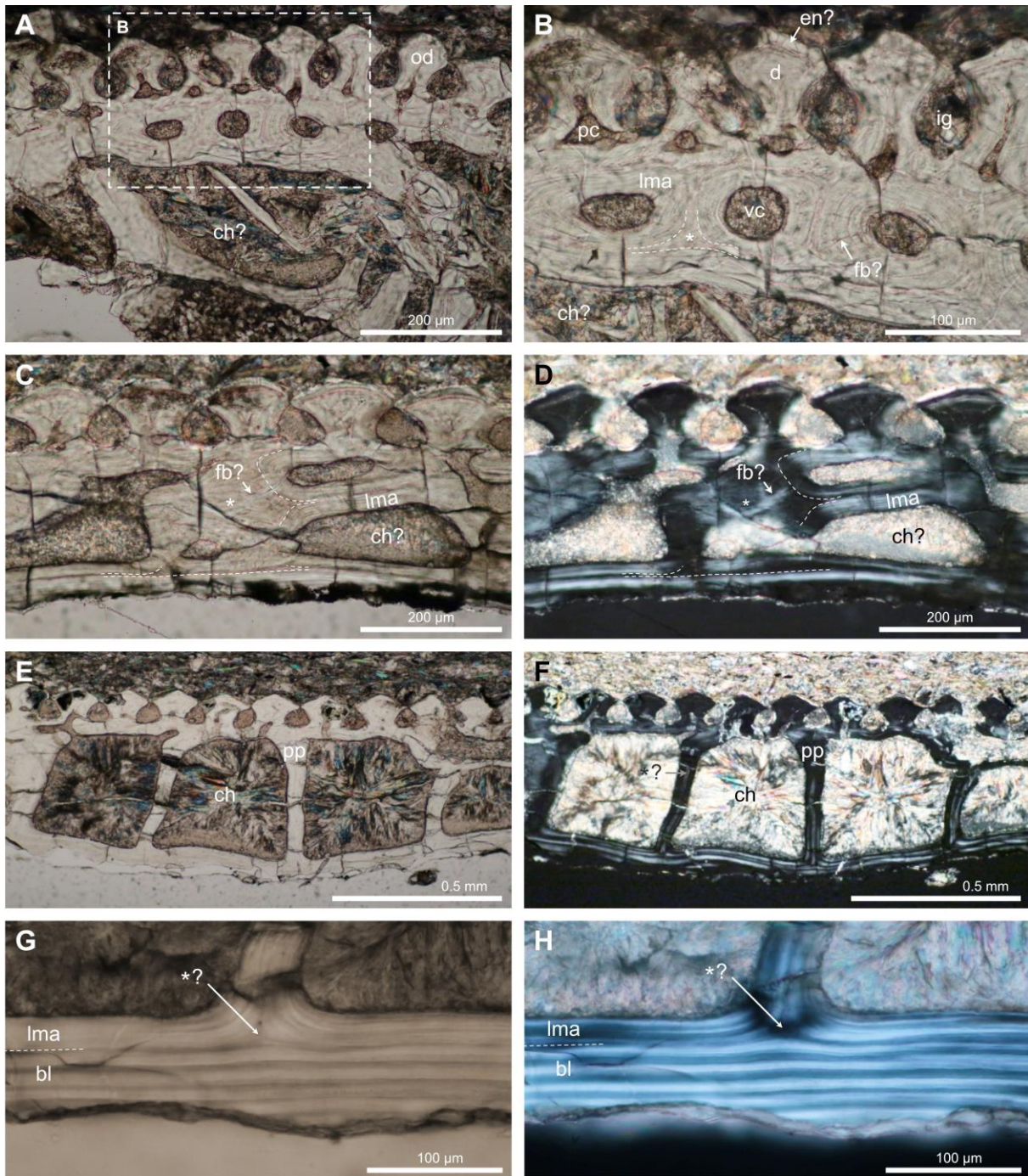


FIGURE V-6. Histological sections of another heterostracan pteraspidomorph (probably a cyathaspid; MNHN.F.SVD2998) in polarized (A-C, E, G) and cross-polarized light (D, F, H). In this taxon, the inner chambers are much larger relative to odontodes and each chamber extends over two or three odontodes, whereas in *Anglaspis* each chamber is capped by one single odontode. A, B, presence of a well-differentiated vascular network forming aspidones. B-D, lamellar aspidin was deposited at the periphery of cavities, while non-lamellar aspidin (*) may have formed the initial trabeculae (see growth lines following the dashed lines). E, F,

presence of large chambers delimited by parallel pillars, without a well-defined vascular network, such as in *Anglaspis*. G, H, potential remnants of non-lamellar aspidin forming the initial trabeculae at the base of a pillar. bl, basal layer. ch, chamber. d, dentin. en, enameloid. fb, fiber. ig, intercostal groove. lma, lamellar aspidin. od, odontode. pc, pulp cavity. pp, parallel pillars. vc, vascular canal. *, non-laminated aspidin.

V.4. Discussion

Characterization of Anglaspis and other pteraspidomorphs' mineralized skeleton

A 3D diagram interpreting the histomorphological data of *Anglaspis* was created based on its histological and structural description of the dermal skeleton (Fig. V-7). CT-scan data confirmed that the dermal skeleton of *Anglaspis* is composed of an internal honeycomb-like bone structure, overlaid with fingerprint-like odontodes, as suspected (Janvier, 1996). This 3D study demonstrated that the honeycomb-like microstructure is uniformly present throughout the plate, contrasting significantly with the less organized spongy structure found in modern or other pteraspidomorphs' dermal bones (Keating *et al.*, 2015, 2018). This kind of bony structure should rather be called 'lacunar bone' than 'spongy bone'. Even more surprisingly, the hexagonal chambers of this structure appear to be almost perfectly aligned with the overlying odontodes. This suggests that the patterning and morphogenesis of odontodes constrains those of lacunar bone, or vice versa, or that both are subject to the same initial patterning.

In terms of odontode composition, the presence of distinguishable orthodontine from an intermediate anosteocytic bony tissue connecting the odontodes has been highlighted. We can nevertheless note that *Anglaspis* orthodontine is composed of a low density of tubules (corresponding to the former location of cellular projections)

compared to what is typically observed in orthodontine (Berkovitz & Shellis, 2016). No hypermineralized capping tissue was clearly identified, contrary to Keating *et al.* (2015) findings, suggesting its absence or non-preservation in the specimen MNHN.F.SVD2219b.

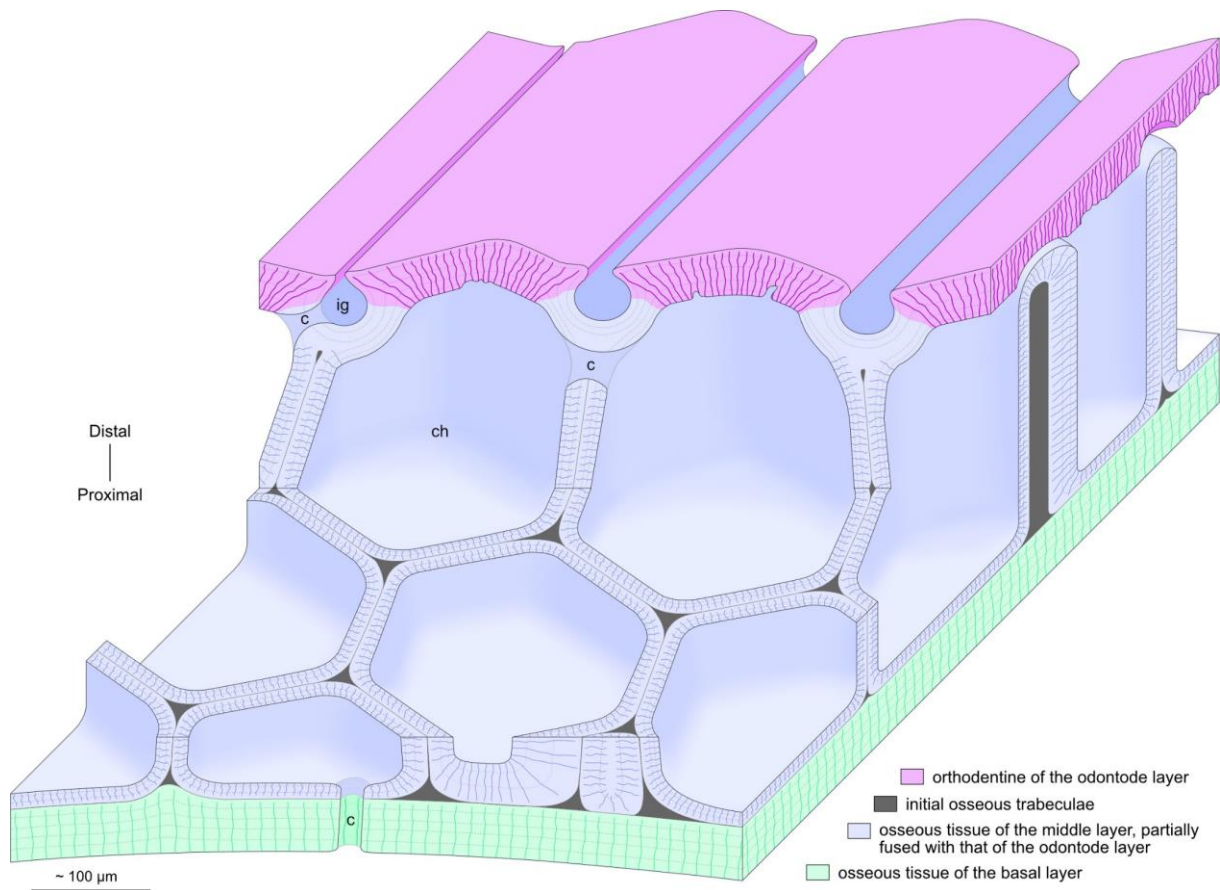


FIGURE V-7. Summary diagram of the histomorphological properties of *Anglaspis*' dermal mineralized skeleton. The odontode layer is composed by odontodes of orthodontine (potentially capped by enameloid, which is not represented here) connected by an intermediate osseous tissue (presence of fibers needs to be confirmed). The middle layer is composed of a lacunar, fibrous (collagen fibers (Keating *et al.*, 2018)), anosteocytic osseous tissue. Putative initial trabeculae can be distinguished from the centrifugal lamellar deposit. The basal layer is composed of a compact, lamellar, fibrous (Sharpey's fibres), anosteocytic osseous tissue. the canals that connect the intercostal grooves with the chambers, link chambers with each other, and connect chambers with the proximal part of the animal. c, canal. ch, chamber. ig, intercostal groove.

Regarding the middle layer, in addition to the deposition of lamellar bone found at the periphery of the chambers, we suspect the presence of initial trabeculae. Indeed, in extant vertebrates, dermal bone formation begins with the formation of initial trabeculae that can fuse and create cavities, which are then partially filled through centripetal deposition (Dubansky & Dubansky, 2018; Setiawati & Rahardjo, 2019; Biga *et al.*, 2020). These initial trabeculae are readily observable in other taxa of pteraspidomorphs and seem to be less structured and rich in wide fibers (Fig. V-6, *, and see Keating *et al.* (2015, 2018)). In *Anglaspis*, the initial trabeculae appear to be significantly reduced. Another important observation in *Anglaspis* is the absence of a well-defined vascular layer between the odontodes and the chambers. Generally in pteraspidomorphs, a layer of aspidin is found with structures very similar to osteons, referred to as aspidones (Fig. V-6A, B and see Denison (1964), Keating *et al.* (2015)). Unlike the chambers, these cavities appear to take on a canal-like form when viewed in 3D (Keating *et al.*, 2018). The implications of this absence are discussed in the next section. It is worth noting that in certain pteraspidomorphs, the structure of this middle layer can vary depending on the anatomical position: a geometric *Anglaspis*-like chambered structure may be found towards the center of the plate (Fig. V-6E), while a less organized chambered structure with vascular elements may be observed towards the edges (Fig. V-6A). This does not appear to be the case for *Anglaspis*, which maintains an uniform organization across the entire plate.

The basal layer is quite similar to what can be observed in other vertebrates, and the visible tubules inside can be interpreted as Sharpey's fibers (de Buffr enil *et al.*, 2021).

Canal networks: looking for the vascular network

As the vascular network is crucial for the formation and maintenance of the mineralized skeleton (Percival & Richtsmeier, 2013; Sivaraj & Adams, 2016), it is

essential to identify its spatiotemporal distribution to infer the development of *Anglaspis*' dermal plates.

As the chambers present in the middle layer do not take the form of canals, their morphogenesis does not appear to be constrained by the initial presence of a vascular network. This confirms Denison (1964) suspicion, namely that the chambers are not analogous to osteons. Hence, when studying sections, it is likely incorrect to associate these large cavities with a vascular network, unlike osteons and aspidones (e.g. Figure 15.9F in Mondéjar Fernández & Janvier (2021)).

As discussed earlier, *Anglaspis* lacks a distinct layer of vascular aspidin between the chambers and odontodes, unlike the majority of other pteraspidomorphs (Keating *et al.*, 2015). However, even if small canals also pass through the basal layer (Fig. V-3A), the highest concentration of canals is found at the interface between aspidin and odontode layers (Fig. V-2D), as suspected by Denison (1964) with cross-sections. Indeed, in this area, numerous canals connect the chambers and pulp cavities with each other. This interface could therefore correspond to a secondary reduced layer of vascularized aspidin. This network of canals should be connected with the outside by the ventral canals passing through the basal layer, and/or by the dorsal canals that connect pulp cavities and chambers with the intercostal grooves (Fig. V-2D arrow head). Additionally, these intercostal grooves have a cylindrical shape and are also interconnected (Fig. V-2D igc). Considering their connection with the pulp cavities and the chambers with the small canals, they also could be part of this network of canals. Thus, if a vascular network, or another kind of network, crossed these plates, it would likely pass through the basal canals and/or the intercostal grooves to enter and exit.

Lateral line systems are known to be present in a diversity of vertebrates, playing critical roles in feeding, swimming, navigation, and communication behaviors (Coombs *et al.*, 2014). The network of pores and wide canals found in heterostracans, as well as in those of other stem-gnathostomes, has been interpreted as probably

representing a system of lateral lines involved in sensory functions, rather than a vascular network (Denison, 1964). The absence of wide canals within the ventral plate, thereby refuting past interpretations (Denison, 1964), further contradicts their interpretation as parts of a vascular network. The different parts of this network are not connected inside the dorsal dermal plate, but they could have been outside this mineralized area. The identification of pores associated with wide canals allows us to infer the network's position when 3D data is unavailable.

Developmental hypotheses of Anglaspis and other pteraspidomorphs' dermal skeleton

The wide canal network and the pineal macula should have been present before the formation, or at least the mineralization, of the epithelial fingerprint-like pattern and the potential intercostal canal network (Fig. V-8A). Indeed, the presence of the wide canals appears to have influenced the fingerprint-like pattern, promoting the formation of truncated odontodes. Additionally, the termination of the strips is observed when they are not parallel to the wide canals (Fig. V-1A, C, F). The absence of a secondary branch in the right part of the dorsal plate, where no end of strips is visible on the surface compared to the left side with the secondary branch, supports this hypothesis (Fig. V-1C).

The epithelial fingerprint-like pattern, and the intercostal canal network, should have formed before the mineralization of odontodes and intercostal groove periphery (Fig. V-8B). Indeed, odontode tissues form at an epithelium-mesenchyme interface, the curvature of which strongly influences the final morphology of dental structures (Berkovitz & Shellis, 2016; Nanci, 2017; Berio & Debiais-Thibaud, 2021).

The growth lines parallel to peripheries observed in the orthodontine suggests a synchronous formation along the whole internal periphery of the odontode (Fig. V-8C), as discussed in Chapters III and IV. Moreover, the potential continuity of these growth lines with those of the intermediate osseous tissue linking odontodes together

extends this synchronous formation to neighbouring odontodes. The observation of mineralized odontodes already linked by the intermediate osseous tissue in putative juveniles of other pteraspidomorphs supports this idea (see Denison (1964), his Fig. 159, and Denison (1973), his Text-fig. 2).

The presumed initial aspidin trabeculae may have formed prior to the peripheral deposition of the chambers, because it corresponds to the deeper tissue of the middle layer (Fig. V-8C). Then, the lamellar bone tissue must have deposited centripetally within the chambers. We can note that the first layers of orthodontine and osseous tissue around the intercostal grooves may have formed before the deposition of the initial peripheral layers of the chambers. Indeed, inner growth lines that are closest to the chamber and the pulp cavity are continuous between chambers and pulp cavities, suggesting that they formed at the same time (Fig. V-8D, E). We can also note that, the pillars of the middle layer can fuse with the odontode layer (preferentially with the intermediate osseous tissue between odontodes), or not (leaving space for forming a canal).

The basal compact layer forms after the initial trabeculae, synchronously across the entire periosteum surface, through the activity of well-aligned osteoblasts, a process observed in the formation of contemporary dermal bones (Fig. V-8D, E) (Setiawati & Rahardjo, 2019; Biga *et al.*, 2020).

Finally, different small canals can form, probably corresponding to the vascular network as previously discussed, eroding the mineralized tissues and inducing the formation of discordances in growth lines (Fig. V-8F).

It is difficult to determine which, between odontodes and putative initial trabeculae, start to mineralize first. If the mechanisms were similar to those in extant gnathostomes, they likely initiate formation simultaneously and fuse later. In contrast, Denison (1964) proposed that odontodes formed first, followed by the aspidin and the basal layer. This hypothesis was based on the observation of putative juveniles

presenting only the odontode layer. However, this observation does not exclude that the aspidin trabeculae and odontodes formed at the same time, without being initially fused, which could also explain the absence of preserved aspidin with odontodes in juveniles.

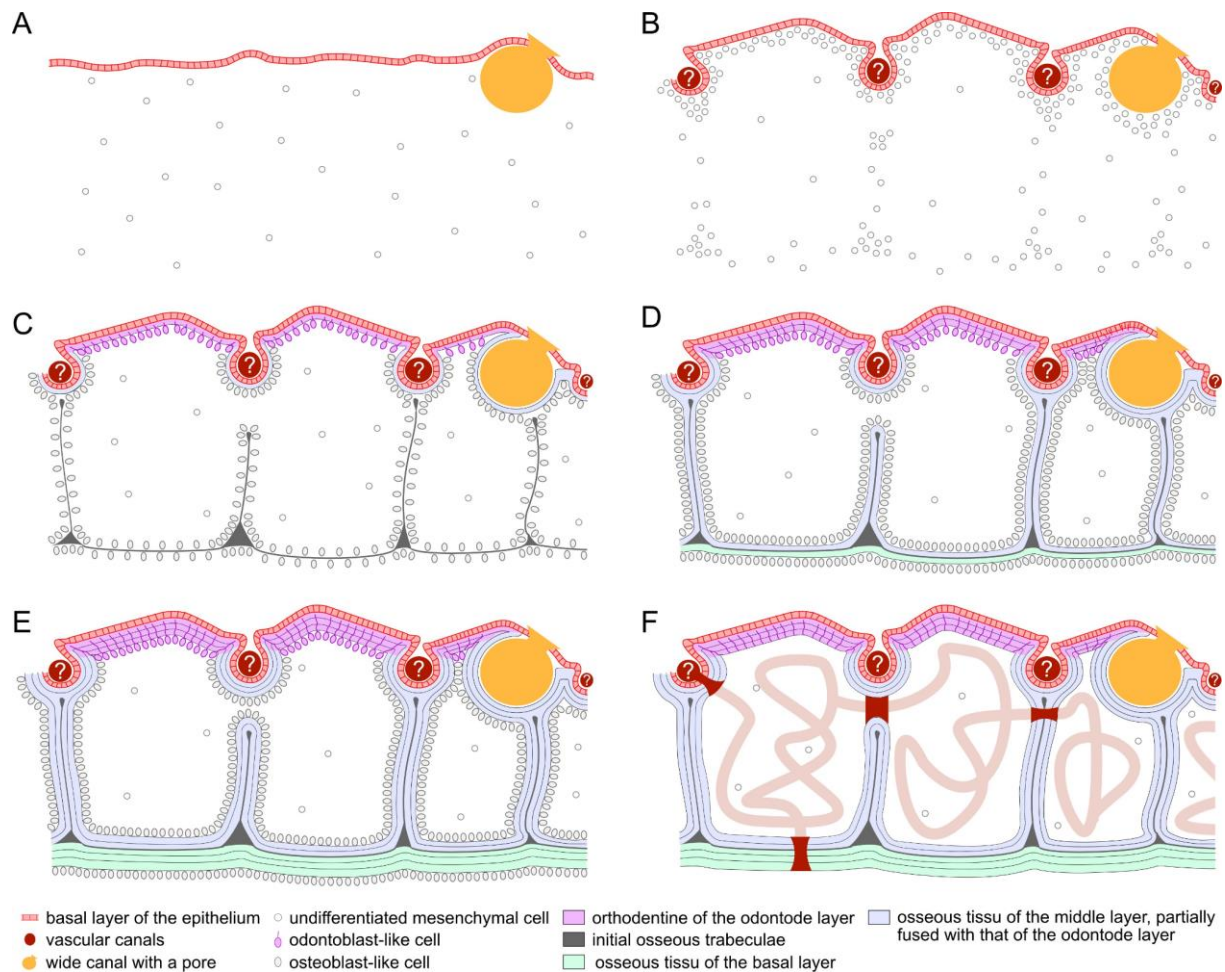


FIGURE V-8. Putative development of the dermal skeleton in *Anglaspis*. The detailed description is available in the main body of the text. Please note that the distribution and timing of the vascular network establishment remain enigmatic.

Contrary to other pteraspitomorphs, which are composed of numerous tesserae more or less fused together (Tarlo, 1967), no demarcation is visible between potential tesserae in *Anglaspis*. Similarly, one would expect to observe prominent concentric growth lines extending from the center of the plate to the edges, as seen in

other pteraspidomorphs (White, 1935; Greeniaus & Wilson, 2003). Their absence in *Anglaspis* raises questions about the growth mechanisms of its plates. It is possible that the plate forms in multiple stages, gradually growing from the edges (Greeniaus & Wilson, 2003), but it is also possible that it mineralizes all at once (Denison, 1964). A key point to address this question is the morphology of the growth lines connecting the odontodes. Indeed, as previously discussed and also observed in *Astraspis* (Chapter IV), the growth lines of *Anglaspis*' orthodontine run parallel to both the internal and external surfaces, suggesting simultaneous activation of cells (Chapters III and IV). Given that these growth lines in orthodontine are interconnected through those of the intermediate bony tissue at the periphery of the canals, this suggests that odontodes and the intermediate tissue form synchronously (Fig. V-8C). Therefore, if this continuity of growth lines is confirmed across the entire plate, it would corroborate the hypothesis that they mineralize as a single event, as proposed by Denison (1964).

This study is still ongoing, but in the future, it would be pertinent to investigate the patterning mechanisms that may have led to the formation of a honeycomb-like bony structure overlying a 'dental' fingerprint structure. Preliminary considerations suggest that simple modifications of a reaction-diffusion mechanism, constraining cellular differentiation zones, could explain the formation of these structures (Garfinkel *et al.*, 2004). According to our previous results, it also appears that the spatiotemporal distribution of the vascular network is a key factor in the formation of spongy or lacunar bone. A 3D study of a taxon displaying both lacunar and spongy bone (e.g. our comparative taxon, see Fig. V-6), would confirm the distinction between a network of chambers and blood channels.

V.5. Conclusion

This study has allowed for a better characterization of the 3D histomorphology of *Anglaspis* (Pteraspimorphi, Heterostraci), an early vertebrate showing an intriguing combination of patterns in its dermal skeleton. It confirmed the presence of honeycomb-like lacunar bone throughout the surface of the dorsal and ventral plates, highlighting the alignment of this pattern with the overlying fingerprint-like odontodes. This 3D study also confirmed the presence of a system of wide canals/pores in the dorsal plate of *Anglaspis* and negated its presence in the ventral plate. Regarding the vascular network, there is no evidence of its significant early presence in the dermis, so it appears to develop later in the lacunar aspidin, leading to bone secondary resorption. Moreover, the connection between the chambers and intercostal grooves raises questions about their functions, potentially allowing for the accommodation of a network of channels, such as vascular structures. This study also suggests that the plates of *Anglaspis* mineralized simultaneously across their entire surface, unlike pteraspimorphs that exhibit concentric growth lines throughout the entire plate. Future research will focus more specifically on the morphogenetic mechanisms that may have led to the formation of the honeycomb-like and fingerprint structure in the dermal skeleton of certain heterostracans, such as reaction-diffusion mechanisms.

Acknowledgements. We warmly thank Alan PRADEL for providing access to the collections of the MNHN, Vincent ROMMEVAUX for preparing the thin sections, as well as Patricia WILS and Marta BELLATO for the scanning of specimens.

Contributions. **Conceptualization** Guillaume Houée (GH), Damien Germain (DG), Nicolas Goudemand (NG), Jérémie Bardin (JB); **Data Curation** GH; **Formal Analysis** GH; **Investigation** GH; **Methodology** GH; **Project Administration** GH; **Resources** GH, DG, NG; **Supervision** DG, NG, JB; **Validation** GH, DG, NG, JB; **Visualization** GH, NG, DG; **Writing – Original Draft Preparation** GH, DG, NG, JB.

Conclusion on the objectives of Chapter V

In Chapter V we:

- Highlighted the interactions between the honeycomb-like bony structure and the fingerprint-like dental structure found in the skeleton of *Anglaspis*.
- Characterized in 3D the different canal networks present in *Anglaspis*' dermal plates, discussing their impacts on the formation of the mineralized skeleton.
- Proposed a developmental scenario explaining the formation of heterostracan dermal skeletons composed by lacunar bone (Fig. 2-V).

GENERAL CONCLUSIONS AND PERSPECTIVES

This manuscript questioned the origins of the diversity of compositions and structures in the mineralized skeleton of vertebrates. The objective of this thesis was to focus on understanding the developmental mechanisms that could be a source of histomorphogenetic diversification to shed a new light on the phylogenetic and temporal distribution of these tissues.

A first step emphasized that this type of evo-devo research is based on phylogenetic distributions of tissues and is therefore heavily dependent on tissue identifications as well as the definition of associated concepts. This is why it is crucial to establish a rigorous taxonomy and nomenclature for tissues, as well as reliable identification methods. A first revision of concepts, terms, and identification criteria for enamel and enameloid tissues was proposed, opening the door to discussions about the reliability of previous identifications and paleohistological distributions.

The second step compared developmental mechanisms among extant vertebrates in order to propose hypotheses of histogenetic modifications that could explain the formation of the observed diversity of dental tissues and structures. Histogenetic models were created to test these hypotheses by exploring the impact of developmental parameters using computer-based simulations. This has notably revealed that (1) the morphology of cellular arrangements, such as the initial curvature of the epithelium during dental structure formation, (2) the intercellular activation timings, such as the timing offset of neighboring cells' activation, and (3) the intracellular secretion timings, such as the onset of vesicle secretion, all constrain the presence and arrangement of various tissues (e.g. dentin, enameloid, and enamel) within a dental structure, notably by influencing matrix blends. These results confirmed that, in addition to the acquisition or loss of genes, small developmental changes could provoke significant morphological changes through evolution. In addition to the *in silico* models developed on Embryomaker, this first part also indirectly led to the development of a new approach for exploring and analyzing a

multiparametric space. These new tools notably open the door to new ways of addressing evo-devo questions.

A third step studied and integrated the fossil record into these evo-devo scenarios. Studying fossils provides access to plesiomorphic developmental mechanisms as well as phylogenetic anchor points. The paleohistological revision of remains from the key taxon, *Astraspis*, thus allowed us to determine that these early 'dental' structures could be produced by a development generally similar to that of present-day structures. However, a difference was suggested regarding the timing of epithelial structure formation, as well as the timing of intercellular activation of mesenchymal cells. This also strengthened the hypothesis that their hypermineralized tissue had a dual origin, aligning it more closely with current concepts of enameloid rather than enamel. These inferences were obtained through the development of a new paleodevelopmental approach based on exploring various ontogenetic scenarios. The characterization of the different layers of *Anglaspis*' dermal skeleton, as well as their interactions, highlighted the morphogenetic constraints that may have existed in early vertebrates. However, the precise mechanisms for the formation of honeycomb-like chambers remain somewhat enigmatic in light of current dermal ossification processes, and these mechanisms will need to be studied in the future in the light of reaction-diffusion processes. Ultimately, these works represent the beginnings of a larger project aiming at reconstructing the paleodevelopmental mechanisms in early vertebrates.

More generally, this thesis has highlighted the advantages of modeling approaches in the context of paleo-evo-devo questions: it allows us to synthesize our knowledge about a system while also highlighting our knowledge gaps (e.g. the creation of a histogenetic model for dental tissues; Fig. I-4), to manipulate hard-to-access systems (e.g. the development of biomineralized structures, especially in the case of non-model or fossil species; e. g. Chapters II-V), to determine the underlying

GENERAL CONCLUSIONS AND PERSPECTIVES

mechanisms controlling the evolution of complex systems (e.g. the synthesis of the underlying mechanisms controlling the transition between enameloid and enamel; Fig. II-8), and to test evolutionary hypotheses (e.g. the assessment of transitions between enameloid and enamel; Chapter II). These various advantages make *in silico* research a guide for paleo-evo-devo questions, the propositions of which must be subsequently tested through experimental studies.

Finally, a concluding figure synthesizes the major drivers affecting histomorphogenetic diversification in vertebrates identified during this thesis (Fig. 7). The construction of this diagram leads to numerous other research topics, with detailed examples provided just below, which will enable its continual refinement as our knowledge advances.

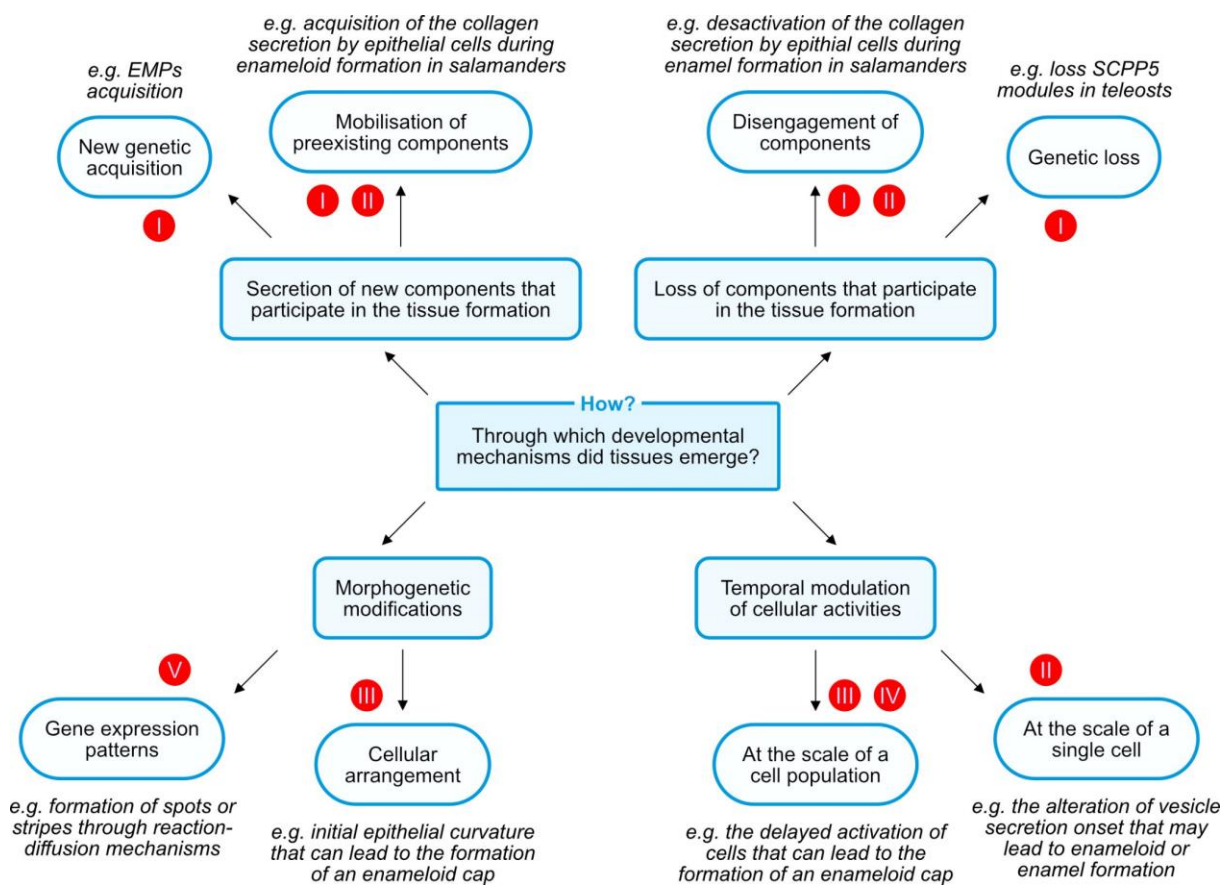


FIGURE 7. Summary of the key identified actors that can influence the diversification of mineralized tissues, in terms of structure and composition, identified during this thesis. Red circles refer to the contribution of the different chapters of the thesis.

In addition to previously presented projects, other projects could be envisioned to further explore the mechanisms of diversification of the mineralized skeleton in vertebrates:

- 1) **Study of the growth line cyclicities in mineralized tissues of non-amniote vertebrates.** During my study of the *Astraspis* development, I highlighted intriguing growth lines similar to the daily growth lines described in amniotes. If these vertebrate Ordovician growth lines are indeed daily ones, they would be the oldest known. Unfortunately, there are only a few data on non-amniote vertebrates. Therefore, I would like to set up new *in vivo* studies to better understand the osteichthyans and chondrichthyans mineralization cyclicities to propose solid interpretations for fossils.
- 2) **Characterize the morphogenesis of dentin growth lines.** Indeed, the implementation of growth line formation mechanisms in my models made me realize that this was not such a straightforward question, and that multiple perspectives exist. For instance, the formation of the lines is based on mineralization timings in my models, but we could instead make them dependent on the secretion timings of matrix elements such as collagen fibers. I would like to explore the impact of various mechanisms on the morphogenesis of these lines.
- 3) **Study the developmental mechanisms of tissue cellularization.** The mineralized tissues studied during this thesis were acellular, but the acquisition of cellularity in bone tissues has been a significant step in vertebrate evolution. For instance, odontocytic dentin exists in many clades of early vertebrates (pteraspidomorphs,

osteostracans, placoderms, acanthodians), and osteocytic bone appears as early as the osteostracans (and possibly in some arandaspids). However, many events leading to anosteocytic bones occurred, especially in teleosts. Therefore, I aim at developing models that can test the impact of developmental parameters such as orientation, motility, and cell cohesion on a tissue's ability to become cellular. Given multiple acquisitions, even losses, of cellularity throughout evolution, I suspect that independent parametric modifications could explain this phenomenon.

4) **Pursue the matter of the evolution of bone in stem and crown-chondrichthyans.**

Indeed, even though it is assumed that chondrichthyans lost dermal and perichondral ossification, we suspect a presence of bone in early and extant chondrichthyans. Moreover, as potential endochondral ossification was identified in a stem-gnathostome (Brazeau *et al.*, 2020), chondrichthyans potentially also have or lost this kind of bone. I would therefore like to pursue histological and developmental studies in extant and extinct chondrichthyans to better understand bone evolution in gnathostomes.

5) **Study the potential oldest known remains of chondrichthyans.**

Indeed, some of the odontodes found in the Ordovician have been attributed to stem-chondrichthyans. These attributions are only based on their histology, and are questionable. However, the origin of these odontodes is key to better understanding the vertebrate early evolutionary steps, because that may delay the divergence time of chondrichthyans and osteichthyans to the middle Ordovician. I would like to use a developmental approach to reinterpret these remains, which could clarify their nature and affiliation within vertebrates.

6) **Figure out the development of conodont elements.** Even though it has been extensively studied, the process of repairing broken structures remains mysterious.

Indeed, following the loss of a tip, the initial morphology is able to recover through the growth of subsequent layers. I would like to propose hypotheses for repair mechanisms using my models on EmbryoMaker.

- 7) **Develop a phylodevelopmental approach taking phylogeny into account during *in silico* explorations of transformation mechanisms.** We investigated the enamel-enameloid transitions and showed that many developmental modifications could explain them. A way to select a solution would be to include the model calculation during the tree search in order to select the best transitions given the distribution of other characters.

EXPERIENCE FEEDBACK

To conclude this manuscript, I wanted to share, in a more personal manner, the experience I went through during the completion of this doctoral journey. Alongside the scientific contribution of a thesis, I attach great importance to the human experience lived during it. Given the pressure on non-tenured researchers, I believe it is crucial to consider both the impact of research projects on the careers of young researchers, as well as on their mental well-being. This introspective work will notably enable me to design future research projects that are as balanced as possible, promoting both innovation pushing beyond our comfort zone and more traditional studies, crucial for maintaining a foothold. This concerns both my own projects and those I will be able to, I hope, supervise.

The review was a difficult but very formative work. It enabled me to become aware of what we know and don't know about my research area, but also to better use the various concepts linked to dental tissue definitions and identifications. It was a key work to propose studies with a clear theoretical framework.

However, I gradually developed a problem of legitimacy because of my limited experience in this discipline. I principally questioned the relevance of my proposals, and even the overall contribution of this review.

Finally, I felt reassured when I had the opportunity to discuss dental tissue concepts with several researchers. In addition to noting that this highly specialized synthesis work was of interest to various researchers, I realized that the concepts related to these tissues were not consistent, confirming the relevance of my review project. Thus, even though I couldn't master the concepts perfectly and provide perfect solutions to the related issues as a young researcher, I could still understand that I could contribute some useful elements of reflection. This work was also particularly beneficial for me during my oral presentations because it allowed me to respond in a much more informed manner to various questions.

Modeling was at the heart of my training. As the main axis of this project initiated by Damien Germain was to study the development of fossils through computer developmental reconstructions, I had to spend a lot of time learning how to build and execute this type of research projects.

One of the main unsuspected difficulties was to understand the role of modeling. Why should I take time to create models that will never be perfectly identical to real systems, and therefore untrue? This question is an essential point when we plan to do modeling, as it allows us to understand what we want it to say, and therefore, how we have to build our models. Another PhD student of the ED227 working on a modeling project, Teddy Gaiddon, once said that it enables us 'to detect underlying mechanisms' of a complex system. I really liked this manner of summarizing a central point of modeling. It means that, similarly to multivariate analysis like PCA, modeling is not intended to dissect the role of each component and their interactions, but rather to detect tendencies to guide future research. It is like building a portrait robot of a poorly understood system to have a basis for discussion. Thus, we do not expect to build models identical to the real systems for this kind of objective. In addition to this central point, modeling has different other objectives. Similar to the review work, modeling requires synthesizing and connecting our knowledge, thereby highlighting our gaps in the process. It is therefore a good complement to a review to master a subject of research. Moreover, modeling can also enable us to work on reproductions of inaccessible systems, such as the development of fossil organisms.

Once the objectives of a modeling project are defined, the software selection and the learning of its use were the next challenging difficulties. We chose to work on EmbryoMaker, a wonderful open access software enabling us to model developmental mechanisms in 3D and at the cellular level. However, it was quite challenging to manage, especially when we don't have much programming experience. The operation under Ubuntu and Fortran90 made things even more complicated. To summarize what EmbryoMaker is: it is a set of folders, filled with a set of files,

themselves filled with a set of lines of code with undetermined roles. To use it, I therefore spend a lot of time learning how to use Ubuntu, the Fortran90 language and dissecting EmbryoMaker to understand how it works. Finally, and notably thanks to the help of Roland Zimm, one of the developers of the software, I was able to create my first models and simulations. Today, I can create more sophisticated models. Nevertheless, I've been cautious about limiting the time I spend on EmbryoMaker, as I don't want to confine my research profile to programming. In the future, I intend to further develop this aspect, particularly the computer modeling projects that I had temporarily set aside. Another problem linked to this coding part is that we mainly develop our computer models alone, limiting the possibilities of assistance from our supervisors when we encounter difficulties. However, the self-training part of computer science can be at some points very stimulating when things start to work, and I am very pleased with the skills it has allowed me to acquire!

I also realized that modeling was not limited to software, but could also be applied with a pen and a paper. I have always sketched my ideas on paper to progress in my thought, but I did not realize that it could be called 'modeling' and become strong figures of discussion for a study. After this, even if this modeling on paper is a first step to more precise computer modeling, this makes modeling quickly accessible to everyone and, notably for students with short deadlines.

The acquisition and analysis of data from models was certainly the more challenging point. I particularly felt a lot of pressure regarding their validity. My acquisitions heavily rely on the quality of my models and the chosen range of parametric exploration. Moreover, my analysis methodologies are also 'handmade'. I was, therefore, very concerned about potential 'unexpected errors' that could make the associated results obsolete. It was crucial for me to validate my methodologies and results with other researchers, not only with my supervisors but also with members of my monitoring committee and at conferences I attended. It was a pleasure to challenge myself in this way, which was precisely what I sought when I applied for a PhD. I

EXPERIENCE FEEDBACK

spent a lot of time scribbling down ideas to resolve a problem, and many of them were questioned and invalidated during meetings, giving me the sense of going in circles. However, in addition to the pleasure of having to think, what a wonderful feeling it was to have one idea very well received by the team.

To give some examples of challenges I had to face, due to the large amount of simulations I wanted to do, I had to find ways to optimize the calculation time. I therefore learned autonomously how to parallelize Fortran90 code, allowing me to split the calculation on the different processors of my computer, and how to use the supercomputing and algorithmic platform of the MNHN (PCIA) to access more processors. Thanks to this, I was finally able to automatically calculate simulations twenty by twenty on the PCIA, reducing the calculation time by a factor of twenty and freeing up access to my computer. This experience enables me to acquire new very useful skills for my future studies.

After acquiring the large dataset resulting from the exploration, in addition to its complex management, I faced challenges in extracting impactful results from it. Indeed, the conventional methods of multivariate analysis that we tried were not very convincing. It was not possible to factually determine which parametric changes allowed transitioning from one group to another, and if they were different independent manners to do it, from these analyses. I spent a lot of time trying to find a good way to achieve it, considering the interaction between all variables. I was particularly relieved when I finally found a way to do it and represented it in a simplified figure. I wish to pursue the development of this multivariate analysis, in order to improve it and explore potential other applications for it.

Finally, considering my relatively limited programming experience, I now recognize that I made several optimization mistakes. On one hand, it was very satisfying to gradually learn how to build faster codes. On the other hand, it was stressful not being fully aware of the coding errors I might have made. I made efforts to correct optimization mistakes as much as possible, but due to time constraints, this

wasn't always feasible. Nevertheless, with the progress I've made in programming, I am confident in my ability to produce increasingly optimized codes.

The histological and microanatomical parts were true breaths of fresh air. Contrary to the other more abstract parts, these more concrete anatomical aspects were very comforting. I had the great pleasure of taking the time to observe the composition and structure of tissues, taking photos, and thinking about how could I use the histomorphological properties to create paleodevelopmental projects. The main awesome discovery was that of Harding sandstone histology. The combination of exceptional preservation with the key phylogenetic position of these skeletal tissues made these fossils a wonderful treasure for people interested in the origin of the vertebrate mineralized skeleton. Even after more than one hundred years of study, the histology of Harding fossils allows us to realize great discoveries. Small details can convey important developmental information, especially when we study them together. Moreover, as for the review and modeling approach, when we synthesize histomorphological information in a draw, we can identify lacks in our observations or knowledge. The addition of a third dimension involving morphogenetic mechanisms of 3D patterning makes projects even more stimulating. The only frustration that I have concerning this part, is that I have the feeling there is still a lot to do, but I didn't have time to look further into it.

Once someone told me that 'everything had globally already been done regarding paleohistology'. I was already surprised to hear that at the time, but now, I am sure of the opposite! I think paleohistological studies have much more to reveal, especially if we take care of small details and their interactions. Sometimes, surprising paleohistological observations can highlight gaps in our knowledge of extant organisms and initiate studies about them, like the discovery of potential daily growth lines in early vertebrates.

To conclude my experience with an exploratory PhD subject, I would say that it is a stressful but wonderful journey into the unknown. Setting aside the linked pressure, it is very stimulating to work on transversal areas, having the opportunity to develop new creative projects, as well as new methodologies, and to express one's personality. I would therefore highly recommend this kind of PhD to autonomous students who are looking for challenging subjects to test their abilities. A key point should be to keep a strong 'conventional part' that would be there to reassure the student, but also the other researchers with whom you wish to share your research. In the same vein, it should be important to start the project with a less ambitious publication to avoid the pressure linked to the difficulty of finalizing an exploratory study.

Concerning the future of this PhD subject initially designed by Damien Germain, Nicolas Goudemand and Jérémie Bardin, I am convinced that it has great potential. To my mind, this kind of 'Jurassic Park' project (J. Bardin), aiming to reconstruct the ontogenesis of extinct organisms with modeling, could become a well-developed area of research. I have the feeling that these three years are just the first steps, highlighting the different kinds of studies that are possible to achieve, on the path for a research project with much greater potential.

As far as I am concerned, I am extremely happy to have conducted this research topic. The palaeohistology enthusiast I was in my master's program couldn't have dreamed of anything better than working on the origin and evolution of the vertebrate mineralized skeleton. I am proud to have taken the time to challenge myself in various disciplines, learning and developing new methodologies, as well as creating synthetic figures as much as possible. I am pleased to have been involved in various projects alongside my research, as the creation of a fieldwork project (General appendix). These were things that were close to my heart, and they will ultimately be very useful to me in the future. I am also very fulfilled by the human experience I had during my thesis. The cohesion with my supervisors was really great, and I had the chance to meet and work with many other great people. I am a bit frustrated by the lack of publications

EXPERIENCE FEEDBACK

and of time to explore in detail pattern modeling, but I have no regrets because I did my best to manage my PhD as effectively as possible while also taking care of my mental health. This balance of life that I have acquired, between the pressure of the research and the break times, allowed me to transition from a low motivation to pursue a postdoctoral position abroad at the beginning of my thesis, to a strong desire for adventure by continuing in this field after the end of my PhD.

REFERENCES

REFERENCES

- ABRÀMOFF, M.D., MAGALHÃES, P.J. & RAM, S.J. (2004) Image processing with ImageJ. *Biophotonics international* **11**, 36–42. Laurin Publishing.
- ALLULEE, J.L. & HOLLAND, S.M. (2005) The sequence stratigraphic and environmental context of primitive vertebrates: Harding Sandstone, Upper Ordovician, Colorado, USA. *Palaios* **20**, 518–533. SEPM Society for Sedimentary Geology.
- ASSARAF-WEILL, N., GASSE, B., SILVENT, J., BARDET, C., SIRE, J.-Y. & DAVIT-BEAL, T. (2014) Ameloblasts Express Type I Collagen during Amelogenesis. *Journal of dental research* **93**, 502–507.
- BARDIN, J., ROUGET, I. & CECCA, F. (2017) Ontogenetic data analyzed as such in phylogenies. *Systematic biology* **66**, 23–37. Oxford University Press.
- BAUME, L.J. (1980) II. Definitions and classifications of the pulpodentinal tissues. In *The biology of pulp and dentine* pp. 41–66. Karger Publishers.
- BENDIX-ALMGREEN, S.E. (1983) *Carcharodon megalodon* from the Upper Miocene of Denmark, with comments on elasmobranch tooth enameloid: coronoin. *Bulletin of the Geological Society of Denmark* **32**, 1–32.
- BERIO, F. & DEBIAIS-THIBAUD, M. (2021) Evolutionary developmental genetics of teeth and odontodes in jawed vertebrates: a perspective from the study of elasmobranchs. *Journal of Fish Biology* **98**, 906–918. Wiley Online Library.
- BERKOVITZ, B.K. & SHELLIS, R.P. (2016) *The teeth of non-mammalian vertebrates*. Academic Press.
- BIGA, L.M., DAWSON, S., HARWELL, A., HOPKINS, R., KAUFMANN, J., LEMASTER, M., MATERN, P., MORRISON-GRAHAM, K., QUICK, D. & RUNYEON, J. (2020) *Anatomy & physiology*. OpenStax/Oregon State University.
- BLIECK, A., GOUJET, D. & JANVIER, P. (1987) The vertebrate stratigraphy of the lower devonian (red bay group and wood bay formation) of spitsbergen. *Modern Geology* **11**, 197–2017.
- BRAASCH, I., GEHRKE, A.R., SMITH, J.J., KAWASAKI, K., MANOUSAKI, T., PASQUIER, J., AMORES, A., DESVIGNES, T., BATZEL, P., CATCHEN, J., BERLIN, A.M., CAMPBELL, M.S., BARRELL, D., MARTIN, K.J., MULLEY, J.F., ET AL. (2016) The spotted gar genome illuminates vertebrate evolution and facilitates human-teleost comparisons. *Nature Genetics* **48**, 427–437. Nature Publishing Group.
- BRAUER, D.S., MARSHALL, G.W. & MARSHALL, S.J. (2010) Variations in human DEJ scallop size with tooth type. *Journal of dentistry* **38**, 597–601.

REFERENCES

- BRAUNN, P.R., FERIGOLO, J. & RIBEIRO, A.M. (2021) Enamel microstructure of permanent and deciduous teeth of a species of notoungulate *Toxodon*: Development, functional, and evolutionary implications. *Acta Palaeontologica Polonica* **66**, 449–464.
- BRAZEAU, M.D., GILES, S., DEARDEN, R.P., JERVE, A., ARIUNCHIMEG, Y.A., ZORIG, E., SANSOM, R., GUILLERME, T. & CASTIELLO, M. (2020) Endochondral bone in an Early Devonian ‘placoderm’ from Mongolia. *Nature Ecology & Evolution* **4**, 1477–1484. Nature Publishing Group UK London.
- BRINK, K.S., CHEN, Y.-C., WU, Y.-N., LIU, W.-M., SHIEH, D.-B., HUANG, T.D., SUN, C.-K. & REISZ, R.R. (2016) Dietary adaptations in the ultrastructure of dinosaur dentine. *Journal of the Royal Society Interface* **13**, 20160626. The Royal Society.
- BRYANT, W.L. (1936) A study of the oldest known vertebrates, *Astraspis* and *Eriptychius*. *Proceedings of the American Philosophical Society* **76**, 409–427. JSTOR.
- DE BUFFRÉNIL, V., DE RICQLÈS, A.J., ZYLBERBERG, L. & PADIAN, K. (2021) *Vertebrate skeletal histology and paleohistology*. CRC Press.
- BURROW, C.J., TRINAJSTIC, K. & LONG, J. (2012) First acanthodian from the Upper Devonian (Frasnian) Gogo Formation, Western Australia. *Historical Biology* **24**, 349–357. Taylor & Francis.
- COOMBS, S., BLECKMANN, H., FAY, R.R. & POPPER, A.N. (eds) (2014) *The Lateral Line System*. Springer New York.
- CUNY, G., GUINOT, G. & ENAULT, S. (2018) *Evolution of Dental Tissues and Paleobiology in Selachians*. Elsevier.
- DARWIN, C. (1859) On the origin of species by means of natural selection. *London: Murray* **247**, 1859.
- DAVESNE, D., MEUNIER, F.J., SCHMITT, A.D., FRIEDMAN, M., OTERO, O. & BENSON, R.B.J. (2019) The phylogenetic origin and evolution of acellular bone in teleost fishes: insights into osteocyte function in bone metabolism. *Biological Reviews of the Cambridge Philosophical Society* **94**, 1338–1363.
- DAVIT-BEAL, T., ALLIZARD, F. & SIRE, J.Y. (2007) Enameloid/enamel transition through successive tooth replacements in *Pleurodeles waltl* (Lissamphibia, Caudata). *Cell and tissue research* **328**, 167–183. Springer.
- DEAN, M.C. (1987) Growth layers and incremental markings in hard tissues; a review of the literature and some preliminary observations about enamel structure in *Paranthropus boisei*. *Journal of Human Evolution* **16**, 157–172.

REFERENCES

- DEAN, M.C. (1998) Comparative observations on the spacing of short-period (von Ebner's) lines in dentine. *Archives of Oral Biology* **43**, 1009–1021.
- DEAN, M.C. (2017) How the microstructure of dentine can contribute to reconstructing developing dentitions and the lives of hominoids and hominins. *Comptes Rendus Palevol* **16**, 557–571.
- DEAN, M.C., BEYNON, A.D., REID, D.J. & WHITTAKER, D.K. (1993) A longitudinal study of tooth growth in a single individual based on long- and short-period incremental markings in dentine and enamel. *International Journal of Osteoarchaeology* **3**, 249–264.
- DEAN, M.C. & SCANDRETT, A.E. (1996) The relation between long-period incremental markings in dentine and daily cross-striations in enamel in human teeth. *Archives of Oral Biology* **41**, 233–241. Elsevier.
- DEANG, J.F., PERSONS, A.K., OPPEDAL, A.L., RHEE, H., MOSER, R.D. & HORSTEMEYER, M.F. (2018) Structure, property, and function of sheepshead (*Archosargus probatocephalus*) teeth. *Archives of Oral Biology* **89**, 1–8. Elsevier.
- DEBIAIS-THIBAUD, M., CHIORI, R., ENAULT, S., OULION, S., GERMON, I., MARTINAND-MARI, C., CASANE, D. & BORDAY-BIRRAUX, V. (2015) Tooth and scale morphogenesis in shark: an alternative process to the mammalian enamel knot system. *BMC Evolutionary Biology* **15**, 292.
- DELGADO, S., FERNANDEZ-TRUJILLO, M., HOUÉE, G., SILVENT, J., LIU, X., CORRE, E. & SIRE, J. (2023) Expression of 20 SCPP genes during tooth and bone mineralization in Senegal bichir. *Development Genes and Evolution* **233**, 91–106.
- D'EMIC, M.D., WHITLOCK, J.A., SMITH, K.M., FISHER, D.C. & WILSON, J.A. (2013) Evolution of high tooth replacement rates in sauropod dinosaurs. *PLoS One* **8**, e69235. Public Library of Science San Francisco, USA.
- DENG, Z., LOH, H.-C., JIA, Z., STIFLER, C.A., MASIC, A., GILBERT, P.U., SHAHAR, R. & LI, L. (2022) Black drum fish teeth: built for crushing mollusk shells. *Acta Biomaterialia* **137**, 147–161. Elsevier.
- DENIS, C., RYBICKI, K.R., SCHREIDER, A.A., TOMECKA-SUCHOŃ, S. & VARGA, P. (2011) Length of the day and evolution of the Earth's core in the geological past. *Astronomische Nachrichten* **332**, 24–35. Wiley Online Library.
- DENISON, R.H. (1964) The Cyathaspididae; a family of Silurian and Devonian jawless vertebrates. *Fieldiana* **13**, 309–473. Chicago Natural History Museum Press.
- DENISON, R.H. (1967) Ordovician vertebrates from western United States. *Fieldiana, Geology* **16**, 131–192. Field Museum of Natural History.

REFERENCES

- DENISON, R.H. (1973) Growth and wear of the shield in Pteraspidae (Agnatha). *Palaeontographica Abteilung A* **A143**, 1–10. Schweizerbart'sche Verlagsbuchhandlung.
- DIDIER, D.A., STAHL, B.J. & ZANGERL, R. (1994) Development and growth of compound tooth plates in *Callorhynchus milii* (chondrichthyes, holocephali). *Journal of Morphology* **222**, 73–89. John Wiley & Sons, Ltd.
- DONOGHUE, P.C.J. (1998) Growth and patterning in the conodont skeleton. *Philosophical Transactions of the Royal Society of London. Series B: Biological Sciences* **353**, 633–666.
- DONOGHUE, P.C.J. & KEATING, J.N. (2014) Early vertebrate evolution. *Palaeontology* **57**, 879–893.
- DONOGHUE, P.C.J. & SANSOM, I.J. (2002) Origin and early evolution of vertebrate skeletonization. *Microscopy research and technique* **59**, 352–372. Wiley Online Library.
- DONOGHUE, P.C.J., SANSOM, I.J. & DOWNS, J.P. (2006) Early evolution of vertebrate skeletal tissues and cellular interactions, and the canalization of skeletal development. *Journal of Experimental Zoology Part B: Molecular and Developmental Evolution* **306**, 278–294. Wiley Online Library.
- DUBANSKY, B.H. & DUBANSKY, B.D. (2018) Natural development of dermal ectopic bone in the american alligator (*Alligator mississippiensis*) resembles heterotopic ossification disorders in humans. *The Anatomical Record* **301**, 56–76.
- ELLIOTT, D.K. (1987) A reassessment of *Astraspis desiderata*, the oldest North American vertebrate. *Science* **237**, 190–192. American Association for the Advancement of Science.
- EMKEN, S., WITZEL, C., KIERDORF, U., FRÖLICH, K. & KIERDORF, H. (2021) Characterization of short-period and long-period incremental markings in porcine enamel and dentine—Results of a fluorochrome labelling study in wild boar and domestic pigs. *Journal of Anatomy* **239**, 1207–1220. Wiley Online Library.
- ENAULT, S. (2015) Évolution et diversité des structures minéralisées chez les sélaciens: approche paléo-développementale. PhD Thesis, Université Montpellier.
- ENAULT, S., GUINOT, G., KOOT, M.B. & CUNY, G. (2015) Chondrichthyan tooth enameloid: past, present, and future. *Zoological Journal of the Linnean Society* **174**, 549–570.

REFERENCES

- ERICKSON, G.M. (1996a) Incremental lines of von Ebner in dinosaurs and the assessment of tooth replacement rates using growth line counts. *Proceedings of the National Academy of Sciences* **93**, 14623–14627. National Acad Sciences.
- ERICKSON, G.M. (1996b) Daily deposition of dentine in juvenile *Alligator* and assessment of tooth replacement rates using incremental line counts. *Journal of Morphology* **228**, 189–194. Wiley Online Library.
- FANCHON, S., BOURD, K., SEPTIER, D., EVERTS, V., BEERTSEN, W., MENASHI, S. & GOLDBERG, M. (2004) Involvement of matrix metalloproteinases in the onset of dentin mineralization. *European journal of oral sciences* **112**, 171–176. Wiley Online Library.
- FRANCILLON-VIEILLOT, H., DE BUFFRÉNIL, V., CASTANET, J.D., GÉRAUDIE, J., MEUNIER, F.J., SIRE, J.Y., ZYLBERBERG, L. & DE RICQLÈS, A. (1990) Microstructure and mineralization of vertebrate skeletal tissues. *Skeletal biomineralization: patterns, processes and evolutionary trends* **1**, 471–530.
- FRASER, G.J., CERNY, R., SOUKUP, V., BRONNER-FRASER, M. & STREELMAN, J.T. (2010) The odontode explosion: the origin of tooth-like structures in vertebrates. *Bioessays* **32**, 808–817. Wiley Online Library.
- FRIEDMAN, M. & BRAZEAU, M.D. (2010) A reappraisal of the origin and basal radiation of the Osteichthyes. *Journal of Vertebrate Paleontology* **30**, 36–56.
- GARCÍA, R.A. & ZURRIAGUZ, V. (2016) Histology of teeth and tooth attachment in titanosaurs (Dinosauria; Sauropoda). *Cretaceous Research* **57**, 248–256. Elsevier.
- GARFINKEL, A., TINTUT, Y., PETRASEK, D., BOSTRÖM, K. & DEMER, L.L. (2004) Pattern formation by vascular mesenchymal cells. *Proceedings of the National Academy of Sciences* **101**, 9247–9250. Proceedings of the National Academy of Sciences.
- GIBSON, C.W., YUAN, Z.-A., HALL, B., LONGENECKER, G., CHEN, E., THYAGARAJAN, T., SREENATH, T., WRIGHT, J.T., DECKER, S., PIDDINGTON, R., HARRISON, G. & KULKARNI, A.B. (2001) Amelogenin-deficient Mice Display an Amelogenesis Imperfecta Phenotype*. *Journal of Biological Chemistry* **276**, 31871–31875.
- GILES, S., RÜCKLIN, M. & DONOGHUE, P.C.J. (2013) Histology of “placoderm” dermal skeletons: Implications for the nature of the ancestral gnathostome. *Journal of Morphology* **274**, 627–644.
- GOLDBERG, M., SEPTIER, D., BOURD, K. & MENASHI, S. (2004) Role of matrix proteins in signalling and in dentin and enamel mineralisation. *Comptes Rendus Palevol* **3**, 573–581. Elsevier.

REFERENCES

- GRAHAM, E.E. (1984) Protein biosynthesis during spiny dogfish (*Squalus acanthias*) enameloid formation. *Archives of Oral Biology* **29**, 821–825.
- GRAHAM, E.E. (1985) Isolation of enamelinlike proteins from blue shark (*Prionace glauca*) enameloid. *Journal of Experimental Zoology* **234**, 185–191.
- GREENIAUS, J.W. & WILSON, M.V.H. (2003) Fossil juvenile Cyathaspididae (Heterostraci) reveal rapid cyclomerial development of the dermal skeleton. *Journal of Vertebrate Paleontology* **23**, 483–487.
- GREN, J.A. & LINDGREN, J. (2014) Dental histology of mosasaurs and a marine crocodylian from the Campanian (Upper Cretaceous) of southern Sweden: incremental growth lines and dentine formation rates. *Geological Magazine* **151**, 134–143. GeoScienceWorld.
- GROSS, W. (1930) *Die fische des mittleren Old Red Südlivlands*. Geologische und paläontologische Abhandlungen.
- HAECKEL, E. (1866) *Generelle Morphologie der Organismen: Allgemeine Grundzüge der organischen Formen-Wissenschaft, mechanisch begründet durch die von Charles Darwin reformierte Descendenz-Theorie*. Band 1: Allgemeine Anatomie. Band 2: Allgemeine Entwicklungsgeschichte. De Gruyter, Berlin, New York.
- HAGOLANI, P.F., ZIMM, R., MARIN-RIERA, M. & SALAZAR-CIUDAD, I. (2019) Cell signaling stabilizes morphogenesis against noise. *Development* **146**, dev179309.
- HAGOLANI, P.F., ZIMM, R., VROOMANS, R. & SALAZAR-CIUDAD, I. (2021) On the evolution and development of morphological complexity: A view from gene regulatory networks. *PLOS Computational Biology* **17**, e1008570. Public Library of Science.
- HALL, B.K. (2002) Palaeontology and Evolutionary Developmental Biology: A Science of the Nineteenth and Twenty-first Centuries. *Palaeontology* **45**, 647–669.
- HALL, B.K. (2015) *Bones and Cartilage: Developmental and Evolutionary Skeletal Biology (Second Edition)*. Academic Press.
- HALSTEAD, L.B. (1987) Evolutionary aspects of neural crest derived skeletogenic cells in the earliest vertebrates. In *Developmental and evolutionary aspects of the neural crest* pp. 339–358. Wiley.
- HEROLD, R.C. (1974) Ultrastructure of odontogenesis in the pike (*Esox lucius*). Role of dental epithelium and formation of enameloid layer. *Journal of Ultrastructure Research* **48**, 435–454.

REFERENCES

- HEROLD, R.C., GRAVER, H.T. & CHRISTNER, P. (1980) Immunohistochemical Localization of Amelogenins in Enameloid of Lower Vertebrate Teeth. *Science* **207**, 1357–1358.
- HEROLD, R.C. & LANDINO, L. (1970) The development and mature structure of dentine in the pike, *Esox lucius*, analyzed by bright field, phase and polarization microscopy. *Archives of Oral Biology* **15**, 747–IN7.
- HEROLD, R.C., ROSENBLOOM, J. & GRANOVSKY, M. (1989) Phylogenetic distribution of enamel proteins: immunohistochemical localization with monoclonal antibodies indicates the evolutionary appearance of enamelines prior to amelogenins. *Calcified tissue international* **45**, 88–94. Springer.
- HILLSON, S. (2005) *Teeth*. Cambridge university press.
- HILLSON, S. (2014) *Tooth development in human evolution and bioarchaeology*. Cambridge University Press.
- HIRASAWA, T., OISI, Y. & KURATANI, S. (2016) *Palaeospondylus* as a primitive hagfish. *Zoological Letters* **2**, 1–9. BioMed Central.
- HUYSEUNE, A., TAKLE, H., SOENENS, M., TAERWE, K. & WITTEN, P.E. (2008) Unique and shared gene expression patterns in Atlantic salmon (*Salmo salar*) tooth development. *Development Genes and Evolution* **218**, 427–437.
- IJIMA, M. & ISHIYAMA, M. (2020) A unique mineralization mode of hypermineralized pleromin in the tooth plate of *Chimaera phantasma* contributes to its microhardness. *Scientific reports* **10**, 18591. Nature Publishing Group UK London.
- IINUMA, Y., SUZUKI, M., YOKOYAMA, M., TANAKA-NAKAMURA, Y. & OHTAISHI, N. (2002) Daily incremental lines in sika deer (*Cervus nippon*) dentine. *Journal of Veterinary Medical Science* **64**, 791–795. Japanese society of veterinary science.
- ISHIYAMA, M. (1984) Comparative histology of tooth enamel in several toothed whales. *Japanese Journal of Oral Biology* **26**, 1054–1071. Japanese Association for Oral Biology.
- ISHIYAMA, M. (1994) Immunocytochemical detection of enamel proteins in dental matrix of certain fishes. *Bulletin de l'Institut Oceanographique, Monaco*. **14**, 175–182.
- ISHIYAMA, M. & TERAOKI, Y. (1990) The fine structure and formation of hypermineralized petrodentine in the tooth plate of extant lungfish (*Lepidosiren paradoxa* and *Protopterus* sp.). *Archives of histology and cytology* **53**, 307–321. International Society of Histology and Cytology.

REFERENCES

- JAEKEL, O. (1891) Die Selachier aus dem oberen Muschelkalk Lothringens. *Geologische Landesanstalt von Elsass-Lothringen.*, 273–332.
- JANVIER, P. (1996) *Early Vertebrates*. Oxford: Clarendon Press.
- JANVIER, P. (2015) Facts and fancies about early fossil chordates and vertebrates. *Nature* **520**, 483–489.
- KAWASAKI, K. (2009) The SCPP gene repertoire in bony vertebrates and graded differences in mineralized tissues. *Development Genes and Evolution* **219**, 147–157.
- KAWASAKI, K. (2013) Odontogenic ameloblast-associated protein (ODAM) and amelotin: Major players in hypermineralization of enamel and enameloid. *Journal of Oral Biosciences* **55**, 85–90.
- KAWASAKI, K. & AMEMIYA, C.T. (2014) SCPP genes in the coelacanth: Tissue mineralization genes shared by sarcopterygians. *Journal of Experimental Zoology Part B: Molecular and Developmental Evolution* **322**, 390–402.
- KAWASAKI, K., KEATING, J.N., NAKATOMI, M., WELTEN, M., MIKAMI, M., SASAGAWA, I., PUTTICK, M.N., DONOGHUE, P.C.J. & ISHIYAMA, M. (2021) Coevolution of enamel, ganoin, enameloid, and their matrix SCPP genes in osteichthyans. *Iscience* **24**, 102023. Elsevier.
- KAWASAKI, K., MIKAMI, M., GOTO, M., SHINDO, J., AMANO, M. & ISHIYAMA, M. (2020) The Evolution of Unusually Small Amelogenin Genes in Cetaceans; Pseudogenization, X–Y Gene Conversion, and Feeding Strategy. *Journal of molecular evolution* **88**, 122–135.
- KAWASAKI, K., SASAGAWA, I., MIKAMI, M., NAKATOMI, M. & ISHIYAMA, M. (2022) Ganoin and acrodin formation on scales and teeth in spotted gar: A vital role of enamelin in the unique process of enamel mineralization. *Journal of Experimental Zoology Part B: Molecular and Developmental Evolution* **340**, 455–468.
- KAWASAKI, K. & SUZUKI, T. (2011) Molecular evolution of matrix metalloproteinase 20. *European Journal of Oral Sciences* **119**, 247–253.
- KAWASAKI, K., SUZUKI, T. & WEISS, K.M. (2005) Phenogenetic drift in evolution: The changing genetic basis of vertebrate teeth. *Proceedings of the National Academy of Sciences* **102**, 18063–18068. Proceedings of the National Academy of Sciences.
- KAWASAKI, K., TANAKA, S. & ISHIKAWA, T. (1979) On the daily incremental lines in human dentine. *Archives of Oral Biology* **24**, 939–943.
- KAWASAKI, K. & WEISS, K.M. (2008) SCPP Gene Evolution and the Dental Mineralization Continuum. *Journal of Dental Research* **87**, 520–531.

REFERENCES

- KEATING, J.N. & DONOGHUE, P.C.J. (2016) Histology and affinity of anaspids, and the early evolution of the vertebrate dermal skeleton. *Proceedings of the Royal Society B: Biological Sciences* **283**, 20152917. The Royal Society.
- KEATING, J.N., MARQUART, C.L. & DONOGHUE, P.C.J. (2015) Histology of the heterostracan dermal skeleton: insight into the origin of the vertebrate mineralised skeleton. *Journal of morphology* **276**, 657–680. Wiley Online Library.
- KEATING, J.N., MARQUART, C.L., MARONE, F. & DONOGHUE, P.C.J. (2018) The nature of aspidin and the evolutionary origin of bone. *Nature Ecology & Evolution* **2**, 1501–1506.
- KEMP, A. (2003) Ultrastructure of developing tooth plates in the Australian lungfish, *Neoceratodus forsteri* (Osteichthyes: Dipnoi). *Tissue and Cell* **35**, 401–426.
- KEMP, N.E. & WESTRIN, S.K. (1979) Ultrastructure of calcified cartilage in the endoskeletal tesserae of sharks. *Journal of Morphology* **160**, 75–101. Wiley Online Library.
- KEREBEL, L.-M. & LE CABELLEC, M.-T. (1979) Structure and ultrastructure of dentine in the teleost fish, *Lophius*. *Archives of Oral Biology* **24**, 745–751.
- KERR, T. (1960) Development and structure of some actinopterygian and urodele teeth. *Proceedings of the Zoological Society of London* **133**, 401–422.
- KLÆR, J. (1932) The Downtonian and Devonian vertebrates of Spitsbergen. IV, Suborder Cyathaspida. *Skifter om Svalbard og Ishavet* **52**, 1–26.
- KOGAYA, Y. (1999) Immunohistochemical localisation of amelogenin-like proteins and type I collagen and histochemical demonstration of sulphated glycoconjugates in developing enameloid and enamel matrices of the larval urodele (*Triturus pyrrhogaster*) teeth. *The Journal of Anatomy* **195**, 455–464. Cambridge University Press.
- KONDO, S. & MIURA, T. (2010) Reaction-diffusion model as a framework for understanding biological pattern formation. *science* **329**, 1616–1620. American Association for the Advancement of Science.
- KVAM, T. (1946) Comparative study of the ontogenetic and phylogenetic development of dental enamel. *Den Norske Tannlaegefor Tidsskr* **56**, 1–198.
- KVAM, T. (1960) The development of the tooth tip in *Triton cristatus* laur. *Acta Odontologica Scandinavica* **18**, 503–519. Taylor & Francis.
- LÊ, S., JOSSE, J. & HUSSON, F. (2008) FactoMineR: an R package for multivariate analysis. *Journal of statistical software* **25**, 1–18.

REFERENCES

- LEBLANC, A.R.H., PALCI, A., ANTHWAL, N., TUCKER, A.S., ARAÚJO, R., PEREIRA, M.F.C. & CALDWELL, M.W. (2023) A conserved tooth resorption mechanism in modern and fossil snakes. *Nature Communications* **14**, 742. Nature Publishing Group UK London.
- LEMIERRE, A. & GERMAIN, D. (2019) A new mineralized tissue in the early vertebrate *Astraspis*. *Journal of anatomy* **235**, 1105–1113. Wiley Online Library.
- LEURS, N., MARTINAND-MARI, C., MARCELLINI, S. & DEBIAIS-THIBAUD, M. (2022) Parallel Evolution of Ameloblastic scpp Genes in Bony and Cartilaginous Vertebrates. *Molecular Biology and Evolution* **39**, msac099.
- LEUZINGER, L., CAVIN, L., LÓPEZ-ARBARELLO, A. & BILLON-BRUYAT, J.-P. (2020) Peculiar tooth renewal in a Jurassic ray-finned fish (Lepisosteiformes, †*Scheenstia* sp.). *Palaeontology* **63**, 117–129.
- LIANG, T., HU, Y., SMITH, C.E., RICHARDSON, A.S., ZHANG, H., YANG, J., LIN, B., WANG, S.-K., KIM, J.-W., CHUN, Y.-H., SIMMER, J.P. & HU, J.C.-C. (2019) AMBN mutations causing hypoplastic amelogenesis imperfecta and Ambn knockout-NLS-lacZ knockin mice exhibiting failed amelogenesis and Ambn tissue-specificity. *Molecular Genetics & Genomic Medicine* **7**, e929.
- LISI, S., PETERKOVA, R., PETERKA, M., VONESCH, J.L., RUCH, J.V. & LESOT, H. (2003) Tooth morphogenesis and pattern of odontoblast differentiation. *Connective tissue research* **44**, 167–170. Taylor & Francis.
- LV, Y., KAWASAKI, K., LI, J., LI, Y., BIAN, C., HUANG, Y., YOU, X. & SHI, Q. (2017) A genomic survey of SCPP family genes in fishes provides novel insights into the evolution of fish scales. *International journal of molecular sciences* **18**, 2432. MDPI.
- MAHO, T., MAHO, S., SCOTT, D. & REISZ, R.R. (2022) Permian hypercarnivore suggests dental complexity among early amniotes. *Nature Communications* **13**, 4882. Nature Publishing Group.
- MARGOLIS, H.C., KWAK, S.-Y. & YAMAZAKI, H. (2014) Role of mineralization inhibitors in the regulation of hard tissue biomineralization: relevance to initial enamel formation and maturation. *Frontiers in Physiology* **5**.
- MARIN-RIERA, M., BRUN-USAN, M., ZIMM, R., VÄLIKANGAS, T. & SALAZAR-CIUDAD, I. (2016) Computational modeling of development by epithelia, mesenchyme and their interactions: a unified model. *Bioinformatics* **32**, 219–225.
- MARIN-RIERA, M., MOUSTAKAS-VERHO, J., SAVRIAMA, Y., JERNVALL, J. & SALAZAR-CIUDAD, I. (2018) Differential tissue growth and cell adhesion alone drive early

REFERENCES

- tooth morphogenesis: An ex vivo and in silico study. *PLOS Computational Biology* **14**, e1005981. Public Library of Science.
- MARSHALL, S.J., BALOOCH, M., HABELITZ, S., BALOOCH, G., GALLAGHER, R. & MARSHALL, G.W. (2003) The dentin–enamel junction—a natural, multilevel interface. *Journal of the European Ceramic Society* **23**, 2897–2904.
- MEINKE, D.K. & THOMSON, K.S. (1983) The Distribution and Significance of Enamel and Enameloid in the Dermal Skeleton of Osteolepiform Rhipidistian Fishes. *Paleobiology* **9**, 138–149. Paleontological Society.
- MEREDITH SMITH, M., CLARK, B., GOUJET, D. & JOHANSON, Z. (2017) Evolutionary origins of teeth in jawed vertebrates: conflicting data from acanthothoracid dental plates ('Placodermi'). *Palaeontology* **60**, 829–836.
- MEUNIER, F.J., GERMAIN, D. & OTERO, O. (2018) A histological study of the lingual molariform teeth in *Hyperopisus bebe* (Mormyridae; Osteoglossomorpha). *Cybium: Revue Internationale d'Ichtyologie* **42**, 87–90.
- MILLER, W.A. & HOBDELL, M.H. (1968) Preliminary report on the histology of the dental and paradental tissues of *Latimeria chalumnae* (Smith) with a note on tooth replacement. *Archives of Oral Biology* **13**, 1289-IN37.
- MONDÉJAR-FERNÁNDEZ, J. & JANVIER, P. (2021) Finned Vertebrates. In *Vertebrate Skeletal Histology and Paleohistology* pp. 294–324. CRC Press.
- MOSS, M.L. (1964) Development of cellular dentin and lepidosteal tubules in the bowfin, *Amia calva*. *Acta Anatomica* **58**, 333–354. S. Karger AG.
- MOY-THOMAS, J.A. (1971) Class Pteraspidomorphi. In *Palaeozoic Fishes* pp. 35–60. Springer US, Boston, MA.
- MURDOCK, D.J.E., DONG, X.-P., REPETSKI, J.E., MARONE, F., STAMPANONI, M. & DONOGHUE, P.C.J. (2013) The origin of conodonts and of vertebrate mineralized skeletons. *Nature* **502**, 546–549.
- MURDOCK, D.J.E. & DONOGHUE, P.C.J. (2011) Evolutionary Origins of Animal Skeletal Biomineralization. *Cells Tissues Organs* **194**, 98–102.
- NANCI, A. (2017) *Ten Cate's Oral Histology: Development, Structure, and Function (9th Edition)*. Elsevier Health Sciences.
- NEUMANN, P.E. & NEUMANN, E.E. (2021) General histological woes: Definition and classification of tissues. *Clinical Anatomy* **34**, 794–801.

REFERENCES

- OHTSUKA-Isoya, M., HAYASHI, H. & SHINODA, H. (2001) Effect of suprachiasmatic nucleus lesion on circadian dentin increment in rats. *American Journal of Physiology-Regulatory, Integrative and Comparative Physiology* **280**, R1364–R1370. American Physiological Society Bethesda, MD.
- OLIVEIRA, C.A., BERGQVIST, L.P. & LINE, S.R.P. (2001) A comparative analysis of the structure of the dentinoenamel junction in mammals. *Journal of Oral Science* **43**, 277–281. Nihon University School of Dentistry.
- ØRVIG, T. (1958) *Pycnaspis splendens*, new genus, new species, a new ostracoderm from the Upper Ordovician of North America. *Proceedings of the United States National Museum* **108**, 1–23.
- ØRVIG, T. (1967) Phylogeny of tooth tissues: evolution of some calcified tissues: evolution of some calcified tissues in early vertebrates. *Structural and chemical organization of teeth*, 45–110. Academic Press.
- ØRVIG, T. (1973) Fossila fisktänder i svepelektronmikroskopet: gamla frågeställningar i ny belysning. *Fauna flora* **68**, 166–173.
- ØRVIG, T. (1976) Palaeohistological Notes 3. The interpretation of pleromin (pleromic hard tissue) in the dermal skeleton of psammosteid heterostracans. *Zoologica Scripta* **5**, 35–47.
- ØRVIG, T. (1978a) Microstructure and Growth of the Dermal Skeleton in Fossil Actinopterygian Fishes: *Birgeria* and *Scanilepis*. *Zoologica Scripta* **7**, 33–56.
- ØRVIG, T. (1978b) Microstructure and Growth of the Dermal Skeleton in Fossil Actinopterygian Fishes: *Nephrotus* and *Colobodus*, with Remarks on the Dentition in Other Forms 1. *Zoologica Scripta* **7**, 297–326. Wiley Online Library.
- ØRVIG, T. (1978c) Microstructure and Growth of the Dermal Skeleton in Fossil Actinopterygian Fishes: *Boreosomus*, *Plegmolepis* and *Gyrolepis*. *Zoologica Scripta* **7**, 125–144.
- ØRVIG, T. (1989) Histologic studies of ostracoderms, placoderms and fossil elasmobranchs. 6. Hard tissues of Ordovician vertebrates. *Zoologica Scripta* **18**, 427–446. Wiley Online Library.
- O'SHEA, J., KEATING, J.N. & DONOGHUE, P.C.J. (2019) The dermal skeleton of the jawless vertebrate *Tremataspis mammillata* (Osteostraci, stem-Gnathostomata). *Journal of Morphology* **280**, 999–1025.
- PAPAKYRIKOS, A.M., ARORA, M., AUSTIN, C., BOUGHNER, J.C., CAPELLINI, T.D., DINGWALL, H.L., GREBA, Q., HOWLAND, J.G., KATO, A. & WANG, X.-P. (2020)

REFERENCES

- Biological clocks and incremental growth line formation in dentine. *Journal of Anatomy* **237**, 367–378. Wiley Online Library.
- PERCIVAL, C.J. & RICHTSMEIER, J.T. (2013) Angiogenesis and intramembranous osteogenesis. *Developmental Dynamics* **242**, 909–922.
- PERNEGRE, V.N. (2003) Un nouveau genre de Pteraspidiiformes (Vertebrata, Heterostraci) de la Formation de Wood Bay (Dévonien inférieur, Spitsberg). *Geodiversitas* **25**, 261–272.
- POOLE, D.F.G. (1967) Enameloid and enamel in recent vertebrates, with a note on the history of cementum: Phylogeny of tooth tissue. *Structure and chemical organization of teeth volume I*, 111–149. Academic Press Inc.
- POOLE, D.F.G. (1971) An introduction to the phylogeny of calcified tissues. *Dental morphology and evolution*. Chicago University Press.
- PRONDVAL, E., STEIN, K.H., DE RICQLÈS, A. & CUBO, J. (2014) Development-based revision of bone tissue classification: the importance of semantics for science. *Biological Journal of the Linnean Society* **112**, 799–816.
- QU, Q., BLOM, H., SANCHEZ, S. & AHLBERG, P. (2015a) Three-dimensional virtual histology of silurian osteostracan scales revealed by synchrotron radiation microtomography. *Journal of Morphology* **276**, 873–888.
- QU, Q., HAITINA, T., ZHU, M. & AHLBERG, P.E. (2015b) New genomic and fossil data illuminate the origin of enamel. *Nature* **526**, 108–111. Nature Publishing Group UK London.
- RADLANSKI, R.J. & RENZ, H. (2007) Insular dentin formation pattern in human odontogenesis in relation to the scalloped dentino-enamel junction. *Annals of Anatomy - Anatomischer Anzeiger* **189**, 243–250.
- RANDLE, E., KEATING, J.N. & SANSOM, R.S. (2022) A Phylogeny for Heterostraci (stem-gnathostomes). bioRxiv.
- REPETSKI, J.E. (1978) A Fish from the Upper Cambrian of North America. *Science* **200**, 529–531. American Association for the Advancement of Science.
- RICHTER, M. & SMITH, M.M. (1995) A microstructural study of the ganoine tissue of selected lower vertebrates. *Zoological Journal of the Linnean Society* **114**, 173–212. Oxford University Press.
- DE RICQLÈS, A. (1995) Les vertébrés des grès de Harding: ce que Vaillant a pu observer. *Geobios* **28**, 51–56. Elsevier.

REFERENCES

- RIPLEY, B., VENABLES, B., BATES, D.M., HORNIK, K., GEBHARDT, A., FIRTH, D. & RIPLEY, M.B. (2013) Package 'mass'. *Cran r* **538**, 113–120.
- RÖSE, C. (1898) *Über die verschiedenen Abänderungen der Hartgewebe bei niederen Wirbeltieren*. *Anat. Anz.*
- ROSENBERG, G.D. & SIMMONS, D.J. (1980) Rhythmic dentinogenesis in the rabbit incisor: circadian, ultradian, and infradian periods. *Calcified Tissue International* **32**, 29–44. Springer.
- RÜCKLIN, M. & DONOGHUE, P.C.J. (2015) *Romundina* and the evolutionary origin of teeth. *Biology Letters* **11**, 20150326. Royal Society.
- RÜCKLIN, M. & DONOGHUE, P.C.J. (2016) Reply to 'placoderms and the evolutionary origin of teeth': Burrow et al. (2016). *Biology Letters* **12**, 20160526. Royal Society.
- RÜCKLIN, M. & DONOGHUE, P.C.J. (2019) Evolutionary Origin of Teeth. In *eLS* pp. 1–7, 1st edition. Wiley.
- SADEK, S., SULTAN, R. & LAGZI, I. (2010) Liesegang patterns in nature: A diverse scenery across the sciences. *Precipitation patterns in reaction-diffusion systems* **661**, 1–43. Research Signpost: Trivandrum, India.
- SANSOM, I.J., DONOGHUE, P.C.J. & ALBANESI, G. (2005) Histology and affinity of the earliest armoured vertebrate. *Biology Letters* **1**, 446–449. The Royal Society London.
- SANSOM, I.J., SMITH, M.M. & SMITH, M.P. (1996) Scales of thelodont and shark-like fishes from the Ordovician of Colorado. *Nature* **379**, 628–630. Nature Publishing Group.
- SANSOM, I.J., SMITH, M.P., SMITH, M.M. & TURNER, P. (1997) *Astraspis* the anatomy and histology of an Ordovician fish. *Palaeontology* **40**, 625–644. London: Palaeontological Association.
- SASAGAWA, I. (1984) Formation of cap enameloid in the jaw teeth of dog salmon, *Oncorhynchus keta*. *Japanese Journal of Oral Biology* **26**, 477–495. Japanese Association for Oral Biology.
- SASAGAWA, I. (1988) The appearance of matrix vesicles and mineralization during tooth development in three teleost fishes with well-developed enameloid and orthodontine. *Archives of Oral Biology* **33**, 75–86. Elsevier.
- SASAGAWA, I. (1997) Fine structure of the cap enameloid and of the dental epithelial cells during enameloid mineralisation and early maturation stages in the tilapia, a teleost. *The Journal of Anatomy* **190**, 589–600. Cambridge University Press.

REFERENCES

- SASAGAWA, I. (1998) Mechanisms of Mineralization in the Enameloid of Elasmobranchs and Teleosts. *Connective Tissue Research* **39**, 207–214. Taylor & Francis.
- SASAGAWA, I. (1999) Fine structure of dental epithelial cells and the enameloid during the enameloid formation stages in an elasmobranch, *Heterodontus japonicus*. *Anatomy and Embryology* **200**, 477–486.
- SASAGAWA, I. (2002) Mineralization patterns in elasmobranch fish. *Microscopy Research and Technique* **59**, 396–407.
- SASAGAWA, I. & AKAI, J. (1992) The Fine Structure of the Enameloid Matrix and Initial Mineralization during Tooth Development in the Sting Rays, *Dasyatis akajei* and *Urolophus aurantiacus*. *Journal of Electron Microscopy* **41**, 242–252.
- SASAGAWA, I. & FERGUSON, M.W. (1991) The development of enamel tubules during the formation of enamel in the marsupial *Monodelphis domestica*. *Journal of anatomy* **179**, 47. Wiley-Blackwell.
- SASAGAWA, I. & ISHIYAMA, M. (1988) The structure and development of the collar enameloid in two teleost fishes, *Halichoeres poecilopterus* and *Pagrus major*. *Anatomy and Embryology* **178**, 499–511.
- SASAGAWA, I., ISHIYAMA, M. & AKAI, J. (2006) Cellular influence in the formation of enameloid during odontogenesis in bony fishes. *Materials Science and Engineering: C* **26**, 630–634.
- SASAGAWA, I., ISHIYAMA, M., YOKOSUKA, H. & MIKAMI, M. (2013) Teeth and ganoid scales in *Polypterus* and *Lepisosteus*, the basic actinopterygian fish: An approach to understand the origin of the tooth enamel. *Journal of Oral Biosciences* **55**, 76–84.
- SASAGAWA, I., ISHIYAMA, M., YOKOSUKA, H., MIKAMI, M., OKA, S., SHIMOKAWA, H. & UCHIDA, T. (2019) Immunolocalization of enamel matrix protein-like proteins in the tooth enameloid of spotted gar, *Lepisosteus oculatus*, an actinopterygian bony fish. *Connective Tissue Research* **60**, 291–303. Taylor & Francis.
- SASAGAWA, I., ISHIYAMA, M., YOKOSUKA, H., MIKAMI, M. & UCHIDA, T. (2009) Tooth enamel and enameloid in actinopterygian fish. *Frontiers of Materials Science in China* **3**, 174–182. Springer.
- SASAGAWA, I., YOKOSUKA, H., ISHIYAMA, M., MIKAMI, M., SHIMOKAWA, H. & UCHIDA, T. (2012) Fine structural and immunohistochemical detection of collar enamel in the teeth of *Polypterus senegalus*, an actinopterygian fish. *Cell and Tissue Research* **347**, 369–381.

REFERENCES

- SATCHELL, P.G., ANDERTON, X., RYU, O.H., LUAN, X., ORTEGA, A.J., OPAMEN, R., BERMAN, B.J., WITHERSPOON, D.E., GUTMANN, J.L., YAMANE, A., ZEICHNER-DAVID, M., SIMMER, J.P., SHULER, C.F. & DIEKWISCH, T.G.H. (2002) Conservation and variation in enamel protein distribution during vertebrate tooth development. *Journal of Experimental Zoology* **294**, 91–106.
- SCHMIDT, W.J. (1957) Zur Durodentinbildung bei Urodelen-Zähnen. *Zeitschrift für Zellforschung und mikroskopische Anatomie* **46**, 281–285. Springer.
- SCHULTZE, H.-P. (2016) Scales, Enamel, Cosmine, Ganoine, and Early Osteichthyans. *Comptes Rendus Palevol* **15**, 83–102.
- SETIAWATI, R. & RAHARDJO, P. (2019) Bone development and growth. *Osteogenesis and bone regeneration* **10**. IntechOpen London, UK.
- SHELLIS, R.P. (1978) The role of the inner dental epithelium in the formation of the teeth in fish. *Development, function and evolution of teeth*, 31–42. Academic Press London.
- SHELLIS, R.P. & BERKOVITZ, B.K.B. (1976) Observations on the dental anatomy of piranhas (Characidae) with special reference to tooth structure. *Journal of Zoology* **180**, 69–84.
- SHELLIS, R.P. & MILES, A.E.W. (1974) Autoradiographic Study of the Formation of Enameloid and Dentine Matrices in Teleost Fishes Using Tritiated Amino Acids. *Proceedings of the Royal Society of London. Series B, Biological Sciences* **185**, 51–72. The Royal Society.
- SHELLIS, R.P., MILES, A.E.W. & HARRISON, R.J. (1997) Observations with the electron microscope on enameloid formation in the common eel (*Anguilla anguilla*; Teleostei). *Proceedings of the Royal Society of London. Series B. Biological Sciences* **194**, 253–269. Royal Society.
- SHELLIS, R.P. & POOLE, D.F.G. (1978) The structure of the dental hard tissues of the coelacanthid fish *Latimeria chalumnae* Smith. *Archives of Oral Biology* **23**, 1105–1113.
- SHIRLEY, B., GROHGANZ, M., BESTMANN, M. & JAROCHOWSKA, E. (2018) Wear, tear and systematic repair: testing models of growth dynamics in conodonts with high-resolution imaging. *Proceedings of the Royal Society B: Biological Sciences* **285**, 20181614. The Royal Society.
- SIMMER, J.P. & HU, J.C.-C. (2002) Expression, Structure, and Function of Enamel Proteinases. *Connective Tissue Research* **43**, 441–449. Taylor & Francis.

REFERENCES

- SIRE, J.-Y., DONOGHUE, P.C.J. & VICKARYOUS, M.K. (2009) Origin and evolution of the integumentary skeleton in non-tetrapod vertebrates. *Journal of Anatomy* **214**, 409–440. Wiley Online Library.
- SIRE, J.-Y. & KAWASAKI, K. (2012) Origin and evolution of bone and dentin and of acidic secretory calcium-binding phosphoproteins. *Phosphorylated extracellular matrix proteins of bone and dentin. Sharjah, UAE: Bentham Science. p*, 3–60.
- SIRE, Y., GÉRAUDIE, J., MEUNTER, F.J. & ZYLBERBERG, L. (1987) On the origin of ganoine: Histological and ultrastructural data on the experimental regeneration of the scales of *Calamolchthys calabaricus* (osteichthyes, brachyopterygii, polypteridae). *American Journal of Anatomy* **180**, 391–402.
- SIVARAJ, K.K. & ADAMS, R.H. (2016) Blood vessel formation and function in bone. *Development* **143**, 2706–2715. The Company of Biologists Ltd.
- SLAVKIN, H.C., SAMUEL, N., BRINGAS, P.J., NANJI, A. & SANTOS, V. (1983) Selachian tooth development: II. Immunolocalization of amelogenin polypeptides in epithelium during secretory amelogenesis in *Squalus acanthias*. *Journal of craniofacial genetics and developmental biology* **3**, 43–52.
- SMITH, C.E., HU, Y., HU, J.C. -C. & SIMMER, J.P. (2016) Ultrastructure of early amelogenesis in wild-type, *Amelx*^{-/-}, and *Enam*^{-/-} mice: enamel ribbon initiation on dentin mineral and ribbon orientation by ameloblasts. *Molecular Genetics & Genomic Medicine* **4**, 662–683.
- SMITH, M.M. (1995) Heterochrony in the evolution of enamel in vertebrates. *Evolutionary change and heterochrony*, 125–150. John Wiley & Sons.
- SMITH, M.M. & HALL, B.K. (1990) Development and evolutionary origins of vertebrate skeletogenic and odontogenic tissues. *Biological Reviews* **65**, 277–373. Blackwell Publishing Ltd Oxford, UK.
- SMITH, M.M. & SANSOM, I.J. (1997) Exoskeletal micro-remains of an Ordovician fish from the Harding Sandstone of Colorado. *Palaeontology* **40**, 645–658.
- SMITH, M.M., SANSOM, I.J. & SMITH, P. (1995) Diversity of the dermal skeleton in Ordovician to Silurian vertebrate taxa from North America: histology, skeletogenesis and relationships. *Geobios* **28**, 65–70. Elsevier.
- SMITH, M.P., SANSOM, I.J. & COCHRANE, K.D. (2001) The Cambrian origin of vertebrates. *Systematics Association Special Volume* **61**, 67–84. London; Chapman & Hall; 1998.
- SMITH, P. & TCHERNOV, E. (1992) *Structure, Function and Evolution of Teeth*. Freund Publishing House Ltd.

REFERENCES

- SOLER-GIJÓN, R. (1999) Occipital spine of *Orthacanthus* (Xenacanthidae, Elasmobranchii): Structure and growth. *Journal of Morphology* **242**, 1–45.
- STERN, D.N., SONG, M.J. & LANDIS, W.J. (1992) Tubule formation and elemental detection in developing opossum enamel. *The Anatomical Record* **234**, 34–48. Wiley Online Library.
- TARLO, L.B.H. (1967) The tessellated pattern of dermal armour in the Heterostraci. *Zoological Journal of the Linnean Society* **47**, 45–54.
- TEAM, RS. (2020) RStudio Team (2022) RStudio: Integrated Development Environment for R. RStudio, PBC, Boston. *RStudio: Integrated Development for R*.
- THESLEFF, I., KERANEN, S. & JERNVALL, J. (2001) Enamel knots as signaling centers linking tooth morphogenesis and odontoblast differentiation. *Advances in dental research* **15**, 14–18. SAGE Publications Sage CA: Los Angeles, CA.
- THEWISSEN, J.G.M., COOPER, L.N. & BEHRINGER, R.R. (2012) Developmental biology enriches paleontology. *Journal of Vertebrate Paleontology* **32**, 1223–1234.
- THIERY, A.P., STANDING, A.S., COOPER, R.L. & FRASER, G.J. (2022) An epithelial signalling centre in sharks supports homology of tooth morphogenesis in vertebrates. *eLife* **11**, e73173. eLife Sciences Publications, Ltd.
- TURING, A.M. (1952) The chemical basis of morphogenesis. *Philosophical Transactions of the Royal Society B: Biological Sciences* **237**, 37–72.
- UCHIDA, T., TANABE, T. & FUKAE, M. (1989) Immunocytochemical localization of amelogenins in the deciduous tooth germs of the human fetus. *Archives of Histology and Cytology* **52**, 543–552. International Society of Histology and Cytology.
- UNGAR, P.S. & SUES, H.-D. (2019) Tetrapod Teeth: Diversity, Evolution, and Function. In *Feeding in Vertebrates* (eds V. BELS & I.Q. WHISHAW), pp. 385–429. Springer International Publishing, Cham.
- VAILLANT, L. (1902) Sur la présence du tissu osseux chez certains Poissons des terrains paléozoïques de Canyon City (Colorado). *Comptes rend Acad Sci* **134**, 1321–1322.
- VELASCO-HOGAN, A., HUANG, W., SERRANO, C., KISAILUS, D. & MEYERS, M.A. (2021) Tooth structure, mechanical properties, and diet specialization of Piranha and Pacu (Serrasalminidae): A comparative study. *Acta Biomaterialia* **134**, 531–545.
- VICKARYOUS, M.K. & SIRE, J.-Y. (2009) The integumentary skeleton of tetrapods: origin, evolution, and development. *Journal of Anatomy* **214**, 441–464. Wiley Online Library.

REFERENCES

- WALCOTT, C.D. (1892) Preliminary notes on the discovery of a vertebrate fauna in Silurian (Ordovician) strata. *Bulletin of the geological Society of America* **3**, 153–172. Geological Society of America.
- WAUGH, D.A., SUYDAM, R.S., ORTIZ, J.D. & THEWISSEN, J.G.M. (2018) Validation of Growth Layer Group (GLG) depositional rate using daily incremental growth lines in the dentin of beluga (*Delphinapterus leucas* (Pallas, 1776)) teeth. *PLOS ONE* **13**, e0190498. Public Library of Science.
- WEBSTER, M. & ZELDITCH, M.L. (2005) Evolutionary modifications of ontogeny: heterochrony and beyond. *Paleobiology* **31**, 354–372. Cambridge University Press.
- WHITE, E.I. (1935) X-The ostracoderm *Pteraspis* Kner and the relationships of the agnathous vertebrates. *Philosophical Transactions of the Royal Society of London. Series B, Biological Sciences* **225**, 381–457.
- WHITTAKER, D.K. (1978) The enamel–dentine junction of human and *Macaca irus* teeth: a light and electron microscopic study. *Journal of Anatomy* **125**, 323. Wiley-Blackwell.
- WILLIAMS, J.L. (1923) Disputed points and unsolved problems in the normal and pathological histology of enamel. *Journal of Dental Research* **5**, 27–116. SAGE Publications Sage CA: Los Angeles, CA.
- WILLIAMSON, W.C. (1849) XXIII. On the microscopic structure of the scales and dermal teeth of some ganoid and placoid fish. *Philosophical Transactions of the Royal Society of London* **139**, 435–475. Royal Society.
- WILLS, L.J. (1936) XVIII.—Rare and New Ostracoderm Fishes from the Downtonian of Shropshire. *Earth and Environmental Science Transactions of The Royal Society of Edinburgh* **58**, 427–447. Royal Society of Edinburgh Scotland Foundation.
- WITTEN, P.E., SIRE, J.-Y. & HUYSEUNE, A. (2014) Old, new and new-old concepts about the evolution of teeth. *Journal of Applied Ichthyology* **30**, 636–642. Wiley Online Library.
- YILMAZ, S., NEWMAN, H.N. & POOLE, D.F.G. (1977) Diurnal periodicity of von Ebner growth lines in pig dentine. *Archives of oral biology* **22**, 511–513. Elsevier.
- YU, D., REN, Y., UESAKA, M., BEAVAN, A.J., MUFFATO, M., SHEN, J., LI, Y., SATO, I., WAN, W. & CLARK, J.W. (2023) Hagfish genome illuminates vertebrate whole genome duplications and their evolutionary consequences. *bioRxiv*, 2023–04. Cold Spring Harbor Laboratory.

REFERENCES

- ZHURAVLEV, A.V. (2017) Comparative histology of conodonts and Early vertebrates. *Вестник института геологии Коми научного центра Уральского отделения РАН*, 37–42. Учреждение Российской академии наук Институт геологии Коми научного центра Уральского отделения РАН, Россия, Сыктывкар.
- ZIMM, R., BERIO, F., DEBIAIS-THIBAUD, M. & GOUEMAND, N. (2023) A shark-inspired general model of tooth morphogenesis unveils developmental asymmetries in phenotype transitions. *Proceedings of the National Academy of Sciences* **120**, e2216959120. National Acad Sciences.

GENERAL APPENDIX

DETAIL OF ANCILLARY ACTIVITIES CARRIED OUT DURING MY DOCTORAL STUDIES

2021-2023 PALAEOLOGICAL EXCAVATION CAMPAIGNS

- (*still in preparation*) • Co-organization of a campaign to collect the remains of Ordovician vertebrates (Cañon City, United States)
- (*1 week*) • Co-organization of a campaign in collaboration with the local town hall (Buxières-les-Mines, France)
- (*1 day*) • Prospecting for Cretaceous terrestrial deposits on an island (Shimonoseki, Japan)
- (*2 weeks*) • Reopening of the Permian site of Buxières-les-Mines and continuation of the excavations in Franchesse (Allier, France)
- (*1 week*) • Reopening of the Permian site of Franchesse (Allier, France)

2023 INTERNATIONAL EXCHANGE (JAPAN)

- (*1 month*) • Work at the Museum of the University of Kyushu (Fukuoka)
- Visit other institutions to meet palaeontologists (Kyushu University, Mine Fossil Museum, Kitakyushu Museum of Natural History & Human History, National Museum of Nature and Science)
- Participation in the congress « Japan Palaeontological Society No. 172 »
- Participation in a prospecting campaign

2021 - 2023 TEACHING MISSION (SORBONNE UNIVERSITÉ)

- (*2 * 64h*) • 1ST002 (1st year): Geosciences 2 (UFR 918)
- 1ST031-PEIP (1st year): Earth Climate Environment (UFR 918)
- 2ST044 (2nd year): Laboratory internship (UFR 918)
- LU3SV602 (3rd year): Comparative biology and animal evolution (UFR 927)
- 5BEB52 (5th year): Paleohistology (UFR 918)

2022 INTERNSHIP CREATION AND SUPERVISION (CR2P)

- (*1 week*) • Supervision of two undergraduate students: creation of a subject, selection of candidates, training, creation of a poster and evaluation

2020 - 2023 INVOLVEMENT

- CR2P doctoral student representative (2020-2023)
- ED227 doctoral student representative (2021-2022)

PUBLICATIONS

With peer review

Delgado, S., Fernandez-Trujillo, M.-A., **Houée, G.**, Silvent, J., Liu, X., Corre, E., Sire, J.-Y. (2023). *Expression of 20 SSCP genes during tooth and bone formation in Senegal bichir*. Development Genes and Evolution. DOI: 10.1007/s00427-023-00706-w

Houssaye, A., Perthuis, A., **Houée, G.** (2021). *Sesamoid bones also show functional adaptation in their microanatomy – The example of the patella in Perissodactyla*. Journal of Anatomy. DOI: 10.1111/joa.13530

Without peer review

Houée, G., Oyama, N. (2023). *Importance des échanges internationaux pour les jeunes chercheurs*. Pal-Échos 35(20-22), journal interne du CR2P.

→ Translation: *"Importance of international exchanges for young researchers."*

Logghe, A., Courville, E., Rebillard, A., Luccisano, V., Li, J.-C., **Houée, G.** (2023). *Poursuite des fouilles à Buxières-les-Mines : campagne 2023*. Pal-Échos 35(13-19), journal interne du CR2P.

→ Translation: *"Continuation of the excavations at Buxières-les-Mines: campaign 2023."*

Buffa, V., Bento Da Costa, L., Goedert, J., Gônet, J., **Houée, G.**, Laville, T., Le Verger, K. (2022). « **Maman, plus tard, je serai paléontologue !** ». Paléontologie d'aujourd'hui. DOI: 10.1051/978-2-7598-2718-3.c018

→ Translation: *"Mom, when I grow up, I will be a palaeontologist."*

Houée, G., Logghe, A., Steyer, J.-S. (2022). *Franchesse : reprise des campagnes de fouilles*. Pal-Échos 31(7-8), journal interne du CR2P.

→ Translation: *"Franchesse: resumption of excavation campaigns."*

Houée, G., Logghe, A., Steyer, J.-S. (2022). *Poursuite des fouilles à Franchesse et réouverture du site de Buxières-les-Mines*. Pal-Échos 33(16-17), journal interne du CR2P.

→ Translation: *"Continuation of the excavations at Franchesse and reopening of the site of Buxières-les-Mines."*

Quilhac, A., **Houée, G.** (2022). *Dans l'intimité de l'os*. Paléontologie d'aujourd'hui. DOI: 10.1051/978-2-7598-2718-3.c087

→ Translation: *"In the bone intimacy."*

Steyer, J.-S., Pouillon, J.-M., Courville, E., **Houée, G.**, Logghe, A., Elbaz, L., Cremer, C., Fabre, J.-E., Pohl, B., Lacombat, F. (2022). *Les fouilles paléontologiques dans le Permien de Franchesse (bassin de Bourbon-l'Archambault, Allier, France) en septembre 2021 : Bilan et perspectives*. Bulletin de la Société d'Histoire Naturelle et des Amis du Muséum d'Autun 217(30-36).

→ Translation: *"Palaeontological excavations in the Permian of Franchesse (Bourbon-l'Archambault basin, Allier, France) in September 2021: Assessment and prospects."*

PRESENTATIONS

Houée, G., Germain, D., Goudemand, N., Bardin, J. (2023). *Patterns de Turing et mécanismes d'ossification chez les premiers Vertébrés*. Troisième Colloque scientifique de l'Association paléontologique de Villers-sur-Mer (APVSM). Villers-sur-mer, France.

→ Translation: *"Turing patterns and ossification mechanisms in early vertebrates."*

Houée, G., Bardin, J., Germain, D., Janvier, P., Goudemand, N. (2023). *La formation des premiers tissus dentaires mise en lumière par des modèles développementaux : l'exemple d'Astraspis*. Congrès de l'Association Paléontologique Française 2023 (APF). Villers-sur-mer, France.

→ Translation: *"Developmental models shed light on the earliest dental tissues, an example on Astraspis."*

- Houée, G., Germain, D., Goudemand, N., Bardin, J. (2022).** *Modeling the histogenetic switch from enameloid to enamel.* 18th International Symposium on Dental Morphology, 3rd Congress of the International Association for Paleodontology (ISDM). Frankfurt am Main, Germany.
- Houée, G., Germain, D., Goudemand, N., Bardin, J. (2022).** *Modélisation de la transition histogénétique entre émailloïde et émail.* Congrès de l'Association Paléontologique Française 2022 (APF). Montpellier, France.
→ Translation: "*Modeling the histogenetic switch from enameloid to enamel.*"
- Houée, G., Germain, D., Goudemand, N., Bardin, J. (2022).** *Turing patterns and ossification mechanisms in early vertebrates.* Internal seminar at the Institut de génomique fonctionnelle de Lyon (IGFL, ENS). Lyon, France.
- Houée, G., Germain, D., Goudemand, N., Bardin, J. (2021).** *Modeling the histogenetic switch from enameloid to enamel.* 3rd Paleontological Virtual Congress. Online.
- Houée, G. (2021).** *Origine des tissus squelettiques minéralisés des vertébrés : L'apport des premiers vertébrés.* ApéroScience. Online.
→ Translation: "*Origin of vertebrate mineralized skeletal tissues: The contribution of early vertebrates.*"

POSTERS

- Houée, G., Bardin, J., Germain, D., Janvier, P., Goudemand, N. (2023).** *Developmental models shed light on the earliest dental tissues, an example based on Astraspis.* 67th Annual Meeting of the Palaeontological Association 2023. Cambridge, United Kingdom.
- Houée, G., Houssaye, A. (2022).** *Adaptation of perissodactyl long bone inner structure - Focus on tapirs.* International Symposium on Palaeohistology (ISPH) 2022. Online.

LES GRES DE HARDING : SUR LES TRACES DE BOULE ET GAUDRY

G. Houée, A. Lemierre, P. Janvier, D. Germain, J. Bardin, N. Goudemand

A la fin du XIX^{ème} siècle, l'exploitation des grès ordoviciens de la Formation de Harding (Cañon City, Colorado, Etats-Unis) a permis la découverte de nombreux fragments biominéralisés. L'origine de ces restes fut attribuée à des squelettes de vertébrés ordoviciens, faisant de ce site le témoin des plus anciens vertébrés connus de l'époque (Fig. 1). Suite à une première publication par le Pr. Walcott, deux taxons de ptéraspidomorphes furent proposés : *Astraspis desiderata* et *Eryptichus americanus* (Walcott, 1892). Depuis, la Formation de Harding a fait l'objet de nombreuses autres études ayant notamment permis d'identifier de nouveaux taxons de vertébrés et de discuter de l'évolution des tissus osseux et dentaires (Bryant, 1936; Ørvig, 1951; Denison, 1967; Sansom *et al.*, 1995; Sansom, Smith & Smith, 1996; Smith & Sansom, 1997; Andreev *et al.*, 2016). Bien que des sites comprenant des vertébrés plus anciens ont pu être mis à jour depuis la découverte de la Formation de Harding, ce site reste d'une importance paléontologique majeure, notamment en raison de sa diversité taxonomique et de la préservation exceptionnelle des tissus.

Les grès bioclastiques de Harding sont présents au Muséum National d'Histoire Naturelle (MNHN) depuis la découverte de leur importance paléontologique. En effet, lors du congrès international de géologie de 1891, Marcellin Boule et Albert Gaudry ont pu récolter des échantillons de grès, sous les conseils du Pr. Walcott lui-même (Boule, 1893). Ces échantillons ont rapidement été étudiés au MNHN par le Pr. Vaillant qui, via la réalisation de lames minces, a pu identifier des restes de cellules osseuses, une première dans l'Ordovicien (Vaillant, 1902). Le taxon correspondant à ces tissus, *Skiichthys halsteadi*, ne fut formellement décrit que 95 ans plus tard (Smith & Sansom, 1997). Cette collection de grès de Harding fut également étoffée par E. Stensiö, qui donna des échantillons supplémentaires en 1922. Cette collection fut malheureusement oubliée, et les lames minces considérées comme perdues, avant sa redécouverte par Armand de Ricqlès bien des années plus tard (De Ricqlès, 1995). De nouvelles lames minces furent alors réalisées, mettant une nouvelle fois en avant la préservation exceptionnelle de ces tissus de l'Ordovicien, ainsi que la possibilité de réaliser des observations inédites de grande importance en ce qui concerne notre compréhension des mécanismes de formation des premiers squelettes (Lemierre & Germain, 2019; Houée *et al.*, accepted). L'étude de ces restes semble en effet clé afin de mieux comprendre l'origine et l'évolution précoce des différents tissus squelettiques des vertébrés.

Or, les échantillons présents au MNHN posent aujourd'hui plusieurs problèmes. En effet, il n'est à l'heure actuelle pas possible de retrouver ou d'inférer l'origine stratigraphique de ces échantillons et donc leurs âges relatifs. De plus, l'extraction de spécimens n'étant pas possible dans ces nos échantillons très indurés, nous sommes fortement limités dans l'identification taxonomique et anatomique des fragments que nous étudions. De la même manière, il est difficilement possible de contrôler l'orientation des coupes histologiques, limitant la précision de nos études. Finalement, ces grès ayant une importance historique pour les collections du MNHN, la destruction de ces échantillons n'est pas souhaitable.

Afin de répondre à ces différents problèmes, nous souhaitons retourner sur les pas de Boule et Gaudry pour récolter de nouveaux échantillons de la Formation de Harding. En effet, à l'aide de l'étude stratigraphique de Allulee & Holland (2005), il sera possible de récupérer des spécimens à la position stratigraphique et la datation plus précise. Allulee & Holland (2005) ayant aussi mis en avant des lithologies et des préservations différentielles dans cette formation, il sera aussi possible de récupérer des spécimens plus ou moins indurés, ouvrant la possibilité de dégagement des fossiles. D'après les fouilleurs amateurs de cette formation, il est notamment possible d'avoir accès à des fragments squelettiques isolés de leur matrice, ouvrant la possibilité à la réalisation d'étude taxonomiques, anatomiques, morphologiques, microanatomiques et histologiques plus précises. Finalement, bien que leur découverte reste rare, sachant que seulement quatre spécimens sub-complets ont pu être mis à jour depuis le XIX^{ème} siècle (e.g. Fig. 1A), nous serons aussi à la recherche de restes articulés de vertébrés durant cette mission.

Ces spécimens, une fois inventoriés dans les collections du MNHN, pourront servir pour de multiples projets :

- D'un point de vue développement méthodologique, nous souhaitons faire des tests de marquage sur des spécimens fossiles. Effectivement, les coupes histologiques du MNHN permettent de mettre en avant une préservation exceptionnelle des spécimens de Harding, et particulièrement lorsqu'un probable fluide riche en oxydes s'est introduit dans les cavités et tubules lors de la taphonomie. Nous pensons qu'il serait possible de procéder à des tests de marquages artificiels sur des spécimens isolés afin de faire ressortir les propriétés histologiques des spécimens récoltés.
- À la vue de la préservation exceptionnelle des restes de vertébrés de Harding et de leur position phylogénétique clé, une diversité d'études histologiques est envisagée dans le but de mieux comprendre les mécanismes de mise en place du squelette minéralisé chez les premiers vertébrés. Basé sur les observations préalables réalisées sur les coupes du MNHN

: (1) L'une d'entre elles pourrait notamment se concentrer sur l'étude de la cyclicité des lignes de croissance chez les premiers vertébrés, avec la possibilité de caractériser les plus anciennes lignes de croissance journalières de vertébrés, (2) tandis qu'une autre pourrait se concentrer sur l'origine de l'ossification périchondrale, voire endochondrale.

- À partir de la description morphologique et microanatomique (scans) d'éléments squelettiques dégagés, nous pourrions étudier les mécanismes morphogénétiques dirigeant la formation du squelette minéralisé chez ces vertébrés.
- D'autre part, nous sommes intéressés à mieux comprendre les facteurs environnementaux qui ont pu contraindre l'évolution des tissus minéralisés des vertébrés, notamment pouvoir inférer les interactions trophiques et l'écologie des différents vertébrés primitifs présents dans la formation de Harding. Dans cette perspective, nous souhaitons aussi échantillonner des spécimens sur lesquels nous pourrions effectuer des analyses isotopiques (Martin *et al.*, 2015; Balter *et al.*, 2019), partiellement destructives.

Faisabilité du projet

Il existe plusieurs affleurements, à la position GPS et au log connus, où il est possible d'échantillonner des restes de vertébrés (Fig. 2). Ces différentes localités sont proches l'une de l'autre et sont facilement accessibles car proches des routes. L'accessibilité des sites, ainsi que les autorisations de prélèvement, ont été confirmées par des membres d'anciennes missions sur Harding avec qui nous sommes en contact. La majorité des sites sont sous la responsabilité du Bureau of Land Management (BLM), entité fédérale américaine. Pour tout prélèvement sur ces sites, un permis de fouille est nécessaire. La demande, à faire sur le site du BLM, est prête à être déposée. Il est à noter que l'affleurement type n'est accessible qu'avec l'autorisation des carriers. Nous allons rentrer en contact avec ces derniers, afin d'obtenir une autorisation de visite et prélèvement.

Planning prévisionnel

Nous prévoyons provisoirement de partir en mai-juin 2024 pour une durée de 21 jours. L'arrivée et le départ se feront à Denver, Colorado, et les déplacements se feront en voiture, notamment pour accéder au camp de base à Canon City. Une fois sur place, nous planifions d'étudier au moins quatre affleurements gérés par le Bureau of Land Management et nous tenterons aussi d'accéder à la Carrière-type (Fig. 2). La présence de vertébrés a pu être vérifiée

Fieldwork project

pour chacun de ces affleurements. Nous souhaitons rester deux jours par affleurement, modifiable en fonction de la richesse et accessibilité de l'affleurement, incluant (1) récolte, (2) tri et identification du matériel, et (3) compte-rendu de terrain. Une visite au Muséum d'histoire Naturelle de Denver est également prévue.

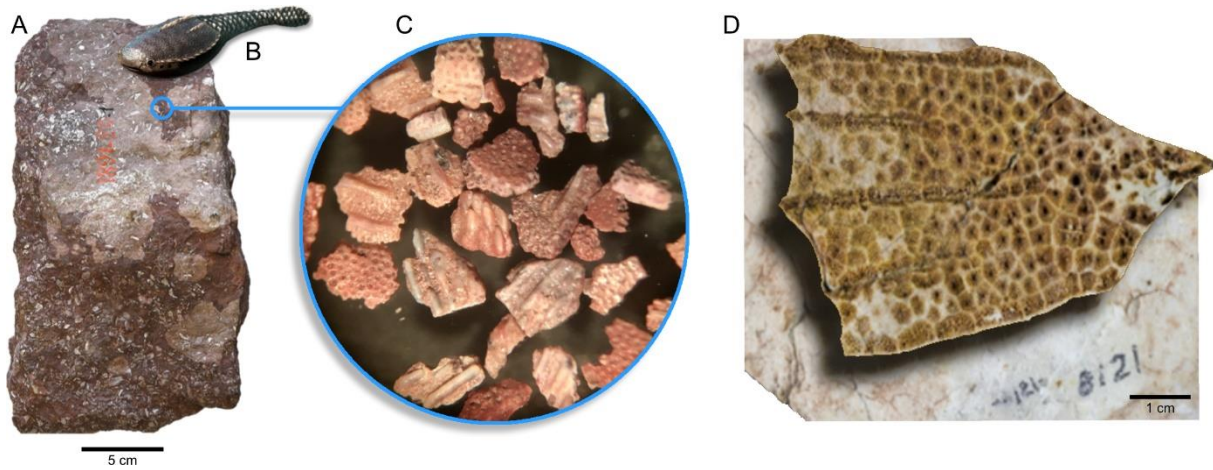


Figure 1 : Exemple de vertébrés fossiles Harding. A, Echantillon de grès de Harding du MNHN récoltés par Boule et Gaudry en 1891 ; B, Reconstruction d'*Astraspis*. C, Exemples d'éléments isolés de vertébrés de Harding (© ThePhysicist, récolte amateur, sans échelle). D, Toit crânien d'*Astraspis* (collection du Smithsonian Institute, DC, Etats-Unis).

Fieldwork project

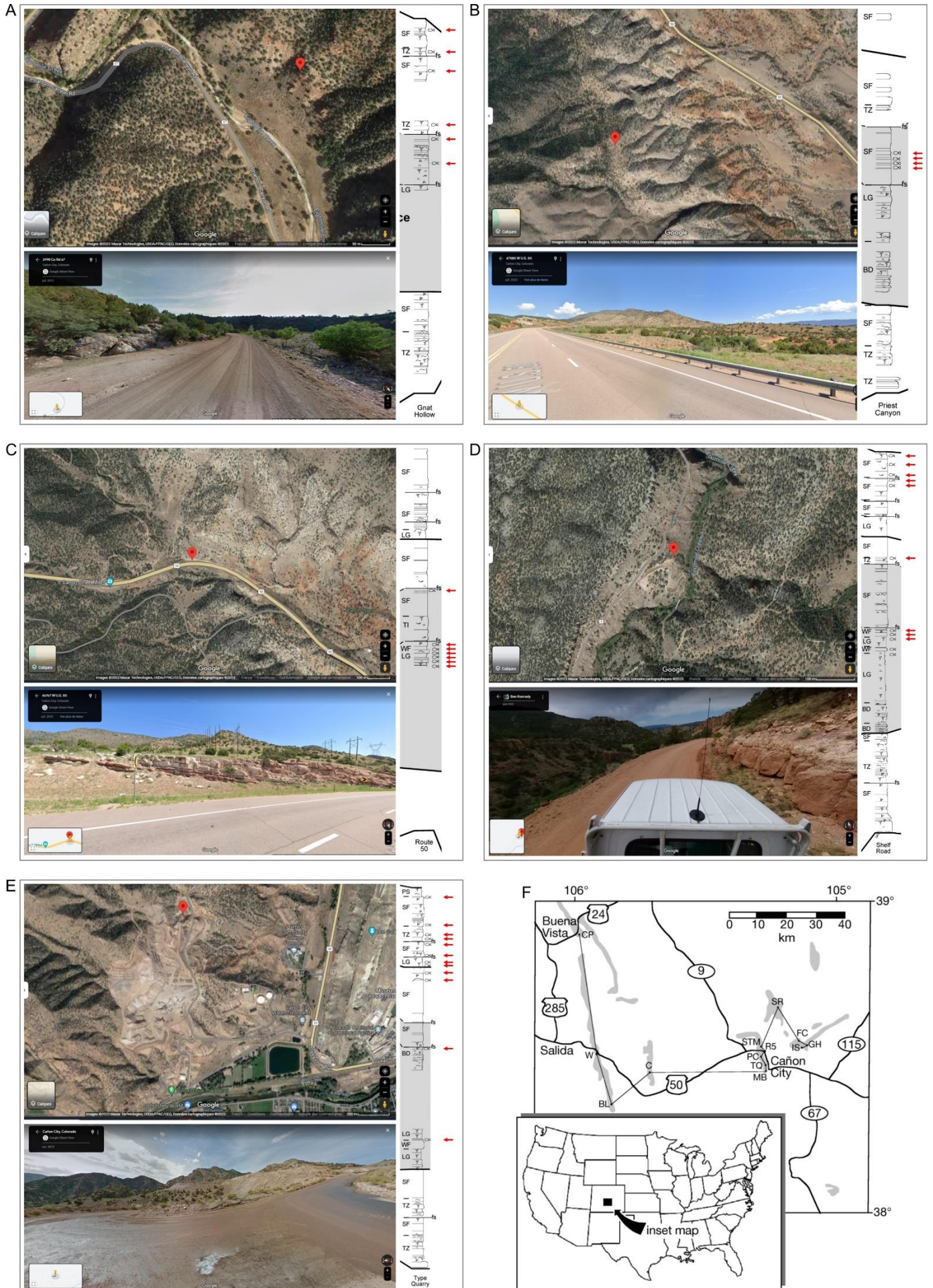


Figure 2 : Localisation des affleurements. A, Gnat Hallow (38°30.729' N, 105°6.680' W.). B, Priest Canyon (38°28.975' N, 105°17.006' W.). C, Route 50 (38°29.763' N, 105°17.387' W.). D, Shelf Road (38°37.070' N, 105°13.097' W.). E, Type Quarry (38°26.663' N, 105°15.832' W.). F, Occurrences de la Formation de Harding dans le Colorado (gris clair). FC, Phantom Canyon. GH, Gnat Hollow. PC, Priest Canyon. R5, Route 50. SR, Shelf Road. TQ, Type Quarry. Les flèches rouges indiquent les niveaux à vertébrés. Les logs et la carte sont tirés de Allulee & Holland (2005), et les photos de Google Maps.

Bibliographie

- ALLULEE, J.L. & HOLLAND, S.M. (2005) The sequence stratigraphic and environmental context of primitive vertebrates: Harding Sandstone, Upper Ordovician, Colorado, USA. *Palaios* **20**, 518–533. SEPM Society for Sedimentary Geology.
- ANDREEV, P., COATES, M.I., KARATAJŪTĒ-TALIMAA, V., SHELTON, R.M., COOPER, P.R., WANG, N.-Z. & SANSOM, I.J. (2016) The systematics of the Mongolepidida (Chondrichthyes) and the Ordovician origins of the clade. *PeerJ* **4**, e1850. PeerJ Inc.
- BALTER, V., MARTIN, J.E., TACAİL, T., SUAN, G., RENAUD, S. & GIRARD, C. (2019) Calcium stable isotopes place Devonian conodonts as first level consumers. *Geochemical Perspectives Letters* **10**, 36–39. European Association of Geochemistry.
- BOULE, M. (1893) Une excursion géologique dans les montagnes rocheuses. *Bulletin de l'association française pour l'avancement des sciences: Conférences de Paris.*, 16.
- BRYANT, W.L. (1936) A study of the oldest known vertebrates, *Astraspis* and *Eriptychius*. *Proceedings of the American Philosophical Society*, 409–427. JSTOR.
- DE RICQLES, A. (1995) Les vertébrés des grés de Harding: ce que Vaillant a pu observer. *Geobios* **28**, 51–56. Elsevier.
- DENISON, R.H. (1967) Ordovician vertebrates from western United States. *Fieldiana, Geology* **16**, 131–192. Field Museum of Natural History.
- HOUÉE, G., BARDIN, J., GERMAIN, D., JANVIER, P. & GOUEMAND, N. (accepted) Developmental models shed light on the earliest dental tissues, an example on *Astraspis*. *Palaeontology*.
- LEMIERRE, A. & GERMAIN, D. (2019) A new mineralized tissue in the early vertebrate *Astraspis*. *Journal of anatomy* **235**, 1105–1113. Wiley Online Library.
- MARTIN, J.E., TACAİL, T., ADNET, S., GIRARD, C. & BALTER, V. (2015) Calcium isotopes reveal the trophic position of extant and fossil elasmobranchs. *Chemical Geology* **415**, 118–125.
- ØRVIG, T. (1951) Histologic studies of Placoderms and fossil Elasmobranchs. I. The endoskeleton, with remarks on the hard tissues of lower vertebrates in general. *Ark. Zool* **2**, 321–454.
- SANSOM, I.J., PAUL SMITH, M., SMITH, M.M. & TURNER, P. (1995) The harding sandstone revisited -a new look at some old bones. *Geobios* **28**, 57–59.

Fieldwork project

SANSOM, I.J., SMITH, M.M. & SMITH, M.P. (1996) Scales of thelodont and shark-like fishes from the Ordovician of Colorado. *Nature* **379**, 628–630. Nature Publishing Group.

SMITH, M.M. & SANSOM, I.J. (1997) Exoskeletal micro-remains of an Ordovician fish from the Harding Sandstone of Colorado. *Palaeontology* **40**, 645–658. BLACKWELL PUBL LTD 108 COWLEY RD, OXFORD, OXON, ENGLAND OX4 1JF.

VAILLANT, L. (1902) Sur la présence du tissu osseux chez certains Poissons des terrains paléozoïques de Canyon City (Colorado). *Comptes rend Acad Sci* **134**, 1321–1322.

WALCOTT, C.D. (1892) Preliminary notes on the discovery of a vertebrate fauna in Silurian (Ordovician) strata. *Bulletin of the geological Society of America* **3**, 153–172. Geological Society of America.

RESUME - ABSTRACT

Le squelette des vertébrés est composé d'une diversité de tissus minéralisés tels que l'os, la dentine et l'émail. La plupart de ces tissus ont une origine ancienne, on les retrouve notamment dans le squelette dermique de premiers vertébrés, comme les ptéraspidomorphes ayant vécu de l'Ordovicien au Dévonien. Leur squelette était composé de plusieurs structures osseuses surplombées d'éléments « dentaires » faits de dentine et parfois d'émailloïde, un tissu similaire à l'émail. Cette thèse explore, de manière intégrée, le développement et l'évolution de ces premiers tissus. Une première étape s'est concentrée sur la redéfinition de concepts clés concernant les tissus hyperminéralisés, uniformisant les identifications et discussions évo-dévo associées. Une seconde étape de création de modèles histomorphogénétiques, basée sur l'étude des tissus actuels, a permis d'explorer les mécanismes développementaux de diversification des structures squelettiques. Cette étape est aussi passée par la création d'une nouvelle approche *in silico* d'exploration d'hypothèses évo-dévo, testant notamment l'impact de paramètres développementaux sur la formation de structures dentaires. Finalement, une troisième étape d'inférence sur des taxons fossiles clés comme *Astraspis* et *Anglaspis* a permis de proposer des reconstructions paléodéveloppementales pour les premières structures squelettiques minéralisées. En comparaison avec l'actuel, cela semble notamment mettre en avant que le timing d'activation des cellules mésenchymateuses ait pu changer durant l'évolution du squelette des vertébrés.

Mots-clés : *paléodéveloppement, vertébrés, ptéraspidomorphes, squelette minéralisé, histologie, microanatomie, modélisation.*

The vertebrate skeleton is composed of a variety of mineralized tissues such as bone, dentin, and enamel. Most of these tissues have an ancient origin, and they are notably found in the dermal skeleton of early vertebrates, like the pteraspidomorphs that lived from the Ordovician to the Devonian. Their skeleton was composed of multiple bony structures topped with 'dental' elements made of dentin and sometimes enameloid, a tissue similar to enamel. This thesis explores, in an integrated manner, the development and evolution of these early tissues. The first step focused on redefining key concepts regarding hypermineralized tissues, standardizing identifications and associated evo-devo discussions. A second step of creating histomorphogenetic models, based on the study of present-day tissues, allowed exploration of the developmental mechanisms diversifying skeletal structures. This step also involved creating a new *in silico* approach to explore evo-devo hypotheses, testing notably the impact of developmental parameters on the formation of dental structures. Finally, a third step of inference on key fossil taxa like *Astraspis* and *Anglaspis* enabled proposing paleodevelopmental reconstructions for the first mineralized skeletal structures. In comparison with the present, this notably suggests that the timing of activation of mesenchymal cells may have changed during the evolution of the vertebrate skeleton.

Keywords: *paleodevelopment, vertebrates, pteraspidomorphs, mineralized skeleton, histology, microanatomy, modeling.*